TITLE:

BASIC STUDIES OF CONVECTION HEAT TRANSFER RELATED TO PASSIVE SAFETY OF FAST BREEDER REACTORS(Dissertation_全文)

AUTHOR(S):

Takeuchi, Yuto

CITATION:

Takeuchi, Yuto. BASIC STUDIES OF CONVECTION HEAT TRANSFER RELATED TO PASSIVE SAFETY OF FAST BREEDER REACTORS. 京都大学, 1998, 博士(工学)

ISSUE DATE:

1998-03-23

URL:

https://doi.org/10.11501/3135662

RIGHT:

京都大学学術情報リポジトリ
KURENAI 紅
Kyoto University Research Information Repository

BASIC STUDIES OF CONVECTION HEAT TRANSFER RELATED TO PASSIVE SAFETY OF FAST BREEDER REACTORS

by

Yuto TAKEUCHI

KYOTO UNIVERSITY

1997

Acknowledgment

The author wishes to gratefully acknowledge the unsparing advice and reliable guidance received from Professor Akimi Serizawa, Graduate School of Engineering of the Kyoto University, in completing this dissertation. The author would like to express his gratitude to Professor Kenjiro Suzuki, and to Professor Fumimaru Ogino, Graduate School of Engineering of the Kyoto University, for the fruitful discussion and valuable comments.

The author wishes to express his gratitude to Emeritus Professor Akira Sakurai of the Kyoto University for the careful advice and encouragement, and to Professor Masahiro Shiotsu, Graduate School of Energy Science of the Kyoto University, for the valuable discussions and helpful advice over the many years that this research was in progress. The author is also grateful to Dr. Koichi Hata, the Institute of Advanced Energy of the Kyoto University, for his skillful technical assistance. The experimental achievements throughout the course of this work have been greatly assisted by the effort of Dr. Koichi Hata.

The author also wishes to express his heartfelt gratitude to Professor Isao Kataoka, Graduate School of Engineering of the Osaka University, for his warm and unswerving encouragement during the preparation of this dissertation. The author is indebted to Dr. Osamu Takahashi, Graduate School of Engineering of the Kyoto University, for the valuable comments on several points in the thesis.

The author also extends his grateful acknowledgments to Shinzo Kikkawa, Hajime Fujimoto, Jiro Senda, Mamoru Senda, and Tsutao Katayama—Professors of the Doshisha University Graduate School of Engineering, and to Mr. Shigeo Nakamura, a general manager of engine measurement system division, Horiba, Ltd., for their untiring encouragement.

Abstract

Basic Studies of Convection Heat Transfer

Related to

Passive Safety of Fast Breeder Reactors

Yuto Takeuchi

This thesis provides the basic information on a couple of heat transfer problems—for assessment of reactor passive safety to make provision against severe accident such as loss of flow encountered in fast breeder reactors and/or in water cooled nuclear reactors—based on theoretical and experimental findings. All the parts of the thesis are devoted to the basic investigations of heat transfer by natural convection or by mixed convection including conjugate heat transfer problem.

In chapter 1, natural convection heat transfer coefficients on single horizontal cylinders with uniform surface heat fluxes and/or with uniform surface temperatures were derived numerically from the basic equations without the boundary layer approximation using finite difference method. The numerical analysis was performed for a wide range of the Rayleigh numbers for the Prandtl numbers ranging from 0.005 to 3000. Experiments of the natural convection heat transfer have been made by the research group including the author for various liquids such as water, ethanol, glycerin, sodium, nitrogen and helium under a wide range of bulk liquid temperatures and system pressures with a variety of horizontal cylinder diameters. Comparison between the experimental and numerical results has revealed that the

local and average Nusselt numbers obtained experimentally for liquid sodium are well described by the numerical solutions for the surface boundary condition of uniform heat flux. On the basis of the numerical results, a correlation capable of describing all the numerical solutions of the average Nusselt numbers for uniform surface heat fluxes within $\pm$ 5 percent errors is presented. The average Nusselt numbers calculated from the correlation were compared with the author's experimental results as well as with other workers' experimental data obtained for various fluids such as air, helium, argon, hydrogen, oxygen, nitrogen, carbon dioxide gases, silicone oils and some liquid metals such as sodium, mercury and tin: the author's experimental results covering the Prandtl number range from 0.005 to 18000 agree well with the correlation within $\pm$ 10 percent errors, provided the fluid properties are evaluated at the reference temperature defined as $T_f = T_W - 0.7(T_W - T_\infty)$ where T_W and T_∞ denote the cylinder surface temperature and the bulk fluid temperature respectively. Comparison of the average Nusselt numbers evaluated by the new correlation with those by some conventional correlations based on published experimental data or on simplified physical models has exhibited that the conventional correlations are invalid for predicting the experimental results for extremely high or low Prandtl numbers.

In chapter 2, heat transfer from the inner rod surface of a vertical concentric annulus to upward laminar forced flow of liquid sodium was numerically analyzed for the Péclet numbers ranging from 0.7 to 71.7 using a numerical model which incorporates the effects of buoyancy force as well as heat conduction in annulus walls. The numerical solutions for fully developed Nusselt number on the surface of a heated section in various lengths ranged approximately between 6 and 7 for the Péclet number range. Some theoretical analyses based on the model disregarding the effects of both buoyancy and axial heat conduction have predicted apparently that the fully developed Nusselt number is about 6 for the same Péclet

number range. It was found, however, that the simplified model underestimates both heated wall and liquid bulk mean temperatures. Experiments were made of forced convection heat transfer from a heated surface of 52 mm in length on an inner cylinder of 7.6 mm in diameter to liquid sodium flowing in a vertically orientated concentric annulus with 14.3 mm inside diameter. The author's experimental data of heated surface temperatures and outlet liquid sodium temperatures at all measuring points agree well with the corresponding numerical solutions. However, the Nusselt numbers, obtained from the measured wall surface temperatures and the local bulk mean temperatures estimated by a simple method based on linear interpolation between the measured inlet and outlet temperatures by taking account of axial conduction effect, decreased from the value of 6 with a decrease in the Péclet number from around 20. It is made clear that the local bulk mean temperatures are not properly estimated by the linear interpolation method at low Péclet numbers. Finally, approximate analytical solution, capable of describing the numerical solution for local bulk mean temperature obtained for a variety of heated lengths, is derived.

In chapter 3, experiments were made of unsteady forced convection heat transfer in liquid sodium in the vertical concentric annulus identical to that used for the steady forced convection heat transfer experiments described in chapter 2. With constant heat flux of 1.0×10^6 W/m^2, liquid sodium flow rate was reduced ramp-wise within about 25 seconds from an initial equilibrium state (T_{in}=573 K, U=5 l/min, Pe=72) to the value of 0.46 l/min (Pe=6.4) and then it was maintained constant; where T_{in}, U, and Pe denote inlet liquid temperature, flow rate, and the Péclet number respectively. And another experimental condition of the flow rate range was from Pe=141(U=10 l/min) to 11.5 (U=0.8 l/min). The qualitative characteristics obtained experimentally for the two flow transiency cases are described as follows: after the flow rate begins to decrease, the surface temperatures at first

remain almost unchanged from the initial values, however, they turn to increase remarkably after a certain period of time has passed. After the flow rate finishes decreasing and reaches a lower constant value, the heated surface temperature at a specific location still keeps on rising with larger time delay as a position is closer to the end of the heated section, and finally converges into a constant value depending on the location on the heated surface. Along with the experimental research, a numerical model for analyzing *unsteady forced convection heat transfer* (*UFCHT*) caused by a variation in liquid sodium flow rate in a concentric annulus was developed by extending a model for *steady forced convection heat transfer* (*SFCHT*) for constant sodium flow rate, which incorporates the effect of heat conduction in the inner and outer walls of an annulus as well as in liquid sodium. With the *UFCHT* model, numerical analysis was first performed with the same parameters—heat flux, inlet temperature of liquid sodium, and transient flow rate—as the experimental conditions mentioned above. The time variations in heated surface temperature obtained numerically agree with the experimental results for the two different flow transient conditions. The numerical model proved to be valid for expressing the unsteady laminar combined forced and free convection heat transfer caused by a decrease in sodium flow rate in a concentric annular passage. The numerical results for various flow reduction periods revealed that the time delays in heated wall temperature rise from those predicted by the *SFCHT* model for constant flow rate were little influenced by the flow reduction periods ranging from about 25 down to 2 sec. As the surface temperatures calculated by the *UFCHT* model become always equal to or lower than those by the *SFCHT* model over the investigated flow reduction range and periods, the *SFCHT* model is regarded as a simple but effective method for safety evaluation of transient heated wall temperature rise caused by rapid decrease in liquid sodium flow rate.

Table of Contents

List of Figures

Chapter 1

Figures

Chapter 2

Figures

Chapter 3

Figures

List of Tables

Chapter 1

Tables

Chapter 2

Tables

Preface

Everybody living on the earth has the desire and right to lead a healthy way of life. Since electricity had been adopted as a clean and effective power source, peoples' ordinary life has been greatly improved by the expansion of a variety of electrical appliances. On the other hand, instinctively human beings once experiencing the material civilization will never go back even only one step to the life in the past. As a consequence of an increase in the population especially in the developing countries of Southeast Asia in recent years as well as in the near future, nobody or nothing would stop an exponentially increase in the consumption of energy. Soon after electrical appliances penetrate the undeveloped markets, they will deeply propagate into those countries and will become firmly established among the people.

Although energy crisis arising from depletion of fossil fuels has been one of the most serious social problems for a long time, the issue still remains fundamentally unresolved and will keep on hanging over us in the future. With a growth in population, electric power consumption will undoubtedly amount to many times as much as it is now, resulting in raising the price of crude oil. Strongly required is the prompt development of alternative source of energy which is stably obtainable without being affected by the price and production of crude oil, and simultaneously which contributes to environmental protection, and more importantly, which has a realizable possibility in the near future. Even if undiscovered deposits of oil or coal will be available in the future and even if they will be sufficient in quantity and in quality, environmental destruction and/or environmental pollution is more or less inevitably accompanied by installation as well as by operations of both hydraulic and thermal power

plants. Indeed, boundless deforestation and limitless emission of CO_2 gas have been causing global warming. On the contrary, nuclear power generation is essentially clean in terms of a local environmental protection as far as it is operating normally, there is, however, a possibility of causing extensive damage to human beings and to environments for a long time in cases of severe accidents. Accordingly, for prevention of such severe accidents that might be occurred in a nuclear power plant as well as for establishment of its safety standard, it is necessary to develop measures with more prudence compared to those employed for thermal or hydroelectric power plants.

Because a fast breeder reactor (FBR) has been attractive by the features such as its fuel breeding characteristic and its effectiveness as a plutonium recycling system, advanced countries have been developing FBR aiming at its practical use. In Japan, for example, plutonium recycling by FBRs has been recognized as one of the important kernels of national project for atomic energy development and utilization since Japan is poor in natural uranium resources. As for the recent trends in the research and development of FBRs, several advanced countries in the world have stopped or suspended its development project one after another. Some of the reasons for such a trend are possibly attributed to difficulties in establishment of either nuclear fuel cycle or sodium technology. In fact, the sodium leakage accident which occurred in "Monju" has shown that there still remain a lot of problems to be solved before the realization of FBR's practical use.

Among safety principles of FBRs, so-called *defense in depth* is a fundamental concept, which is classified into three levels according to the objects of safety measures. As one of the subdivisions of defense in depth, a concept of *passive safety* ranks as the second level of the defense in depth. In estimating the passive safety design of FBR in terms of thermal hydraulics, it is essential to consider how to secure the level of liquid sodium used as a

coolant to keep necessary flow rate, and also how to maintain the capacity of natural circulation independent of an external power source. Liquid sodium—having high thermal conductivity and high boiling point—permits the FBR's primary coolant circuit to operate at pressures less than about 1 MPa, which prevents rapid loss of coolant due to flashing followed by pipe rupture. In addition, a FBR vessel is equipped with a guard-vessel which contributes to maintain liquid sodium level, providing against loss of coolant by its leakage. And also, the temperature difference between inlet and outlet in FBR core is designed to be large enough to enhance buoyancy driven flow of liquid sodium, which allows the coolant to remove decay heat by its natural circulation. Thus, by making good use of the thermophysical characteristics of liquid sodium, decay heat removal by natural circulation of coolant is one of the rational and effective methods concerning passive safety design of FBR.

For constructing more accurate and reliable standards of the passive safety, it is very important to investigate in detail the basic physical mechanisms encountered in various thermal hydraulic phenomena associated with the natural circulation characteristic of FBR. Based on the above mentioned technological background and motivation, all the parts of this thesis are devoted to basic studies of convective heat transfer concerning reactor passive safety design, especially focusing on the problems related to decay heat removal by natural circulation of coolant in reactor core as well as in intermediate heat exchanger. The thesis consists of four chapters. A brief description of the content of each chapter is as follows.

Chapter 1 presents a general correlation derived from numerical results for natural convection heat transfer from single horizontal cylinders in liquids and gases. The applicability of the correlation is discussed by comparison with the author's and other researchers' experimental results for various fluids with the Prandtl numbers ranging from 0.005 to 18000. The correlation is also compared with a couple of well-known

conventional correlation equations for natural convection heat transfer from a horizontal cylinder.

Chapter 2 deals with combined forced and free convection heat transfer of liquid sodium in a concentric annulus at low Péclet numbers. The heated surface temperatures obtained experimentally are compared with numerical results based on a rigorous numerical model for the Péclet numbers ranging from 72 down to 0.7. The theoretical analysis has clarified the mechanism of the heat transfer at extremely low Péclet numbers, and has pointed out that a simple method for predicting local bulk mean temperature by a linear interpolation between the inlet and outlet temperatures is invalid in estimation of heat transfer coefficients. Based on the theoretical results, an approximate analytical solution for local bulk mean temperature of liquid sodium in a concentric annulus is presented.

Chapter 3 discusses unsteady combined forced and free convection heat transfer caused by rapid decrease in liquid sodium flow rate in a concentric annulus. Measurements have been made of heated surface temperatures for the Péclet numbers decreasing from 141 down to 11.5 and from 72 to 6.4. In both cases, heat flux was maintained at a constant value of 1×10^6 W/m^2. The numerical model presented in chapter 2 was extended to analyze unsteady heat transfer problem accompanied by the flow transiency. The validity of the model is first verified by the experimental results with the flow transient conditions of two different types. Then, the effect of flow reduction period on time variation in heated surface temperature and on transient heat transfer coefficient is investigated by numerical analysis using the extended numerical model.

Chapter 4 summarizes the major results and conclusions described in the prior chapters.

Chapter 1

A General Correlation for Laminar Natural Convection Heat Transfer from Single Horizontal Cylinders

1.1 Introduction

A number of correlations for natural convection heat transfer from single horizontal cylinders have been presented by many researchers up to the present. A correlation representing experimental data for air, water and various oils for the Rayleigh numbers ranging from 10^3 to 10^9 was presented by McAdams (1954). Kutateladze (1958) derived theoretically a correlation for liquid metals based on boundary layer approximation. These correlations, however, become inapplicable in the region of low Rayleigh numbers where the curvature effect on heat transfer is no longer negligible, and several empirical correlations have been presented to correlate the experimental data at low Rayleigh numbers. Churchill and Chu (1975) have proposed a correlation by employing the method developed by Churchill and Usagi (1972) to combine an equation derived theoretically for high Rayleigh number region with an empirically assumed constant value for extremely low Rayleigh

number region. Raithby and Hollands (1985) have presented a correlation based on existing experimental data for a wide range of Rayleigh and Prandtl numbers. Although many correlations for natural convection heat transfer from single horizontal cylinders have been published as mentioned above, there is no general correlation derived purely by numerical analysis. Table 1.1 summarizes published numerical studies of natural convection heat transfer from a horizontal cylinder. As seen in the table, most of the numerical analyses have employed constant temperature as a boundary condition at cylinder surface, and also, they are restricted within the narrow ranges of the Prandtl and Rayleigh numbers.

Recently, the local and average natural convection heat transfer coefficients on the single horizontal cylinders of 7.6 and 10.7 mm in diameters in liquid sodium were obtained experimentally by Hata et al (1991): the results indicated that the average heat transfer coefficients are about 36 to 100 percent higher than those predicted by the Kutateladze's correlation. Along with the experiments, numerical analysis was made of natural convection heat transfer from single horizontal cylinders in liquid sodium for constant surface heat fluxes and for constant surface temperatures (Takeuchi et al, 1992). Comparison between the experimental results and the numerical solutions for the two different types of boundary conditions has revealed that the theoretical local and average Nusselt numbers obtained for constant surface heat flux agree with the experimental results within $\pm$ 10 percent errors. On the contrary, the theoretical local Nusselt numbers obtained with the boundary condition of constant surface temperature did not agree with the experimental results, and also the average Nusselt numbers become about 10 percent lower than those for constant heat flux.

The purpose of the present study described in chapter 1 is threefold. First is to obtain the numerical solutions of heat transfer coefficients on single horizontal cylinders for a wide range of the Rayleigh and Prandtl numbers using finite difference method, and based on the

computational results, to derive a correlation capable of expressing all the numerical solutions of the average Nusselt numbers.

Second is to accumulate the experimental data of natural convection heat transfer coefficients on single horizontal cylinders for various liquids—helium, nitrogen, glycerin, water, ethanol, and sodium—under a wide range of experimental conditions such as cylinder diameter, system pressure, and liquid temperatures. In connection with the experimental data analysis, the effect of the temperature-dependent fluid properties on natural convection heat transfer will be also discussed.

Third is to compare the average Nusselt numbers predicted by the new correlation with the author's and other workers' experimental results for various liquids and gases, as well as with some correlations presented by other researchers based on their experimental or theoretical investigations.

1.2 Numerical Analysis

1.2.1 Physical Model and Basic Equations

By assuming that the physical properties other than the density of the fluid around a horizontal cylinder are constant irrespective of temperature variation, we can express the basic equations in the cylindrical coordinates in Fig. 1.1 as follows:

(Vorticity Equation)

$$\frac{\partial \zeta}{\partial \tau}+\frac{1}{r}\left\{\frac{\partial}{\partial r}\left(rv_r\zeta\right)+\frac{1}{\pi}\frac{\partial}{\partial \theta}\left(v_\theta\zeta\right)\right\}=\Pr\left\{\frac{\partial^2\zeta}{\partial r^2}+\frac{1}{r}\frac{\partial \zeta}{\partial r}+\frac{1}{(\pi r)^2}\frac{\partial^2\zeta}{\partial \theta^2}\right\}$$

$$+\frac{\mathrm{Ra}}{8}\Pr\left\{\sin(\pi\theta)\frac{\partial \Theta}{\partial r}+\frac{\cos(\pi\theta)}{\pi r}\frac{\partial \Theta}{\partial \theta}\right\}\quad , \qquad (1.1)$$

(Stream Function Equation)

$$\frac{\partial^2\varphi}{\partial r^2}+\frac{1}{r}\frac{\partial\varphi}{\partial r}+\frac{1}{(\pi r^2)}\frac{\partial^2\varphi}{\partial\theta^2}+\zeta=0 \quad , \tag{1.2}$$

(Energy Equation)

$$\frac{\partial\Theta}{\partial\tau}+\frac{1}{r}\left\{\frac{\partial}{\partial r}(rv_r\Theta)+\frac{1}{\pi}\frac{\partial}{\partial\theta}(v_\theta\Theta)\right\}=\frac{\partial^2\Theta}{\partial r^2}+\frac{1}{r}\frac{\partial\Theta}{\partial r}+\frac{1}{(\pi r)^2}\frac{\partial^2\Theta}{\partial\theta^2} \quad . \tag{1.3}$$

In Eq. (1.1), the Rayleigh number, Ra, is defined as Ra_T $(=g\beta(T_W-T_\infty)D^3/(a\nu))$ for constant surface temperature and as Ra_q $(=g\beta qD^4/\lambda a\nu)$ for constant surface heat flux respectively. The dimensionless temperature, Θ, in Eqs. (1.1) and (1.3) is defined as $\Theta=(T-T_L)/(T_W-T_L)$ for constant surface temperature and $\Theta=(T-T_L)/(qD/\lambda)$ for constant surface heat flux respectively. The radial and angular velocity components involved in Eqs. (1.1) and (1.3) are expressed by

$$v_r=\frac{1}{\pi r}\frac{\partial\varphi}{\partial\theta} \quad , \tag{1.4}$$

$$v_\theta=-\frac{\partial\varphi}{\partial r} \quad . \tag{1.5}$$

These basic equations are numerically analyzed under the following boundary conditions by using the finite difference method .

$$r=1 \quad : \quad \varphi=0, \quad \zeta=\frac{\partial^2\varphi}{\partial r^2},$$

$$\begin{cases}\Theta = 1 & (\text{for constant temperature}),\\ \dfrac{\partial\Theta}{\partial r}=-\dfrac{1}{2} & (\text{for constant heat flux}),\end{cases} \tag{1.6}$$

$$r = r_\infty \ : \ \frac{\partial \varphi}{\partial r} = 0, \quad \zeta = -\frac{1}{(\pi r_\infty)^2} \frac{\partial^2 \varphi}{\partial \theta^2},$$

$$\Theta = 0 \text{ (for inflow)}, \quad \frac{\partial \Theta}{\partial r} = 0 \text{ (for outflow)} \tag{1.7}$$

$$\theta = 0, 1 \ : \ \varphi = 0, \quad \zeta = 0, \quad \frac{\partial \Theta}{\partial \theta} = 0. \tag{1.8}$$

As given by Eq. (1.7), a set of boundary conditions for dimensionless temperature, Θ, developed by Kuehn (1976) were employed for separation of the outer boundary into two sections; one is the boundary where the ambient fluid flows into the calculation domain at its bulk temperature, and the other is the one where heated fluid flows outward conveying thermal energy only by convection with negligible radial temperature gradient. The angular location dividing the inflow and outflow sections of the outer boundary was determined by the angle at which the absolute value of stream function has a maximum, since the sign of the radial velocity component is reversed at this point. Equation (1.8) implies that the fields of both flow and temperature are symmetrical to the line, parallel to the direction of gravity, passing through the center of a horizontal cylinder. The outer boundary of a calculation domain, constructed in a concentric form around a horizontal cylinder, was set far enough so that it will become larger than the boundary layer thickness except the thermal plume region at the top of a horizontal cylinder. As listed in Table 1.2, the ratios of the radial distance of the outer boundary of a calculation domain measured from the center of a horizontal cylinder to the cylinder radius, r_∞, were ranged from 4 to 25000 according to the magnitude of the modified Rayleigh number, Ra_q. Since the thickness of velocity and thermal boundary layer varies with the Rayleigh and the Prandtl numbers, the radial mesh-size adjacent to a cylinder surface was varied from $0.0005 \times R$ to $0.1 \times R$. The radial grid spacing was

increased in a geometrical ratio as it extends outward until the outermost node surface reaches the outer boundary of calculation domain. The number of radial grid points was ranged from 51 to 101, and the angular grid spacing was reduced from 5 to 1.25 deg with an increase in the Rayleigh number.

1.2.2 Procedure of Numerical Analysis

All the numerical solutions reported in this chapter have been obtained by solving unsteady natural convection heat transfer so that it can be checked sequentially whether the computational analysis properly proceeds. Every numerical execution starting with the initial condition of stepwise increase in surface heat flux was performed until a steady state was established. Upon the beginning of a numerical calculation, the initially stagnant fluid around a horizontal cylinder at its bulk temperature starts being heated, thereby increasing its flow velocity to the limiting value that may cause divergence of numerical solution. To prevent the numerical divergence and to maintain numerical stability during calculation, hybrid difference scheme was employed for discretization of the convection terms, while central difference scheme was used for the diffusion terms in the vorticity and energy equations. By fully implicit method the vorticity and energy equations were solved, while the stream function equation was iterated by successive over relaxation method at every time step. The program developed for the present analysis as well as its flowchart are summarized in Appendix B at the end of this chapter.

Figure 1.2(a) and 1.2(b) show the typical transient behavior of the average Nusselt numbers obtained numerically for Pr = 0.005 and 1000 respectively. The exact solution of unsteady heat conduction equation for stepwise increase in surface heat flux on a circular cylinder in infinite medium is given by Carslaw and Jaeger (1959) as

$$\mathrm{Nu}=\left[-\frac{1}{\pi}\int_0^{\infty}\left(1-e^{-u^2\tau}\right)\frac{J_0(u)Y_1(u)-Y_0(u)J_1(u)}{u^2\left\{J_1^{\,2}(u)+Y_1^{\,2}(u)\right\}}du\right]^{-1}, \qquad (1.9)$$

where $J_n(u)$ is the Bessel function of n-th order and $Y_n(u)$ is the Neumann function of n-th order respectively. The transient Nusselt numbers calculated from Eq. (1.9) are also shown in each figure as a bold solid curve for comparison. As shown in the figures, the numerically obtained Nusselt numbers for all the Prandtl and Rayleigh numbers first decrease along with the transient heat conduction curve given by Eq. (1.9), then each of them departs from the curve and approaches their asymptotic value depending on the Prandtl and the Rayleigh numbers. At this stage, the fluid flow above a horizontal cylinder still keeps fluctuating slightly for a certain period even after a stable temperature field was formed around a cylinder. Provided that variations in the calculated values of stream function and temperature at each node fall within 0.01 percent from the values obtained at 50 time steps before, the numerical solutions were regarded to be converged, and steady state local heat transfer coefficients on the circumference of a cylinder were obtained. By integrating these local values, an average steady state heat transfer coefficient was obtained.

1.3 Results and Discussion

1.3.1 Comparison of Experimental Results for Liquid Sodium with Numerical Results and Conventional Correlations

The local and average natural convection heat transfer coefficients on single horizontal cylinders of 7.6 and 10.7 mm in diameters in liquid sodium were obtained experimentally by Hata et al (1991) for a wide range of Rayleigh numbers at the bulk liquid temperature of 673 K under atmospheric pressure. (see Appendix A.1)

Kutateladze (1958) presented the following correlation for natural convection heat

transfer from a horizontal cylinder in liquid metals based on boundary layer approximation:

$$\mathrm{Nu} = 0.67\left(\frac{\mathrm{Gr\,Pr}^2}{1+\mathrm{Pr}}\right)^{1/4}, \tag{1.10}$$

where Nu is the average Nusselt number, and Gr, Pr are the Grashof and the Prandtl numbers respectively. Sugiyama et al (1991) obtained numerical solutions without boundary layer approximation for laminar natural convection heat transfer from an isothermal horizontal cylinder in liquid metals for the range $4 \le \mathrm{GrPr}^2 \le 7000$ $(0.004 \le \mathrm{Pr} \le 0.02)$ and presented a correlation for liquid metals based on their numerical results:

$$\mathrm{Nu} = 1.11\left(\mathrm{Gr\,Pr}^2\right)^{0.196}, \quad \text{for} \quad 4 \le \mathrm{Gr\,Pr}^2 \le 7000. \tag{1.11}$$

The numerical solutions of the average Nusselt number for Pr = 0.005 for uniform heat flux and for uniform surface temperature obtained by the present analysis are compared with the author's experimental data in Fig. 1.3 in a plot of $\log_{10}\mathrm{Nu}$ vs. $\log_{10}\mathrm{Gr\,Pr}^2/(1+\mathrm{Pr})$. The curves calculated from the correlations proposed by Kutateladze and by Sugiyama et al are also shown in the figure for comparison.

The prediction by the Kutateladze's correlation curve is found to be 30 to 60 percent lower than the experimental data. This discrepancy arises from the boundary layer approximation employed for derivation of his correlation. The experimental data are in agreement with the author's numerical results for uniform surface heat flux within ± 10 percent errors over the range of $\mathrm{GrPr}^2/(1+\mathrm{Pr})$, however, the numerical solutions for uniform temperature are about 10 percent lower than those for uniform heat flux. The Nusselt number calculated by the Sugiyama et al's correlation agrees with the author's numerical solutions for uniform surface temperature within the application range of Eq. (1.11). However, as Eq. (1.11) is merely a linear approximation of the actually nonlinear

relationship on the graph, the Nusselt number obtained from Eq. (1.11) becomes about 15 percent lower than the present numerical solution for uniform surface temperature at $GrPr^2/(1+Pr) = 0.2$.

Takeuchi et al (1992) have discussed which cylinder surface boundary condition should be selected in predicting more properly the experimental data of the local Nusselt number. The experimental data of local Nusselt number at different circumferential positions on the 7.6 and 10.7 mm diameter single horizontal cylinders in liquid sodium—whose average Nusselt number is about 2 at $Gr \approx 5 \times 10^5$—are compared with the numerical solutions for uniform heat flux and for uniform temperature in Figs. 1.4 and 1.5 respectively. The local position is specified by the angle on the circumference, θ_d, measured from the lower stagnation point $(\theta_d = 0 \text{ deg})$ of the horizontal cylinder, and Nu_θ denotes the Nusselt number at the position corresponding to θ_d.

As shown in Fig. 1.4, the numerical results for uniform heat flux at Gr*Pr = 5000 agree with the experimental data within ± 10 percent errors. In contrast, the numerical solutions for uniform surface temperature at GrPr = 2510 shown in Fig. 1.5 tend to decrease with increasing θ_d, and become about 45 percent lower than the experimental data at $\theta_d = 180$ deg, though they are almost in agreement with each other in the range of θ_d from 0 to about 60 deg. The distribution of local heat transfer coefficient obtained numerically for the boundary condition of uniform surface heat flux has proved to be in better agreement with the experimental data than that for uniform surface temperature. This fact was also confirmed by a comparison of the experimental data whose average Nusselt number is about 2.33 at $Gr = 1.4 \times 10^6$ with the numerical solutions for uniform heat flux at Gr*Pr = 16300 and with those for uniform surface temperatures at GrPr = 7000. From the above results, it is concluded that the natural convection heat transfer on an electrically heated horizontal

cylinder is well predicted by the numerical solutions obtained with the surface boundary condition of uniform heat flux.

1.3.2 Derivation of General Correlation for Natural Convection Heat Transfer Based on the Numerical Results

Fujii et al (1976) derived a correlation for natural convection heat transfer on vertical flat plates with uniform heat flux, which describes the theoretical local Nusselt numbers for the Prandtl numbers ranging from near zero to near infinity with an accuracy of ± 1.7 percent. This correlation for vertical plates can be transformed to the following correlation for a horizontal cylinder by using Hermann's transformation (Hermann, 1936) :

$$Nu = 1.03\ R_f^{1/5} \quad , \tag{1.12}$$

where $R_f = Gr^*Pr^2/(4+9Pr^{1/2}+10Pr)$, and Gr* is a modified Grashof number for uniform heat flux (Gr* = Nu Gr). The coefficient of 1.03 in Eq. (1.12) was introduced as a result of the transformation. As shown in Table 1.2, the author has obtained the numerical solutions of natural convection heat transfer from single horizontal cylinders with constant surface heat flux for the Prandtl numbers ranging from 0.005 to 3000, and the modified Rayleigh numbers from 1.3×10^{-5} to 9.4×10^{11}. Figure 1.6 shows the numerical solutions of the average Nusselt number on the graph of $\log_{10}$ Nu versus $\log_{10} R_f$. The numerical solutions for the Prandtl numbers less than or equal to 10 are expressed by a single curve approaching asymptotically the curve of Eq. (1.12) in the region of high R_f where the boundary layer approximation appears to be appropriate. Based on this fact, the author derived a correlation capable of expressing the theoretical Nusselt number for the Prandtl numbers ranging from 0.005 to 10 within ± 4 percent errors by using least square fitting (Takeuchi et al, 1992):

$$\log_{10} \mathrm{Nu} = 0.193385 + (0.145037)\,A + (0.664323 \times 10^{-2})\,A^2 - (0.232432 \times 10^{-3})\,A^3 - (0.238613 \times 10^{-4})\,A^4 , \quad (1.13)$$

where $A = \log_{10} \mathrm{R}_f$.

As shown in Fig. 1.6, the numerical solutions of the average Nusselt number for the Prandtl numbers greater than 10 tend to become higher with the increase in the Prandtl number at a fixed value of R_f. This tendency is seen to be more remarkable as R_f decreases. To improve the applicability of Eq. (1.13) to wider range of the Prandtl numbers, the author has first assumed that the average Nusselt number for the Prandtl numbers converge in the curve expressed by Eq. (1.12) at large R_f, then Eq. (1.13) can be modified as

$$\log_{10} \mathrm{Nu} = 0.194 + (0.141)\,A + (0.6 \times 10^{-2})\,A^2 - (0.1 \times 10^{-3})\,A^3 - (0.9 \times 10^{-5})\,A^4 , \quad (1.14)$$

which describes the numerical solution for the Prandtl numbers ranging from 0.005 to 10 within $\pm$ 5 percent errors. Next, the dimensionless parameter, R_f, was modified to R_m by multiplying a correction factor, F, as

$$\mathrm{R}_m = F\,\mathrm{R}_f . \quad (1.15)$$

The values of F were determined so that all the theoretical Nusselt numbers coincide with the values obtained from an equation equivalent to Eq. (1.14) in which the dimensionless number, R_f, is replaced by R_m. On the hypothesis that essentially no correction to R_f is required for all the Prandtl numbers at high Grashof numbers where the boundary layer approximation is valid, then we have

$$F = 1 . \quad (1.16)$$

In the region of relatively low R_f where the values of F do not satisfy Eq. (1.16), the correction factors are expressed by another dimensionless quantity, H, which is a function of

the Prandtl and the modified Grashof numbers:

$$\log_{10} H = \log_{10} \frac{\mathrm{Pr}^{0.2}}{\mathrm{Gr}^{*0.1}} + 0.4 - 0.5\left\{1+\left(\frac{2\log_{10}\mathrm{Pr}-1}{5}\right)^{10}\right\}^{0.1} . \qquad (1.17)$$

Finally, Equations (1.16) and (1.17) are combined to yield the following equation for the correction factor, F, as

$$F = \left(1+H^{2.5}\right)^{1/2.5} . \qquad (1.18)$$

Consequently, an extended correlation for natural convection heat transfer from single horizontal cylinders takes the final form as

$$\log_{10} \mathrm{Nu} = 0.194 + 0.141B + \left(0.6\times10^{-2}\right)B^2 - \left(0.1\times10^{-3}\right)B^3 - \left(0.9\times10^{-5}\right)B^4 , \qquad (1.19)$$

where $B = \log_{10} \mathrm{R}_m$.

The numerical solutions of the average Nusselt number, obtained for the Prandtl numbers ranging from 0.005 to 3000 and for the modified Rayleigh numbers ranging from 1.3×10^{-5} to 9.4×10^{11}, are plotted on the graph of $\log_{10}$ Nu vs. $\log_{10}$ R_m in Fig. 1.7 in comparison with the curve by Eq. (1.19). As shown in the figure, the extended correlation generally describes the numerical solutions of the average Nusselt numbers for the dimensionless number of R_m ranging from 1.09×10^{-7} to 2.15×10^{9} within ± 5 percent errors.

1.3.3 Experimental Results for Various Liquids

In this section, the natural convection heat transfer coefficients on single horizontal cylinders obtained experimentally for various liquids will be compared with those predicted by the general correlation derived in the previous section. The experimental data for various

liquids such as sodium, water, ethanol, glycerin, nitrogen, and helium have been obtained for long years by some the members of the research section of nuclear reactor engineering of the Institute of Atomic Energy, Kyoto University. The experiments for water, nitrogen, and ethanol have been carried out mainly by Hata, Shiotsu, and Sakurai. The details of the apparatus as well as of the data acquisition and processing methods employed in the experiments have been described by Sakurai et al (1990), Shiotsu et al (1989) and by Hata et al (1991). The outline of their works are summarized in Appendix A. The experimental conditions such as test heater diameter, system pressure, bulk liquid temperature for each liquid are listed in Table 1.3. Figure 1.8 demonstrates some of the experimental results obtained under the conditions shown in Table 1.3 as the relationship between surface heat flux and surface superheat from bulk liquid temperature.

1.3.3.1 Reference temperature accounting for property variation

For correlating experimental results, the effect of temperature dependence of fluid properties on heat transfer has been discussed by many researchers: the physical properties have been evaluated at the mean film temperature, $T_f = T_W - 0.5(T_W - T_\infty)$, in many literature on natural convection heat transfer from bodies with various shapes. Sparrow and Gregg (1958) recommended, for natural convection heat transfer from isothermal vertical plates, that fluid properties be evaluated at the reference temperature defined as $T_f = T_W - 0.38(T_W - T_\infty)$. For natural convection heat transfer from a horizontal cylinder, Fand et al (1977), who conducted the experiments with horizontal cylinders in air, water, and three kinds of silicone oils at room temperatures, have reported that their experimentally obtained Nusselt number were best fitted to their correlation with the fluid properties evaluated at the reference temperature defined as

$$T_f = T_\infty + 0.32\left(T_W - T_\infty\right), \tag{1.20}$$

which can be rewritten as

$$T_f = T_w - m\left(T_W - T_\infty\right) \quad ; \quad m = 0.68 . \tag{1.21}$$

For low Prandtl number fluids such as liquid metals as well as for any fluids at low cylinder surface superheats, heat transfer is generally little influenced by the choice of the reference temperature, however, the statistical analysis of the author's experimental results exhibited that the data were best arranged into a smooth continuous curve on the graph of $\log_{10}$ Nu vs. $\log_{10} R_m$ provided the coefficient m in Eq. (1.21) takes the value of 0.7, which is almost the same value as that suggested by Fand et al as mentioned above. Consequently, the experimental data of natural convection heat transfer from single horizontal cylinders with a variety of diameters in various liquids exist within minimum errors from the general correlation curve given by Eq. (1.19) when the dimensionless numbers such as Pr and Gr* involved in the correlation are evaluated at the reference temperature;

$$T_f = T_W - 0.7\left(T_W - T_\infty\right) \quad . \tag{1.22}$$

The curves of Eq. (1.19) shown in Fig. 1.8 are also obtained by using the fluid properties evaluated at the reference temperature calculated from Eq. (1.22).

1.3.3.2 Comparison of Experimental Results with General Correlation

In this section, the general correlation based on the numerical analysis is compared, on the graph of $\log_{10}$ Nu versus $\log_{10} R_m$, with a large number of experimental data obtained for various fluids. The average Nusselt numbers as well as the values of R_m obtained from the author's experimental results were calculated by using the fluid properties evaluated by

Eq. (1.22). On the contrary, most of the experimental results obtained by other workers were directly converted onto the graph since the fluid properties cannot be estimated due to the lack of information on the cylinder surface and fluid temperatures.

Figure 1.9 shows the author's and other workers' (Kovalev and Zhukov, 1973; Fedynskii, 1958) experimental results obtained for various liquid metals—sodium, mercury, and tin—with extremely low Prandtl numbers (0.005 to 0.02). The author's experimental data obtained for liquid sodium with the single horizontal cylinders of 7.6 and 10.7 mm in diameters agree well with the curve calculated from Eq. (1.19) with an error not exceeding ± 10 percent over the experimental range. Kovalev's data, existing in far narrower range of R_m than the author's data, are scattered and at most 20 percent higher than the correlation curve. Fedynskii's data for sodium and tin are about 10 percent lower than the author's data but the tendency of dependence on R_m is similar. However, the data for mercury depart upward from the curve with increasing R_m in the range of $\log_{10} R_m > 6.5$ where the convective flow possibly changes from laminar to turbulent. Further investigation is required to verify whether this disagreement essentially arises from the occurrence of flow transition.

In Figs. 1.10 and 1.11, other workers' data with horizontal cylinders in air (Langmuir, 1912; Koch, 1927; Rice, 1929; Arajs and Legvold, 1958; Gebhart and Pera, 1970; Parsons, Jr. and Mulligan, 1978; Fujii et al, 1982) and the data for various gases (Petavel, 1901; Arajs and Legvold, 1958; Hesse and Sparrow, 1974) with the Prandtl number of around 0.7 are shown respectively for comparison: the data for air and the gases agree well with the average Nusselt numbers calculated from Eq. (1.19) within ± 12 percent errors.

Recently, data of natural convection heat transfer from a horizontal cylinder in cryogenic fluids such as liquid helium and liquid nitrogen have been obtained experimentally

by the research group including the author, and they are plotted in Figs. 1.12 and 1.13 respectively. Although the dependence of the liquid nitrogen data, with the cylinder of 1.2 mm in diameter, on R_m is observed to be slightly different from that of the correlation curve by Eq. (1.19), the average Nusselt number data for both cryogenic liquids agree with the correlation within ± 10 percent errors.

Figures 1.14 and 1.15 show the experimental data for water and ethanol respectively as examples of ordinary liquids with the Prandtl numbers ranging from about 2 to 10. From the water data obtained with the single horizontal cylinders of 0.5, 1.2, and 2 mm in diameters, it is seen that the data with the 0.5 mm diameter cylinder are distributed within -10 to +15 percent difference from Eq. (1.19), and those with the cylinders of 1.2 and 2 mm in diameters agree with Eq. (1.19) within ± 10 percent errors. Good agreement between the correlation and the experimental results is also observed for ethanol as shown in Fig. 1.15.

Figure 1.16 shows the author's and other workers' (Davis, 1922; Gebhart and Pera, 1970; Fand et al, 1977) data for high Prandtl number liquids such as glycerin and silicone oils. Generally, the fluid properties of high Prandtl number liquids vary markedly with temperature. Consequently, at a fixed bulk liquid temperature of about 15 degC, the Prandtl number for the author's glycerin data obtained with a cylinder of 1.2 mm in diameter ranged from 18000 at the cylinder surface temperature of T_W = 19 degC down to 200 at T_W = 256 degC; nevertheless, the author's glycerin data agree with the correlation with an error of not over ± 10 percent over the Prandtl number range. In correlating the data of three kinds of silicone oils reported by Fand et al (1977), the values of Nu and R_m were calculated by using fluid properties evaluated at the reference temperatures defined as Eq. (1.22) since the experimental conditions such as cylinder diameter (11.57 mm), cylinder surface temperature, fluid temperature, and heat flux are explicitly described in their paper: the Prandtl number

for their data ranges from about 3000 down to 100. It is seen from the figure that the Nusselt number data for 350 cS oil are about 20 percent lower than the value calculated by Eq. (1.19) at $\log_{10} R_m = 2.4$ (Pr = 3070), though the data for these silicon oils tend to converge in the correlation curve as the Prandtl number decreases with increasing R_m. In low R_m region, the 0.65 cS and 5.8 cS oil data obtained by Gebhart and Pera are in good agreement with Eq. (1.19), however, all the data for the liquids of Pr = 69, 1400, and 7640 reported by Davis fall below the correlation curve by at most 30 percent at $\log_{10} R_m = 4.2$. In summary, since the numerical solutions of the average Nusselt number have been obtained only for the Prandtl numbers below 3000, an endorsement based on experiments with various test cylinder diameters will be required to make clear the application range of Eq. (1.19) for the Prandtl numbers greater than 3000.

1.3.4 Comparison of Conventional Correlations with General Correlation

The Nusselt numbers calculated from a couple of well-known conventional correlations are compared with those obtained from the general correlation, Eq. (1.19), on the graph of $\log_{10}$ Nu versus $\log_{10} R_m$ in Figs. 1.17, 1.18 and 1.19.

A correlation representing experimental data for air, water and oils for the Rayleigh numbers ranging from 10^3 to 10^9 was presented by McAdams (1954):

$$\mathrm{Nu} = 0.53\, \mathrm{Ra}_T^{1/4} . \tag{1.23}$$

Figure 1.17 shows the average Nusselt numbers for Pr = 0.005, 0.7, and 1000 calculated by Eq. (1.23) in comparison with Eq. (1.19). The range of R_m for each curve obtained from the McAdams's correlation corresponds to its application range, $10^3 < \mathrm{Ra}_T < 10^9$, for each Prandtl number. The curve for Pr = 0.7 agrees with Eq. (1.19) within -7 to +12 percent

errors, whereas the curve for Pr = 0.005 is 60 to 130 percent higher and that for Pr = 1000 is 7 to 24 percent lower than Eq. (1.19). Hence, the McAdams's correlation appears invalid to predict the average Nusselt numbers for fluids of extremely high or low Prandtl numbers.

Churchill and Chu (1975) have proposed a correlation for single horizontal cylinders by employing the method presented by Churchill and Usagi (1972) to combine an equation for high Rayleigh numbers with an empirical limiting value of Nu = 0.36 determined by the experimental results for silicon oil, spindle oil, toluene and air at low Rayleigh numbers obtained by Tsubouchi and Masuda (1967/68):

$$\mathrm{Nu}^{1/2} = 0.60 + 0.387\left[\frac{\mathrm{Ra}_T}{\left\{1+\left(0.559/\mathrm{Pr}\right)^{9/16}\right\}^{16/9}}\right]^{1/6} . \qquad (1.24)$$

Figure 1.18 shows the Nusselt numbers calculated from Eq. (1.24) for Pr = 0.005, 10, 1000, and 10000. All the curves by Eq. (1.24) for the Prandtl numbers tend to become lower than Eq. (1.19) within almost the entire range of R_m on the graph. At $\log_{10} R_m = 1$, the Nusselt numbers given by Eq. (1.24) for Pr = 0.005 and 10 agree with each other, however, they are about 20 percent lower than those obtained from Eq. (1.19). Furthermore, the Nusselt numbers calculated by Eq. (1.24) for Pr = 1000 and 10000 coincide with each other, indicating about 36 percent lower value than that by Eq. (1.19) at $\log_{10} R_m = 0$. It is concluded therefore that the correlation presented by Churchill and Chu does not agree with the general correlation or with the experimental results for the Prandtl numbers.

Raithby and Hollands (1985) proposed a correlation for natural convection heat transfer from single horizontal cylinders as

$$\mathrm{Nu} = \left[\left(\mathrm{Nu}_l\right)^{3.3} + \left(\mathrm{Nu}_t\right)^{3.3}\right]^{1/3.3} , \qquad (1.25)$$

where Nu_l and Nu_t are the average Nusselt numbers for fully laminar flow based on so-called

conduction-layer model and for fully turbulent flow respectively:

$$\mathrm{Nu}_l = \frac{2f}{\ln\left\{1+2f/\left(0.772C_l\mathrm{Ra}_T^{1/4}\right)\right\}}, \tag{1.26}$$

$$f = 1-\frac{0.13}{\left(0.772C_l\mathrm{Ra}_T^{1/4}\right)^{0.16}}, \tag{1.27}$$

$$\mathrm{Nu}_t = C_t\,\mathrm{Ra}_T^{1/3}. \tag{1.28}$$

The coefficients designated by C_l in Eqs. (1.26), (1.27) and C_t in Eq. (1.28), which were introduced to express the effect of the Prandtl number on heat transfer for laminar and turbulent flow respectively, were determined from other workers' experimental data obtained for a wide range of Prandtl numbers. The value of C_l is given by $C_l = 0.67/\left[1+\left(0.492/\mathrm{Pr}\right)^{9/16}\right]^{4/9}$, and the values of C_t become, for example, $C_t = 0.077$ for Pr = 0.01, $C_t = 0.103$ for Pr = 0.71, and $C_t = 0.088$ for Pr = 2000 respectively. Figure 1.19 shows the curves obtained from Eq. (1.25) for Pr = 0.01, 0.71 and 2000. The curve given by Eq. (1.25) for Pr = 0.71 agrees with the curve by Eq. (1.19) within ± 6 percent errors in the range $-7 < \log_{10}\mathrm{R}_m < 7$. The curve obtained from Eq. (1.25) for Pr = 0.01 agrees with that from Eq. (1.19) within the range $-7 < \log_{10} R_m < 3$. At $\log_{10}\mathrm{R}_m > 3$, however, it departs upward rapidly from the curve of Eq. (1.19) with increasing R_m, indicating about 50 percent higher value than Eq. (1.19) at $\log_{10}\mathrm{R}_m = 7$ where the contribution of Nu_t in Eq. (1.25) becomes more dominant than that of Nu_l. The values calculated from Eq. (1.25) for Pr = 2000 is from 10 to 20 percent lower than those from Eq. (1.19) over the range of R_m. It seems that the Raithby and Hollands's correlation describes the natural convection heat transfer coefficients with the same accuracy as the other researchers' experimental errors.

1.4 Conclusions

1) The natural convection heat transfer coefficients on single horizontal cylinders with uniform surface heat fluxes were obtained numerically from the basic equations by finite difference method for a wide range of Rayleigh numbers for Pr = 0.005, 0.7, 10, 100, 1000 and 3000. On the basis of the numerical results, a general correlation for laminar natural convection heat transfer from single horizontal cylinders was derived. The correlation describes the numerical solutions of the average Nusselt number for the dimensionless numbers of R_m ranging from 1.09×10^{-7} to 2.15×10^{9} within $\pm$ 5 percent errors.

2) The author's experimental results, for various liquids such as water, ethanol, glycerin, sodium, nitrogen, and helium obtained for a wide range of bulk liquid temperatures and system pressures with a variety of cylinder diameters, agree with the general correlation on the graph of $\log_{10}$ Nu vs. $\log_{10}$ R_m within $\pm$ 10 percent errors for the Prandtl numbers ranging from 0.005 to 18000, provided the liquid properties are evaluated at the reference temperature given by $T_f = T_W - 0.7(T_W - T_\infty)$. Other researchers' experimental data obtained for air, He, Ar, H_2, O_2, N_2, CO_2 gases, silicone oils and some liquid metals such as sodium, mercury and tin agree with the general correlation within $\pm$ 20 percent errors.

3) Some conventional correlations were compared with the general correlation: McAdams's correlation appears to be inappropriate for prediction of the average Nusselt numbers for fluids of extremely high or low Prandtl numbers even in a region where the boundary layer approximation is appropriate; the correlation presented by Churchill and Chu does not agree with the general correlation or with the experimental results for the Prandtl numbers tested in this work; Raithby and Hollands's correlation, based on other workers' experimental data, seems to predict natural convection heat transfer from a horizontal cylinder with the same accuracy as experimental errors.

Nomenclature

a	thermal diffusivity, m^2/s
C_l	function of the Prandtl number in Eqs. (1.26) and (1.27)
C_t	function of the Prandtl number in Eq. (1.28)
D	cylinder diameter, m
F	dimensionless quantity given by Eq. (1.18)
Gr	Grashof number
Gr*	modified Grashof number, $g\beta qD^4/(\lambda\ \nu^2)$
g	acceleration of gravity, m/s^2
H	dimensionless quantity given by Eq. (1.17)
Nu	average Nusselt number
Nu_l	average Nusselt number in fully laminar flow given by Eq. (1.26)
Nu_t	average Nusselt number in fully turbulent flow given by Eq. (1.28)
Pr	Prandtl number
q	heat flux, W/m^2
R	cylinder radius, m
R_f	$Gr^* Pr^2/(4+9Pr^{1/2}+10Pr)$
R_m	dimensionless number defined as Eq. (1.15)
Ra_T	Rayleigh number, $g\beta(T_W - T_\infty) D^3/(a\nu)$
Ra_q	modified Rayleigh number, $g\beta q D^4/(\lambda a \nu)$
r	dimensionless radial distance, r_d/R
r_d	radial distance, m
r_∞	dimensionless radial distance between the center of a cylinder and the outer boundary of calculation domain, $(r_d)_\infty/R$

T temperature, K

T_W surface temperature, K

T_∞ bulk liquid temperature, K

t time, sec

Greek Symbols

β volumetric expansion coefficient, K^{-1}

ζ dimensionless vorticity, $\zeta_d R^2/a$

ζ_d vorticity, sec^{-1}

φ dimensionless stream function, φ_d/a

φ_d stream function, m^2/s

Θ dimensionless temperature, $(T-T_\infty)/(qD/\lambda)$

θ dimensionless angle, θ_d/π

θ_d angle measured from the lower stagnation point of a horizontal cylinder, deg

λ thermal conductivity, W/(mK)

ν kinematic viscosity, m^2/s

τ dimensionless time, ta/R^2

References

Arajs, S., and Legvold, S., 1958, "Free-Convectional Heat Transfer from a Single Horizontal Wire," *J. Chem. Phys.*, Vol. 29, pp. 697-699.

Carslaw, H. S., and Jaeger, J. C., 1959, "*Conduction of Heat in Solids, 2nd ed.*," Oxford University Press, Oxford, p. 338.

Churchill, S. W., and Chu, H. H. S., 1975, "Correlating Equations for Laminar and Turbulent Free Convection from a Horizontal Cylinder," *Int. J. Heat Mass Transfer*, Vol. 18, pp. 1049-1053.

Churchill, S. W., and Usagi, R., 1972, "A General Expression for the Correlation of Rates of Transfer and Other Phenomena," *AIChE Journal*, Vol. 18, No. 6, pp. 1121-1128.

Davis, A. H., 1922, "Natural Convection Cooling in Fluids," *Philos. Mag.*, Vol. 44, pp. 920-940.

Fand, R.M., Morris, E.W., and Lum, M., 1977, "Natural Convection Heat Transfer from Horizontal Cylinders to Air, Water and Silicone Oils for Rayleigh Numbers between 3×10^2 and 2×10^7," *Int. J. Heat Mass Transfer*, Vol. 20, pp. 1173-1184.

Fedynskii, O. S., 1958, "*Heat Transfer and Thermal Modeling*(*in Russian*)," AN USSR, p. 107.

Fujii, T., and Fujii, M., 1976, "The Dependence of Local Nusselt Number on Prandtl Number in the Case of Free Convection along a Vertical Surface with Uniform Heat Flux," *Int. J. Heat Mass Transfer*, Vol. 19, pp. 121-122.

Fujii, T., Fujii, M., and Honda, T, 1982, "Theoretical and Experimental Studies of the Free Convection around a Long Horizontal Thin Wire in Air," *Proceedings, 7th International Heat Transfer Conference*, U. Grigull et al, ed., Hemisphere Publishing Corp., Washington, D.C., Vol. 2, pp. 311-316.

Gebhart, B., and Pera, L., 1970, "Mixed Convection from Long Horizontal Cylinders," *J. Fluid Mech.*, Vol. 45, pp. 49-64.

Hata, K., Takeuchi, Y., Shiotsu, M., and Sakurai, A., 1991, "A Generalized Correlation for Natural Convection Heat Transfer from a Horizontal Cylinder in Liquid Sodium," *Proceedings, International Conference on Fast Reactors and Related Fuel Cycles*, Vol. 1, pp. 10.9-1 - 10.9-10.

Hermann, R., 1936, "Wärmeübergang bei freier Strömung an Waagerechten Zylinder in zweiatomigen Gasen," *VDI Forschungsheft*, Vol. 7(379), pp. 1-24.

Hesse, G., and Sparrow, E.M., 1974, "Low Rayleigh Number Natural Convection Heat Transfer from High-Temperature Horizontal Wires to Gases," *Int. J. Heat Mass Transfer*, Vol. 17, pp. 796-798.

Koch, W., 1927, *Gesundh-Ing*, Vol. 22, pp. 1-27.

Kovalev, S. A., and Zhukov, V. M., 1973, "Experimental Study of Heat Transfer During Sodium Boiling Under Conditions of Low Pressures and Natural Convection," *Progress in Heat and Mass Transfer*, Pargamon Press, Oxford, Vol. 7, pp. 347-354.

Kuehn, T. H., 1976, "Natural Convection Heat Transfer from a Horizontal Circular Cylinder to a Surrounding Cylindrical Enclosure," Ph.D. Thesis, Univ. of Minnesota, MN.

Kutateladze, S. S. et al, 1958, "*Zhidkometallitsheskye Teplonositeli,*" Atomizdat, Moscow.

Langmuir, I., 1912, "Convection and Conduction of Heat in Gases," *Phys.Rev.*, Vol. 34, pp. 401-422.

McAdams, W. H., 1954, "*Heat Transmission, 3rd ed.*," McGraw-Hill, New York, p. 176.

Parsons, Jr., J. R., and Mulligan, J. C., 1978, "Transient Free Convection from a Suddenly Heated Horizontal Wire," ASME *Journal of Heat Transfer*, Vol. 100, pp. 423-428.

Petavel, J. E., 1901, "On the Heat Dissipated by a Platinum Surface at High Temperatures--- Part IV. Thermal Emissivity in High Pressure Gases," *Phil. Trans. Roy. Soc. London*, A197, pp. 229-254.

Raithby, G. D., and Hollands, K. G. T., 1985, "Natural Convection," *Handbook of Heat Transfer Fundamentals*, W. M. Rohsenow et al, ed., McGraw-Hill, New York, pp. 6-1 - 6-94.

Rice, C. W., 1929, "Free and Forced Convection of Heat from Bodies of Simple Shape in Gases and Liquids," *International Critical Tables*, McGraw-Hill, New York, Vol. 5, pp. 234-236.

Sakurai, A., Shiotsu, M., and Hata, K., 1990, "A General Correlation for Pool Film Boiling Heat Transfer from a Horizontal Cylinder to Subcooled Liquid: Part 2 ---Experimental Data for Various Liquids and Its Correlation," ASME *Journal of Heat Transfer*, Vol. 112, pp. 441-450.

Shiotsu, M., Hata, K., and Sakurai, A., 1989,"Effects of Diameter and System Pressure on Critical Heat Flux for Horizontal Cylinder in Saturated Liquid He I," Cryogenics, Vol. 29, pp. 593-596.

Sparrow, E. M., and Gregg, J. L., 1958, "The Variable Fluid Property Problem in Free Convection," ASME *Journal of Heat Transfer*, Vol. 80, pp. 879-886.

Sugiyama, K., Ma, Y., and Ishiguro, R., 1991, "Laminar Natural Convection Heat Transfer from a Horizontal Circular Cylinder to Liquid Metals," ASME *Journal of Heat Transfer*, Vol. 113, pp. 91-96.

Takeuchi, Y., Hata, K., Shiotsu, M., and Sakurai, A., 1992, "A General Correlation for Natural Convection Heat Transfer from Horizontal Cylinders in Liquids and Gases," *General Papers in Heat Transfer*, ASME Publication HTD-Vol. 204, pp. 183-189.

Tsubouchi, T., and Masuda, H., 1967/68, "Heat Transfer by Natural Convection from Horizontal Cylinders at Low Rayleigh Numbers," *Rep. Inst. High Sp. Mech.*, Japan, Vol. 19, pp. 205-219.

Table 1.1 Published numerical analyses for natural convection heat transfer from a horizontal cylinder.

Author	Surface Boundary Condition	Prandtl Number range	Grashof number range	Rayleigh number range	Ref. #
Kuehn et al	Isothermal	0.01	—	10^4	4
Kuehn et al	Isothermal	0.1	—	10^4	4
Kuehn et al	Isothermal	0.7	—	$10^0 \sim 10^7$	4
Kuehn et al	Isothermal	1.0	—	10^4	4
Kuehn et al	Isothermal	5.0	—	10^4	4
Kuehn et al	Isothermal	10.0	—	10^4	4
Wang et al	Uniform heat flux	0.7	—	$10^6 \sim 2.5 \times 10^8$	2
Wang et al	Isothermal	0.7	—	$10^5 \sim 2 \times 10^7$	2
Wang et al	Mixed	0.7	—	$2 \times 10^7, 2 \times 10^{8*}$	2
Fujii et al	Isothermal	0.7, 10, 100	$10^{-4} \sim 10^4$	—	1
Saitoh et al	Isothermal	0.7	—	10^3, 10^4, 10^5	5
Sugiyama et al	Isothermal	0.004~0.07	$2.5 \times 10^5 \sim 7 \times 10^6$	—	3
Sako et al	Isothermal	1.0	$1 \sim 10^4$	—	6

* $Ra = g\beta D^3 (T_w' - T_0') / \mu a$, T_w' : temperature of cylinder surface T_0' : temperature inside cylinder

1. Fujii, T., Fujii, M., and Matsunaga, T., A Numerical Analysis of Laminar Free Convection Around an Isothermal Horizontal Circular Cylinder, Numerical Heat Transfer, Vol. 2, pp.329-344, (1979).
2. Wang, P., Kahawita, R., and Nguyen, T. H., Numerical Computation of the Natural Convection Flow About a Horizontal Cylinder Using Splines, Numerical Heat Transfer, Part A, Vol. 17, pp.191-215, (1990).
3. Sugiyama, K., Ma. Y., and Ishiguro, R., Laminar Natural Convection Heat Transfer From a Horizontal Circular Cylinder to Liquid Metals, Journal of Heat Transfer, Vol. 113, pp.91-96, (1991).
4. Kuehn, T. H., and Goldstein, R. J., Numerical Solution to the Navier-Stokes Equations for Laminar Natural Convection About a Horizontal Isothermal Circular Cylinder, Int. J. Heat Mass Transfer, Vol. 23, pp. 971-979, (1980).
5. Saitoh, T., Sajiki, T., and Maruhara, K., Bench Mark Solutions to Natural Convection Heat Transfer Problem Around a Horizontal Circular Cylinder, Int. J. Heat Mass Transfer, Vol. 36, No. 5, pp.1251-1259, (1993).
6. Sako, M., Salinas Garza. J. M., Yanagida, A., and Chiba, Y., Numerical Calculation on Unsteady Free Convection From a Horizontal Cylinder, in Japanese, JSME Series B, Vol. 48, No. 434, pp. 2005-2012, (1982).

Table 1.2 Parameters for numerical analysis.

Pr	Ra_q	r_∞	Pr	Ra_q	r_∞
0.005	9.37×10^{11}	100	10	4.19×10^{6}	30
	2.01×10^{9}	5		1.32×10^{1}	127
	2.96×10^{8}	10		4.19×10^{-2}	15000
	2.01×10^{7}	20		3.16×10^{-4}	25000
	2.01×10^{6}	30		1.32×10^{-5}	15000
	7.00×10^{4}	127	100	1.09×10^{5}	500
	5.00×10^{3}	127		3.46×10^{3}	1000
	2.51×10^{2}	127		3.46×10^{2}	1000
	5.10×10^{1}	843		1.09×10^{0}	10000
	1.00×10^{0}	3000		3.16×10^{-3}	20000
	1.00×10^{-2}	3000	1000	1.80×10^{10}	2000
	1.00×10^{-4}	16500		1.03×10^{6}	5000
0.7	5.68×10^{7}	4		3.25×10^{4}	4000
	8.37×10^{6}	6		1.03×10^{3}	1000
	2.65×10^{4}	20		1.78×10^{1}	10000
	4.71×10^{2}	50		3.25×10^{-1}	10000
	2.65×10^{-1}	3000	3000	7.37×10^{2}	5000
	2.65×10^{-3}	3000			

Table 1.3 Experimental conditions.

Liquid	Heater Diameter (mm)	System Pressure (kPa)	Bulk-Liquid Temperature (deg C)
Sodium	7.6～10.7	101.3	400～406
Water	0.5～2.0	3.3～101.3	18～80
Ethanol	1.2	52～200	62～79
Glycerin	1.2	101.3	15.3
Nitrogen	0.2～1.2	101.3～1016	-196 ～-194
Helium	0.2	5.3～101.3	-271 ～-269

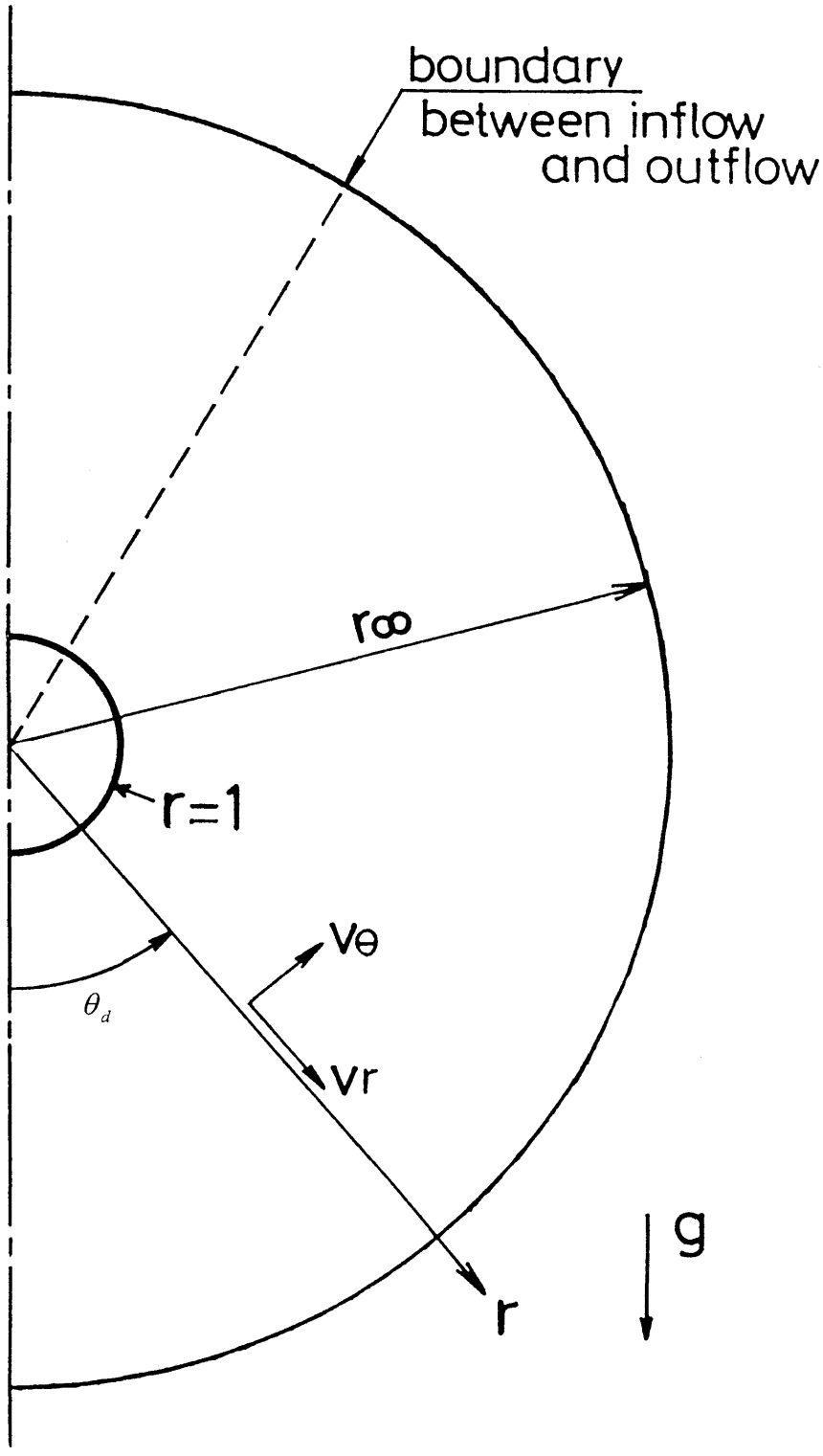

Fig. 1.1 Physical model and coordinates for numerical analysis.

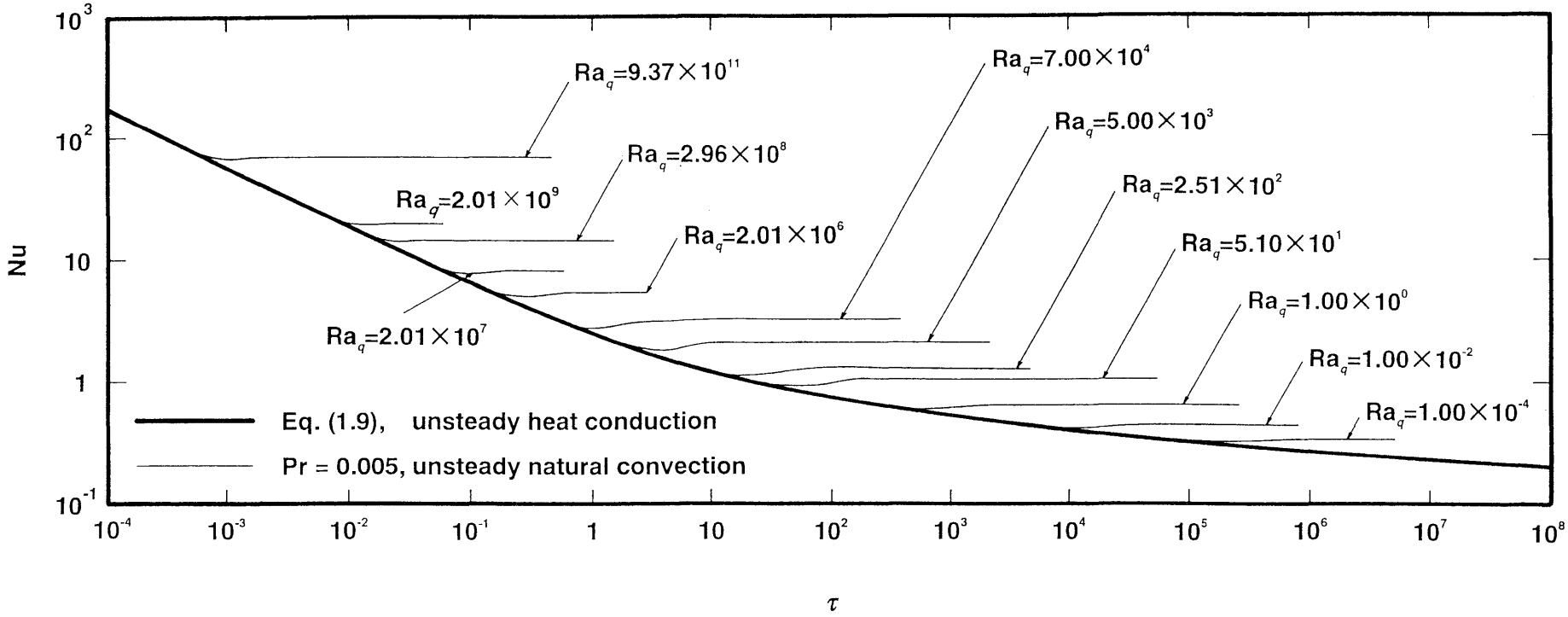

Fig. 1.2(a) Transient behavior of the average Nusselt numbers for Pr=0.005 compared with the exact solution of unsteady heat conduction equation for constant heat flux.

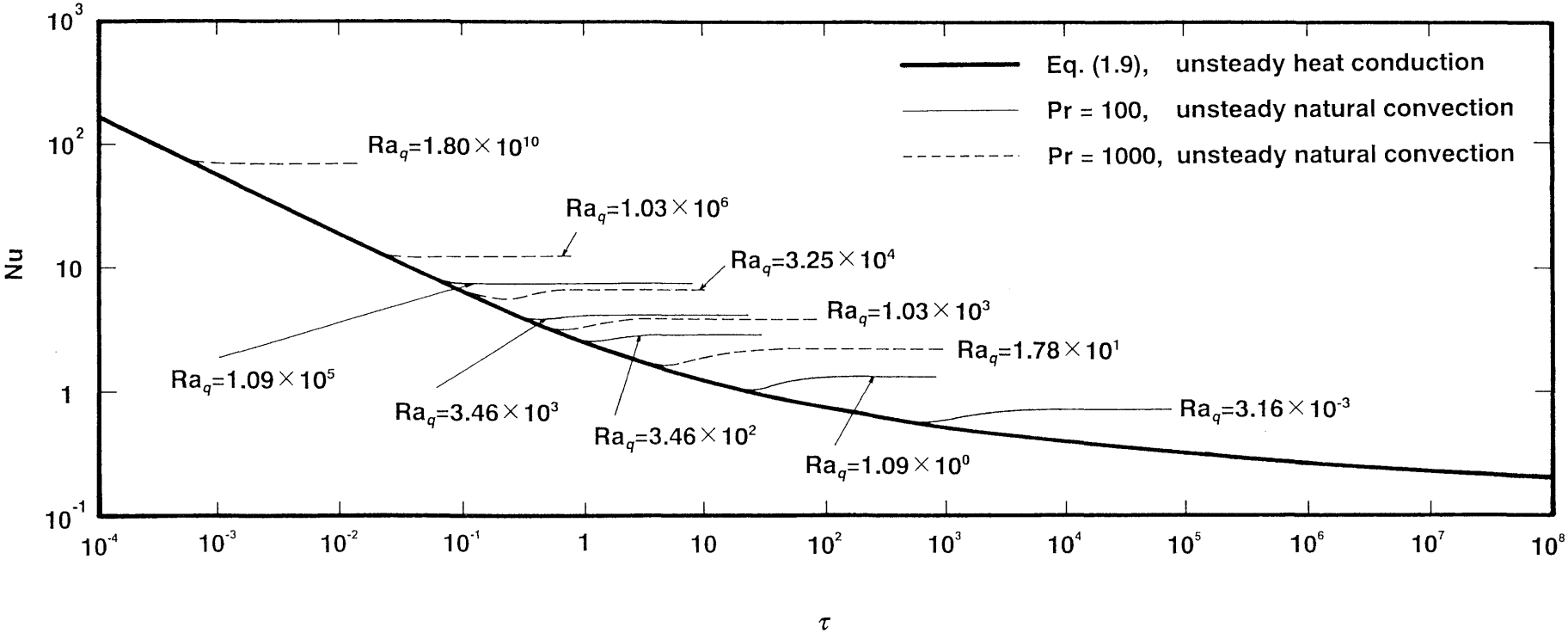

Fig. 1.2(b) Transient behavior of the average Nusselt numbers for Pr=100 and 1000 compared with the exact solution of unsteady heat conduction equation for constant heat flux.

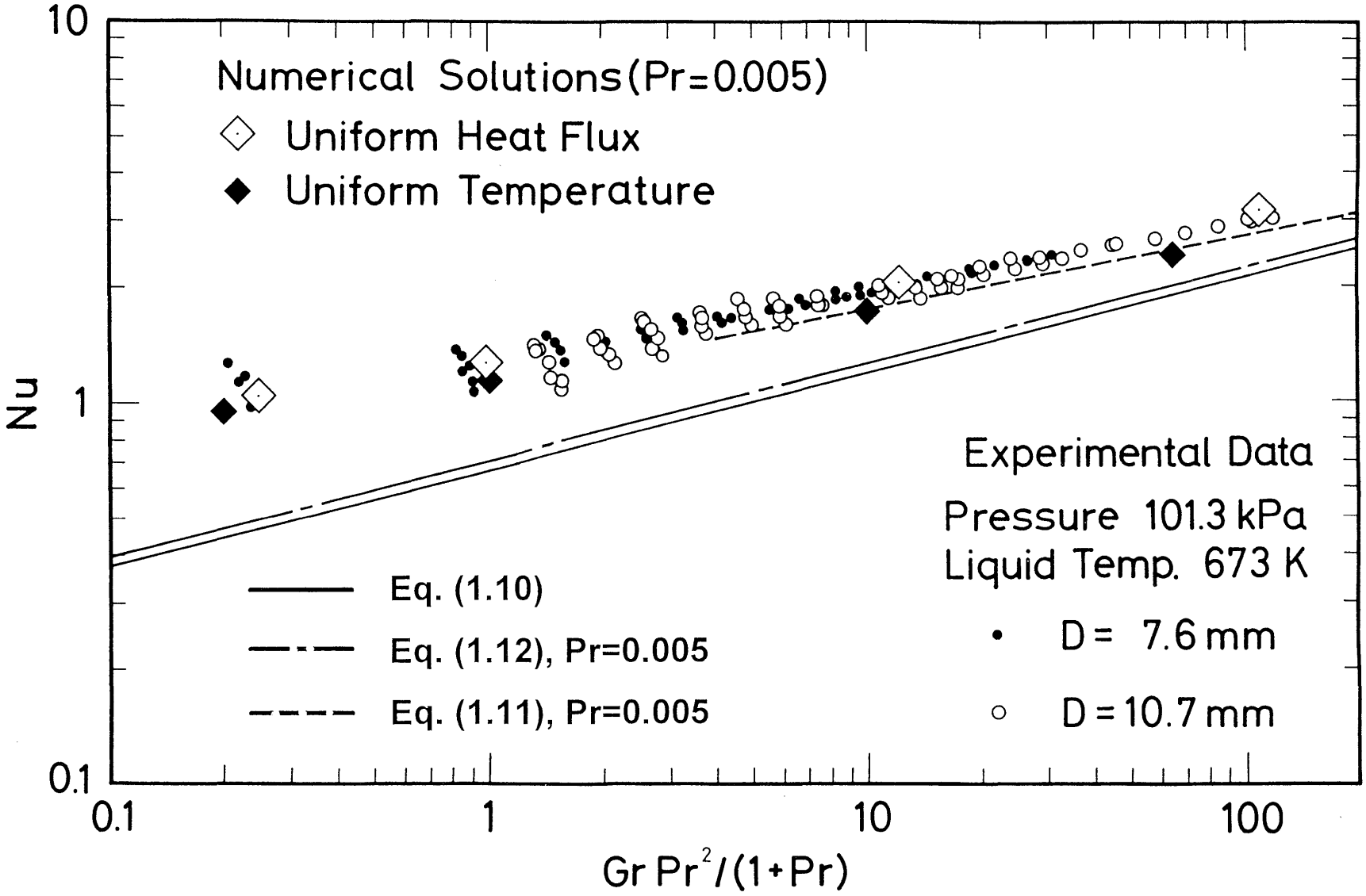

Fig. 1.3 Average Nusselt numbers experimentally obtained with single horizontal cylinders of 7.6 and 10.7 mm in diameter compared with numerical solutions and with conventional correlations.

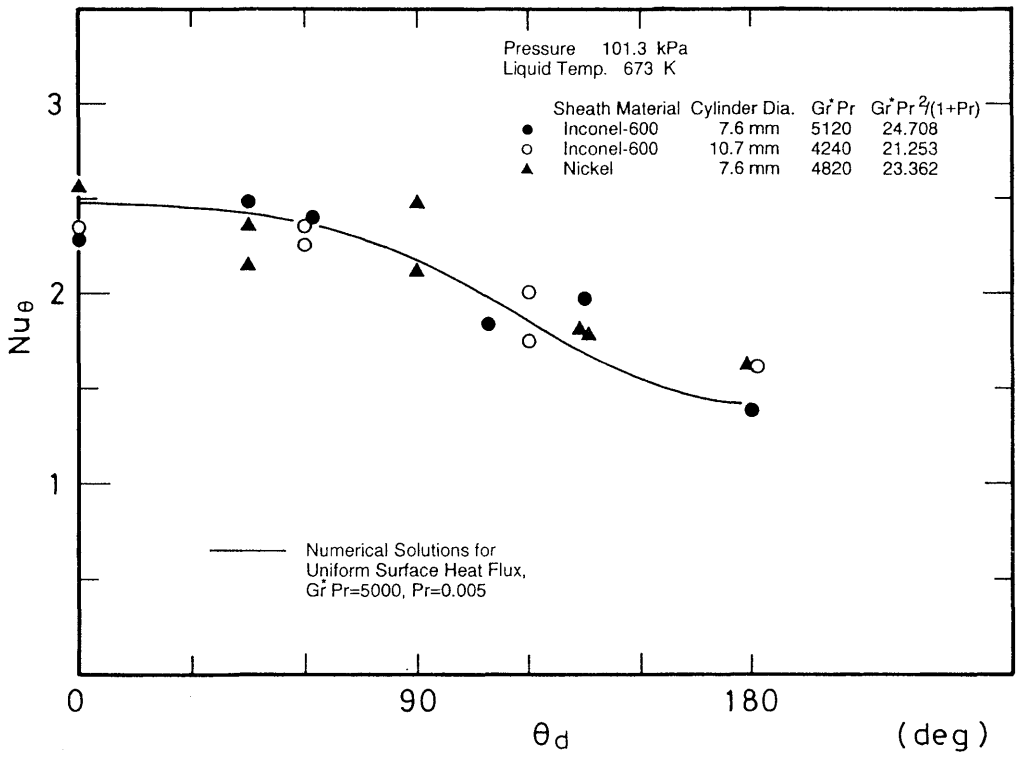

Fig. 1.4 **Comparison of experimental results for local Nusselt number on peripheral surface of a horizontal cylinder for Gr*Pr around 5000 with numerical solutions for constant surface heat flux.**

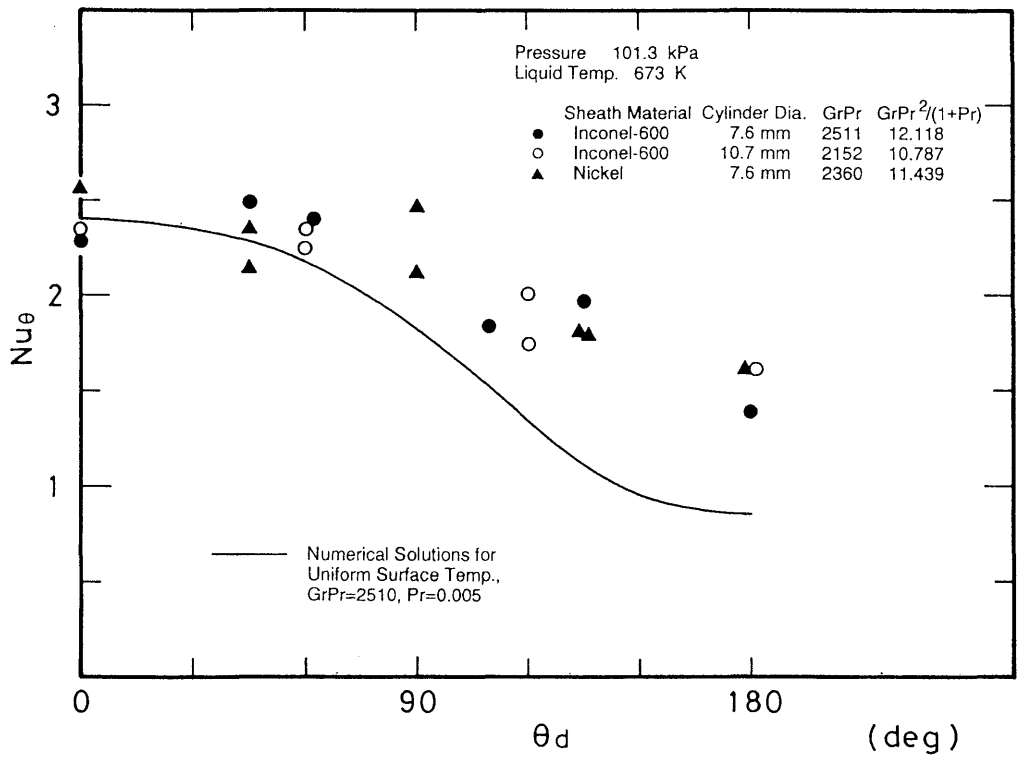

Fig. 1.5 **Comparison of experimental results for local Nusselt number identical to those shown in Fig. 1.4 with numerical solutions for constant surface temperature.**

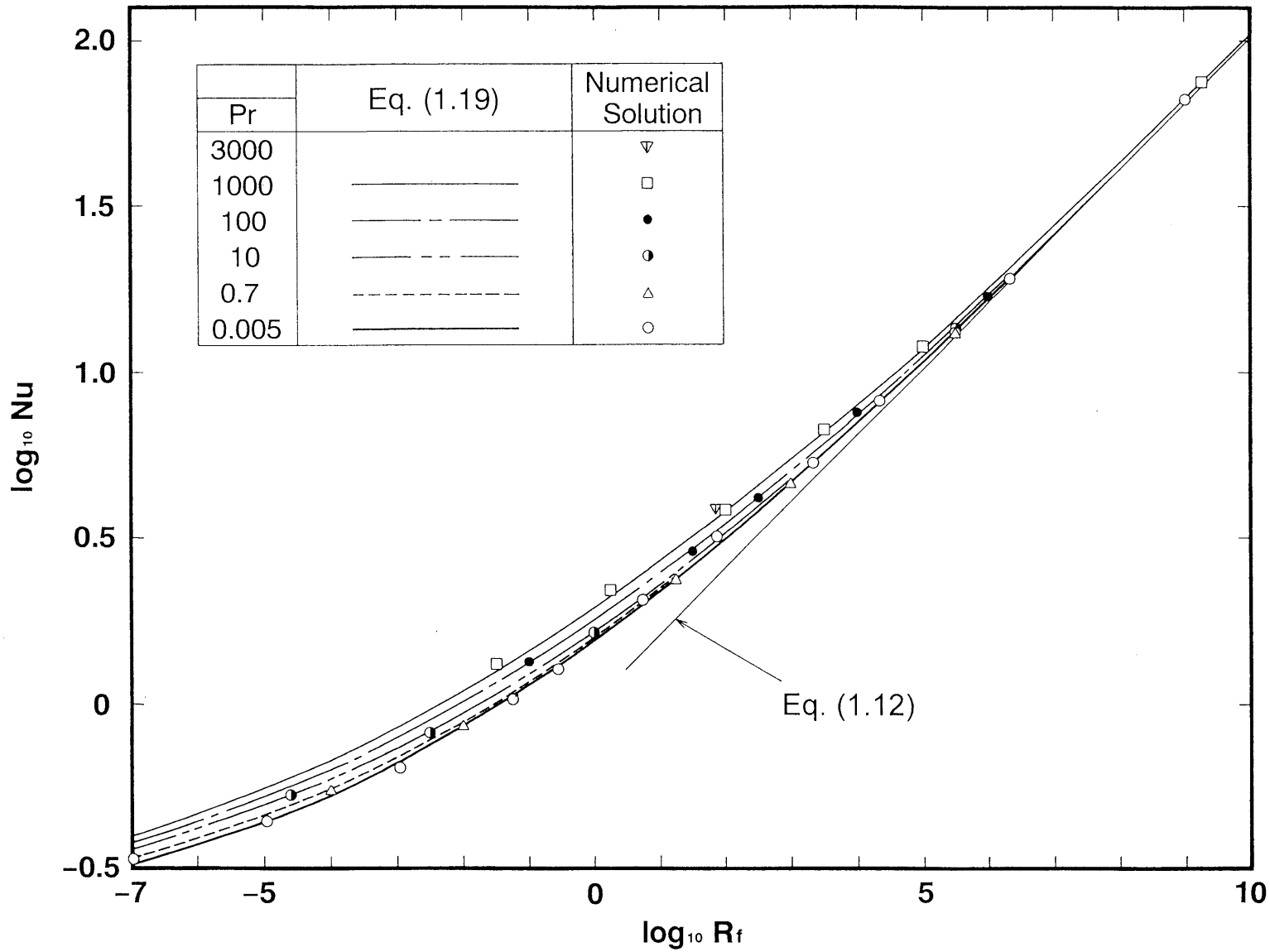

Fig. 1.6 **Numerical solutions of the average Nusselt number for the Prandtl numbers ranging from 0.005 to 3000 plotted on the graph of Nu vs. R_f.**

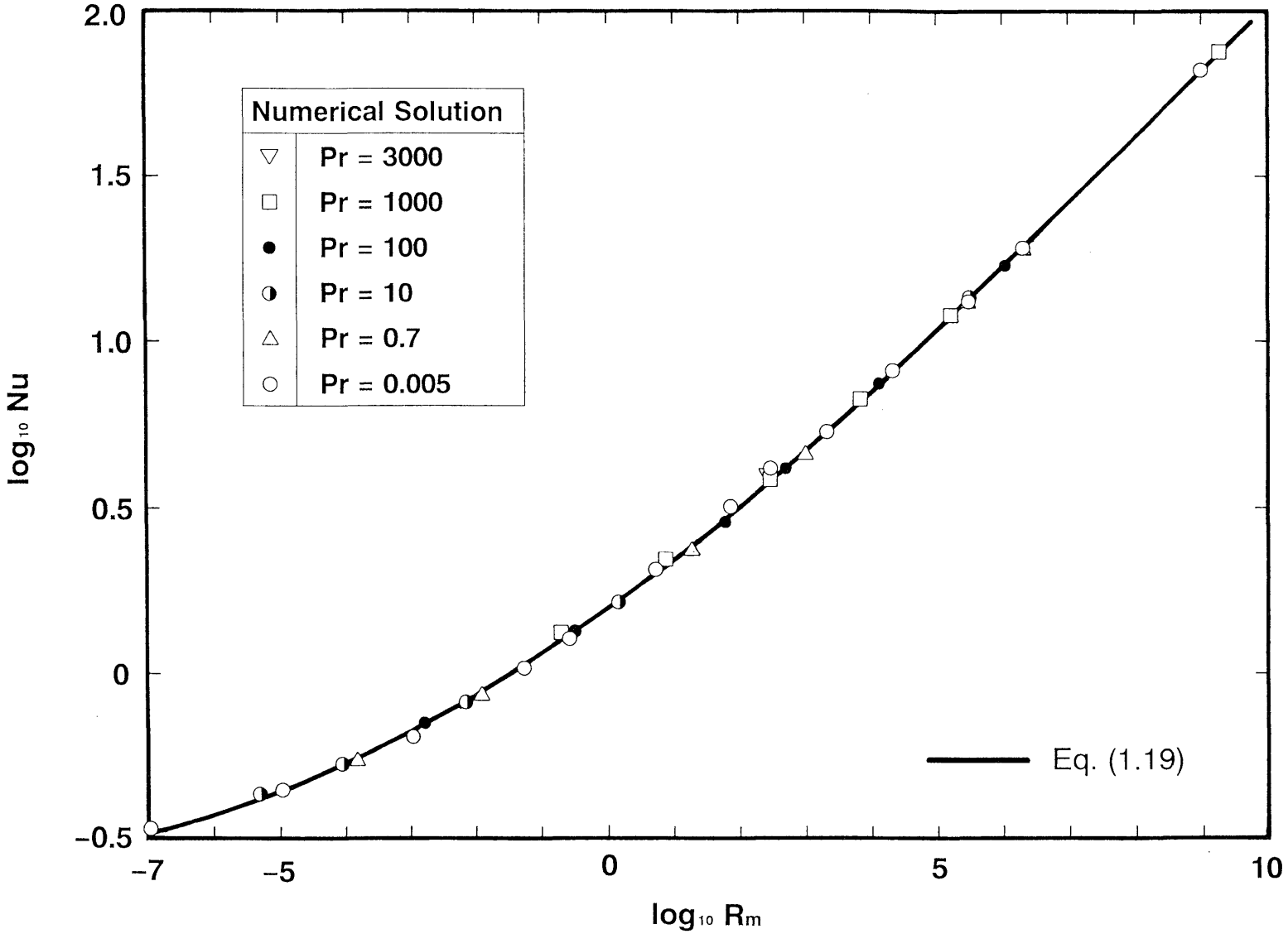

Fig. 1.7 Numerical solutions of the average Nusselt number for the Prandtl numbers ranging from 0.005 to 3000 compared with general correlation on the graph of Nu vs. R_m.

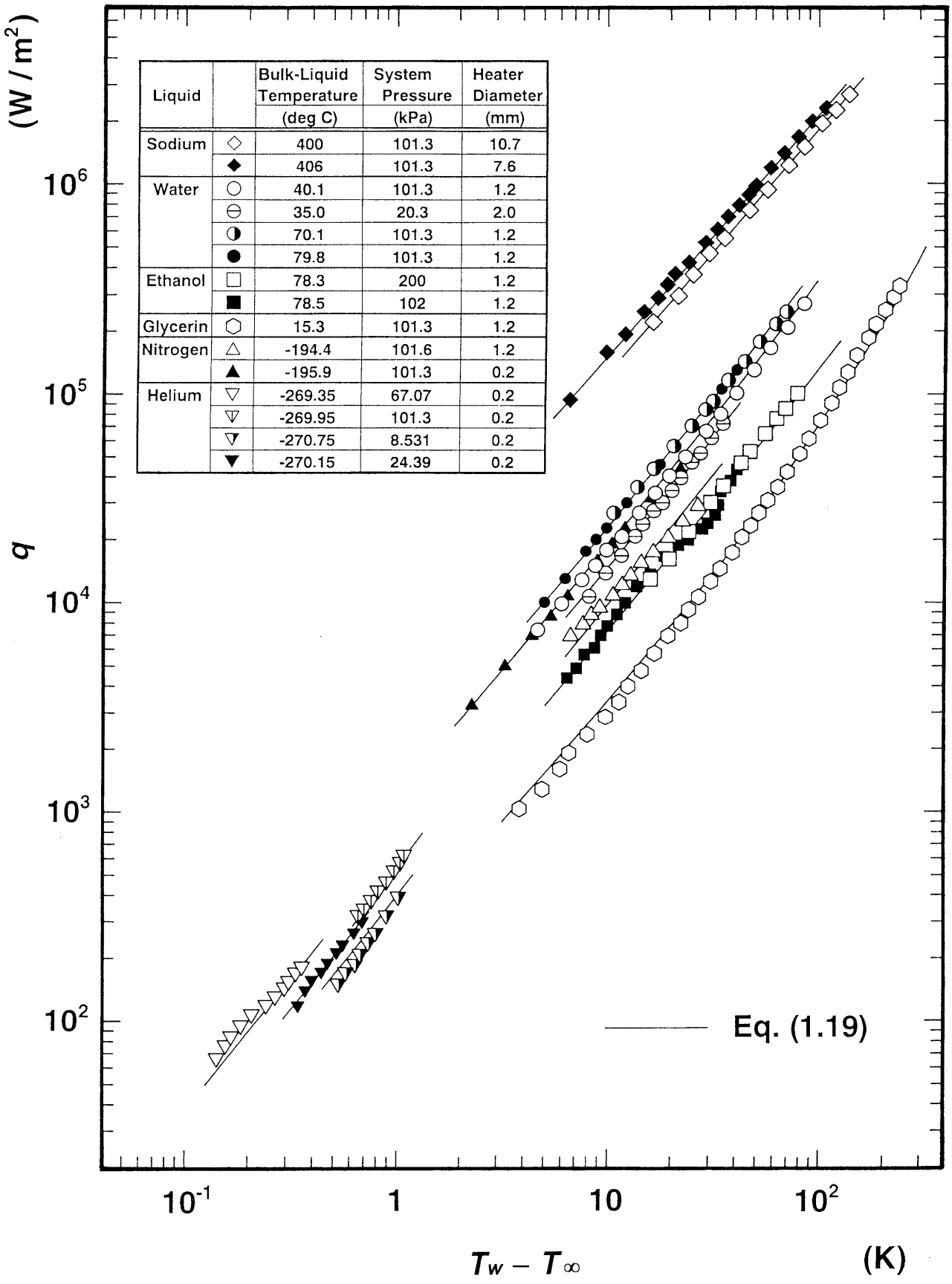

Liquid		Bulk-Liquid Temperature (deg C)	System Pressure (kPa)	Heater Diameter (mm)
Sodium	◇	400	101.3	10.7
	◆	406	101.3	7.6
Water	○	40.1	101.3	1.2
	⊖	35.0	20.3	2.0
	◑	70.1	101.3	1.2
	●	79.8	101.3	1.2
Ethanol	□	78.3	200	1.2
	■	78.5	102	1.2
Glycerin	⬡	15.3	101.3	1.2
Nitrogen	△	-194.4	101.6	1.2
	▲	-195.9	101.3	0.2
Helium	▽	-269.35	67.07	0.2
	▽	-269.95	101.3	0.2
	▽	-270.75	8.531	0.2
	▼	-270.15	24.39	0.2

Fig. 1.8 **Experimental results of natural convection heat transfer for various liquids compared with the values calculated from general correlation.**

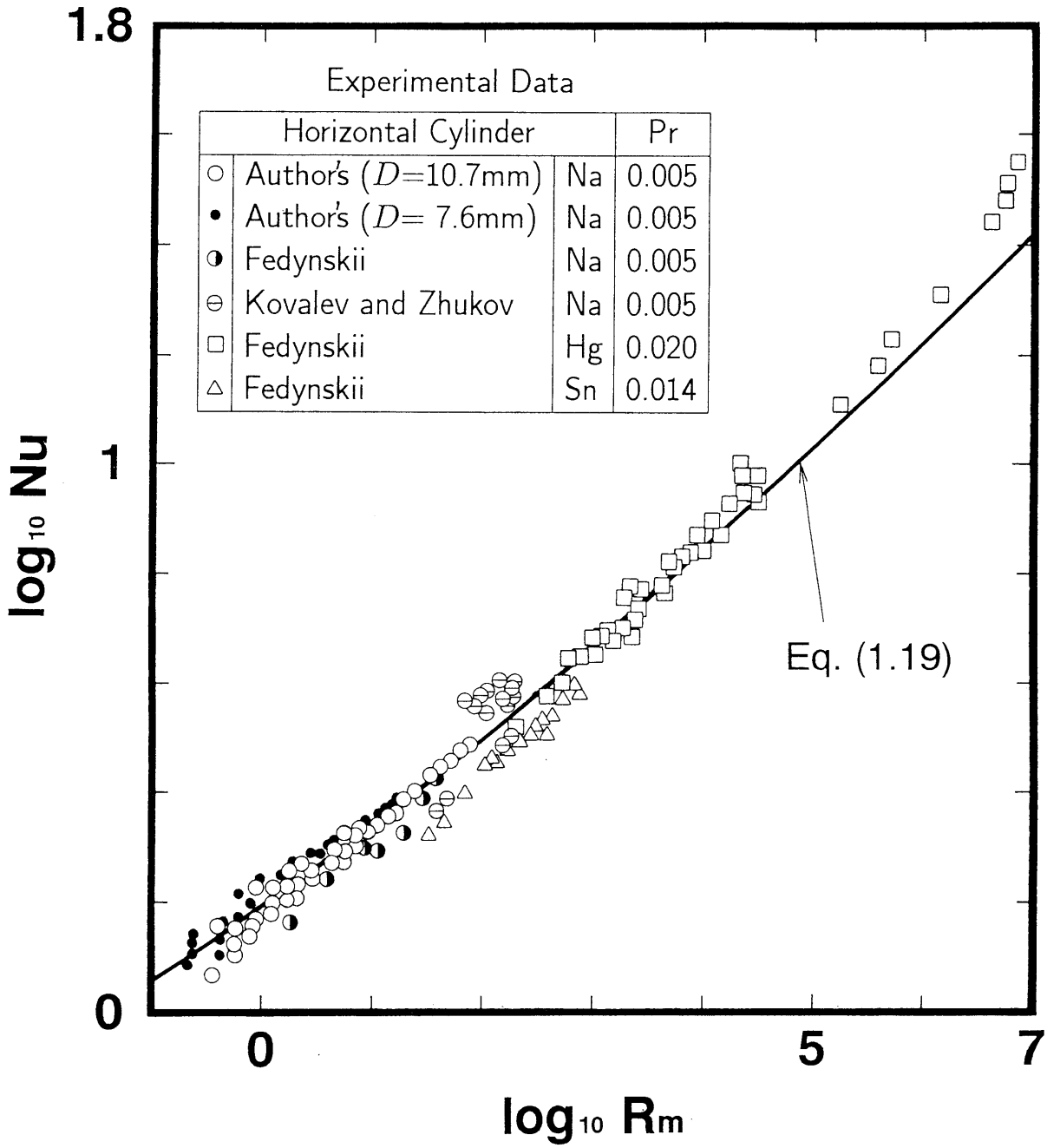

Fig. 1.9 **Comparison of experimental results for various liquid metals (Pr=0.005～0.020) with the general correlation.**

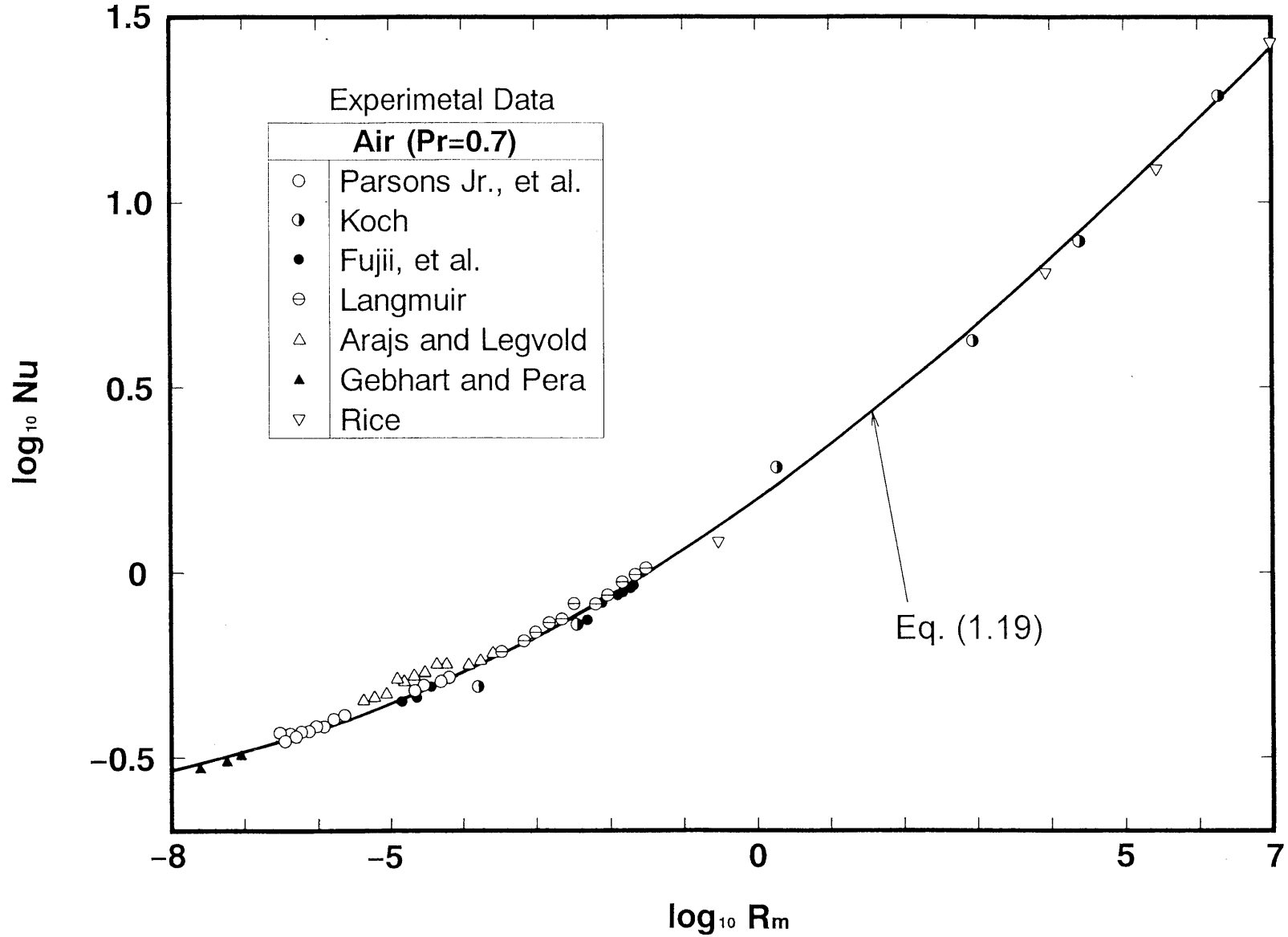

Fig. 1.10 Comparison of other researchers' experimental results for air (Pr=0.7) with the general correlation.

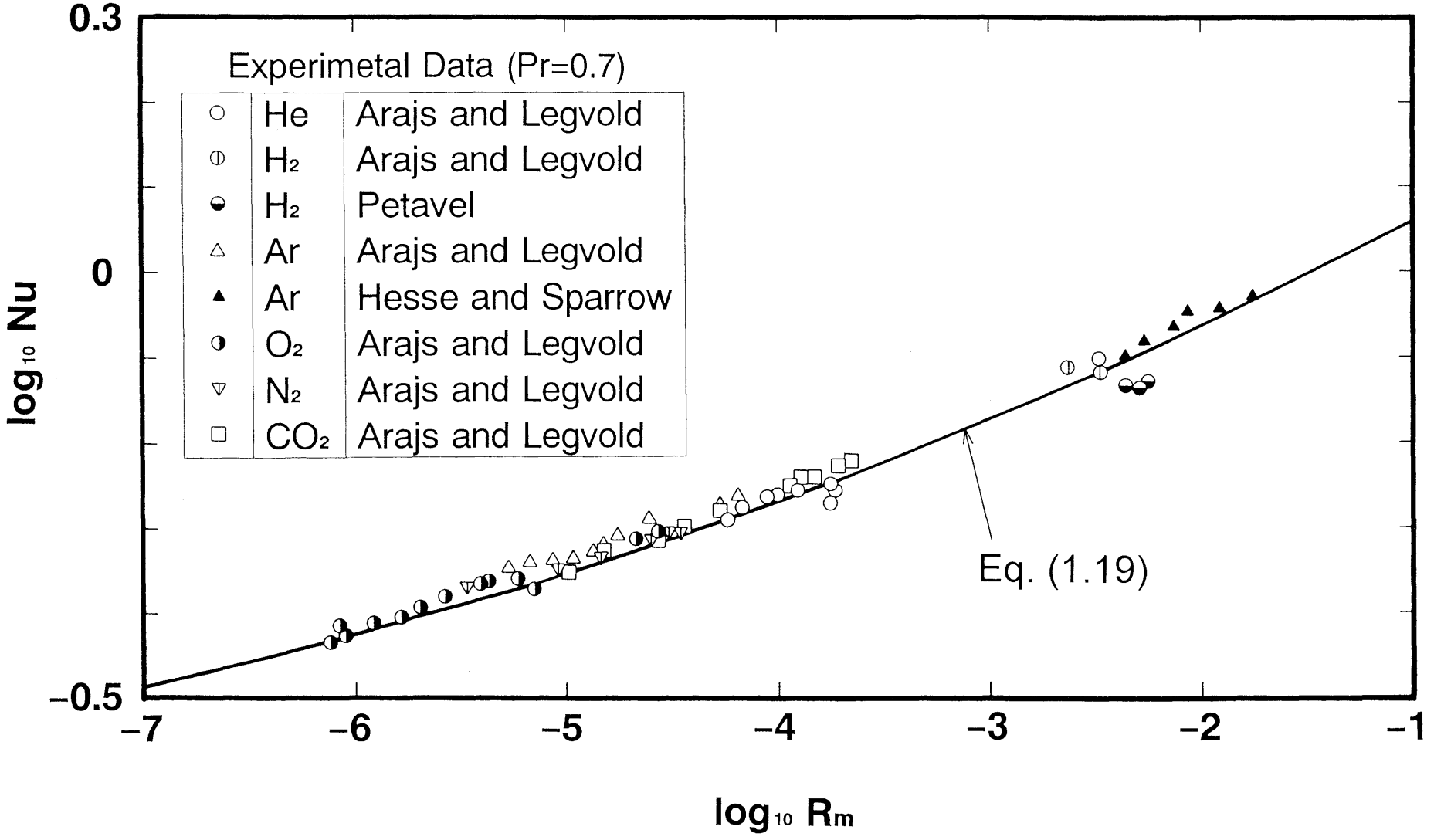

Fig. 1.11 **Comparison of other researchers' experimental results for various gases (Pr=0.7) with the general correlation.**

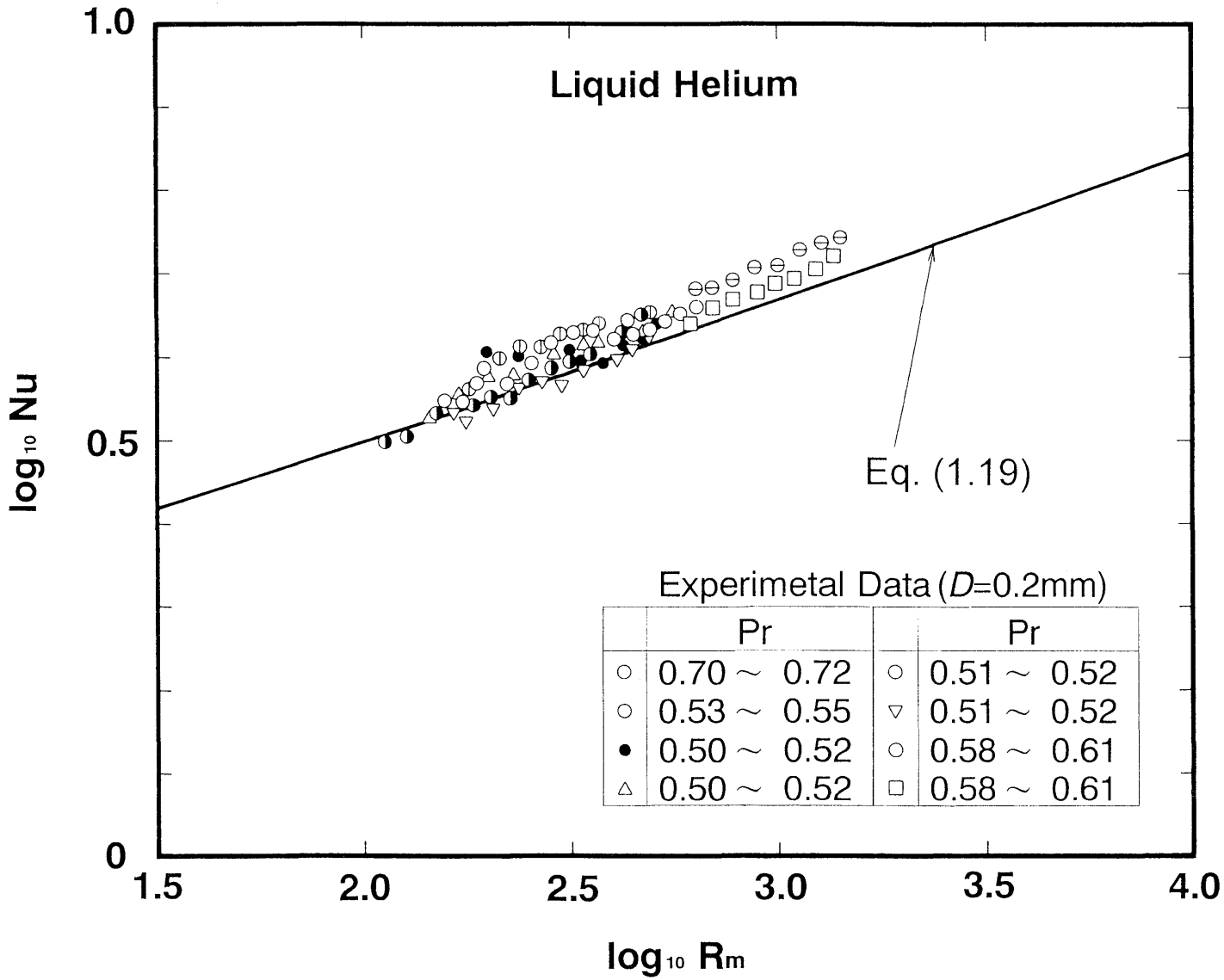

Fig. 1.12 **Comparison of experimental results for liquid helium (Pr=0.50～0.72) with the general correlation.**

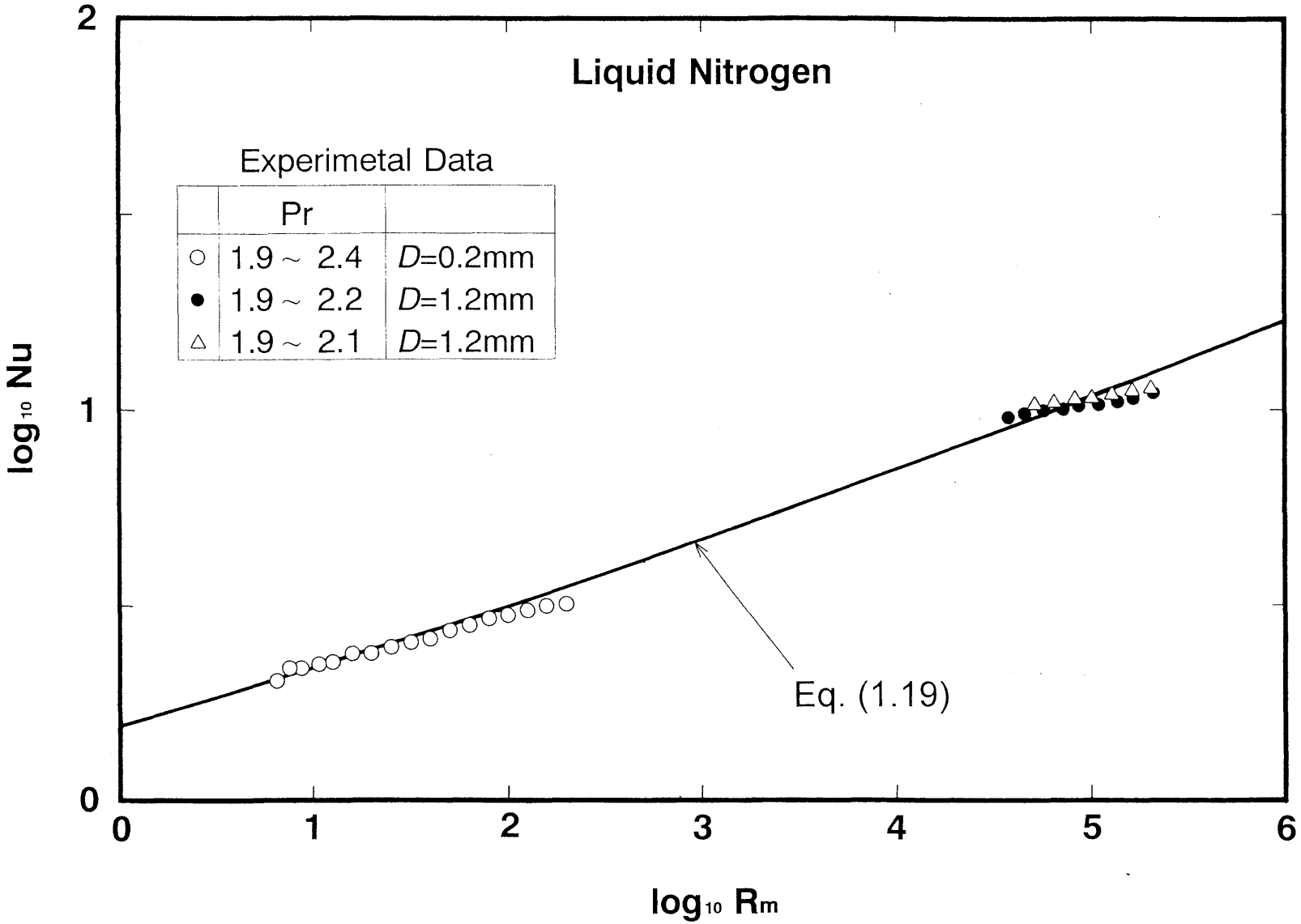

Fig. 1.13 Comparison of experimental results for liquid nitrogen (Pr=1.9～2.4) with the general correlation.

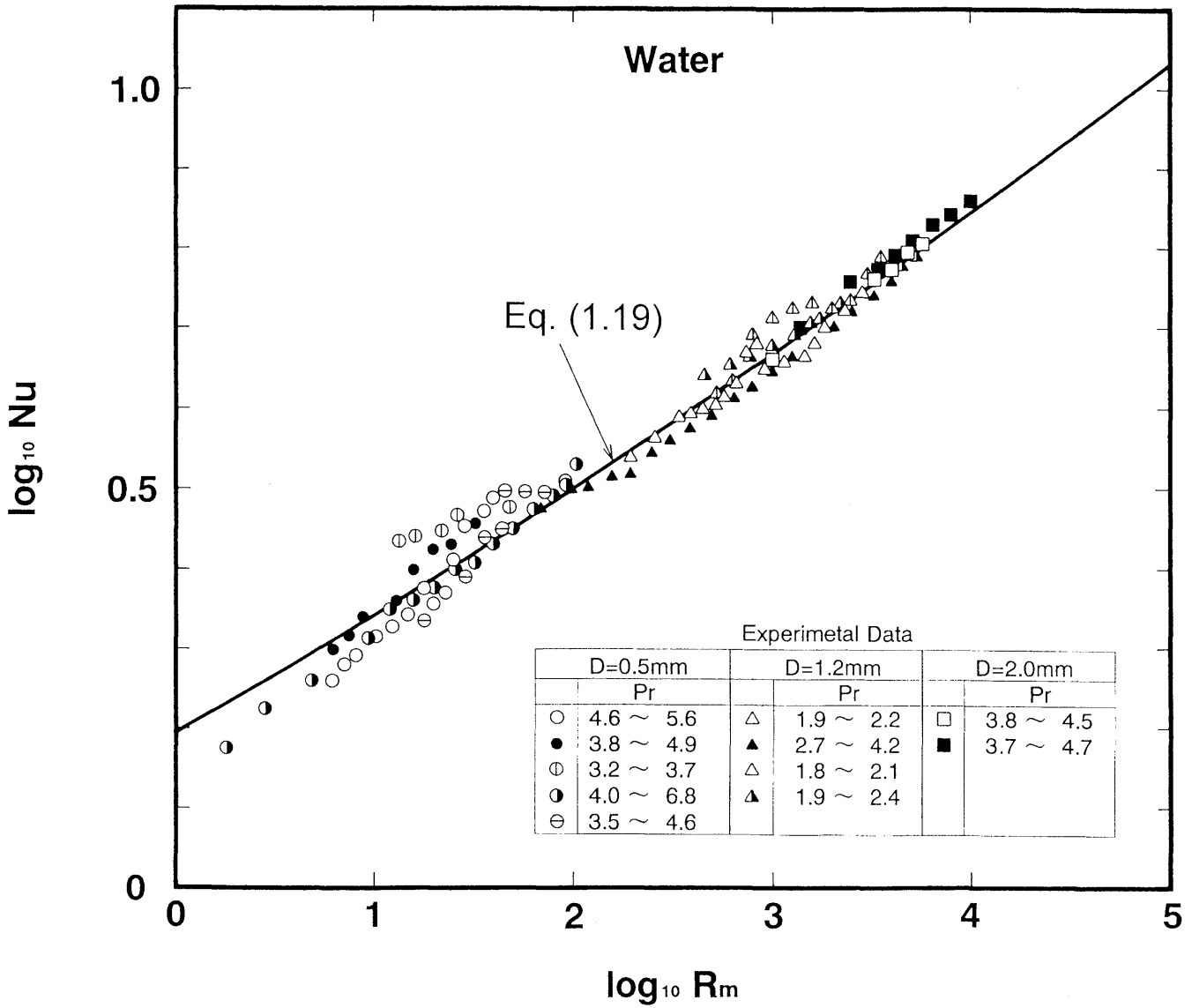

Fig. 1.14 Comparison of experimental results for water (Pr=1.8～6.8) with the general correlation.

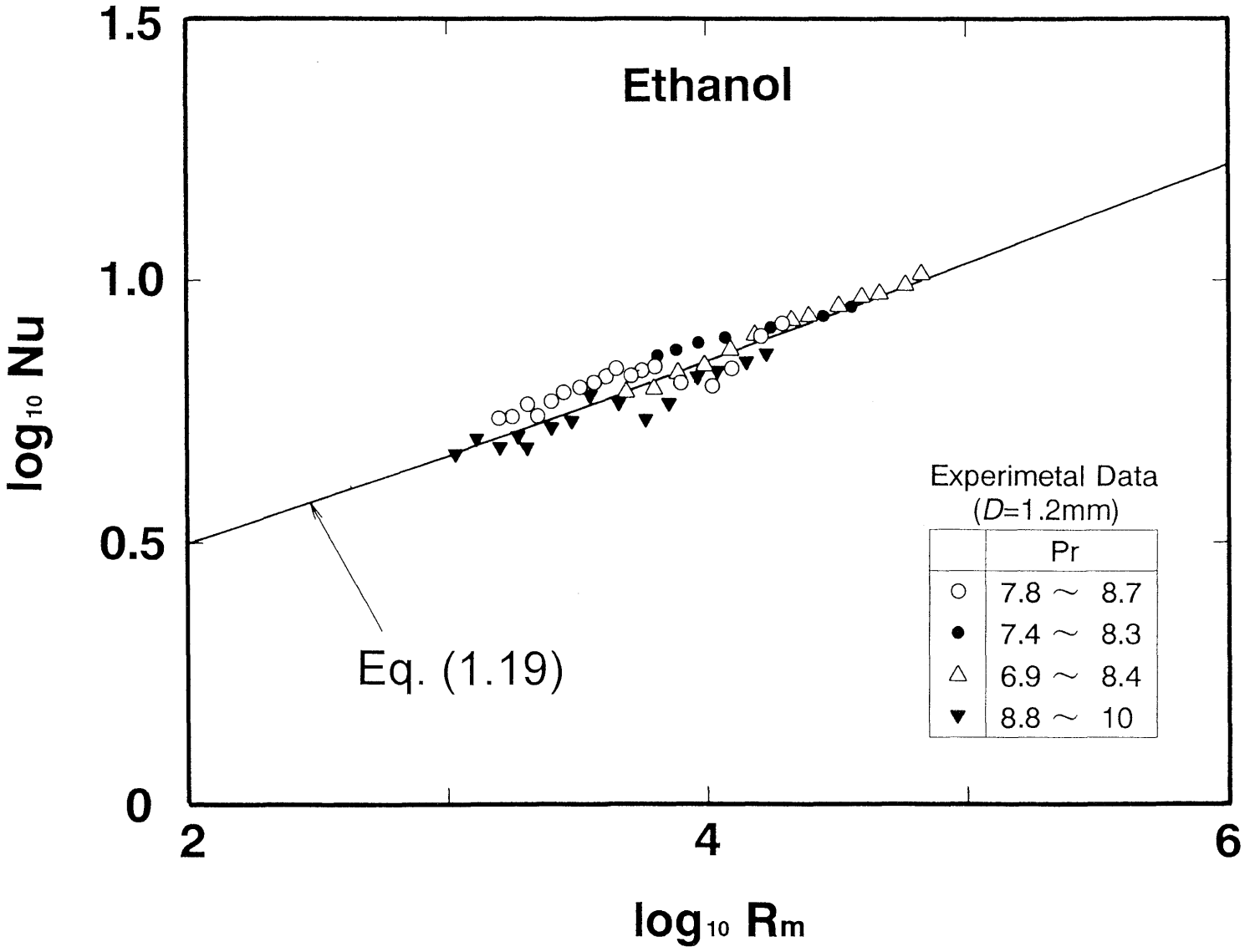

Fig. 1.15 **Comparison of experimental results for ethanol (Pr=6.8～10) with the general correlation.**

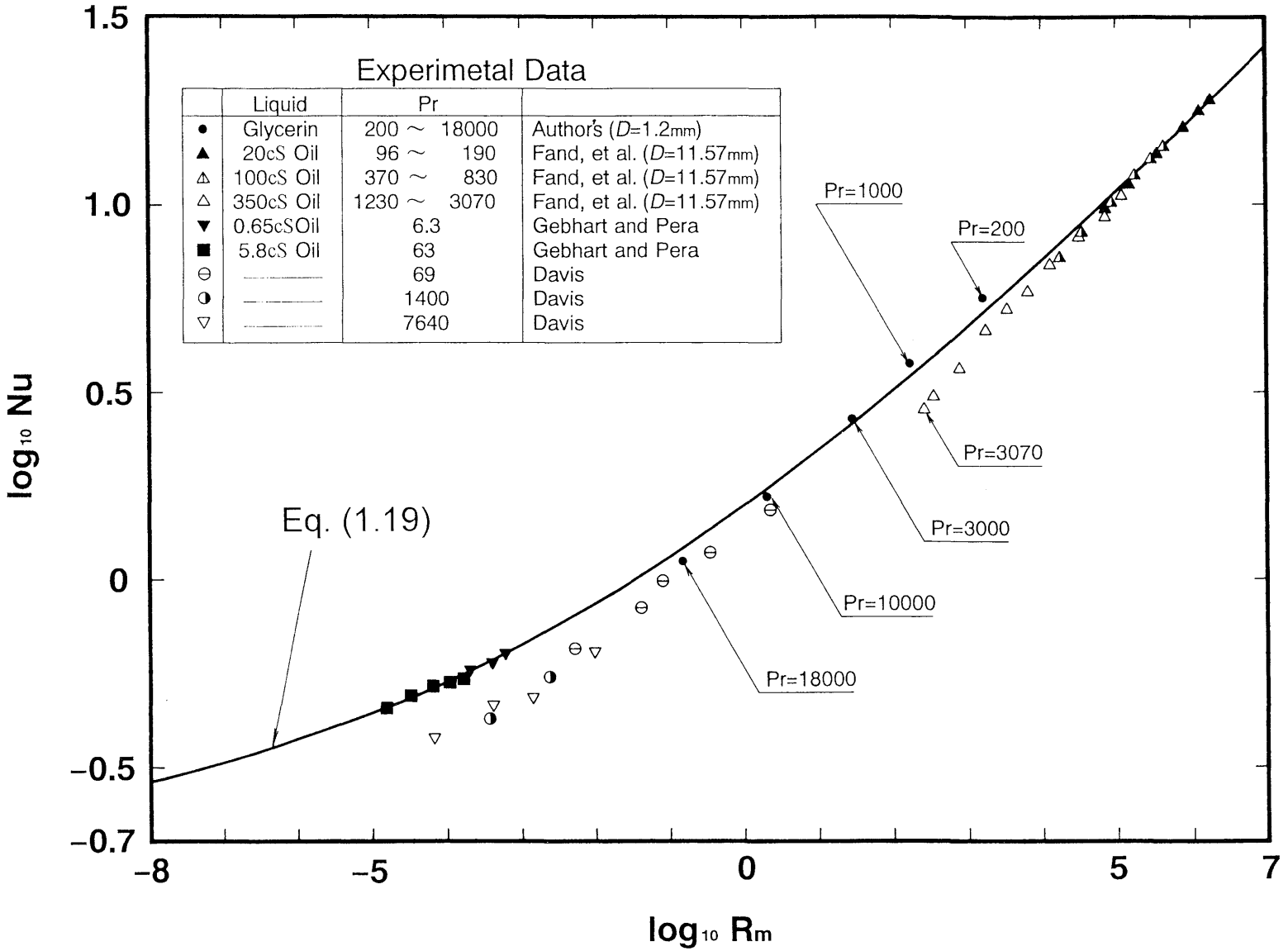

Fig. 1.16 Comparison of experimental results for various liquids of high Prandtl numbers (Pr=6.3～18000) with the general correlation.

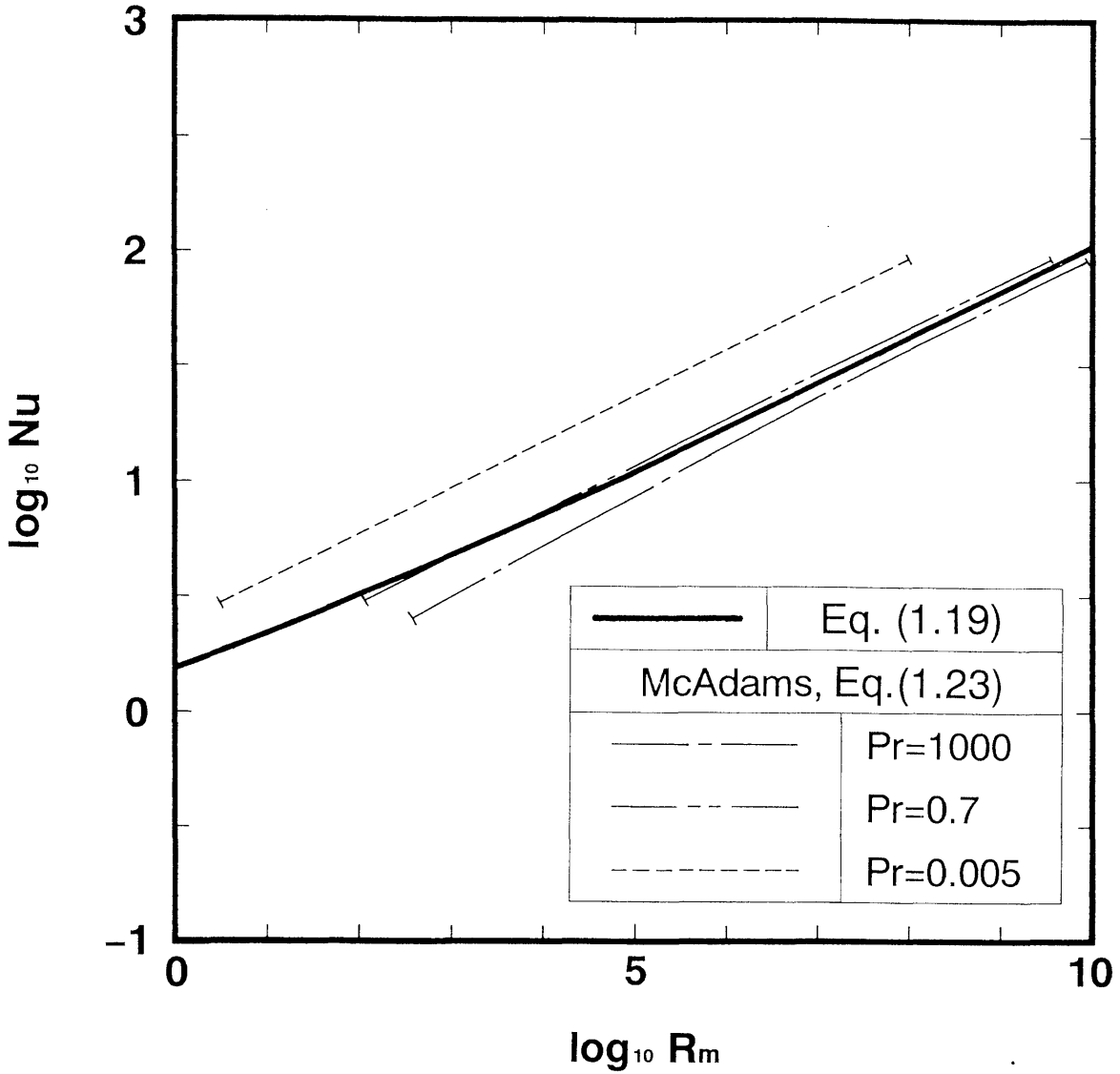

Fig. 1.17 **Comparison of average Nusselt numbers predicted by McAdams's correlation for Pr=0.005, 0.7, and 1000 with those calculated by the general correlation on the graph of Nu vs. R_m.**

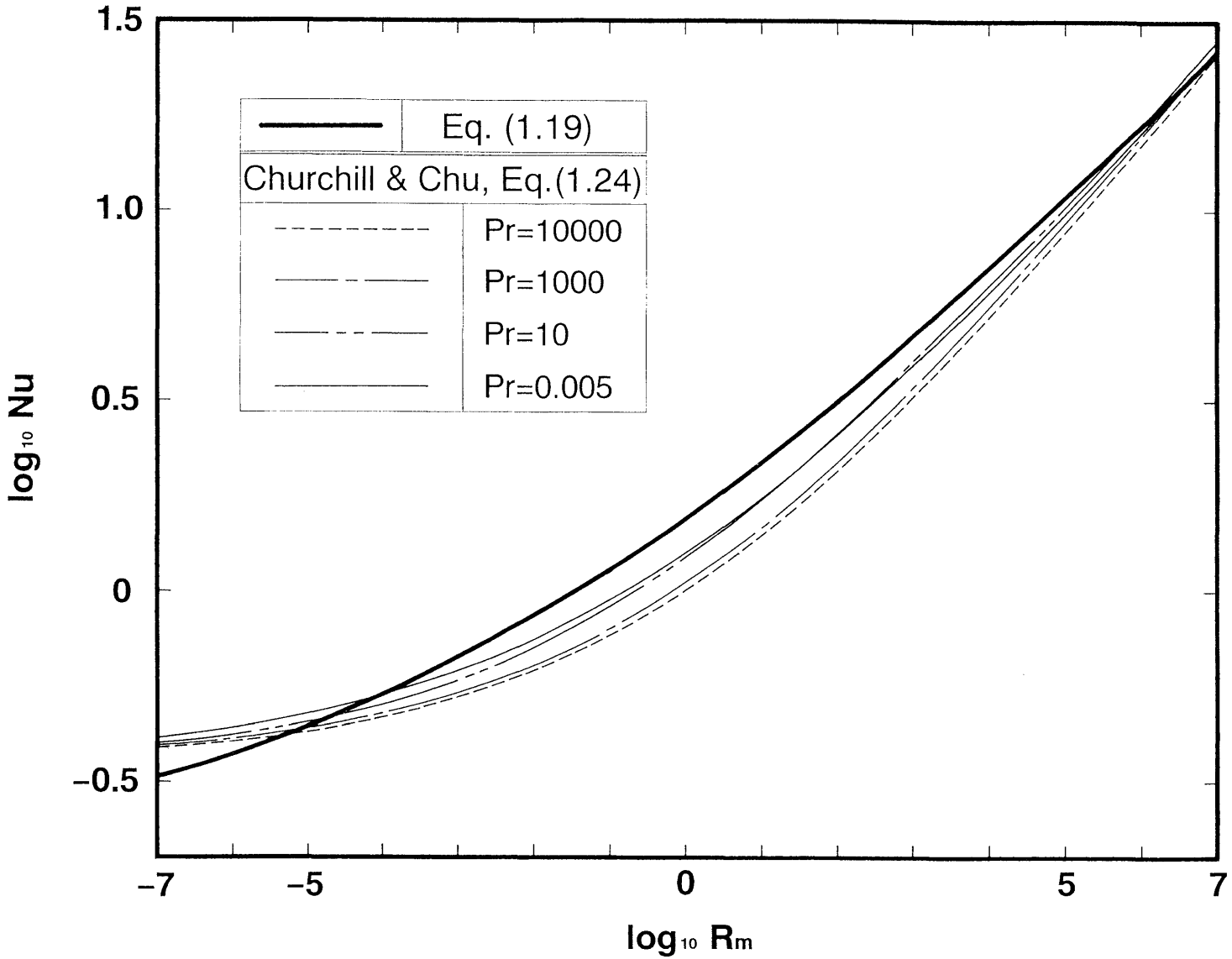

Fig. 1.18 **Comparison of average Nusselt numbers predicted by Churchill and Chu's correlation for Pr=0.005, 10, 1000, and 10000 with those calculated by the general correlation on the graph of Nu vs. R_m.**

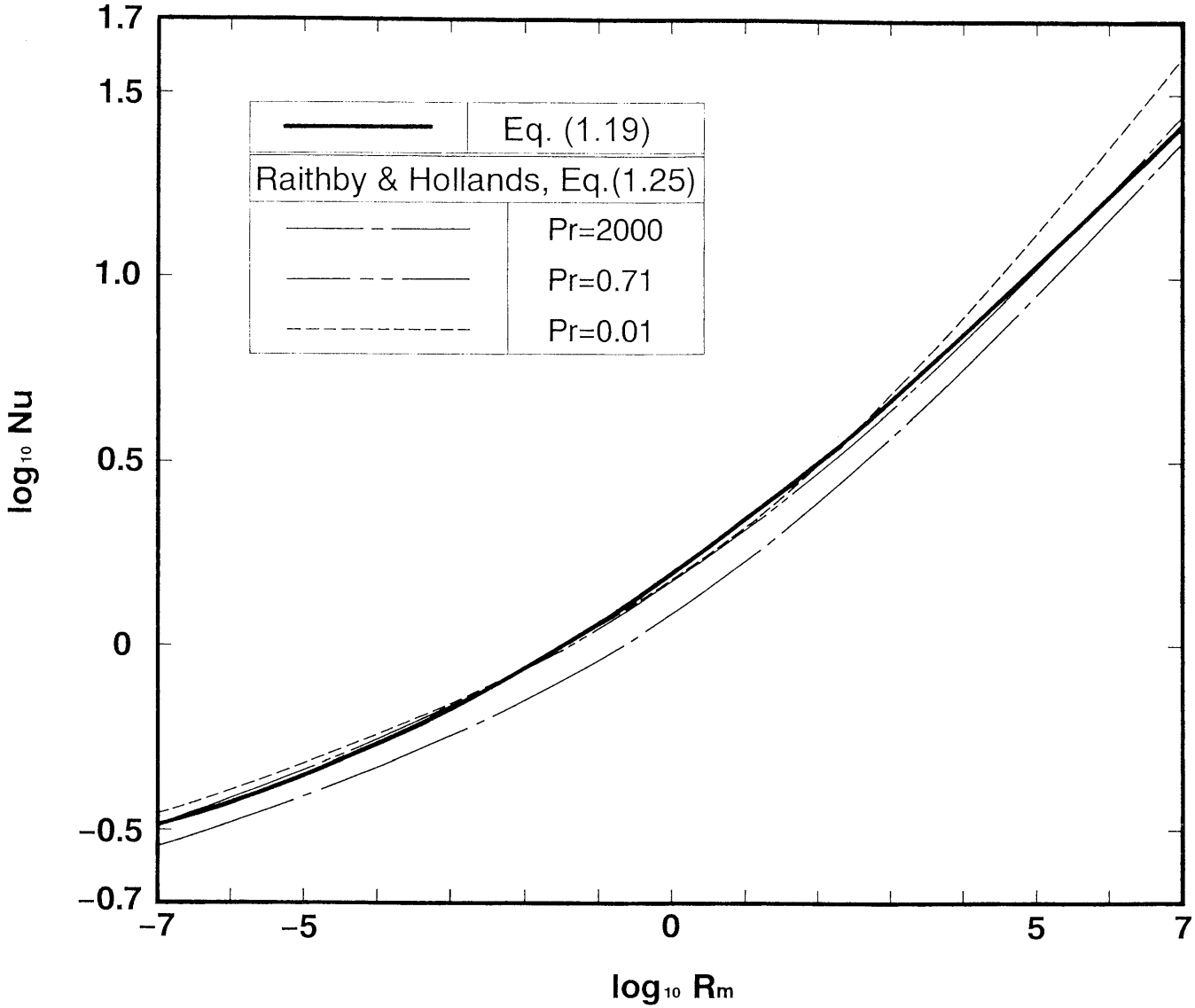

Fig. 1.19 Comparison of average Nusselt numbers predicted by Raithby and Hollands's correlation for Pr=0.01, 0.71, and 2000 with those calculated by the general correlation on the graph of Nu vs. R_m.

Appendix A

This appendix provides a brief description of the experimental apparatus and methods developed at a research section of nuclear reactor engineering of the Institute of Atomic Energy, Kyoto University.

Experimental Apparatus and Methods

A.1 Experiments in liquid sodium (Hata, et al, 1991)

Figure A-1 shows the schematic layout of experimental facilities which consist of pool boiling test sections (1) and (2), a forced convection test section, a vapor condenser, a main heater section, an economizer, a sodium purification section, a sodium pump system, an inert gas supply, and a vacuum system. All the components possibly coming into contact with high temperature liquid and/or vapor sodium are made of Hastelloy X. Figure A-2 shows a schematic of the pool boiling test section (1) which was used as a test vessel for natural convection heat transfer experiments described in this thesis. The test vessel is 30 cm in inside diameter and 70 cm in height. A cylindrical test heater is mounted horizontally at the height of 110 mm from the inner bottom of this vessel. The vertical temperature distribution of the liquid sodium was measured by several chromel-alumel thermocouples in conjunction with a standard PR thermocouple. The liquid temperature was kept at a desired value by an electric furnace covering the test vessel from its bottom up to the height of 500 mm.

Natural convection heat transfer coefficient on horizontal cylinders with various diameters immersed in a pool of liquid sodium was measured for the bulk liquid temperature of 673 K with a liquid head above the cylinder of about 200 mm under atmospheric pressure.

The Inconel sheathed cylindrical heaters of 7.6 and 10.7 mm in diameters as well as the nickel sheathed cylindrical heater of 7.6 mm in diameter were used. Each of the Inconel sheathed heater of different diameters has six and nickel sheathed heater has eight sheathed chromel-alumel thermocouples of 0.5 mm in diameter. The thermocouples are embedded to a surface depth of 0.25 mm at regular intervals of 60 degrees around the Inconel sheathed heaters and at 45 degrees intervals around the nickel one including both upper and lower stagnation points of each heater. From the temperatures measured by the thermocouples, the heater surface temperatures were evaluated by solving a radially one dimensional steady heat conduction equation.

In Fig. A-3, experimental results of the average Nusselt numbers expressed by the average heat transfer coefficients $(h = q/(T_W - T_L))$ on the circumference of the heater for the various constant heat fluxes are plotted on the graph of Nu versus $GrPr^2/(1+Pr)$ for the Inconel sheathed heater and the nickel one of 7.6 mm in diameter. The values of the average Nusselt number obtained with the different types of heaters are seen to be in good agreement with each other over the experimental range. This means that the surface temperatures are accurately estimated from the temperatures measured by the thermocouples embedded in the heaters with the sheath materials of fairly different thermal conductivities. Complete description on the experimental apparatus, instrumentation and procedure are available in the paper published by Hata et al (1991).

A.2 Experiments in glycerin

Figure A-4 illustrates schematically the apparatus used for glycerin experiment. The test vessel is a 600 mm long stainless steel tube with 200 mm inside diameter. Liquid temperature was increased from room temperature by a sheathed heater mounted at the

bottom of the vessel, and was maintained at almost constant by thermal insulator covering the vessel. Bulk liquid temperature was measured with high precision mercury thermometer. A platinum test heater of 1.2 mm in diameter is horizontally supported in the vessel. For voltage drop measurement, two fine platinum wires of 30 μm in diameter were spot welded on the test heater surface. The effective length between the potential taps was 82 mm. The test heater was heated by electrical current supplied by a direct current source. The average temperature of the test heater was measured by resistance thermometry using the heater itself. A double bridge circuit including the heater as a branch was first balanced at bulk liquid temperature. During data acquisition, the output voltages of the bridge circuit, together with the voltage drops across the potential taps of the heater and across a standard resistance, were amplified and passed through the A-D converters installed in a digital computer. The average temperature of the heater was calculated using a calibrated resistance-temperature relationship. By assuming that the heater surface is isothermal, the heater surface temperature was evaluated by solving one dimensional heat conduction equation for the test cylinder together with the measured average temperature and heat generation rate. During one experimental run, the electrical power controlled by the computer was increased progressively from zero to a desired value.

A.3 Experiments in water, ethanol, and liquid nitrogen (e.g. Sakurai, et al, 1990)

Figure A-5 shows the schematic of apparatus used for the experiments in water or in ethanol. The test vessel is a cylindrical stainless steel pressure vessel having an inside diameter of 20 cm and a height of 60 cm. The bulk liquid temperature was measured by a chromel-alumel thermocouple of 1 mm in diameter. A cylindrical platinum test heater is horizontally supported in the vessel. The diameter of the test heater was chosen to be 0.5,

1.2, and 2.0 mm for water and 1.2 mm for ethanol respectively. Two fine platinum wires of 30 μ m in diameter were spot welded on the test heater as potential taps whose distance is about 50 mm from each other. The 50 mm long test section was heated by electrical current supplied through a power amplifier.

Figure A-6 shows a schematic of the experimental apparatus for liquid nitrogen. The test vessel consists of a thermally insulated vacuum cylindrical pressure container of 20 cm inner diameter and 70 cm height. The vessel is connected via a valve to a liquid feed tank. System pressure in the vessel was automatically controlled within $\pm$1 kPa around a desired value by a pressure controlling system which consists of a pressure transducer, a pressure controller, and a control valve. For measurement of bulk liquid temperature, the vessel is equipped with a sheathed 1 mm diameter copper-constantan thermocouple. Each of 0.2 and 1.2 mm diameter test heaters was electrically heated by a fast response, direct current source controlled by a digital computer. The surface temperature of each test heater was calculated in the same way as that described for the glycerin experiment.

A.4 Experiments in liquid helium (e.g. Shiotsu, et al, 1989)

Figure A-7 shows a schematic diagram of the experimental apparatus for liquid helium. The test vessel consists of thermally insulated vacuum chamber and liquid nitrogen cooled cylindrical stainless steel pressure vessel having an inside diameter of 50 cm and a height of 128 cm. System pressure in the vessel was automatically controlled within $\pm$70 Pa around a desired value by a precision pressure control system. A Pt-Co (0.5 weight %) cylinder having a diameter of 0.2 mm was used as a test heater. The method for evaluation of heater surface temperature is identical to that employed for the glycerin experiment.

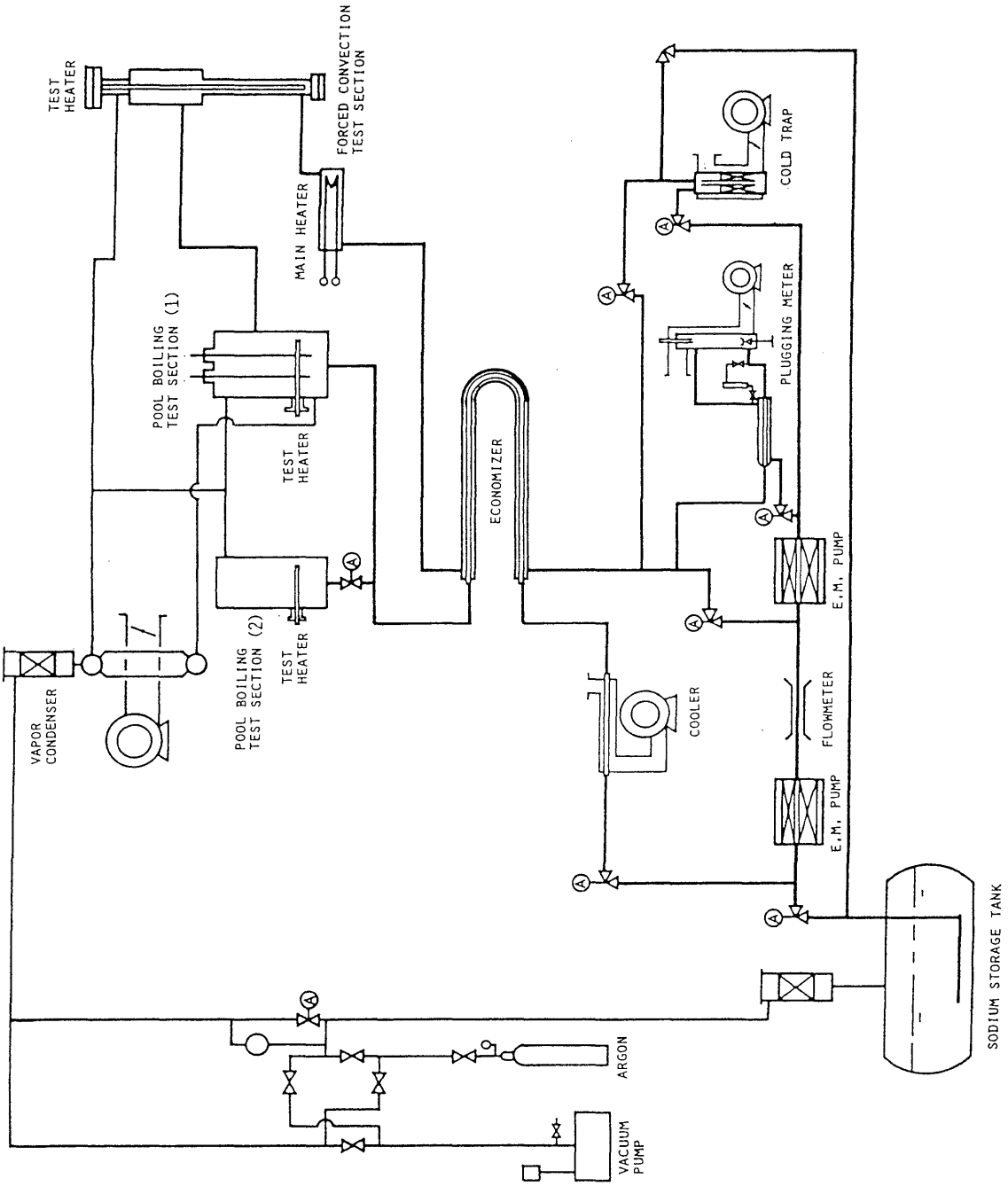

Fig. A-1 Schematic layout of experimental facility for liquid sodium.

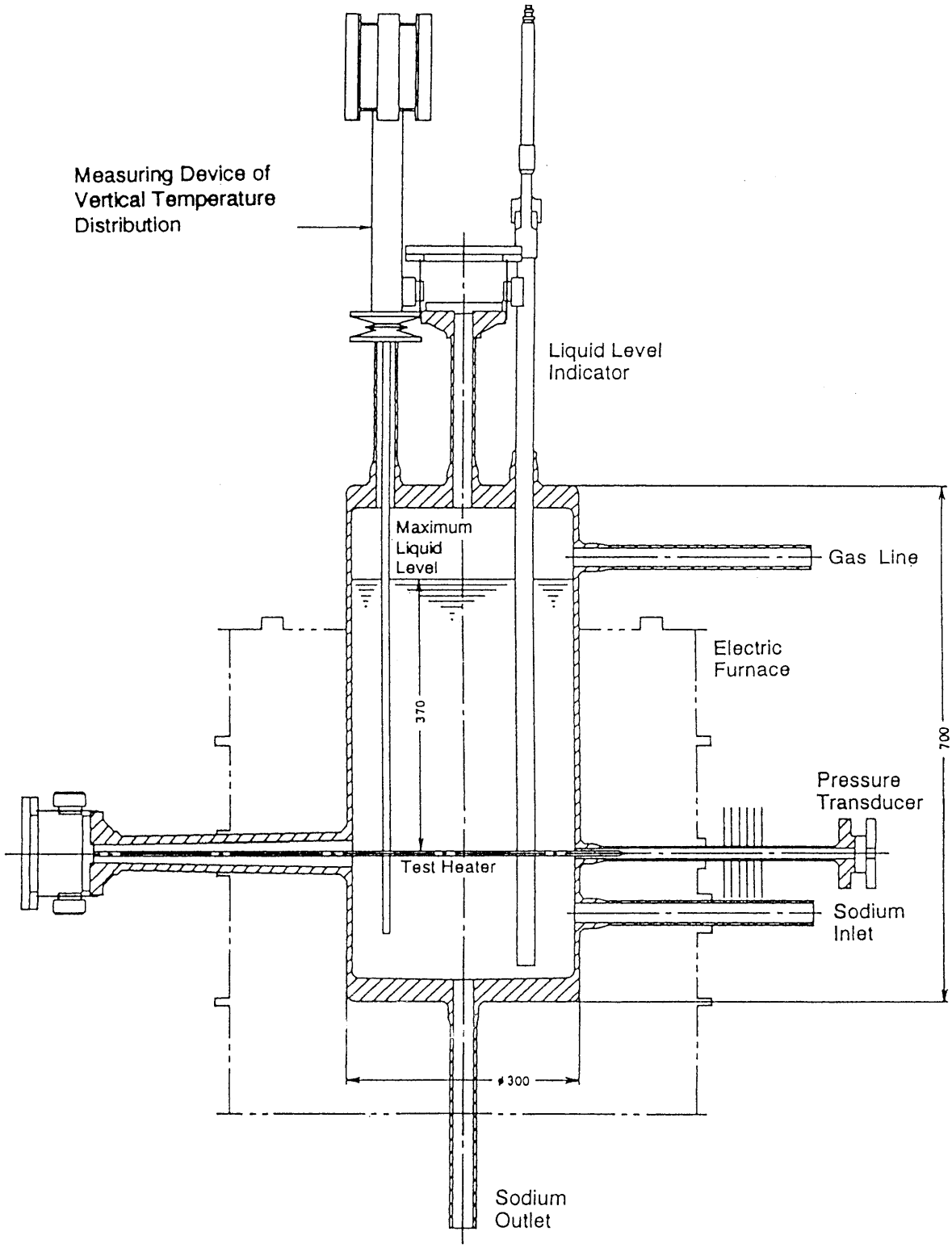

Fig. A-2 Schematic of test section for liquid sodium.

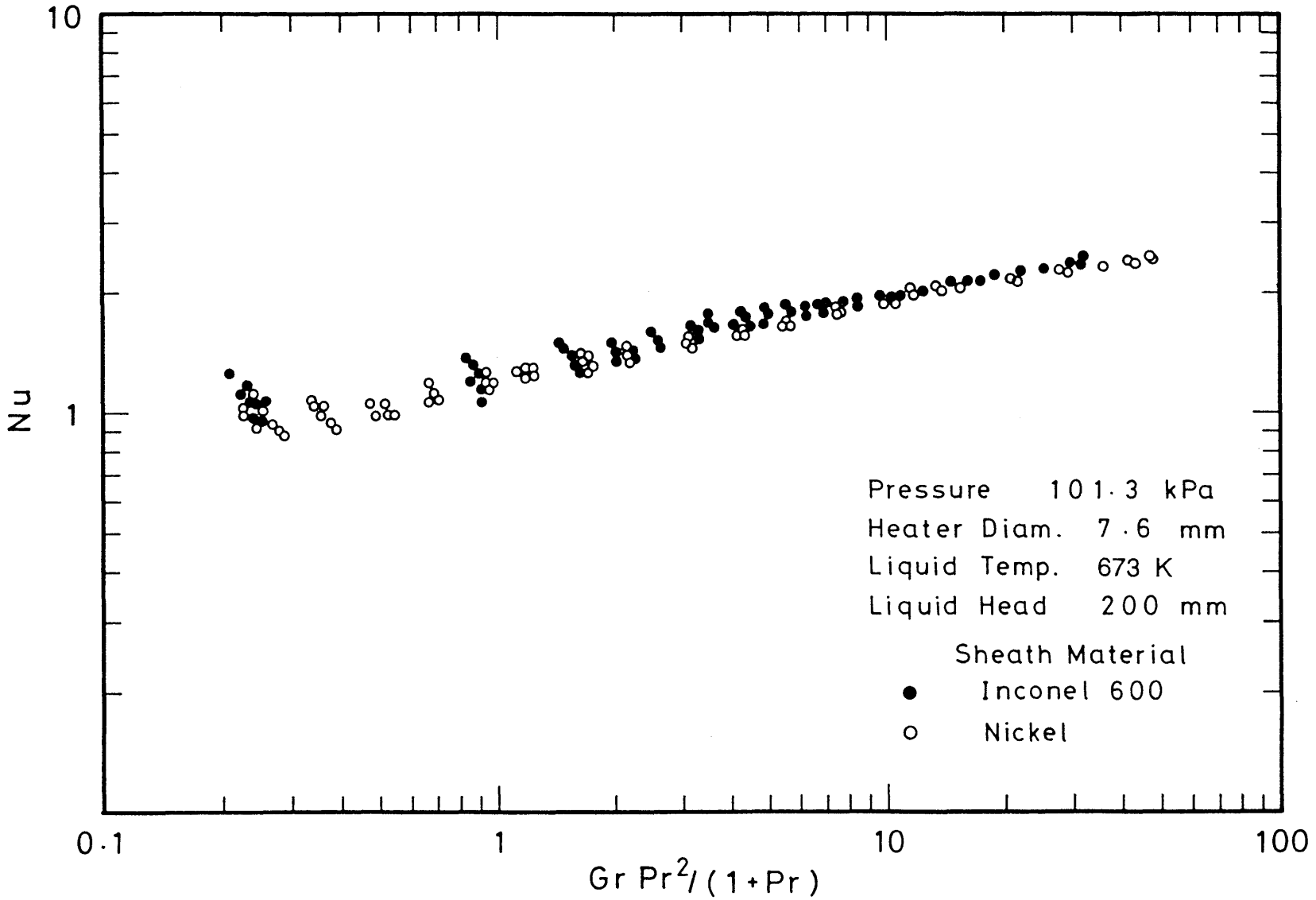

Fig. A-3 **Average Nusselt numbers obtained experimentally with Inconel sheathed 7.6 mm diameter horizontal cylinder compared with those obtained with nickel sheathed cylinder.**

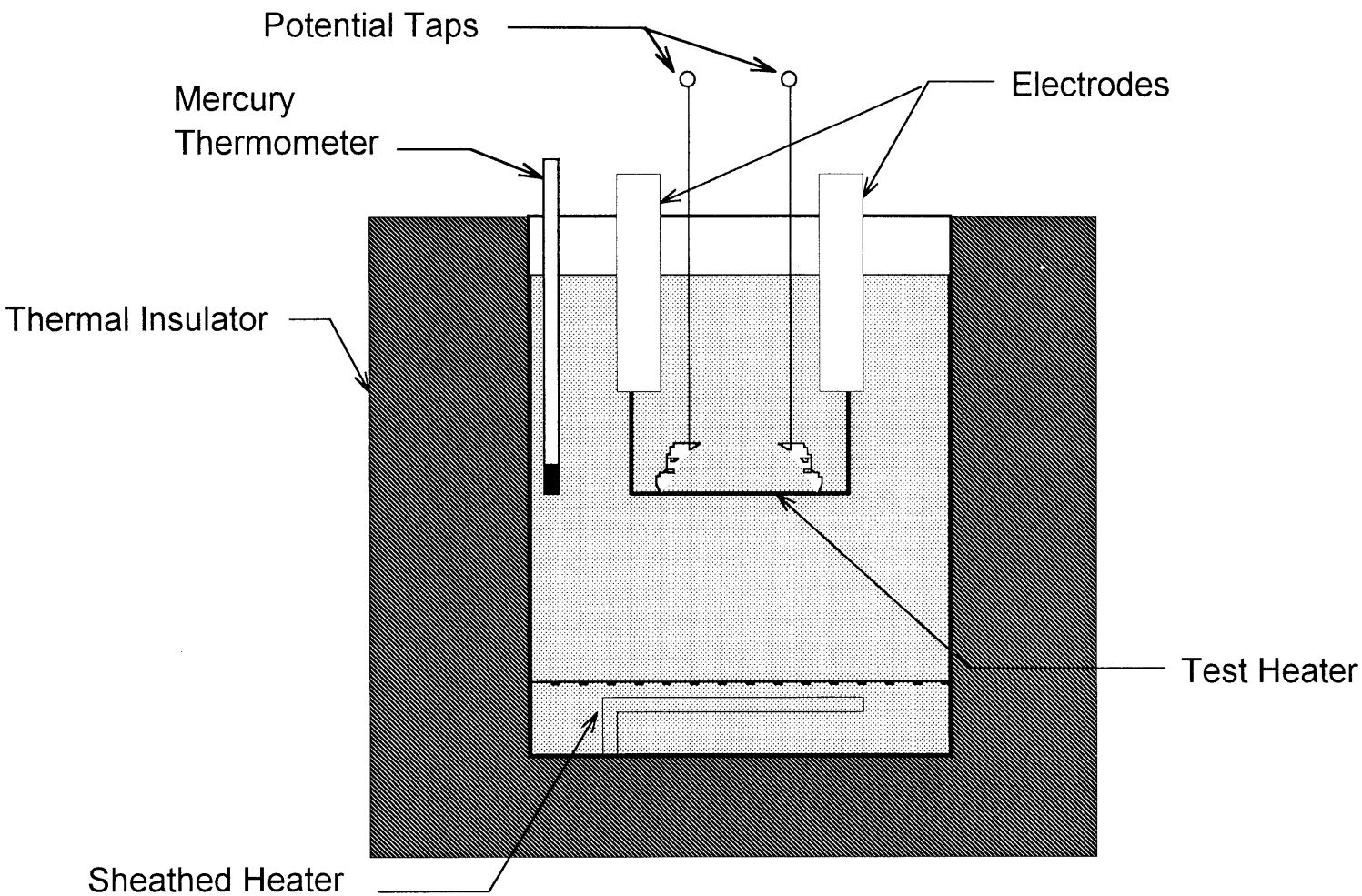

Fig. A-4 Schematic of experimental apparatus for glycerin.

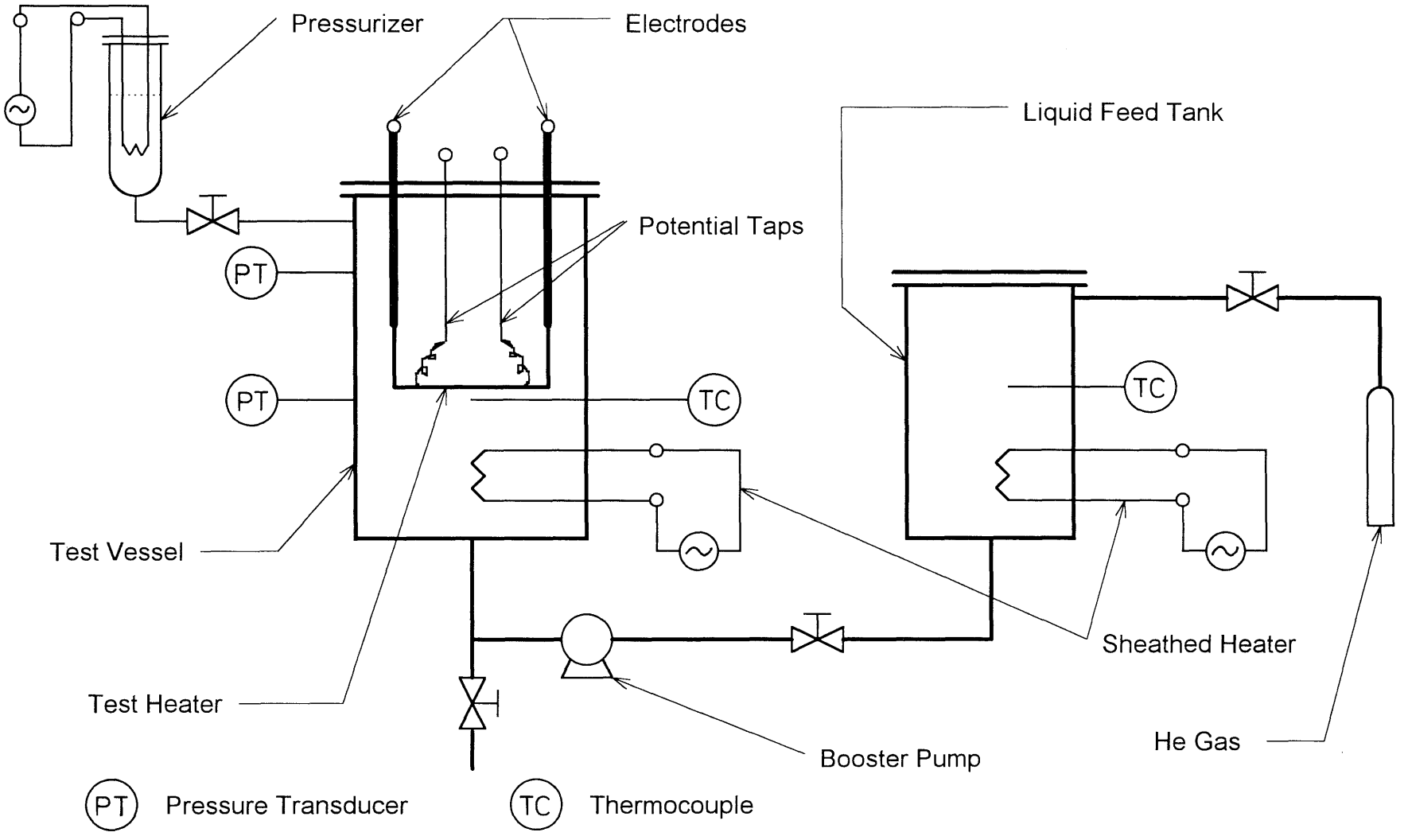

Fig. A-5 Schematic of experimental apparatus for water and ethanol.

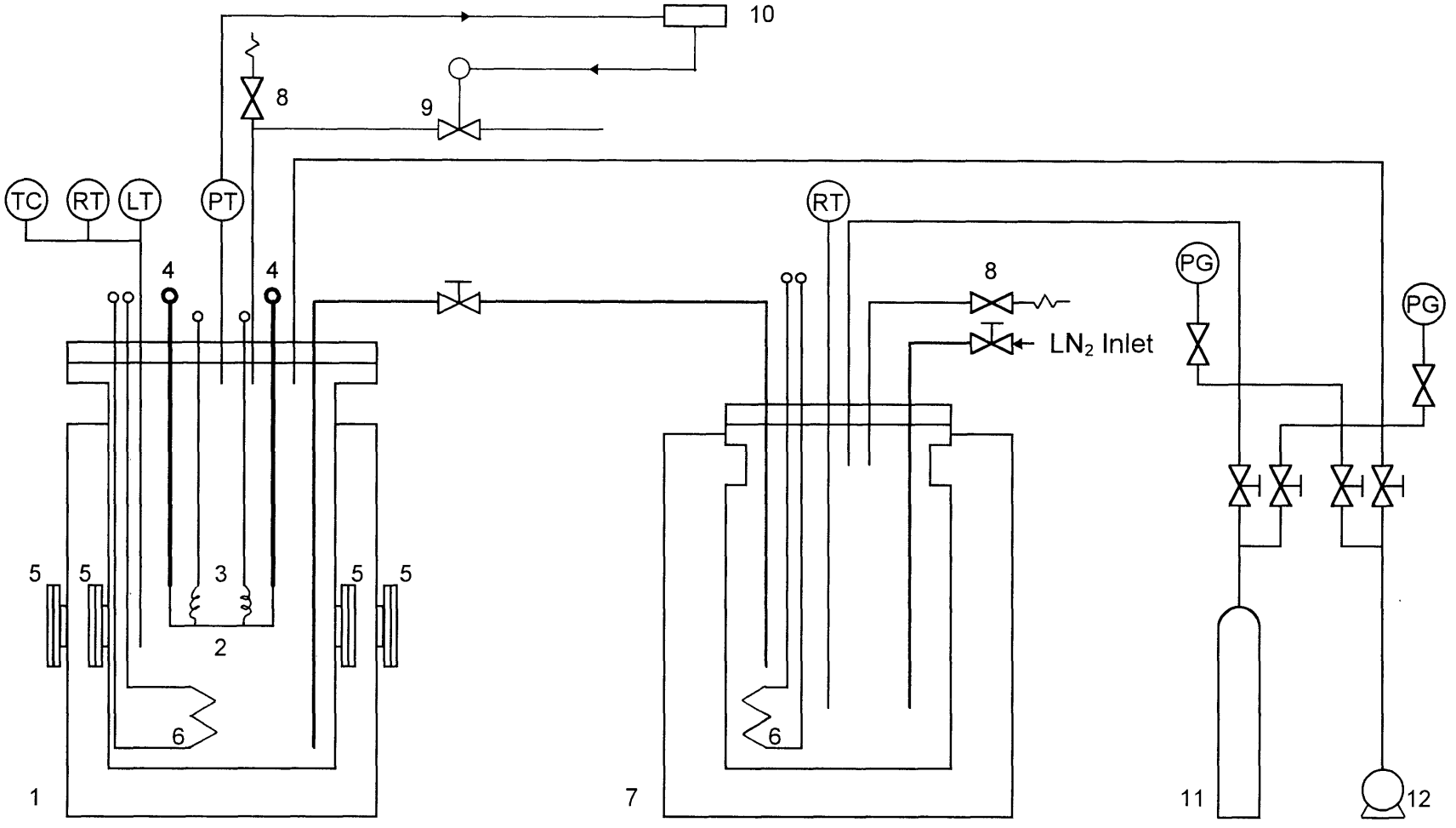

1 Boiling Vessel (Cryostadt) 2 Test Heater 3 Potential Taps 4 Electrodes 5 View Port 6 Sheathed Heater

7 LN_2 Feed Tank 8 Pressure Relief Valve 9 Control Valve 10 Pressure Controller 11 He Gas 12 Vacuum Pump

(PT) Pressure Transducer (TC) Thermocouple (RT) Pt 100 Ω Resistance Thermometer (LT) Liquid Level Transducer

(PG) Pressure Gauge

Fig. A-6 Schematic of experimental apparatus for liquid nitrogen.

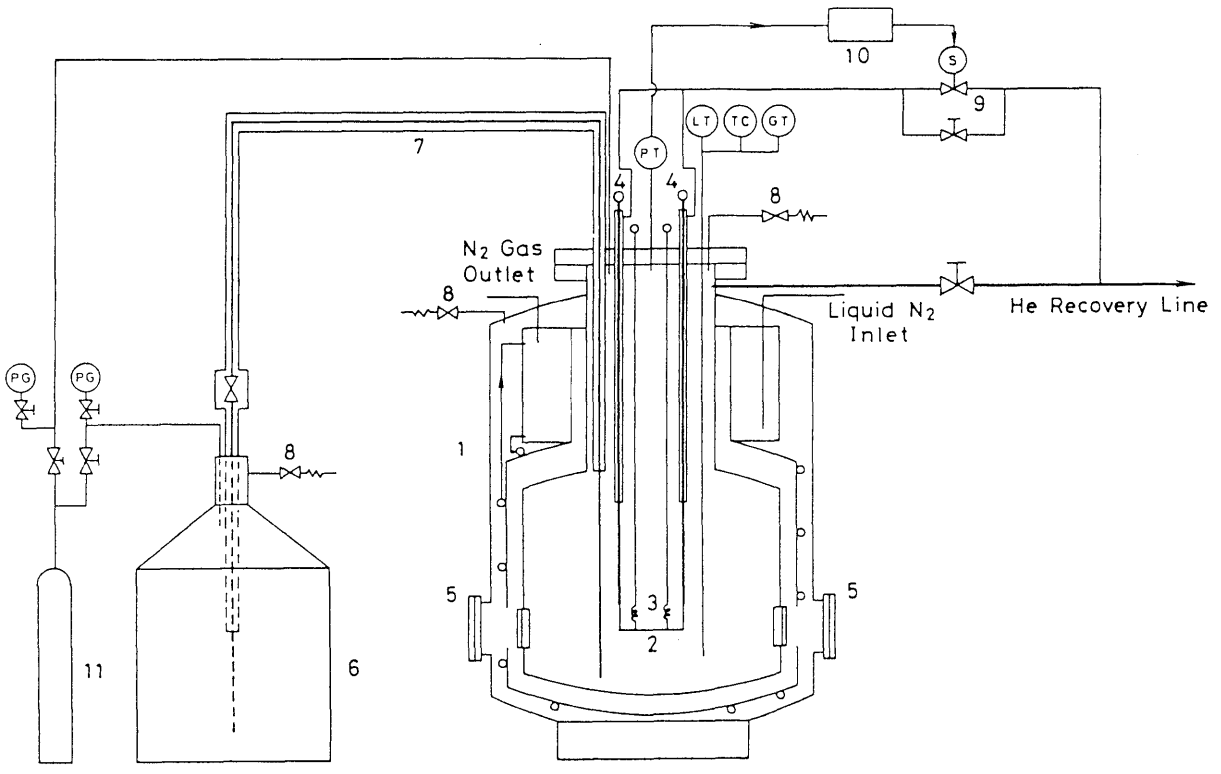

1	Boiling Vessel (Cryostadt)	2	Test Heater	3	Potential Taps
4	Gas-cooled Electrodes	5	View Port	6	Liquid He Feed Tank
7	Liquid He Transfer Tube	8	Pressure Relief Valve	9	Control Valve
10	Pressure Controller	11	He Gas		

(PT) Pressure Transducer (GT) Germanium Resistance Thermometer

(TC) Thermocouple (LT) Liquid Level Transducer (PG) Pressure Gauge

Fig. A-7 Schematic of experimental apparatus for liquid helium.

Appendix B

Source program with flowchart used for numerical analysis

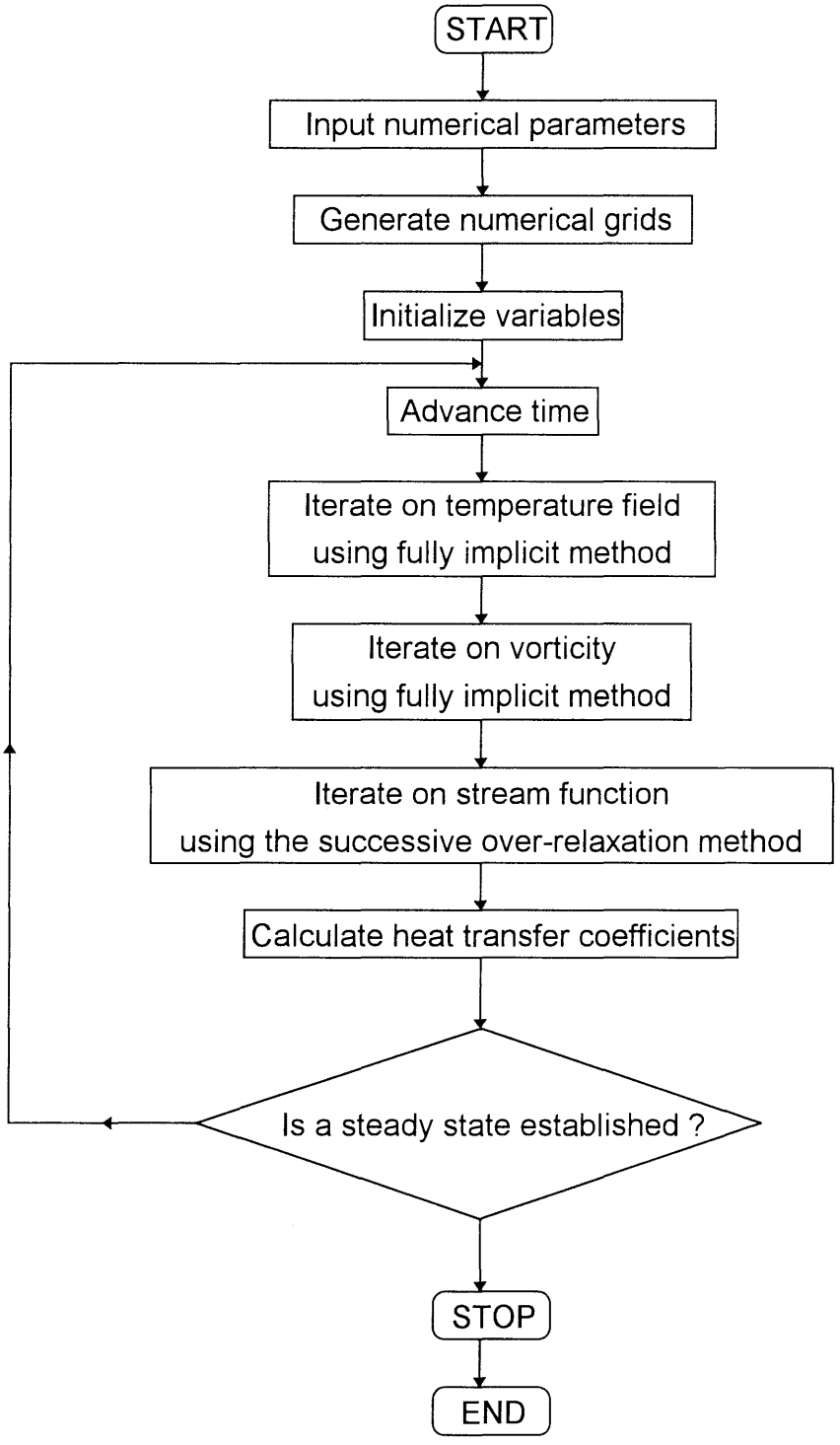

Fig. B-1 Flow chart of the numerical procedure using stream function and vorticity method.

```
C-------- NEW.FORT77(MRCONT) --------------------------
CCCCCCCCCCCCCCCCCCCCC NATURAL CONVECTION
CCCCCCCCCCCCCCCC
C
      IMPLICIT REAL*8 (A-H,O-Z)
C
      COMMON /CO1/ Y(111),R(111),THETA(150),ET(150)
     &           /CO2/ DY(111),DET(150),DA(111),DB(150)
     &           /SOLD/ ST(111,150),VO(111,150),T(111,150),PST(111,150),
     &                  PVO(111,150),PT(111,150),FST(111,150),FVO(111,150),
     &                  FT(111,150)
     &           /CST1/ DIA,RR,RRM,RM
     &           /CST2/ M1,M2,M3,N1,N2,N3
     &           /SOL/ HTNUM
     &           /CST5/ PAI,DTIM,TIM,RDTIM
     &           /CST6/ XX,YY,ZZ
     &           /CST8/ OMG,KST,KVO,KT,KTT,KE,KP,KV,KSS,NM,NB,IMAX,KMAX
     &           /CST9/ ERT,ERVO,ERST
     &           /CST10/ JRAO,JBT,IJCHK,ICON
     &           /CST12/ PAID
     &           /CST14/ IVI
     &           /CST16/ ITE
     &           /BC/ IBCT
      COMMON /PRO/ TCV
     &           /CST20/ COEF,IU,IUST
     &           /PROP/ TCL
     &           /ERMAX/ PTMAX,PSMAX,PTER,PSER,PSM
     &           /TR1/ PR,RA4
     &           /TTIME/ TIM1,TIM2,TIM3,TIM4,TIM5,TIM6,IHT
     &           /IJOB/ JOBITE
     &           /STEP/ CPUTIM,CPU,T000
     &           /DLT/ DLTIM
C
      OPEN(55,FILE='../NCPROG/data_cont100')
      OPEN(2,FILE='../NCPROG/NCDATA/Pr100_Rfm3.5_1240',
     &           FORM='UNFORMATTED')
      OPEN(20,FILE='../NCPROG/NCDATA/Pr100_Rfm3.5_111_1240',
     &           FORM='UNFORMATTED')
      OPEN(21,FILE='../NCPROG/NCDATA/Pr100_Rfm3.5_150_1240',
     &           FORM='UNFORMATTED')
      OPEN(24,FILE='../NCPROG/NCDATA/Pr100_Rfm3.5_111150_1240',
     &           FORM='UNFORMATTED')
c
      OPEN(3,FILE='../NCPROG/NCDATA/Pr100_Rfm3.5_1241',
     &         FORM='UNFORMATTED')
      OPEN(30,FILE='../NCPROG/NCDATA/Pr100_Rfm3.5_111_1241',
     &         FORM='UNFORMATTED')
      OPEN(31,FILE='../NCPROG/NCDATA/Pr100_Rfm3.5_150_1241',
     &         FORM='UNFORMATTED')
      OPEN(34,FILE='../NCPROG/NCDATA/Pr100_Rfm3.5_111150_1241',
     &         FORM='UNFORMATTED')
C
      OPEN(8,FILE='../NCPROG/NCFILE_Pr100_Rfm3.5_1241')
C
      T000=second()
      READ(55,500) DLTIM
  500 FORMAT(9X,D15.8)
      CALL PRDATA
C
      READ(55,50) CPU,DTIM,TIM1,TIM2,TIM3,TIM4,TIM5,TIM6,IHT,NB
   50 FORMAT(10X,F8.1/6X,E11.4,6(/35X,F12.7),/35X,I5/35X,I3)
C
      KMAX=9999999
      KP=1
C
      M0=M1+1
      N0=N1+1
      WRITE(8,601) M0,N0,DTIM
  601 FORMAT(1H ,30X,'M0=',I3,'    N0=',I3,'    DTIM=',E11.4,
     &       '(DIMENSIONLESS)')
C
      WRITE(8,113) JBT
  113 FORMAT(1H ,'      >>>> JBT =',I3)
C
      WRITE(8,6501) RM
 6501 FORMAT(1H ,10X,'RM=',E11.4)
      WRITE(8,678) PR,RA4
  678 FORMAT(1H ,'   PR=',E11.4,'   RA4=',E11.4)
      WRITE(8,650) XX,YY,ZZ
  650 FORMAT(1H ,' XX=',E11.4,' YY=',E11.4,' ZZ=',E11.4)
C
      WRITE(8,603) OMG
  603 FORMAT(1H ,20X,'RELAXATION FACTOR ;   OMG=',F7.4)
C
      WRITE(8,6004) TIM1,TIM2,TIM3,TIM4,TIM5,TIM6
 6004 FORMAT(1H ,'   TIM1=',E11.4,'   TIM2=',E11.4,'   TIM3=',E11.4,'   TIM4
     &=',E11.4,'   TIM5=',E11.4,'   TIM6=',E11.4)
      WRITE(8,660) COEF,NB,IU
  660 FORMAT(1H ,20X,'COEF=',F10.4,'   SHUUSOKUHANTEI(NB)',I3,
     &  ' KAI-OKI   UCHIDASHI-KANKAKU(IU) WA KE GA ',I5,' KAI-OKI DESU')
C
C
 9999 CONTINUE
c
      KE=KE+1
c
      ITE=0
 8888 CONTINUE
```

```
C
C
CC        CALCULATION OF TEMPERATURE DISTRIBUTION
      CALL TEMP
      IF(KT.GE.IMAX) GO TO 1234
C
C         CALCULATION OF VORTICITY DISTRIBUTION
      CALL VORT
      IF(KVO.GE.IMAX) GO TO 1234
C
C          CALCULATION OF STREAM-FUNCTION DISTRIBUTION
 1010 CALL STFU
      IF(KST.GE.IMAX) GO TO 1234
C
      CALL NCCON
      IF(KP.GE.2) GO TO 900
      GO TO 9999
  900 CONTINUE
C
      STOP
 1234 CALL PRINT
      STOP
           CLOSE(2)
           CLOSE(20)
           CLOSE(21)
           CLOSE(22)
           CLOSE(24)
           CLOSE(25)
           CLOSE(3)
           CLOSE(30)
           CLOSE(31)
           CLOSE(32)
           CLOSE(34)
           CLOSE(35)
           CLOSE(55)
           CLOSE(8)
      END
```

```
C
      SUBROUTINE PRDATA
C
      IMPLICIT REAL*8 (A-H,O-Z)
C
      COMMON /CO1/ Y(111),R(111),THETA(150),ET(150)
     &           /CO2/ DY(111),DET(150),DA(111),DB(150)
     &           /SOLD/ ST(111,150),VO(111,150),T(111,150),PST(111,150),
     &                  PVO(111,150),PT(111,150),FST(111,150),FVO(111,150),
     &                  FT(111,150)
     &           /CST1/ DIA,RR,RRM,RM
     &           /CST2/ M1,M2,M3,N1,N2,N3
     &           /SOL/ HTNUM
     &           /CST5/ PAI,DTIM,TIM,RDTIM
     &           /CST6/ XX,YY,ZZ
     &           /CST8/ OMG,KST,KVO,KT,KTT,KE,KP,KV,KSS,NM,NB,IMAX,KMAX
     &           /CST9/ ERT,ERVO,ERST
     &           /CST10/ JRAO,JBT,IJCHK,ICON
     &           /CST12/ PAID
     &           /CST14/ IVI
     &           /BC/ IBCT
      COMMON /PRO/ TCV
     &           /CST20/ COEF,IU,IUST
     &           /PROP/ TCL
     &           /ERMAX/ PTMAX,PSMAX,PTER,PSER,PSM
     &           /TR1/ PR,RA4
     &           /TTIME/ TIM1,TIM2,TIM3,TIM4,TIM5,TIM6,IHT
     &           /DLT/ DLTIM
C
      DIMENSION STST(16650),FSTFST(16650),PSTPST(16650),
     &          VOVO(16650),PVOPVO(16650),TT(16650),PTPT(16650)
      EQUIVALENCE (ST(1,1),STST(1)),(FST(1,1),FSTFST(1)),
     &            (PST(1,1),PSTPST(1)),(VO(1,1),
     &             VOVO(1)),(PVO(1,1),PVOPVO(1)),(T(1,1),TT(1)),
     &            (PT(1,1),PTPT(1))
      READ(20) R
      READ(24) STST
      READ(24) PSTPST
      READ(24) VOVO
      READ(24) PVOPVO
      READ(24) TT
      READ(24) PTPT
      READ(21) THETA
      READ(21) ET
      READ(20) Y
      READ(20) DY
      READ(21) DET
      READ(20) DA
      READ(21) DB
      READ(2) M1
      READ(2) M2
      READ(2) M3
      READ(2) N1
      READ(2) N2
      READ(2) N3
      READ(2) IBCT
      READ(2) PAI
      READ(2) DTIM
      READ(2) TIM
```

```
READ(2) RDTIM
READ(2) DIA
READ(2) RR
READ(2) RRM
READ(2) RM
READ(2) XX
READ(2) YY
READ(2) ZZ
READ(2) OMG
READ(2) KST
READ(2) KVO
READ(2) KT
READ(2) KTT
READ(2) KE
READ(2) KP
READ(2) KV
READ(2) KSS
READ(2) NM
READ(2) NB
READ(2) IMAX
READ(2) KMAX
READ(2) IVI
READ(2) ERT
READ(2) ERVO
READ(2) ERST
READ(2) JRAO
READ(2) JBT
READ(2) IJCHK
READ(2) ICON
READ(2) PAID
READ(2) TCV
READ(2) COEF
READ(2) TCL
READ(2) IU
READ(2) IUST
READ(2) PTMAX
READ(2) PSMAX
READ(2) PTER
READ(2) PSER
READ(2) PSM
READ(2) PR
READ(2) RA4
READ(2) TIM1
READ(2) TIM2
READ(2) TIM3
READ(2) TIM4
READ(2) TIM5
READ(2) TIM6
READ(2) IHT
      READ(2,END=999) DLTIM
  999 print*,'(DLTIM) O.K.'
      RETURN
      END
```

```
C-------- NEW.FORT77(HTR) ----------------------------
C                              (HT)
C         CALCULATION OF HEATTRANSFER COEFFICIENT
      SUBROUTINE NCHT
C
      IMPLICIT REAL*8 (A-H,O-Z)
C
      COMMON /CO1/ Y(111),R(111),THETA(150),ET(150)
     &           /CO2/ DY(111),DET(150),DA(111),DB(150)
     &           /SOLD/ ST(111,150),VO(111,150),T(111,150),PST(111,150),
     &                  PVO(111,150),PT(111,150),FST(111,150),FVO(111,150),
     &                  FT(111,150)
     &           /SOL/ HTNUM
     &           /CST1/ DIA,RR,RRM,RM
     &           /CST2/ M1,M2,M3,N1,N2,N3
     &           /CST4/ DY2,C1,CD3,DD0,D1
     &           /CST5/ PAI,DTIM,TIM,RDTIM
     &           /CST8/ OMG,KST,KVO,KT,KTT,KE,KP,KV,KSS,NM,NB,IMAX,KMAX
     &           /CST14/ IVI
     &           /BC/ IBCT
     &           /PROP/ TCL
     &           /TR1/ PR,RA4
     &           /TR0/ HTN(150),HTNR(150)
     &           /TTIME/ TIM1,TIM2,TIM3,TIM4,TIM5,TIM6,IHT
     &           /NTIME/ MT1,MT2,MT3,MT4,MT5,MT6,ICONV
     &           /DIM/ HTNHI(150),HTNHIR(150)
     &    /IUP/ KT1CT,KT1UP,KTINCT,KTINUP,KTN1CT,KTN1UP,KVOCT,KVOUP
     &           /STEP/ CPUTIM,CPU,T000
C
      RY=DA(2)/DA(1)
      RY1=1.D0+RY
      RY12=RY1*RY1
      RY13=RY12*RY1
      RY2=RY1+RY*RY
      RY22=RY2*RY2
      RY23=RY22*RY2
      AL=RY22/RY1
C
      DO 572 J=1,N1
      IF(IBCT.EQ.0) GO TO 100
      HTN(J)=1.D0/T(1,J)
      HTNR(J)=HTN(J)/RA4
      HTNHI(J)=HTN(J)
```

```
      HTNHIR(J)=HTNR(J)
      GO TO 110
  100 HTN(J)=2.D0/((1.D0-RM)*DA(1)*RY*RY1)*((1.D0-RY12)+RY12*T(2,J)-T(3,J))
      HTNHI(J)=2.D0*((RY23-AL*RY13)*T(2,J)+AL*T(3,J)-T(4,J)-(AL*(1.D0-R
     &            Y13)-(1.D0-RY23))*T(1,J))/(DA(1)*(AL*RY1*(1.D0-RY12)-
     &            RY2*(1.D0-RY22)))/(1.D0-RM)
      HTNR(J)=HTN(J)/RA4
      HTNHIR(J)=HTNHI(J)/RA4
      IF(HTNHI(J).GE.0.) GO TO 110
      WRITE(8,6011) J,T(2,J),T(3,J),HTNHI(J)
 6011 FORMAT(1H ,15X,'AT J=',I3,' T(2,J)=',E10.3,'   T(3,J)=',E10.3/1H ,
     &       'HTNHI=',E11.4,'----- STOP ------')
      CALL PRINT
      CALL BUFFER
      STOP
C
  110 IF(((KE/IHT*IHT-KE).EQ.0).AND.(ICONV.NE.1)) GO TO 572
      IF((KE.EQ.MT1).OR.(KE.EQ.MT2).OR.(KE.EQ.MT3).OR.(KE.EQ.MT4).OR.
     &(KE.EQ.MT5).OR.(KE.EQ.MT6).OR.(ICONV.EQ.1).OR.(CPUTIM.GE.CPU).OR.
     &    (IVI.EQ.1))
     & WRITE(8,6000) THETA(J),HTN(J),HTNR(J),HTNHI(J),HTNHIR(J)
C
 6000 FORMAT(1H ,F6.0,'(DEG)      LOCAL NU =',E15.8,
     &       '   NU/RA4=',E11.4,'   ;; HTNHI=',E15.8,'   HTNHIR=',E15.8)
C
  572 CONTINUE
C
      DO 200 J=1,N2
      IF(HTNHI(J+1).LE.HTNHI(J)) GO TO 200
      GO TO 201
  200 CONTINUE
      GO TO 5721
  201   WRITE(8,6060) KE,KT,KVO,KST,KT1CT,KT1UP,KTINCT,KTINUP,KTN1CT,
     &                  KTN1UP,KVOCT,KVOUP
 6060   FORMAT(1H ,'++++++ NU(J) < NU(J+1) DE STOP ++++++   KE=',I8,
     &          '  KT=',I3,'  KVO=',I3,'  KST=',I3/1H ,'KT1CT=',I4,'  KT1U
     &P=',I4,'  KTINCT=',I4,'  KTINUP=',I4,'  KTN1CT=',I4,'  KTN1UP=',I4
     &,'  KVOCT=',I4,'  KVOUP=',I4)
      DO 5720 J=1,N1
       WRITE(8,6000) THETA(J),HTN(J),HTNR(J),HTNHI(J),HTNHIR(J)
 5720 CONTINUE
        CALL BUFFER
       STOP
 5721 CONTINUE
 5722 CONTINUE
C
           CALL SUBTRP (HTN,N1,HTNUM)
           CALL SUBTRP (HTNHI,N1,HTNUMH)
C
      HJUD=ABS(HTNHI(1)-HTNHI(N1))/HTNUMH
      III=1
      IF(III.EQ.1) GO TO 111
      DLTIM=FLOAT(KE)*DTIM
      WRITE(8,2130) DLTIM,KE,KT,KVO,KST
     &      ,KT1CT,KT1UP,KTINCT,KTINUP,KTN1CT,KTN1UP,KVOCT,KVOUP
 2130 FORMAT(1H ,'<<<<< DLTIM=',F15.6,' >>>>>      KE=',I8,
     &          '  KT=',I4,'  KVO=',I4,'  KST=',I4/1H ,'KT1CT=',I4,'  KT1U
     &P=',I4,'  KTINCT=',I4,'  KTINUP=',I4,'  KTN1CT=',I4,'  KTN1UP=',I4
     &,'  KVOCT=',I4,'  KVOUP=',I4)
      WRITE(8,6002) HTNUM,HTNUMH,HTNHI(1),HTNHI(N1)
 6002 FORMAT(1H ,10X,'NUM=',E11.4,'    ;  HTNUMH=',E11.4,35('-'),
     &       '  NU(1)=',E11.4,' NU(N1)=',E11.4/)
      RETURN
  111 CONTINUE
      IF((KE/IHT*IHT-KE).NE.0) RETURN
C
      WRITE(8,6003) HTNUM,HTNUMH,HTNHI(1),HTNHI(N1)
 6003 FORMAT(1H ,10X,'NUM=',E11.4,'    ;  HTNUMH=',E15.8,31('+'),
     &       '  NU(1)=',E11.4,' NU(N1)=',E11.4/)
      RETURN
      END
```

```
C-------- NEW.FORT77(PRINT) ---------------------------
C                          (PRINT)
C
      SUBROUTINE PRINT
C
      IMPLICIT REAL*8 (A-H,O-Z)
C
      COMMON /CO1/ Y(111),R(111),THETA(150),ET(150)
     &           /CO2/ DY(111),DET(150),DA(111),DB(150)
     &           /SOLD/ ST(111,150),VO(111,150),T(111,150),PST(111,150),
     &                  PVO(111,150),PT(111,150),FST(111,150),FVO(111,150),
     &                  FT(111,150)
     &           /SOL/ HTNUM
     &           /CST2/ M1,M2,M3,N1,N2,N3
     &           /CST5/ PAI,DTIM,TIM,RDTIM
     &           /CST8/ OMG,KST,KVO,KT,KTT,KE,KP,KV,KSS,NM,NB,IMAX,KMAX
     &           /CST10/ JRAO,JBT,IJCHK,ICON
     &           /CST14/ IVI
     &    /IUP/ KT1CT,KT1UP,KTINCT,KTINUP,KTN1CT,KTN1UP,KVOCT,KVOUP
     &           /STEP/ CPUTIM,CPU,T000
C
      WRITE(8,610)   KST,KVO,KT,KE,JBT
      WRITE(8,611)   KT1CT,KT1UP,KTINCT,KTINUP,KTN1CT,KTN1UP,
     &               KVOCT,KVOUP
```

```
C       NP=N2/10
        NP=1
        KW=1
        NS=1
        NE=6
C
    1 IF(KW.EQ.1) GO TO 2
        NS=NS+6
        NE=NE+6
        IF(NE.GE.N1) NE=N1
    2 WRITE(8,614)   (J,J=NS,NE,NP)
        WRITE(8,615)   (THETA(J),J=NS,NE,NP)
        WRITE(8,617)
        NMP=1
        DO 650 I=1,M1,NMP
        WRITE(8,620)   Y(I),(R(I),ST(I,J),J=NS,NE,NP)
  672 WRITE(8,622)   (VO(I,J),J=NS,NE,NP)
  673 WRITE(8,624)   (T(I,J),J=NS,NE,NP)
  650 CONTINUE
C
        KW=KW+1
        IF(NE.LT.N1) GO TO 1
        RETURN
C
  610 FORMAT(/1H ,10X,'KST=',I4,4X,'KVO=',I4,4X,'KT=',I4,' ;; KE=',I10,
     &        '   ; JBT=',I3)
  611 FORMAT(1H ,'KT1CT=',I4,'   KT1UP=',I4,'   KTINCT=',I4,'   KTINUP=',I4
     &       ,'   KTN1CT=',I4,'   KTN1UP=',I4,'   KVOCT=',I4,'   KVOUP=',I4)
  614 FORMAT(//1H ,'   J =       ',7X,I6,5(14X,I6))
  615 FORMAT(1H ,'THETA(DEG)',6X,F7.2,5(13X,F7.2))
  617 FORMAT(/1H ,'Y',4X,6(3X,'    R     ',4X,'ST',4X))
  620 FORMAT(1H ,F6.3,6(E10.3,E10.3))
  621 FORMAT(1H ,1X,' FST ',6(10X,E10.3))
  622 FORMAT(1H ,2X,' VO ',6(10X,E10.3))
  624 FORMAT(1H ,3X,' T ',6(10X,E10.3))
  625 FORMAT(1H ,2X,' PT ',6(10X,E10.3))
  626 FORMAT(1H ,F6.0,'(DEG)',5X,E11.4,'(KCAL/M2HK)')
  627 FORMAT(1H ,10X,'NUM=',E11.4,5X,'NU(MCADAMS) = ',E11.4,' (GR*PR)=',
     &        E11.4)
  630 FORMAT(1H ,1X,' PST ',6(10X,E10.3))
  631 FORMAT(1H ,1X,' PVO ',6(10X,E10.3))
C
        END
```

```
C-------- SOR.FORT77(QCONST1) --------------------------
C ---------------- T(1,J) EXTRAPOLATION ------------------
        SUBROUTINE QCONS1
C
        IMPLICIT REAL*8 (A-H,O-Z)
C
        COMMON /CO2/ DY(111),DET(150),DA(111),DB(150)
       &       /SOLD/ ST(111,150),VO(111,150),T(111,150),PST(111,150),
       &              PVO(111,150),PT(111,150),FST(111,150),FVO(111,150),
       &              FT(111,150)
       &       /CST1/ DIA,RR,RRM,RM
       &       /CST2/ M1,M2,M3,N1,N2,N3
C
        RY=DA(2)/DA(1)
        RY1=1.D0+RY
        RY12=RY1*RY1
        RY13=RY12*RY1
        RY2=RY1+RY*RY
        RY22=RY2*RY2
        RY23=RY22*RY2
        AL=RY22/RY1
        DO 100 J=1,N1
        T(1,J)=(0.5D0*(1.D0-RM)*DA(1)*(AL*RY1*(1.D0-RY12)-RY2*(1.D0-RY22))
       &       -(RY23-AL*RY13)*T(2,J)-AL*T(3,J)+T(4,J))/((1.D0-RY23)-AL*(1
       &        .D0-RY13))
  100 CONTINUE
        RETURN
        END
```

```
C-------- NEW.FORT77(ST) --------------------------
C                       (HYBRIDST)
C
        SUBROUTINE STFU
C
        IMPLICIT REAL*8 (A-H,O-Z)
C
        COMMON /CO1/ Y(111),R(111),THETA(150),ET(150)
       &       /CO2/ DY(111),DET(150),DA(111),DB(150)
       &       /SOLD/ ST(111,150),VO(111,150),T(111,150),PST(111,150),
       &              PVO(111,150),PT(111,150),FST(111,150),FVO(111,150),
       &              FT(111,150)
       &       /CST1/ DIA,RR,RRM,RM
       &       /CST2/ M1,M2,M3,N1,N2,N3
       &       /CST5/ PAI,DTIM,TIM,RDTIM
       &       /CST6/ XX,YY,ZZ
       &       /CST8/ OMG,KST,KVO,KT,KTT,KE,KP,KV,KSS,NM,NB,IMAX,KMAX
       &       /CST9/ ERT,ERVO,ERST
       &       /CST10/ JRAO,JBT,IJCHK,ICON
       &       /CST14/ IVI
       &       /BC/ IBCT
c
```

```
      dimension CL(111,150),CM(111,150),CN(111,150),CO(111,150),
     &          CP(111,150)
C
      KST=0
      RMH1=RM-1.D0
      DD=1.D0/RMH1
      BBB=0.D0
      AF=0.D0
      BF=0.D0
      CF=0.D0
      RY=DA(2)/DA(1)
      RY1=1.D0+RY
      RY2=RY*RY
      RY12=RY1*RY1
      RY21=2.D0*RY+1.D0
      DDDD=DD*DD
C
    1 DO 100 J=2,N2
      DO 200 I=2,M2
      DBJ=DB(J)
      DBJP=DB(J-1)
      DEJ=DET(J)
      DEJP=DET(J-1)
      DEJF=DET(J+1)
C
      DEMOD=0.5D0*(DBJ+DBJP)
C
      IF(J.EQ.2) DEJP=2.D0*DET(1)
      IF(J.EQ.N2) DEJF=2.D0*DET(N1)
C
      DYI=DY(I)
      DYIP=DY(I-1)
      DYIF=DY(I+1)
      IF(I.EQ.2) DYIP=2.D0*DY(1)
      IF(I.EQ.M2) DYIF=2.D0*DY(M1)
      DAI=DA(I)
      DAIP=DA(I-1)
C
      DYMOD=0.5D0*(DAI+DAIP)
C
      YI=Y(I)
      YD=YI*DD
      DD3=1.D0/(YI*(RM-1.D0)+1.D0)
      RI2F=R(I)+0.5D0*RMH1*DYI
      RI2P=R(I)-0.5D0*RMH1*DYI
    3 D=DD3/PAI
      BB=YD*BBB
      DD2=D*D
      ALFA=(DDDD+DD2*BF*BF)
      BETA=2.D0*BF*DD2
      GAMMA=DD2
      DELTA=(DD3*DD+CF*DD2)-AF
      DELPL=DELTA+ABS(DELTA)
      DELMI=DELTA-ABS(DELTA)
C------------ CENTRAL DIFFERENCE -----------------------
      CL(I,J)=-ALFA/DYMOD*(1.D0/DAI+1.D0/DAIP)-GAMMA/DEMOD*(1.D0/DBJ
     &        +1.D0/DBJP)-0.5D0*DELTA/DYI*(DYIP/DAIP-DYIF/DAI)
      IF(CL(I,J).GT.0.D0) GO TO 333
      CM(I,J)=ALFA/DYMOD/DAI+0.5D0*DELTA/DAI
      IF(CM(I,J).LT.0.D0) GO TO 333
      CN(I,J)=ALFA/DYMOD/DAIP-0.5D0*DELTA/DAIP
      IF(CN(I,J).LT.0.D0) GO TO 333
      GO TO 344
C------------ CENTRAL DIFFERENCE -----------------------
  333 CL(I,J)=-ALFA/DYMOD*(1.D0/DAI+1.D0/DAIP)-GAMMA/DEMOD*(1.D0/DBJ
     &        +1.D0/DBJP)-0.5D0*(DELPL/DAI-DELMI/DAIP)
      CM(I,J)=ALFA/DYMOD/DAI+0.5D0*DELPL/DAI
      CN(I,J)=ALFA/DYMOD/DAIP-0.5D0*DELMI/DAIP
  344 CO(I,J)=GAMMA/DEMOD/DBJ
      CP(I,J)=GAMMA/DEMOD/DBJP
  200 CONTINUE
  100 CONTINUE
c
      do 1000 J=2,N2
      do 2000 I=2,M2
      ST(I,J)=(1.D0-OMG)*ST(I,J)
     &        -OMG*(CM(I,J)*ST(I+1,J)+CN(I,J)*ST(I-1,J)
     &        +CO(I,J)*ST(I,J+1)+CP(I,J)*ST(I,J-1)+VO(I,J))/CL(I,J)
 2000 CONTINUE
c
      ST(M1,J)=(RY12*ST(M2,J)-RY2*ST(M3,J))/RY21
 1000 CONTINUE
C
 8000 JUDGE=0
C
      IF(KST.EQ.0) GO TO 330
      JUDGE=0
      IF(KST.GT.(IMAX/5)) GO TO 331
C
      SMAX=0.D0
      DO 320 J=1,N1
      DO 320 I=1,M1
      ERS=ABS(ST(I,J))*ERST
      SAMS=ABS(ST(I,J)-FST(I,J))
C
      IF(ABS(ST(I,J)).LE.SMAX) GO TO 3200
      SMAX=ABS(ST(I,J))
      JBT=J
```

```
 3200 CONTINUE
C
      IF(SAMS.GT.ERS) GO TO 321
  320 CONTINUE
      JUDGE=1
      RETURN
C
  331 SMAX=0.D0
      DO 319 J=1,N1
      DO 319 I=1,M1
      IF(ABS(ST(I,J)).LE.SMAX) GO TO 319
      SMAX=ABS(ST(I,J))
      JBT=J
  319 CONTINUE
      ERS=ERST*SMAX
      DO 332 J=1,N1
      DO 332 I=1,M1
      SAMS=ABS(ST(I,J)-FST(I,J))
      IF(SAMS.GT.ERS) GO TO 321
  332 CONTINUE
      JUDGE=1
      RETURN
  321 IF(KST.LT.IMAX) GO TO 330
      WRITE(6,61) KE,TIM,IMAX,JBT
   61 FORMAT(1H ,'### KE=',I5,'   TIM=',E11.4,'(SEC)     IMAX=',I5,
     &       '   JBT=',I3)
      KSS=1
C
      WRITE(6,30) KE,I,J,ST(I,J),FST(I,J),SAMS,ERS
   30 FORMAT(1H ,'KE=',I5,'   F(',I3,',',I2,')=',E11.4,' FF=',E11.4,
     &       '   SAMS=',E11.4,' >',E11.4,'(ERS) DE STOP')
      IVI=1
      RETURN
C
  330 CONTINUE
      DO 335 J=1,N1
      DO 335 I=1,M1
      FST(I,J)=ST(I,J)
  335 CONTINUE
      KST=KST+1
      GO TO 1
      END
```

```
C-------- NEW.FORT77(TLAST) ---------------------------
C                          (HYBRIDST)
C
      SUBROUTINE TEMP
C
      IMPLICIT REAL*8 (A-H,O-Z)
C
      COMMON /CO1/ Y(111),R(111),THETA(150),ET(150)
     &           /CO2/ DY(111),DET(150),DA(111),DB(150)
     &           /SOLD/ ST(111,150),VO(111,150),T(111,150),PST(111,150),
     &                  PVO(111,150),PT(111,150),FST(111,150),FVO(111,150),
     &                  FT(111,150)
     &           /CST1/ DIA,RR,RRM,RM
     &           /CST2/ M1,M2,M3,N1,N2,N3
     &           /CST5/ PAI,DTIM,TIM,RDTIM
     &           /CST6/ XX,YY,ZZ
     &           /CST8/ OMG,KST,KVO,KT,KTT,KE,KP,KV,KSS,NM,NB,IMAX,KMAX
     &           /CST9/ ERT,ERVO,ERST
     &           /CST10/ JRAO,JBT,IJCHK,ICON
     &           /CST14/ IVI
     &           /BC/ IBCT
c
      dimension VRI1(111),VRIP1(111),VRIF1(111)
      dimension VTJ1(111),VTJP1(111),VTJF1(111)
      dimension VRI(111,150),VRIP(111,150),VRIF(111,150)
      dimension VTJ(111,150),VTJP(111,150),VTJF(111,150)
      dimension VTPQ1(111),VTRS1(111)
     &         ,VRQS1(111),VRPR1(111)
      dimension VTPQ(111,150),VTRS(111,150)
     &         ,VRQS(111,150),VRPR(111,150)
      dimension VTWX1(111),VTYZ1(111)
     &         ,VROT1(111),VRUV1(111)
      dimension VTWX(111,150),VTYZ(111,150)
     &         ,VROT(111,150),VRUV(111,150)
      dimension CL(111,150),CM(111,150),CN(111,150),CO(111,150),
     &          CP(111,150)
      dimension CLI(111),CMI(111),CNI(111),COI(111),CPI(111)
      dimension CLJ(150),CMJ(150),CNJ(150),COJ(150),CPJ(150)
      dimension DYK(111)
      dimension STO(111,150),STP(111,150),STQ(111,150),
     &          STR(111,150),STS(111,150),STT(111,150),
     &          STU(111,150),STV(111,150),STW(111,150),
     &          STX(111,150),STY(111,150),STZ(111,150)
C
      KT=0
      RMH1=RM-1.D0
      DD=1.D0/RMH1
      BBB=0.D0
      AF=0.D0
      BF=0.D0
      CF=0.D0
      RY=DA(2)/DA(1)
c
      DYK(1)=2.D0*DY(1)
```

```
      do 35 I=2,M2
      DYK(I)=DY(I)
   35 continue
      DYK(M1)=2.D0*DY(M1)
c
      DBJ=DB(2)
      DBJP=DB(2)
      DEJ=DET(2)
      DEJP=DET(2)
      DEJF=DET(2)
      DEMOD=0.5D0*(DBJ+DBJP)
      DEJFF=DET(2)
      DEJPP=DET(2)
      DBJF=DB(2)
      DBJPP=DB(2)
      SJ2F=RM*(DEJ+DEJF)/(2.D0*DBJ)
      SJ2P=RM*(DEJ+DEJP)/(2.D0*DBJP)
c
      DB1=DB(1)
      DBN2=DB(N2)
      RZ=DB(2)/DB1
      RY1=1.D0+RY
      RY2=RY*RY
      RY12=RY1*RY1
      RY21=2.D0*RY+1.D0
      DDDD=DD*DD
      ALF=ZZ*DDDD
    1 CONTINUE
      IF(IBCT.EQ.1) CALL QCONS1
      DO 900 I=2,M2
      DYI=DYK(I)
      DYIP=DYK(I-1)
      DYIF=DYK(I+1)
      DYIPP=DYK(I-2)
      DYIFF=DYK(I+2)
      DAI=DA(I)
      DAIP=DA(I-1)
C
      DYMOD=0.5D0*(DAI+DAIP)
      DYM=DYMOD
C
      DD3=1.D0/R(I)
      RI2F=R(I)+0.5D0*RMH1*DYI
      RI2P=R(I)-0.5D0*RMH1*DYI
      IF(I.NE.2)
     & STO(I,1)=(ST(I-1,2)*DYIPP+ST(I-2,2)*DYIP)*DET(1)
     &          /(2.D0*DA(I-2)*DB(1))
      IF(I.NE.M2)
     & STU(I,1)=(ST(I+2,2)*DYIF+ST(I+1,2)*DYIFF)*DET(1)
     &          /(2.D0*DA(I+1)*DB(1))
      STW(I,1)=(DYIP*DET(2)*ST(I,3)+DYIP*DET(3)*ST(I,2)+DYI*DET(2)
     &          *ST(I-1,3)+DYI*DET(3)*ST(I-1,2))/(4.D0*DAIP*DB(2))
      STX(I,1)=(DYI*DET(2)*ST(I+1,3)+DYI*DET(3)*ST(I+1,2)+DYIF*DET(2)
     &          *ST(I,3)+DYIF*DET(3)*ST(I,2))/(4.D0*DAI*DB(2))
   31 STQ(I,1)=DET(1)*(DYIF*ST(I,2)+DYI*ST(I+1,2))/(2.D0*DAI*DB1)
      STP(I,1)=DET(1)*(DYI*ST(I-1,2)+DYIP*ST(I,2))/(2.D0*DAIP*DB1)
      VRQS1(I)=STQ(I,1)/DET(1)/(PAI*RI2F)
      VRPR1(I)=STP(I,1)/DET(1)/(PAI*RI2P)
      VTPQ1(I)=DD*(STP(I,1)-STQ(I,1))/DYI
      VTRS1(I)=-VTPQ1(I)
      VROT1(I)=STO(I,1)/DET(1)/PAI/(R(I-1)-0.5D0*RMH1*DYIP)
      VRUV1(I)=STU(I,1)/DET(1)/PAI/(R(I+1)+0.5D0*RMH1*DYIF)
      VTWX1(I)=(STW(I,1)-STX(I,1))/DYI/RMH1
  900 continue
c
      do 909 I=2,M2
      VTYZ1(I)=-VTWX1(I)
      VRUV1(M2)=VRQS1(M2)+RY*(VRQS1(M2)-VRPR1(M2))
      VRI1(I)=0.5D0*(VRQS1(I)+VRPR1(I))
      VRIP1(I)=0.5D0*(VROT1(I)+VRPR1(I))
      VRIP1(2)=0.D0
      VRIF1(I)=0.5D0*(VRQS1(I)+VRUV1(I))
      VTJ1(I)=0.D0
      VTJF1(I)=0.5D0*(VTPQ1(I)+VTWX1(I))
      VTJP1(I)=-VTJF1(I)
  909 continue
c
      do 950 I=2,M2
      DYI=DYK(I)
      DYIP=DYK(I-1)
      DYIF=DYK(I+1)
      DAI=DA(I)
      DAIP=DA(I-1)
      DYMOD=0.5D0*(DAI+DAIP)
      DYM=DYMOD
      DD3=1.D0/R(I)
      RI2F=R(I)+0.5D0*RMH1*DYI
      RI2P=R(I)-0.5D0*RMH1*DYI
c
      DEL=ZZ*DD/R(I)
      GAM=ZZ/(PAI*PAI*R(I)*R(I))
      DELPL=DEL+ABS(DEL)
      DELMI=DEL-ABS(DEL)
C
C------------------ CENTRAL DIFFERENCE -----------------------------
      CLI(I)=-1.D0/DTIM-ALF/DYMOD*(1.D0/DAI+1.D0/DAIP)
     &          -2.D0*GAM/DB1/DB1+
     &    0.5D0*DEL/DYI*(DYIF/DAI-DYIP/DAIP)
```

```
     &   -0.5D0*DD3*DD*R(I)*VRI1(I)/DYI*(DYIF/DAI-DYIP/DAIP)
      IF(CLI(I).GT.0.D0) GO TO 8880
      CMI(I)=ALF/DYMOD/DAI+DEL/(2.D0*DAI)-0.5D0*DD3*DD/DAI*R(I+1)
     &          *VRIF1(I)
      IF(CMI(I).LT.0.D0) GO TO 8880
      CNI(I)=ALF/DYMOD/DAIP-DEL/(2.D0*DAIP)+0.5D0*DD3*DD/DAIP
     &          *R(I-1)*VRIP1(I)
      IF(CNI(I).LT.0.D0) GO TO 8880
      COI(I)=2.D0*GAM/DB1/DB1-DD3*VTJF1(I)/PAI/DB1
      IF(COI(I).LT.0.D0) GO TO 8880
      GO TO 8881
C---------- CENTRAL DIFFERENCE ----------
C + + + + + + + + + UPWIND   DIFFERENCE + + + + + + + + + + + + + + + +
 8880 CLI(I)=-1.D0/DTIM-ALF/DYM*(1.D0/DAI+1.D0/DAIP)
     &          -GAM/DET(1)/DB(1)-0.5D0
     & *(DELPL/DAI-DELMI/DAIP)-0.5D0*DD3*DD/DYI*(RI2F
     &   *(VRQS1(I)+ABS(VRQS1(I)))
     & -RI2P*(VRPR1(I)-ABS(VRPR1(I))))
     & -DD3*(VTPQ1(I)+ABS(VTPQ1(I))-VTRS1(I)+ABS(VTRS1(I)))/
     &    (4.D0*PAI*DET(1))
      CMI(I)=ALF/DYM/DAI+DELPL/(2.D0*DAI)-0.5D0*DD3*DD/DYI*RI2F
     &          *(VRQS1(I)-ABS(VRQS1(I)))
      CNI(I)=ALF/DYM/DAIP-DELMI/(2.D0*DAIP)+0.5D0*DD3*DD/DYI*RI2P
     &          *(VRPR1(I)+ABS(VRPR1(I)))
      COI(I)=GAM/DET(1)/DB(1)-DD3*(VTPQ1(I)-ABS(VTPQ1(I))
     &          -VTRS1(I)-ABS(VTRS1(I)))
     &          /(4.D0*PAI*DET(1))
C + + + + + + + + + UPWIND   DIFFERENCE + + + + + + + + + + + + + + + +
 8881 CPI(I)=PT(I,1)/DTIM
  950 CONTINUE
c
      do 9000 I=2,M2
      T(I,1)=-(CMI(I)*T(I+1,1)+CNI(I)*T(I-1,1)+COI(I)*T(I,2)+CPI(I))
     &         /CLI(I)
 9000 CONTINUE
c
c
      DO 100 J=2,N2
      IF(J.LE.JBT) T(M1,J)=0.D0
      DO 200 I=2,M2
C
      DYI=DYK(I)
      DYIP=DYK(I-1)
      DYIF=DYK(I+1)
      DAI=DA(I)
      DAIP=DA(I-1)
C
      DYMOD=0.5D0*(DAI+DAIP)
      DYM=DYMOD
C
      YI=Y(I)
      YD=YI*DD
      DD3=1.D0/(YI*(RM-1.D0)+1.D0)
      RI2F=R(I)+0.5D0*RMH1*DYI
      RI2P=R(I)-0.5D0*RMH1*DYI
    3 D=DD3/PAI
      BB=YD*BBB
      DD2=D*D
      ALFA=ZZ*(DDDD+DD2*BF*BF)
      BETA=2.D0*ZZ*BF*DD2
      GAMMA=ZZ*DD2
      DELTA=ZZ*(DD3*DD+CF*DD2)-AF
      DELPL=DELTA+ABS(DELTA)
      DELMI=DELTA-ABS(DELTA)
      DAIF=DA(I+1)
      DYIFF=DYK(I+2)
      DYIPP=DYK(I-2)
      DAIPP=DA(I-2)
      IF(I.EQ.M2) go to 441
      STU(I,J)=(DYIF*DEJ*ST(I+2,J+1)+DYIF*DEJF*ST(I+2,J)+DYIFF*DEJ*
     &                ST(I+1,J+1)+DYIFF*DEJF*ST(I+1,J))/(4.D0*DAIF*DBJ)
      STV(I,J)=(DYIF*DEJP*ST(I+2,J)+DYIFF*DEJ*ST(I+1,J-1)+DYIF*DEJ*
     &                ST(I+2,J-1)+DYIFF*DEJP*ST(I+1,J))/(4.D0*DAIF*DBJP)
  441 IF(I.EQ.2) go to 442
      STO(I,J)=(DYIPP*DEJF*ST(I-1,J)+DYIPP*DEJ*ST(I-1,J+1)+DYIP*DEJ
     &                *ST(I-2,J+1)+DYIP*DEJF*ST(I-2,J))/(4.D0*DAIPP*DBJ)
      STT(I,J)=(DYIP*DEJ*ST(I-2,J-1)+DYIPP*DEJ*ST(I-1,J-1)+DYIP*DEJ
     &                P*ST(I-2,J)+DYIPP*DEJP*ST(I-1,J))/(4.D0*DAIPP*DBJP)
  442 IF(J.EQ.N2) go to 443
      STW(I,J)=(DYIP*DEJF*ST(I,J+2)+DYIP*DEJFF*ST(I,J+1)+DYI*DEJF*
     &          ST(I-1,J+2)+DYI*DEJFF*ST(I-1,J+1))/(4.D0*DAIP*DBJF)
      STX(I,J)=(DYI*DEJF*ST(I+1,J+2)+DYI*DEJFF*ST(I+1,J+1)+DYIF*DEJF*
     &          ST(I,J+2)+DYIF*DEJFF*ST(I,J+1))/(4.D0*DAI*DBJF)
  443 IF(J.EQ.2) go to 51
      STY(I,J)=(DYIP*DEJPP*ST(I,J-1)+DYIP*DEJP*ST(I,J-2)+DYI*DEJPP*
     &          ST(I-1,J-1)+DYI*DEJP*ST(I-1,J-2))/(4.D0*DAIP*DBJPP)
      STZ(I,J)=(DYIF*DEJPP*ST(I,J-1)+DYIF*DEJP*ST(I,J-2)+DYI*DEJPP*
     &          ST(I+1,J-1)+DYI*DEJP*ST(I+1,J-2))/(4.D0*DAI*DBJPP)
   51 STQ(I,J)=(DYIF*DEJF*ST(I,J)+DYI*DEJF*ST(I+1,J)+DYIF*DEJ*ST(I,J+1)
     &           +DYI*DEJ*ST(I+1,J+1))/(4.D0*DAI*DBJ)
      STS(I,J)=(DYIF*DEJP*ST(I,J)+DYI*DEJP*ST(I+1,J)+DYIF*DEJ*ST(I,J-1)
     &           +DYI*DEJ*ST(I+1,J-1))/(4.D0*DAI*DBJP)
      STP(I,J)=(DYIP*DEJF*ST(I,J)+DYI*DEJF*ST(I-1,J)+DYIP*DEJ*ST(I,J+1)
     &           +DYI*DEJ*ST(I-1,J+1))/(4.D0*DAIP*DBJ)
      STR(I,J)=(DYIP*DEJP*ST(I,J)+DYI*DEJP*ST(I-1,J)+DYIP*DEJ*ST(I,J-1)
     &           +DYI*DEJ*ST(I-1,J-1))/(4.D0*DAIP*DBJP)
      VRQS(I,J)=(STQ(I,J)-STS(I,J))/DEJ/(PAI*RI2F)
      VRPR(I,J)=(STP(I,J)-STR(I,J))/DEJ/(PAI*RI2P)
```

```
      VTPQ(I,J)=(STP(I,J)-STQ(I,J))/DYI/(SJ2F-1.D0)
      VTRS(I,J)=(STR(I,J)-STS(I,J))/DYI/(SJ2P-1.D0)
      IF(I.NE.2) VROT(I,J)=(STO(I,J)-STT(I,J))/DEJ
     &                          /(PAI*(R(I-1)-0.5D0*RMH1*DYIP))
      VRUV(I,J)=(STU(I,J)-STV(I,J))/DEJ/(PAI*(R(I+1)+0.5D0*RMH1*DYIF))
      VTWX(I,J)=(STW(I,J)-STX(I,J))/DYI/RMH1
      VTYZ(I,J)=(STY(I,J)-STZ(I,J))/DYI/RMH1
  200 continue
  100 continue
c
      do 102 J=2,N2
      do 102 I=2,M2
      VRI(I,J)=0.5D0*(VRQS(I,J)+VRPR(I,J))
      VRIP(I,J)=0.5D0*(VROT(I,J)+VRPR(I,J))
      VRIF(I,J)=0.5D0*(VRQS(I,J)+VRUV(I,J))
      VTJ(I,J)=0.5D0*(VTPQ(I,J)+VTRS(I,J))
      VTJP(I,J)=0.5D0*(VTYZ(I,J)+VTRS(I,J))
      VTJP(I,2)=0.D0
      VTJF(I,J)=0.5D0*(VTPQ(I,J)+VTWX(I,J))
      VTJF(I,N2)=0.D0
  202 continue
      VRIP(2,J)=0.D0
      VRUV(M2,J)=VRQS(M2,J)+RY*(VRQS(M2,J)-VRPR(M2,J))
  102 continue
C
      do 150 J=2,N2
      do 155 I=2,M2
      DAI=DA(I)
      DAIP=DA(I-1)
      DYMOD=0.5D0*(DAI+DAIP)
      DYM=DYMOD
      YI=Y(I)
      DYI=DYK(I)
      DYIP=DYK(I-1)
      DYIF=DYK(I+1)
      DD3=1.D0/(YI*(RM-1.D0)+1.D0)
      RI2F=R(I)+0.5D0*RMH1*DYI
      RI2P=R(I)-0.5D0*RMH1*DYI
      D=DD3/PAI
      DD2=D*D
      ALFA=ZZ*(DDDD+DD2*BF*BF)
      BETA=2.D0*ZZ*BF*DD2
      GAMMA=ZZ*DD2
      DELTA=ZZ*(DD3*DD+CF*DD2)-AF
      DELPL=DELTA+ABS(DELTA)
      DELMI=DELTA-ABS(DELTA)
C----------------- CENTRAL DIFFERENCE ------------------------------
      CL(I,J)=-1.d0/DTIM-ALFA/DYMOD*(1.D0/DAI+1.D0/DAIP)
     &          -GAMMA/DEMOD*(1.D0/DBJ+
     &    1.D0/DBJP)-0.5D0*DELTA/DYI*(DYIP/DAIP-DYIF/DAI)-DD3*(0.5D0*
     &    DD*R(I)*VRI(I,J)/DYI*(DYIF/DAI-DYIP/DAIP)
     &    +0.5D0*VTJ(I,J)/PAI/DEJ*(DEJF/DBJ-DEJP/DBJP))
      IF(CL(I,J).GT.0.D0) GO TO 8890
      CM(I,J)=ALFA/DYMOD/DAI+DELTA/(2.D0*DAI)-0.5D0*DD3*DD/DAI
     &          *R(I+1)*VRIF(I,J)
      IF(CM(I,J).LT.0.D0) GO TO 8890
      CN(I,J)=ALFA/DYMOD/DAIP-DELTA/(2.D0*DAIP)+0.5D0*DD3*DD/DAIP
     &          *R(I-1)*VRIP(I,J)
      IF(CN(I,J).LT.0.D0) GO TO 8890
      CO(I,J)=GAMMA/DEMOD/DBJ-0.5D0*DD3*VTJF(I,J)/PAI/DBJ
      IF(CO(I,J).LT.0.D0) GO TO 8890
      CP(I,J)=GAMMA/DEMOD/DBJP+0.5D0*DD3*VTJP(I,J)/PAI/DBJP
      IF(CP(I,J).LT.0.D0) GO TO 8890
      GO TO 155
C----------------- CENTRAL DIFFERENCE ------------------------------
C + + + + + + + + + UPWIND   DIFFERENCE + + + + + + + + + + + + + + + +
 8890 CL(I,J)=-1.d0/DTIM-ALFA/DYM*(1.D0/DAI+1.D0/DAIP)-GAMMA/DEJ
     &          *(1.D0/DBJ+1.D0
     &   /DBJP)-0.5D0*(DELPL/DAI-DELMI/DAIP)-DD3*(DD*(RI2F*(VRQS(I,J)
     &   +ABS(VRQS(I,J)))-RI2P*(VRPR(I,J)-ABS(VRPR(I,J))))
     &   /(2.D0*DYI)+0.5D0/DEJ/PAI
     &          *(VTPQ(I,J)+ABS(VTPQ(I,J))-VTRS(I,J)+ABS(VTRS(I,J))))
      CM(I,J)=ALFA/DYM/DAI+0.5D0*DELPL/DAI-0.5D0*DD3*DD*RI2F/DYI
     &          *(VRQS(I,J)-ABS(VRQS(I,J)))
      CN(I,J)=ALFA/DYM/DAIP-0.5D0*DELMI/DAIP+0.5D0*DD3*DD*RI2P/DYI
     &          *(VRPR(I,J)+ABS(VRPR(I,J)))
      CO(I,J)=GAMMA/DEJ/DBJ-0.5D0*DD3/DEJ
     &          *(VTPQ(I,J)-ABS(VTPQ(I,J)))/PAI
      CP(I,J)=GAMMA/DEJ/DBJP+0.5D0*DD3/DEJ
     &          *(VTRS(I,J)+ABS(VTRS(I,J)))/PAI
C + + + + + + + + + UPWIND   DIFFERENCE + + + + + + + + + + + + + + + +
  155 continue
  150 continue
c
      do 1010 J=2,N2
      do 1010 I=2,M2
      T(I,J)=-(CM(I,J)*T(I+1,J)+CN(I,J)*T(I-1,J)+CO(I,J)*T(I,J+1)
     &       +CP(I,J)*T(I,J-1)+PT(I,J)/DTIM)/CL(I,J)
 1010 continue
c
      GAMMA=ZZ/(PAI*PAI*RM*RM)
      do 1011 J=2,N2
      IF(J.LE.JBT) GO TO 1011
      RM2F=RM+RMH1*DY(M1)
      RM2P=RM-RMH1*DY(M1)
      STP(M1,J)=(ST(M2,J+1)*DEJ*2.D0*DY(M1)+ST(M2,J)*DEJF*2.D0*DY(M1)
     &    +ST(M1,J+1)*DY(M2)*DEJ+ST(M1,J)*DEJF*DY(M2))/(4.D0*DBJ*DA(M2))
      STR(M1,J)=(ST(M2,J)*DEJP*2.D0*DY(M1)+ST(M2,J-1)*DEJ*2.D0*DY(M1)
```

```
     &   +ST(M1,J)*DY(M2)*DEJP+ST(M1,J-1)*DEJ*DY(M2))/(4.D0*DBJP*DA(M2))
      VRQS(M1,J)=(STP(M1,J)-STR(M1,J))/DEJ/(PAI*RM2F)
      VRPR(M1,J)=(STP(M1,J)-STR(M1,J))/DEJ/(PAI*RM2P)
      VROT(M1,J)=VRPR(M1,J)-(VRQS(M1,J)-VRPR(M1,J))/RY
      VRUV(M1,J)=VRQS(M1,J)+RY*(VRQS(M1,J)-VRPR(M1,J))
      VRI(M1,J)=0.5D0*(VRQS(M1,J)+VRPR(M1,J))
      VRIP(M1,J)=0.5D0*(VROT(M1,J)+VRPR(M1,J))
      VRIF(M1,J)=0.5D0*(VRQS(M1,J)+VRUV(M1,J))
      CLJ(J)=-1.D0/DTIM-4.D0*ALF/DA(M2)/DA(M2)/(1.D0+RY)-GAMMA/DEJ
     &        *(1.D0/DBJ+1.D0/DBJP)-DD
     & /RM*0.5D0*(RM*(VRI(M1,J)+ABS(VRI(M1,J)))/DA(M2)
     &    +(RM+RY*DA(M2))/RY/DA(M2)
     &    *(VRIF(M1,J)-ABS(VRIF(M1,J)))*(1.D0-RY)
     &    -RM*(VRI(M1,J)-ABS(VRI(M1,J)))/RY/DA(M2))
      CMJ(J)=GAMMA/DEJ/DBJ
      CNJ(J)=GAMMA/DEJ/DBJP
      COJ(J)=4.D0*ALF/DA(M2)/DA(M2)/(1.D0+RY)-DD/RM/2.D0/DA(M2)
     &    *((RM+RY*DA(M2))*(VRIF(M1,J)-ABS(VRIF(M1,J)))
     &     -R(M2)*(VRIP(M1,J)+ABS(VRIP(M1,J))))
      CPJ(J)=PT(M1,J)/DTIM
 1011 continue
c
      do 1012 J=JBT+1,N2
      T(M1,J)=-(CMJ(J)*T(M1,J+1)+CNJ(J)*T(M1,J-1)+COJ(J)*T(M2,J)
     &          +CPJ(J))/CLJ(J)
 1012 CONTINUE
C---------------------- IN CASE JBT=N2 -----------------------
      T(M1,N1)=(RY12*T(M2,N1)-RY2*T(M3,N1))/RY21
C---------------------- IN CASE JBT=N2 -----------------------
      DO 1013 I=2,M2
      DYI=DYK(I)
      DYIP=DYK(I-1)
      DYIF=DYK(I+1)
      DYIPP=DYK(I-2)
      DYIFF=DYK(I+2)
      DAI=DA(I)
      DAIP=DA(I-1)
C
      DYMOD=0.5D0*(DAI+DAIP)
      DYM=DYMOD
C
      DD3=1.D0/R(I)
      RI2F=R(I)+0.5D0*RMH1*DYI
      RI2P=R(I)-0.5D0*RMH1*DYI
      IF(I.NE.2)
     & STT(I,N1)=(ST(I-2,N2)*DYIP+ST(I-1,N2)*DYIPP)*DET(N1)
     &           /(2.D0*DA(I-2)*DBN2)
      IF(I.NE.M2)
     & STV(I,N1)=(ST(I+1,N2)*DYIFF+ST(I+2,N2)*DYIF)*DET(N1)
     &           /(2.D0*DA(I+1)*DBN2)
      STY(I,N1)=(DYIP*DET(N3)*ST(I,N2)+DYIP*DET(N2)*ST(I,N3)
     &          +DYI*DET(N3)*ST(I-1,N2)+DYI*DET(N2)*ST(I-1,N3))
     &          /(4.D0*DAIP*DB(N3))
      STZ(I,N1)=(DYIF*DET(N3)*ST(I,N2)+DYIF*DET(N2)*ST(I,N3)
     &          +DYI*DET(N3)*ST(I+1,N2)+DYI*DET(N2)*ST(I+1,N3))
     &          /(4.D0*DAI*DB(N3))
 611 STR(I,N1)=DET(N1)*(DYIP*ST(I,N2)+DYI*ST(I-1,N2))/(2.D0*DAIP*DBN2)
      STS(I,N1)=DET(N1)*(DYI*ST(I+1,N2)+DYIF*ST(I,N2))/(2.D0*DAI*DBN2)
      VRQS(I,N1)=-STS(I,N1)/DET(N1)/(PAI*RI2F)
      VRPR(I,N1)=-STR(I,N1)/DET(N1)/(PAI*RI2P)
      VTPQ(I,N1)=DD*(STS(I,N1)-STR(I,N1))/DYI
      VTRS(I,N1)=-VTPQ(I,N1)
      VRUV(I,N1)=-STV(I,N1)/DET(N1)/PAI/(R(I+1)+0.5D0*RMH1*DYIF)
      VROT(I,N1)=-STT(I,N1)/DET(N1)/PAI/(R(I-1)-0.5D0*RMH1*DYIP)
      VTWX(I,N1)=(STZ(I,N1)-STY(I,N1))/DYI/RMH1
 1013 continue
c
      do 1023 I=2,M2
      VTYZ(I,N1)=-VTWX(I,N1)
      VRUV(M2,N1)=VRQS(M2,N1)+RY*(VRQS(M2,N1)-VRPR(M2,N1))
   63 VRI(I,N1)=0.5D0*(VRQS(I,N1)+VRPR(I,N1))
      VRIP(I,N1)=0.5D0*(VROT(I,N1)+VRPR(I,N1))
      VRIP(2,N1)=0.D0
      VRIF(I,N1)=0.5D0*(VRQS(I,N1)+VRUV(I,N1))
      VTJ(I,N1)=0.D0
      VTJP(I,N1)=0.5D0*(VTYZ(I,N1)+VTRS(I,N1))
      VTJF(I,N1)=-VTJP(I,N1)
 1023 continue
c
      do 1014 I=2,M2
      DYI=DYK(I)
      DYIP=DYK(I-1)
      DYIF=DYK(I+1)
      DAI=DA(I)
      DAIP=DA(I-1)
      DYMOD=0.5D0*(DAI+DAIP)
      DYM=DYMOD
      DD3=1.D0/R(I)
      RI2F=R(I)+0.5D0*RMH1*DYI
      RI2P=R(I)-0.5D0*RMH1*DYI
c
      DEL=ZZ*DD/R(I)
      GAM=ZZ/(PAI*PAI*R(I)*R(I))
      DELPL=DEL+ABS(DEL)
      DELMI=DEL-ABS(DEL)
C------------------ CENTRAL DIFFERENCE -------------------------
      CLI(I)=-1.D0/DTIM-ALF/DYMOD*(1.D0/DAI+1.D0/DAIP)
     &   -2.D0*GAM/DBN2/DBN2
```

```
     &   +0.5D0*DEL/DYI*(DYIF/DAI-DYIP/DAIP)
     &   -0.5D0*DD3*DD*R(I)*VRI(I,N1)/DYI*(DYIF/DAI-DYIP/DAIP)
      IF(CLI(I).GT.0.D0) GO TO 888
      CMI(I)=ALF/DYMOD/DAI+DEL/(2.D0*DAI)-0.5D0*DD3*DD/DAI*R(I+1)
     &         *VRIF(I,N1)
      IF(CMI(I).LT.0.D0) GO TO 888
      CNI(I)=ALF/DYMOD/DAIP-DEL/(2.D0*DAIP)+0.5D0*DD3*DD/DAIP
     &         *R(I-1)*VRIP(I,N1)
      IF(CNI(I).LT.0.D0) GO TO 888
      COI(I)=2.D0*GAM/DBN2/DBN2+DD3*VTJP(I,N1)/PAI/DBN2
      IF(COI(I).LT.0.D0) GO TO 888
      GO TO 889
C------------------ CENTRAL DIFFERENCE -----------------------------
C + + + + + + + + + UPWIND   DIFFERENCE + + + + + + + + + + + + + + + +
  888 CLI(I)=-1.D0/DTIM-ALF/DYM*(1.D0/DAI+1.D0/DAIP)-GAM/DET(N1)/DB(N2)
     &         -0.5
     &    D0*(DELPL/DAI-DELMI/DAIP)-0.5D0*DD3*DD/DYI
     &    *(RI2F*(VRQS(I,N1)+ABS(VRQS(I,N1)
     &    ))-RI2P*(VRPR(I,N1)-ABS(VRPR(I,N1))))
     &    -DD3*(VTPQ(I,N1)+ABS(VTPQ(I,N1))-VTRS(I,N1)+ABS(VTRS(I,N1)))/
     &    (4.D0*PAI*DET(N1))
      CMI(I)=ALF/DYM/DAI+DELPL/(2.D0*DAI)-0.5D0*DD3*DD/DYI*RI2F*
     &         (VRQS(I,N1)-ABS(VRQS(I,N1)))
      CNI(I)=ALF/DYM/DAIP-DELMI/(2.D0*DAIP)+0.5D0*DD3*DD/DYI*RI2P*
     &          (VRPR(I,N1)+ABS(VRPR(I,N1)))
      COI(I)=GAM/DET(N1)/DB(N2)-DD3
     &     *(VTPQ(I,N1)-ABS(VTPQ(I,N1))-VTRS(I,N1)-ABS(VTRS(I,N1)))/
     &    (4.D0*PAI*DET(N1))
C + + + + + + + + + UPWIND   DIFFERENCE + + + + + + + + + + + + + + + +
  889 CPI(I)=PT(I,N1)/DTIM
 1014 CONTINUE
c
      do 1015 I=2,M2
      T(I,N1)=-(CMI(I)*T(I+1,N1)+CNI(I)*T(I-1,N1)+COI(I)*T(I,N2)
     &          +CPI(I))/CLI(I)
 1015 CONTINUE
C
 8000 JUDGE=0
C
      IF(KT.EQ.0) GO TO 330
      JUDGE=0
      IF(KT.GT.(IMAX/5)) GO TO 331
C
      SMAX=0.D0
      DO 320 J=1,N1
      DO 320 I=1,M1
      ERS=ABS(T(I,J))*ERT
      SAMS=ABS(T(I,J)-FT(I,J))
      IF(SAMS.GT.ERS) GO TO 321
  320 CONTINUE
      JUDGE=1
      RETURN
C
  331 SMAX=0.D0
      DO 319 J=1,N1
      DO 319 I=1,M1
C
      IF(ABS(T(I,J)).LE.SMAX) GO TO 319
      SMAX=ABS(T(I,J))
C
  319 CONTINUE
      ERS=ERT*SMAX
      DO 332 J=1,N1
      DO 332 I=1,M1
      SAMS=ABS(T(I,J)-FT(I,J))
      IF(SAMS.GT.ERS) GO TO 321
  332 CONTINUE
      JUDGE=1
      RETURN
  321 IF(KT.LT.IMAX) GO TO 330
      WRITE(8,61) KE,TIM,IMAX,JBT
   61 FORMAT(1H ,'### KE=',I5,'   TIM=',E11.4,'(SEC)     IMAX=',I5,
     &         '   JBT=',I3)
      KSS=1
C
      WRITE(8,30) KE,I,J,T(I,J),FT(I,J),SAMS,ERS
   30 FORMAT(1H ,'KE=',I5,'   F(',I3,',',I2,')=',E11.4,' FF=',E11.4,
     &         '   SAMS=',E11.4,' >',E11.4,'(ERS) DE STOP')
      IVI=1
      RETURN
C
  330 CONTINUE
      DO 335 J=1,N1
      DO 335 I=1,M1
      FT(I,J)=T(I,J)
  335 CONTINUE
C
      KT=KT+1
      GO TO 1
      END
```

```
C-------- NEW.FORT77(VOLAST) -------------------------
C                          (HYBRIDST)
C
      SUBROUTINE VORT
C
      IMPLICIT REAL*8 (A-H,O-Z)
```

```
C
      COMMON /CO1/ Y(111),R(111),THETA(150),ET(150)
     &            /CO2/ DY(111),DET(150),DA(111),DB(150)
     &            /SOLD/ ST(111,150),VO(111,150),T(111,150),PST(111,150),
     &                   PVO(111,150),PT(111,150),FST(111,150),FVO(111,150),
     &                   FT(111,150)
     &            /CST1/ DIA,RR,RRM,RM
     &            /CST2/ M1,M2,M3,N1,N2,N3
     &            /CST5/ PAI,DTIM,TIM,RDTIM
     &            /CST6/ XX,YY,ZZ
     &            /CST8/ OMG,KST,KVO,KT,KTT,KE,KP,KV,KSS,NM,NB,IMAX,KMAX
     &            /CST9/ ERT,ERVO,ERST
     &            /CST10/ JRAO,JBT,IJCHK,ICON
     &            /CST14/ IVI
     &            /BC/ IBCT
c
      dimension CL(111,150),CM(111,150),CN(111,150),CO(111,150),
     &          CP(111,150),CQ(111,150)
      dimension VRI(111,150),VRIP(111,150),VRIF(111,150)
      dimension VTJ(111,150),VTJP(111,150),VTJF(111,150)
      dimension VTPQ(111,150),VTRS(111,150)
     &         ,VRQS(111,150),VRPR(111,150)
      dimension VTWX(111,150),VTYZ(111,150)
     &         ,VROT(111,150),VRUV(111,150)
      dimension DYK(111)
      dimension STO(111,150),STP(111,150),STQ(111,150),
     &          STR(111,150),STS(111,150),STT(111,150),
     &          STU(111,150),STV(111,150),STW(111,150),
     &          STX(111,150),STY(111,150),STZ(111,150)
C
      KVO=0
      RMH1=RM-1.D0
      DD=1.D0/RMH1
      BBB=0.D0
      AF=0.D0
      BF=0.D0
      CF=0.D0
      RY=DA(2)/DA(1)
      RZ=DB(2)/DB(1)
      RY1=1.D0+RY
      DDDD=DD*DD
c
      DYK(1)=2.D0*DY(1)
      do 35 I=2,M2
      DYK(I)=DY(I)
   35 continue
      DYK(M1)=2.D0*DY(M1)
c
      DBJ=DB(2)
      DBJP=DB(2)
      DEJ=DET(2)
      DEJP=DET(2)
      DEJF=DET(2)
      SJ2F=RM*(DEJ+DEJF)/(2.D0*DBJ)
      SJ2P=RM*(DEJ+DEJP)/(2.D0*DBJP)
C
      DEMOD=0.5D0*(DBJ+DBJP)
      DEJFF=DET(2)
      DBJPP=DB(2)
      DEJPP=DET(2)
      DBJF=DB(2)
c
      do 1010 J=2,N2
      VO(1,J)=2.D0*DDDD*(ST(3,J)-RY1*RY1*RY1*ST(2,J))/(RY*RY1*RY1*DA(1)*
     &          DA(1))
      VO(M1,J)=-2.D0*((ST(M1,J+1)-ST(M1,J))/DBJ-(ST(M1,J)-
     &          ST(M1,J-1))/DBJP)/(DBJ+DBJP)/(PAI*RM)**2
 1010 continue
    1 DO 100 J=2,N2
c
      DO 200 I=2,M2
      DYI=DYK(I)
      DYIP=DYK(I-1)
      DYIF=DYK(I+1)
      DAIF=DA(I+1)
      DYIFF=DYK(I+2)
      DYIPP=DYK(I-2)
      DAIPP=DA(I-2)
      DAI=DA(I)
      DAIP=DA(I-1)
C
       DYMOD=0.5D0*(DAI+DAIP)
       DYM=DYMOD
C
      YI=Y(I)
      YD=YI*DD
      DD3=1.D0/(YI*(RM-1.D0)+1.D0)
      RI2F=R(I)+0.5D0*RMH1*DYI
      RI2P=R(I)-0.5D0*RMH1*DYI
    3 D=DD3/PAI
      BB=YD*BBB
      DD2=D*D
      IF(I.eq.M2) go to 43
          STU(I,J)=(DYIF*DEJ*ST(I+2,J+1)+DYIF*DEJF*ST(I+2,J)+DYIFF*DEJ*
     &                ST(I+1,J+1)+DYIFF*DEJF*ST(I+1,J))/(4.D0*DAIF*DBJ)
          STV(I,J)=(DYIF*DEJP*ST(I+2,J)+DYIFF*DEJ*ST(I+1,J-1)+DYIF*DEJ*
     &                ST(I+2,J-1)+DYIFF*DEJP*ST(I+1,J))/(4.D0*DAIF*DBJP)
   43 IF(I.eq.2) go to 42
```

```
      STO(I,J)=(DYIPP*DEJF*ST(I-1,J)+DYIPP*DEJ*ST(I-1,J+1)+DYIP*DEJ
     &              *ST(I-2,J+1)+DYIP*DEJF*ST(I-2,J))/(4.D0*DAIPP*DBJ)
      STT(I,J)=(DYIP*DEJ*ST(I-2,J-1)+DYIPP*DEJ*ST(I-1,J-1)+DYIP*DEJP
     &              *ST(I-2,J)+DYIPP*DEJP*ST(I-1,J))/(4.D0*DAIPP*DBJP)
   42 IF(J.eq.2) go to 41
      STY(I,J)=(DYIP*DEJPP*ST(I,J-1)+DYIP*DEJP*ST(I,J-2)+DYI*DEJPP
     &              *ST(I-1,J-1)+DYI*DEJP*ST(I-1,J-2))/(4.D0*DAIP*DBJPP)
      STZ(I,J)=(DYIF*DEJPP*ST(I,J-1)+DYIF*DEJP*ST(I,J-2)+DYI*DEJPP
     &              *ST(I+1,J-1)+DYI*DEJP*ST(I+1,J-2))/(4.D0*DAI*DBJPP)
   41 IF(J.eq.N2) go to 31
      STW(I,J)=(DYIP*DEJF*ST(I,J+2)+DYIP*DEJFF*ST(I,J+1)+DYI*DEJF
     &              *ST(I-1,J+2)+DYI*DEJFF*ST(I-1,J+1))/(4.D0*DAIP*DBJF)
      STX(I,J)=(DYI*DEJF*ST(I+1,J+2)+DYI*DEJFF*ST(I+1,J+1)+DYIF*DEJF
     &              *ST(I,J+2)+DYIF*DEJFF*ST(I,J+1))/(4.D0*DAI*DBJF)
   31 STQ(I,J)=(DYIF*DEJF*ST(I,J)+DYI*DEJF*ST(I+1,J)+DYIF*DEJ*ST(I,J+1)
     &            +DYI*DEJ*ST(I+1,J+1))/(4.D0*DAI*DBJ)
      STS(I,J)=(DYIF*DEJP*ST(I,J)+DYI*DEJP*ST(I+1,J)+DYIF*DEJ*ST(I,J-1)
     &            +DYI*DEJ*ST(I+1,J-1))/(4.D0*DAI*DBJP)
      STP(I,J)=(DYIP*DEJF*ST(I,J)+DYI*DEJF*ST(I-1,J)+DYIP*DEJ*ST(I,J+1)
     &             +DYI*DEJ*ST(I-1,J+1))/(4.D0*DAIP*DBJ)
      STR(I,J)=(DYIP*DEJP*ST(I,J)+DYI*DEJP*ST(I-1,J)+DYIP*DEJ*ST(I,J-1)
     &            +DYI*DEJ*ST(I-1,J-1))/(4.D0*DAIP*DBJP)
      VRQS(I,J)=(STQ(I,J)-STS(I,J))/DEJ/(PAI*RI2F)
      VRPR(I,J)=(STP(I,J)-STR(I,J))/DEJ/(PAI*RI2P)
      VTPQ(I,J)=(STP(I,J)-STQ(I,J))/DYI/(SJ2F-1.D0)
      VTRS(I,J)=(STR(I,J)-STS(I,J))/DYI/(SJ2P-1.D0)
      IF(I.NE.2)
     &VROT(I,J)=(STO(I,J)-STT(I,J))/DEJ/(PAI*(R(I-1)-0.5D0*RMH1*DYIP))
      VRUV(I,J)=(STU(I,J)-STV(I,J))/DEJ/(PAI*(R(I+1)+0.5D0*RMH1*DYIF))
      VTWX(I,J)=(STW(I,J)-STX(I,J))/DYI/RMH1
      VTYZ(I,J)=(STY(I,J)-STZ(I,J))/DYI/RMH1
  200 continue
  100 continue
c
      do 102 J=2,N2
      do 202 I=2,M2
      VRI(I,J)=0.5D0*(VRQS(I,J)+VRPR(I,J))
      VRIP(I,J)=0.5D0*(VROT(I,J)+VRPR(I,J))
      VRIF(I,J)=0.5D0*(VRQS(I,J)+VRUV(I,J))
      VTJ(I,J)=0.5D0*(VTPQ(I,J)+VTRS(I,J))
      VTJP(I,J)=0.5D0*(VTYZ(I,J)+VTRS(I,J))
      VTJP(I,2)=0.D0
      VTJF(I,J)=0.5D0*(VTPQ(I,J)+VTWX(I,J))
      VTJF(I,N2)=0.D0
  202 continue
      VRIP(2,J)=0.D0
      VRUV(M2,J)=VRQS(M2,J)+(VRQS(M2,J)-VRPR(M2,J))*RY
  102 continue
c
      do 1011 J=2,N2
      do 2010 I=2,M2
      DYI=DYK(I)
      DYIP=DYK(I-1)
      DYIF=DYK(I+1)
      DAI=DA(I)
      DAIP=DA(I-1)
      DYMOD=0.5D0*(DAI+DAIP)
      DYM=DYMOD
      YI=Y(I)
      YD=YI*DD
      DD3=1.D0/(YI*(RM-1.D0)+1.D0)
      RI2F=R(I)+0.5D0*RMH1*DYI
      RI2P=R(I)-0.5D0*RMH1*DYI
      D=DD3/PAI
      BB=YD*BBB
      DD2=D*D
      ALFA=XX*(DDDD+DD2*BF*BF)
      BETA=2.D0*XX*BF*DD2
      GAMMA=XX*DD2
      DELTA=XX*(DD3*DD+CF*DD2)-AF
      DELPL=DELTA+ABS(DELTA)
      DELMI=DELTA-ABS(DELTA)
C
      DTDY=((DYI*T(I+1,J)+DYIF*T(I,J))/(2.D0*DAI)-(DYIP*T(I,J)
     &        +DYI*T(I-1,J))/(2.D0*DAIP))/DYI
      DTDET=((DEJ*T(I,J+1)+DEJF*T(I,J))/(2.D0*DBJ)-(DEJP*T(I,J)
     &        +DEJ*T(I,J-1))/(2.D0*DBJP))/DEJ
C
C----------------- CENTRAL DIFFERENCE --------------------------
      CL(I,J)=-1.d0/DTIM-ALFA/DYMOD*(1.D0/DAI+1.D0/DAIP)
     &          -GAMMA/DEMOD*(1.D0/DBJ+1.D0/DBJP)
     &  -0.5D0*DELTA/DYI*(DYIP/DAIP-DYIF/DAI)-DD3*(0.5D0*DD
     &  *R(I)*VRI(I,J)/DYI*(DYIF/DAI-DYIP/DAIP)
     &  +0.5D0/PAI*VTJ(I,J)/DEJ*(DEJF/DBJ-DEJP/DBJP))
      IF(CL(I,J).GT.0.D0) GO TO 777
      CM(I,J)=ALFA/DYMOD/DAI+0.5D0*DELTA/DAI
     &          -0.5D0*DD3*DD*R(I+1)/DAI*VRIF(I,J)
      IF(CM(I,J).LT.0.D0) GO TO 777
      CN(I,J)=ALFA/DYMOD/DAIP-0.5D0*DELTA/DAIP+0.5D0*DD3*DD
     &          *R(I-1)/DAIP*VRIP(I,J)
      IF(CN(I,J).LT.0.D0) GO TO 777
      CO(I,J)=GAMMA/DEMOD/DBJ-0.5D0*DD3/DBJ*VTJF(I,J)/PAI
      IF(CO(I,J).LT.0.D0) GO TO 777
      CP(I,J)=GAMMA/DEMOD/DBJP+0.5D0*DD3/DBJP*VTJP(I,J)/PAI
      IF(CP(I,J).LT.0.D0) GO TO 777
      GO TO 7777
C----------------- CENTRAL DIFFERENCE --------------------------
C + + + + + + + + + UPWIND DIFFERENCE + + + + + + + + + + + + + +
```

```
  777 CL(I,J)=-1.d0/DTIM-ALFA/DYM*(1.D0/DAI+1.D0/DAIP)
     &            -GAMMA/DEJ*(1.D0/DBJ+1.D0/DBJP)
     &            -0.5D0*(DELPL/DAI-DELMI/DAIP)
     &            -DD3*(DD*(RI2F*(VRQS(I,J)+ABS(VRQS(I,J)))
     &            -RI2P*(VRPR(I,J)-ABS(VRPR(I,J))))/(2.D0*DYI)
     &            +0.5D0/DEJ/PAI*(VTPQ(I,J)+ABS(VTPQ(I,J))
     &            -VTRS(I,J)+ABS(VTRS(I,J))))
       CM(I,J)=ALFA/DYM/DAI+0.5D0*DELPL/DAI-0.5D0*DD3*DD*RI2F/DYI
     &          *(VRQS(I,J)-ABS(VRQS(I,J)))
       CN(I,J)=ALFA/DYM/DAIP-0.5D0*DELMI/DAIP+0.5D0*DD3*DD*RI2P/DYI
     &          *(VRPR(I,J)+ABS(VRPR(I,J)))
       CO(I,J)=GAMMA/DEJ/DBJ-0.5D0*DD3/DEJ*(VTPQ(I,J)-ABS(VTPQ(I,J)))/PAI
       CP(I,J)=GAMMA/DEJ/DBJP+0.5D0*DD3/DEJ*(VTRS(I,J)+ABS(VTRS(I,J)))
     &          /PAI
C + + + + + + + + + UPWIND DIFFERENCE + + + + + + + + + + + + + +
 7777 CQ(I,J)=PVO(I,J)/DTIM+YY*(SIN(PAI*THETA(J)/180.D0)*DD*DTDY
     &          +COS(PAI*THETA(J)/180.D0)/PAI/R(I)*(DTDET+BB*DTDY))
 2010 CONTINUE
 1011 CONTINUE
c
       do 110 J=2,N2
       do 220 I=2,M2
       VO(I,J)=-(CM(I,J)*VO(I+1,J)+CN(I,J)*VO(I-1,J)
     &          +CO(I,J)*VO(I,J+1)+CP(I,J)*VO(I,J-1)+CQ(I,J))
     &          /CL(I,J)
  220 CONTINUE
  110 CONTINUE
C
 8000 JUDGE=0
C
       IF(KVO.EQ.0) GO TO 330
       JUDGE=0
C
       IO=1
       IF(IO.EQ.1) GO TO 331
C
       IF(KVO.GT.(IMAX/5)) GO TO 331
C
       SMAX=0.D0
       DO 320 J=1,N1
       DO 320 I=1,M1
       ERS=ABS(VO(I,J))*ERVO
       SAMS=ABS(VO(I,J)-FVO(I,J))
       IF(SAMS.GT.ERS) GO TO 321
  320 CONTINUE
       JUDGE=1
       RETURN
C
  331 SMAX=0.D0
       DO 319 J=1,N1
       DO 319 I=1,M1
C      IF(ABS(F(I,J)).GT.SMAX) SMAX=ABS(F(I,J))
C
       IF(ABS(VO(I,J)).LE.SMAX) GO TO 319
       SMAX=ABS(VO(I,J))
C
  319 CONTINUE
       ERS=ERVO*SMAX
       DO 332 J=1,N1
       DO 332 I=1,M1
       SAMS=ABS(VO(I,J)-FVO(I,J))
       IF(SAMS.GT.ERS) GO TO 321
  332 CONTINUE
       JUDGE=1
       RETURN
  321 IF(KVO.LT.IMAX) GO TO 330
       WRITE(8,61) KE,TIM,IMAX,JBT
   61 FORMAT(1H ,'### KE=',I5,'   TIM=',E11.4,'(SEC)    IMAX=',I5,
     &        '   JBT=',I3)
       KSS=1
C
       WRITE(8,30) KE,I,J,VO(I,J),FVO(I,J),SAMS,ERS
   30 FORMAT(1H ,'KE=',I5,'   F(',I3,',',I2,')=',E11.4,' FF=',E11.4,
     &        '   SAMS=',E11.4,' >',E11.4,'(ERS) DE STOP')
       IVI=1
       RETURN
C
  330 CONTINUE
       DO 335 J=1,N1
       DO 335 I=1,M1
       FVO(I,J)=VO(I,J)
  335 CONTINUE
C
       KVO=KVO+1
       GO TO 1
       END
```

```
-
       SUBROUTINE SUBTRP (HNU,NN,HNUSOL)
       IMPLICIT REAL*8(A-H,O-Z)
C
       COMMON /CO1/ Y(111),R(111),THETA(150),ET(150)
       DIMENSION HNU(150)

C
       SOL=0.D0
       DO 10 J=2,NN
```

```
   10 SOL=(ET(J)-ET(J-1))*(HNU(J)+HNU(J-1))+SOL
      HNUSOL=0.5D0*SOL/ET(NN)
C
      RETURN
      END
```

```
C-------- NEW.FORT77(COGKE) ---------------------------
C
      SUBROUTINE NCCON
C
      IMPLICIT REAL*8 (A-H,O-Z)
C
      COMMON /CO1/ Y(111),R(111),THETA(150),ET(150)
     &          /CO2/ DY(111),DET(150),DA(111),DB(150)
     &          /SOLD/ ST(111,150),VO(111,150),T(111,150),PST(111,150),
     &                 PVO(111,150),PT(111,150),FST(111,150),FVO(111,150),
     &                 FT(111,150)
     &          /YYY/ YT(111,150),YST(111,150),VR(111,150),VT(111,150),
     &                AVEL(111,150)
     &          /SOL/ HTNUM
     &          /CST1/ DIA,RR,RRM,RM
     &          /CST2/ M1,M2,M3,N1,N2,N3
     &          /CST4/ DY2,C1,CD3,DD0,D1
     &          /CST5/ PAI,DTIM,TIM,RDTIM
     &          /CST8/ OMG,KST,KVO,KT,KTT,KE,KP,KV,KSS,NM,NB,IMAX,KMAX
     &          /CST9/ ERT,ERVO,ERST
      COMMON /CST10/ JRAO,JBT,IJCHK,ICON
     &          /CST14/ IVI
     &          /PRO/ TCV
     &          /PROP/ TCL
     &          /CST20/ COEF,IU,IUST
     &          /ERMAX/ PTMAX,PSMAX,PTER,PSER,PSM
     &          /TR1/ PR,RA4
     &          /TR0/ HTN(150),HTNR(150)
     &          /TTIME/ TIM1,TIM2,TIM3,TIM4,TIM5,TIM6,IHT
     &          /NTIME/ MT1,MT2,MT3,MT4,MT5,MT6,ICONV
     &          /IJOB/ JOBITE
     &          /STEP/ CPUTIM,CPU,T000
     &          /DLT/ DLTIM
C
      MT1=TIM1/DTIM
      MT2=TIM2/DTIM
      MT3=TIM3/DTIM
      MT4=TIM4/DTIM
      MT5=TIM5/DTIM
      MT6=TIM6/DTIM
      IF(IVI.NE.0) GO TO 570
      IST=0
      IT=0
      ICONV=0
C
      IF(IU.LT.IUST.AND.KE.LT.IUST) GO TO 7
      IF((KE/IU*IU-KE).NE.0) GO TO 7
      WRITE(8,61) KE,PTER,PSER
   61 FORMAT(/1H ,40X,'@@ KE=',I10,'   PTER=',E11.4,'   PSER=',E11.4)
      CALL PRINT
      CALL NCHT
    7 CONTINUE
C
      IF(KE/NB*NB-KE) 564,8,564
    8 IF(KE.EQ.NB) GO TO 564
C
      PSM=PSMAX
      PTMAX=1.D0
      PSMAX=0.D0
      DO 563 J=1,N1
      DO 563 I=2,M2
      IF(ABS(ST(I,J)).GT.PSMAX) PSMAX=ABS(ST(I,J))
  563 CONTINUE
      DPSM=PSMAX-PSM
      IF(PSMAX.NE.0.D0) DPCON=ABS(DPSM/PSMAX)
      PTER=ERT*PTMAX*COEF
      PSER=ERST*PSMAX*COEF
C
      IF(KE.EQ.1) GO TO 564
      DO 562 J=1,N1
      DO 562 I=2,M1
      DTY=ABS(T(I,J)-YT(I,J))
      ITY=I
      JTY=J
      IF(DTY.GT.PTER) GO TO 564
  562 CONTINUE
      IT=1
C
  544 CONTINUE
      DO 566 J=2,N2
      DO 566 I=2,M1
      DSY=ABS(ST(I,J)-YST(I,J))
      IF(DSY.GT.PSER) GO TO 564
  566 CONTINUE
      IST=1
C
      IF((IT.NE.1).OR.(IST.NE.1)) GO TO 564
      ICONV=1
      WRITE(8,1000) PTER,PSER,DPSM,KE,TIM,JBT
 1000 FORMAT(1H ,'$$$$$$$$$$   CONVERGED !!!!!!!!!   PTER=',E11.4,
```

```
     &        '  PSER=',E11.4,'  DPSM=',E11.4,'  KE=',I10,'  TIM=',E11.4,
     &        '(SEC)    ; JBT=',I3)
C
      WRITE(8,666)
  666 FORMAT(/1H ,'  ¥¥¥ CONVERGED !!!')
      GO TO 570
C
  564 CONTINUE
C
      DLTIM=DLTIM+DTIM
 8888 DO 565 J=1,N1
      DO 565 I=1,M1
      PST(I,J)=ST(I,J)
      PVO(I,J)=VO(I,J)
      PT(I,J)=T(I,J)
      IF(KE/NB*NB-KE) 565,567,565
  567 YST(I,J)=ST(I,J)
      YT(I,J)=T(I,J)
  565 CONTINUE
C
      CPUTIM=second()-T000
      IF(CPUTIM.Lt.CPU) GO TO 234
      WRITE(8,667) CPU,CPUTIM,KE
      WRITE(8,668) DLTIM
  667 FORMAT(/1H ,'******** CPUSTEP=',E11.4,
     &        '(SEC) :    CPUTIM =',E11.4,'(SEC);      KE=',I10)
  668 FORMAT(1H ,'+++++ DLTIM=',E15.8)
      call PRINT
      CALL BUFFER
      STOP
  234 CONTINUE
C
      IF((KE/IHT*IHT-KE).EQ.0) WRITE(8,213) TIM,KE,DLTIM,KT,KVO,KST
      CALL NCHT
      IF((CPUTIM.LE.CPU).AND.(KE.NE.MT1).AND.(KE.NE.MT2).AND.
     &   (KE.NE.MT3).AND.(KE.NE.MT4).AND.(KE.NE.MT5).AND.
     &   (KE.NE.MT6).AND.((KE/IHT*IHT-KE).NE.0)) RETURN
  213 FORMAT(1H ,'<<<<< TIM=',F15.6,'(SEC) >>>>>      KE=',I10,' DLTIM=',
     &          E15.8,'    KT=',I4,'   KVO=',I4,'   KST=',I4)
      KV=1
C
      GO TO 5700
C
  570 CONTINUE
C          CALCULATION OF HEATTRANSFER COEFFICIENT
C
      CALL NCHT
C
 5700 CONTINUE
C
      IF(IVI.NE.0) GO TO 2000
      IF((ICONV.NE.1).AND.(CPUTIM.LE.CPU)) RETURN
      KP=KP+1
      CALL PRINT
      CALL BUFFER
C
 2000 INC=1
C
      IF(IVI.EQ.1) RETURN
      RMH1=RM-1.D0
      DO 700 I=2,M2
      DYI=DY(I)
      DYIF=DY(I+1)
      DYIP=DY(I-1)
      IF(I.EQ.2) DYIP=2.D0*DY(1)
      IF(I.EQ.M2) DYIF=2.D0*DY(M1)
      DAI=DA(I)
      DAIP=DA(I-1)
      RI2F=R(I)+0.5D0*RMH1*DYI
      RI2P=R(I)-0.5D0*RMH1*DYI
      STQ=DET(1)*(DYIF*ST(I,2)+DYI*ST(I+1,2))/(2.D0*DAI*DB(1))
      STP=DET(1)*(DYI*ST(I-1,2)+DYIP*ST(I,2))/(2.D0*DAIP*DB(1))
      VRQS=STQ/DET(1)/(PAI*RI2F)
      VRPR=STP/DET(1)/(PAI*RI2P)
      VR(I,1)=0.5D0*(VRQS+VRPR)
  700 CONTINUE
      DO 710 J=2,N2
      DEJ=DET(J)
      DEJF=DET(J+1)
      DEJP=DET(J-1)
      DBJ=DB(J)
      DBJP=DB(J-1)
      IF(J.EQ.2) DEJP=2.D0*DET(1)
      IF(J.EQ.N2) DEJF=2.D0*DET(N1)
      DO 710 I=2,M2
      DYI=DY(I)
      DYIF=DY(I+1)
      DYIP=DY(I-1)
      DAI=DA(I)
      DAIP=DA(I-1)
      IF(I.EQ.2) DYIP=2.D0*DY(1)
      IF(I.EQ.M2) DYIF=2.D0*DY(M1)
      STQ=(DYIF*DEJF*ST(I,J)+DYI*DEJF*ST(I+1,J)+DYIF*DEJ*ST(I,J+1)+DYI*
     &        DEJ*ST(I+1,J+1))/(4.D0*DAI*DBJ)
      STS=(DYIF*DEJP*ST(I,J)+DYI*DEJP*ST(I+1,J)+DYIF*DEJ*ST(I,J-1)+DYI*
     &        DEJ*ST(I+1,J-1))/(4.D0*DAI*DBJP)
      STP=(DYIP*DEJF*ST(I,J)+DYI*DEJF*ST(I-1,J)+DYIP*DEJ*ST(I,J+1)+DYI*
     &        DEJ*ST(I-1,J+1))/(4.D0*DAIP*DBJ)
```

```
      STR=(DYIP*DEJP*ST(I,J)+DYI*DEJP*ST(I-1,J)+DYIP*DEJ*ST(I,J-1)+DYI*
     &          DEJ*ST(I-1,J-1))/(4.D0*DAIP*DBJP)
      RI2F=R(I)+0.5D0*RMH1*DYI
      RI2P=R(I)-0.5D0*RMH1*DYI
      VRQS=(STQ-STS)/DEJ/(PAI*RI2F)
      VRPR=(STP-STR)/DEJ/(PAI*RI2P)
      SJ2F=RM*(DEJ+DEJF)/(2.D0*DBJ)
      SJ2P=RM*(DEJ+DEJP)/(2.D0*DBJP)
      VTPQ=(STP-STQ)/DYI/(SJ2F-1.D0)
      VTRS=(STR-STS)/DYI/(SJ2P-1.D0)
      VR(I,J)=0.5D0*(VRQS+VRPR)
      VT(I,J)=0.5D0*(VTPQ+VTRS)
  710 CONTINUE
      DO 720 I=2,M2
      DYI=DY(I)
      DYIF=DY(I+1)
      DYIP=DY(I-1)
      IF(I.EQ.2) DYIP=2.D0*DY(1)
      IF(I.EQ.M2) DYIF=2.D0*DY(M1)
      DAI=DA(I)
      DAIP=DA(I-1)
      STR=DET(N1)*(DYIP*ST(I,N2)+DYI*ST(I-1,N2))/(2.D0*DAIP*DB(N2))
      STS=DET(N1)*(DYI*ST(I+1,N2)+DYIF*ST(I,N2))/(2.D0*DAI*DB(N2))
      RI2F=R(I)+0.5D0*RMH1*DYI
      RI2P=R(I)-0.5D0*RMH1*DYI
      VRQS=-STS/DET(N1)/(PAI*RI2F)
      VRPR=-STR/DET(N1)/(PAI*RI2P)
      VR(I,N1)=0.5D0*(VRQS+VRPR)
  720 CONTINUE
      DO 730 J=2,N2
      DEJ=DET(J)
      DEJF=DET(J+1)
      DEJP=DET(J-1)
      IF(J.EQ.2) DEJP=2.D0*DET(1)
      IF(J.EQ.N2) DEJF=2.D0*DET(N1)
      DBJ=DB(J)
      DBJP=DB(J-1)
      RM2F=RM+RMH1*DY(M1)
      RM2P=RM-RMH1*DY(M1)
      STP=(ST(M2,J+1)*DEJ*2.D0*DY(M1)+ST(M2,J)*DEJF*2.D0*DY(M1)+ST(M1,J+
     &     1)*DY(M2)*DEJ+ST(M1,J)*DEJF*DY(M2))/(4.D0*DBJ*DA(M2))
      STR=(ST(M2,J)*DEJP*2.D0*DY(M1)+ST(M2,J-1)*DEJ*2.D0*DY(M1)+ST(M1,J)
     &     *DY(M2)*DEJP+ST(M1,J-1)*DEJ*DY(M2))/(4.D0*DBJP*DA(M2))
      VRQS=(STP-STR)/DEJ/(PAI*RM2F)
      VRPR=(STP-STR)/DEJ/(PAI*RM2P)
      VR(M1,J)=0.5D0*(VRQS+VRPR)
  730 CONTINUE
C
      VRMAX=0.
      VTMAX=0.
      AVMAX=0.
      IVR=0
      JVR=0
      IVT=0
      JVT=0
      IAVEL=0
      JAVEL=0
      DO 592 J=1,N1
      DO 592 I=2,M1
      IF(ABS(VR(I,J)).LT.VRMAX) GO TO 701
      IVR=I
      JVR=J
      VRMAX=ABS(VR(I,J))
  701 IF(ABS(VT(I,J)).LT.VTMAX) GO TO 592
      IVT=I
      JVT=J
      VTMAX=ABS(VT(I,J))
  592 CONTINUE
C
      KW=1
      JW=1
      NS=1
      WRITE(8,600)
      N90=N2/2+1
      NP=N2/10
      IF(N2.GE.10) GO TO 110
      N90=6
      NP=1
  110 N91=N90+NP
      NE=N90
  680 CONTINUE
  685 DO 650 I=1,M1,NM
      WRITE(8,601) (R(I),VR(I,J),J=NS,NE,NP)
      WRITE(8,602) (VT(I,J),J=NS,NE,NP)
  650 CONTINUE
   99 KW=KW+1
      IF(KW.GT.2) GO TO 101
      NS=N91
      IF(N1.LE.6) GO TO 101
      NE=N1
      GO TO 680
  101 CONTINUE
C
      WRITE(8,610) IVR,JVR,VRMAX
      WRITE(8,611) IVT,JVT,VTMAX
      RETURN
  600 FORMAT(/1H ,'**********  VELOCITY DISTRIBUTIONS  **********')
  601 FORMAT(1H ,6X,6(E10.3,1X,E9.2))
```

```
  602 FORMAT(1H ,1X,' VTH ',6(11X,E9.2))
  610 FORMAT(/1H ,'VRMAX(',I3,',',I2,')=',E11.4)
  611 FORMAT(1H ,'VTMAX(',I3,',',I2,')=',E11.4)
      END

------------------------------------------------------------------------

      SUBROUTINE BUFFER
C
      IMPLICIT REAL*8 (A-H,O-Z)
C
      COMMON /CO1/ Y(111),R(111),THETA(150),ET(150)
     &       /CO2/ DY(111),DET(150),DA(111),DB(150)
     &       /SOLD/ ST(111,150),VO(111,150),T(111,150),PST(111,150),
     &              PVO(111,150),PT(111,150),FST(111,150),FVO(111,150),
     &              FT(111,150)
     &       /CST1/ DIA,RR,RRM,RM
     &       /CST2/ M1,M2,M3,N1,N2,N3
     &       /SOL/ HTNUM
     &       /CST5/ PAI,DTIM,TIM,RDTIM
     &       /CST6/ XX,YY,ZZ
     &       /CST8/ OMG,KST,KVO,KT,KTT,KE,KP,KV,KSS,NM,NB,IMAX,KMAX
     &       /CST9/ ERT,ERVO,ERST
     &       /CST10/ JRAO,JBT,IJCHK,ICON
     &       /CST12/ PAID
     &       /CST14/ IVI
     &       /BC/ IBCT
      COMMON /PRO/ TCV
     &       /CST20/ COEF,IU,IUST
     &       /PROP/ TCL
     &       /ERMAX/ PTMAX,PSMAX,PTER,PSER,PSM
     &       /TR1/ PR,RA4
     &       /TTIME/ TIM1,TIM2,TIM3,TIM4,TIM5,TIM6,IHT
     &       /STEP/ CPUTIM,CPU,T000
     &       /DLT/ DLTIM
      DIMENSION STST(16650),FSTFST(16650),PSTPST(16650),
     &          VOVO(16650),PVOPVO(16650),TT(16650),PTPT(16650)
      EQUIVALENCE  (ST(1,1),STST(1)),(FST(1,1),FSTFST(1)),
     &             (PST(1,1),PSTPST(1)),(VO(1,1),
     &              VOVO(1)),(PVO(1,1),PVOPVO(1)),(T(1,1),TT(1)),
     &             (PT(1,1),PTPT(1))
C
      REWIND 3
      REWIND 30
      REWIND 31
      REWIND 34
C
      WRITE(30) R
      WRITE(34) STST
      WRITE(34) PSTPST
      WRITE(34) VOVO
      WRITE(34) PVOPVO
      WRITE(34) TT
      WRITE(34) PTPT
      WRITE(31) THETA
      WRITE(31) ET
      WRITE(30) Y
      WRITE(30) DY
      WRITE(31) DET
      WRITE(30) DA
      WRITE(31) DB
      WRITE(3) M1
      WRITE(3) M2
      WRITE(3) M3
      WRITE(3) N1
      WRITE(3) N2
      WRITE(3) N3
      WRITE(3) IBCT
      WRITE(3) PAI
      WRITE(3) DTIM
      WRITE(3) TIM
      WRITE(3) RDTIM
      WRITE(3) DIA
      WRITE(3) RR
      WRITE(3) RRM
      WRITE(3) RM
      WRITE(3) XX
      WRITE(3) YY
      WRITE(3) ZZ
      WRITE(3) OMG
      WRITE(3) KST
      WRITE(3) KVO
      WRITE(3) KT
      WRITE(3) KTT
      WRITE(3) KE
      WRITE(3) KP
      WRITE(3) KV
      WRITE(3) KSS
      WRITE(3) NM
      WRITE(3) NB
      WRITE(3) IMAX
      WRITE(3) KMAX
      WRITE(3) IVI
      WRITE(3) ERT
      WRITE(3) ERVO
      WRITE(3) ERST
      WRITE(3) JRAO
      WRITE(3) JBT
```

```
WRITE(3) IJCHK
WRITE(3) ICON
WRITE(3) PAID
WRITE(3) TCV
WRITE(3) COEF
WRITE(3) TCL
WRITE(3) IU
WRITE(3) IUST
WRITE(3) PTMAX
WRITE(3) PSMAX
WRITE(3) PTER
WRITE(3) PSER
WRITE(3) PSM
WRITE(3) PR
WRITE(3) RA4
WRITE(3) TIM1
WRITE(3) TIM2
WRITE(3) TIM3
WRITE(3) TIM4
WRITE(3) TIM5
WRITE(3) TIM6
WRITE(3) IHT
WRITE(3) DLTIM
print*,'DLTIM o.k.'
STOP
END
```


Fig. B-2 Source program list used for numerical analysis.

Chapter 2

Laminar Combined Forced and Free Convection Heat Transfer of Liquid Sodium in a Concentric Annulus at Low Péclet Numbers

2.1 Introduction

A study of combined forced and free convection heat transfer to liquid sodium flowing inside a concentric annulus at low flow rate is important as a database for a safety design of fast breeder reactors concerning a loss of flow accident caused by pump coastdown. Under rated operating conditions of FBR, the liquid sodium flow rate in reactor core is designed to be between 200 and 400 in terms of the Péclet number. In case of loss of flow accident, however, when a pony-motor acts only as a power source driving a coolant flow, the Péclet number range changes between 30 and 60, and it finally falls between 4 and 10 under natural circulation condition. Most of the forced convection heat transfer investigations using liquid metals have been restricted to pipe flow. Besides, no experiments with a concentric annulus has been carried out under the Péclet number below 30, and therefore almost no information on the mechanism of heat transfer at low Péclet numbers

has been available in the past.

Rensen (1981) investigated experimentally the forced convection heat transfer to liquid sodium flowing in a concentric annulus with a diameter ratio of 1.85 for the Péclet numbers ranging from about 32 to 300, and based on the experimental results, he proposed a correlation for heat transfer coefficient for the inner wall in fully developed region. The Nusselt number predicted by his correlation is about 6.1 for Pe = 30.

Several theoretical studies on laminar forced convection heat transfer in a concentric annular passage have been reported in the past (Hatton and Quarmby, 1962; Lundberg et al, 1963). However, their theoretical approaches were based on the assumption that the effects of axial heat conduction in flowing liquid, the temperature dependence of thermophysical properties, and the effect of natural convection driven by buoyancy force on heat transfer can be ignored. Moreover, the influence of heat conduction in inner cylinder and in outer pipe has not been taken into consideration. Both of their analytical solutions give the constant Nusselt number of about 6.1 for a diameter ratio of 1.85 in a fully developed region independent of the Péclet number for an entire laminar flow region, which coincides with the value obtained from the Rensen's correlation as mentioned above. However, it is not obvious that these analytical solutions based on such simplified physical model are capable of predicting the heat transfer in liquid metals with fairly high thermal conductivities.

Recently, heat transfer from the inner cylinder (7.6 mm in diameter, heater sheath of 1.1 mm in thickness, and heated section of 52 mm in length) to liquid sodium flowing inside a vertical concentric annulus (diameter ratio of 1.88, and outer pipe thickness of 3.7 mm) has been studied experimentally by Shiotsu et al (1993) for the Péclet numbers ranging from 650 down to 0.7. For Pe < 100, little existing experimental data are available, and furthermore, particularly for Pe < 30 no experimental works had been previously performed.

In evaluating local heat transfer coefficients, the local bulk mean temperature distribution of liquid sodium should be known. Petukhov and Yusin (1961) proposed a simple method for estimating the local bulk mean temperatures in a pipe flow by a linear interpolation between inlet and outlet liquid temperatures, which took into account the axial heat conduction effect. For forced convection heat transfer in a concentric annulus, however, an appropriate method for estimating the local bulk mean temperatures has not been established.

The purpose of this study is threefold. First is to obtain the numerical solution to a set of fundamental equations for combined forced and free convection heat transfer in a concentric annulus for a wide range of the Péclet number. Second is, by comparing the numerical solutions for a variety of heated lengths with the experimental results obtained by Shiotsu et al (1993), to examine the validity of the linear interpolation method for estimating local bulk mean temperatures. Third is to derive an approximate analytical solution capable of describing the numerical solutions of local bulk mean temperatures for a variety of heated lengths.

2.2 Numerical Analysis

2.2.1 Numerical Model for a Conjugate Heat Transfer Problem

The problem should be treated as a conjugate heat transfer problem which incorporates the effect of heat conduction in the walls being in contact with liquid sodium, since both inner and outer walls of the concentric annulus used as a test section of the experiments by Shiotsu et al (1993; see Appendix C) are made of metals—a heater sheath made of Tantalum and an outer pipe made of Hastelloy X—with relatively high thermal conductivities and also those heat capacities are not negligible.

2.2.1.1 Fundamental Equations and Boundary Conditions

Supposing that heat generation by viscous dissipation is negligible and that both velocity and temperature fields are uniform in angular direction of a vertical concentric annulus, the fundamental equations for laminar convection heat transfer in liquid sodium and the heat conduction equation for the inner and outer walls of an annulus are expressed in the axisymmetric two dimensional coordinate shown in Fig. 2.1 as follows:

Continuity equation for liquid sodium

$$\frac{\partial \rho}{\partial \tau}+\frac{1}{r}\frac{\partial}{\partial r}(\rho r v_r)+\frac{\partial}{\partial x}(\rho v_x)=0 \quad , \tag{2.1}$$

Momentum equations for liquid sodium

(r direction)

$$\frac{\partial}{\partial \tau}(\rho v_r)+\frac{1}{r}\frac{\partial}{\partial r}(\rho r v_r^{\,2})+\frac{\partial}{\partial x}(\rho v_r v_x)$$

$$=-\frac{\partial p}{\partial r}+\frac{2}{3\mathrm{Re}}\left[\frac{1}{r}\frac{\partial}{\partial r}\left\{\mu r\left(2\frac{\partial v_r}{\partial r}-\frac{v_r}{r}-\frac{\partial v_x}{\partial x}\right)\right\}\right.$$

$$\left.+\frac{\mu}{r}\left(\frac{\partial v_r}{\partial r}-2\frac{v_r}{r}+\frac{\partial v_x}{\partial x}\right)+\frac{3}{2}\frac{\partial}{\partial x}\left\{\mu\left(\frac{\partial v_r}{\partial x}+\frac{\partial v_x}{\partial r}\right)\right\}\right] , \tag{2.2}$$

(x direction)

$$\frac{\partial}{\partial \tau}(\rho v_x)+\frac{1}{r}\frac{\partial}{\partial r}(\rho r v_r v_x)+\frac{\partial}{\partial x}(\rho v_x^{\,2})$$

$$= -\frac{\partial p}{\partial x} + \frac{1}{\mathrm{Re}}\left[\frac{1}{r}\frac{\partial}{\partial r}\left\{\mu r\left(\frac{\partial v_r}{\partial x} + \frac{\partial v_x}{\partial r}\right)\right\}\right.$$

$$\left. + \frac{2}{3}\frac{\partial}{\partial x}\left\{\mu\left(-\frac{\partial v_r}{\partial r} - \frac{v_r}{r} + 2\frac{\partial v_x}{\partial x}\right)\right\}\right] - \frac{1}{\mathrm{Fr}} + \frac{\mathrm{Gr}^*}{\mathrm{Re}^2}T \,, \tag{2.3}$$

Energy equation for liquid sodium

$$c_p\left[\frac{\partial}{\partial r}(\rho T) + \frac{1}{r}\frac{\partial}{\partial r}(\rho r v_r T) + \frac{\partial}{\partial x}(\rho v_x T)\right]$$

$$= \frac{1}{\mathrm{Re}\,\mathrm{Pr}}\left\{\frac{1}{r}\frac{\partial}{\partial r}\left(k r \frac{\partial T}{\partial r}\right) + \frac{\partial}{\partial x}\left(k\frac{\partial T}{\partial x}\right)\right\} \,, \tag{2.4}$$

Heat conduction equation for inner and outer walls

$$\rho c_p \frac{\partial T}{\partial \tau} = \frac{1}{\mathrm{Re}\,\mathrm{Pr}}\left\{\frac{1}{r}\frac{\partial}{\partial r}\left(r k \frac{\partial T}{\partial r}\right) + \frac{\partial}{\partial x}\left(k\frac{\partial T}{\partial x}\right)\right\} \,. \tag{2.5}$$

The above equations are expressed in terms of nondimensional form by introducing the following change of variables;

$$r' = R / L_D, \quad x' = X / L_D, \quad v_r' = V_r / V_0, \quad v_x' = V_x / V_0,$$

$$t' = V_0 t / L_D, \quad T' = (T - T_{in}) k_0 / (q_w L_D)$$

and the superscripts of (′) are omitted for the sake of simplicity. The thermophysical properties such as density, specific heat, viscosity, and thermal conductivity in the above equations are also transformed into nondimensional forms by using the liquid sodium properties at inlet temperature. Consequently, the dimensionless numbers involved in the above fundamental equations are defined as

$$\mathrm{Re} = \rho_0 V_0 L_D / \mu_0, \quad \mathrm{Gr}^* = g\beta_0 q_w L_D^4 / \left(k_0 \nu_0^2\right), \quad \mathrm{Fr} = V_0^2 / \left(g L_D\right), \quad \mathrm{Pr} = \mu_0 c_{p0} / k_0,$$

respectively, where the subscripts, $_0$, denote the values at the inlet temperature of liquid sodium. The reference length designated by L_D is defined as the hydraulic equivalent diameter, $L_D = D_{out} - D_{in}$, where D_{out} and D_{in} are inside diameter of the outer pipe, and outside diameter of the inner cylinder respectively. The boundary conditions are written as

$$\overline{EF} \ : \ v_r = v_x = 0, \qquad (2.6) \qquad \overline{GH} \ : \ v_r = v_x = 0, \qquad (2.7)$$

$$\overline{FH} \ : \ v_r = 0, \ v_x = v_{x_{in}}, \qquad (2.8) \qquad \overline{EG} \ : \ v_r = 0, \ \frac{\partial v_x}{\partial x} = 0 \qquad (2.9)$$

for velocity components and

$$\overline{AB} \ : \ \frac{\partial T}{\partial r} = 0, \qquad (2.10) \qquad \overline{IJ} \ : \ \frac{\partial T}{\partial r} = 0, \qquad (2.11)$$

$$\overline{BC} \ : \ q_w = -k_w \frac{\partial T}{\partial r} = \text{const.} \qquad (2.12) \qquad \overline{DF} \ : \ \frac{\partial T}{\partial x} = 0, \qquad (2.13)$$

$$\overline{CD} \ : \ \frac{\partial T}{\partial r} = 0, \qquad (2.14) \qquad \overline{HJ} \ : \ \frac{\partial T}{\partial x} = 0, \qquad (2.15)$$

$$\overline{FH} \ : \ T = 0, \qquad (2.16) \qquad \overline{AI} \ : \ \frac{\partial T}{\partial x} = 0, \qquad (2.17)$$

for temperature respectively. In Eq. (2.8), $v_{x_{in}}$ denotes a velocity profile obtained analytically for a hydrodynamically developed laminar flow in a concentric annulus (e.g. Andoh, 1979);

$$v_{x_{in}} = a\left\{R^2 - {R_{out}}^2 + \frac{{R_{out}}^2 - {R_{in}}^2}{\ln\left(R_{out}/R_{in}\right)} \ln\left(\frac{R_{out}}{R}\right)\right\} / V_0 \ , \qquad (2.18)$$

where the coefficient, a, is expressed by the following equation as a function of flow rate, Q;

$$a = \frac{2Q}{{R_{in}}^4 - {R_{out}}^4 + \left({R_{out}}^2 - {R_{in}}^2\right)^2 / \ln\left(R_{out}/R_{in}\right)} \ . \qquad (2.19)$$

2.2.1.2 Procedure of Numerical Analysis

The dimensional sizes of calculation domain were determined so as to be identical to the concentric annular test section of the experimental apparatus that consists of the inner cylinder (7.6 mm in diameter, heater sheath made of Tantalum of 1.1 mm in thickness and heated section of 52 mm in length) and the outer pipe made of Hastelloy X (diameter ratio of 1.88 and 3.7 mm in thickness). The surface heat fluxes, flow rates, and liquid inlet temperatures employed in the present numerical analysis and the corresponding nondimensional parameters involved in the fundamental equations are listed in Table 2.1. As will be discussed later, the numerical analysis for the heated length of $L = 104$ mm for Pe = 2.2, 4.5, and 10.1 and of $L = 156$ mm for Pe = 2.2, 10.1, and 71.7 was also performed to investigate the effect of heated length on heat transfer. The longitudinal distance between the upstream end of the heated section and the upstream boundary ($\overline{DJ}$) was varied from 50 to 150 mm according to the Péclet number so that the boundary conditions expressed by Eqs. (2.8), (2.13), (2.15), and (2.16) are not affected by axial heat conduction. The location of an outflow boundary ($\overline{AI}$) is about 100 mm downstream of the exit of the heated section. The fundamental equations, together with the boundary conditions, were discretized by finite difference method and numerically analyzed by SIMPLER algorithm (Patankar, 1980). The calculation domain was radially divided into 24 grid points for all the Péclet numbers investigated in the present analysis, and the number of axial nodes was varied from 75 to 151 according to the length of the heated section and to the magnitude of the Péclet number. As an initial condition a stepwise heat input to the inner surface of a heater sheath was assumed, and the numerical analysis of transient heat transfer due to a sudden heat input was carried out until steady state heat transfer is established. The program developed in the present analysis as well as its flowchart are summarized in Figs. D-2 and D-1 respectively at

the end of this chapter.

2.2.2 Local Bulk Mean Temperature and Local Nusselt number

The local bulk mean temperature of liquid sodium is obtained by substituting the numerical solutions for T and v_x into the following equation

$$T_m(x) = \int_{R_{in}}^{R_{out}} \rho c_p T v_x r dr \Big/ \int_{R_{in}}^{R_{out}} \rho c_p v_x r dr \,. \tag{2.20}$$

Local heat transfer coefficient and the local Nusselt number are defined respectively as

$$h_x = \frac{q_x}{T_w(x) - T_m(x)} \,, \tag{2.21}$$

$$\mathrm{Nu} = \frac{h_x L_D}{k_l} \,, \tag{2.22}$$

where the heat flux, q_x , is calculated from the local temperature gradient normal to the surface of the inner cylinder. Figure 2.2(a) shows transient behavior of $T_m(x)$ for Pe = 2.2, $q = 1.96 \times 10^5$ W/m^2, and T_{in} = 249.1 °C for a heated section of 52 mm in length. The position of $X = 0$ mm in the figure corresponds to the upstream end of the heated section. As shown in the figure, the liquid temperature at a position downstream of the heated section ($X >$ 52 mm) decreases to its inlet temperature with increasing X at t = 4.5 sec. This is because at this stage the heat transferred from the heated section to the liquid sodium is consumed to heat up the non-heated parts of an annulus. The liquid temperature rises with time and becomes almost stable at $X <$ 52 mm in about 80 seconds after a stepwise change in heat input. However, the outlet liquid temperature requires a period of not less than 50 seconds to reach the steady state in the region of $X >$ 52 mm. At the steady state, the bulk mean temperature begins to rise from its inlet temperature at the upstream of the heated

section and the liquid temperature at $X = 0$ mm is 9 K higher than its inlet temperature.

Figure 2.2(b) shows the case for Pe = 0.7, in which the parameters such as heat flux, liquid inlet temperature, and heated length are the same as those in Fig. 2.2(a). In this case, the period required to reach the steady state is found to be 649 seconds after stepwise heat input to the inner surface of the heater sheath. Furthermore, at the steady state the liquid temperature already reaches 80 K at $X = 0$ mm, and 260 K at the exit of the heated section. Obviously the starting point of temperature rise tends to move towards the upstream with a decrease in the Péclet number due to the effect of axial heat conduction in liquid sodium and in the inner and outer walls of the concentric annulus. The local bulk mean temperature at $X = 0$ mm obtained by the numerical analysis is shown against the Péclet numbers in Table 2.2. As shown in the table, the bulk liquid temperature for Pe > 20 does not significantly rise from the inlet temperature T_{in}. However, there is a noticeable tendency for the bulk liquid temperature to increase with decreasing the Péclet number. As mentioned above, the temperature rise reaches as much as 78 K for Pe = 0.7, though in this case the heat flux is reduced to about 1/6 of that for Pe > 7.6. On the contrary, the theoretical results based on the physical model disregarding axial heat conduction effect will predict that the temperature rise at $X = 0$ mm is always equal to 0 K independent of Pe, thus leading to serious underestimation of local liquid temperature especially at low Péclet numbers.

2.3 Results and Discussion

2.3.1 Comparison Between Numerical and Experimental Results and Examination of Linear Interpolation Method for Estimating Local Bulk Mean Temperature

Figure 2.3 shows the numerical solutions for the steady state local Nusselt number for Pe = 0.7, 3.1, 20.2 and 71.7 at the surface of the 52 mm long heated section. In thermal

entrance region, the local Nusselt number becomes higher as the Péclet number becomes larger, however, it decreases with increasing X to almost constant value between 6 and 7 in fully developed region independent of the magnitude of the Péclet number.

As mentioned before, the analytical solution presented by Hatton and Quarmby (1962), based on the simplified model with constant heat flux on the inner rod surface and thermally insulated at the outer wall of an annular channel, predicts that the fully developed Nusselt number will be 6.1 for a concentric annulus of D_{out}/D_{in} = 1.88, which does not significantly differ from the present numerical results. However, this is simply because the temperature difference between the heated surface and bulk liquid in thermally fully developed region predicted by their model is apparently equal to that obtained by the present numerical results. Consequently, not only the absolute value of T_m but also T_w obtained by their model will fall below the present numerical solutions obtained through the conjugate heat transfer analysis.

Figure 2.4 shows the local Nusselt numbers at X = 21.5 mm on a heated section of 52 mm in length for the Péclet numbers ranging from 0.7 to 71.7. It is seen that the numerical solutions of the local Nusselt number based on the calculated surface temperatures and the local bulk mean temperatures calculated from Eq. (2.20) exist between 6 and 7 over the range of the Péclet numbers tested in this work.

Shiotsu et al carried out a series of experiments on liquid sodium forced convection heat transfer in a vertical concentric annulus for the Péclet numbers ranging from 650 down to 0.7 (1993). The local Nusselt number, Nu_{e0}, at X = 21.5 mm obtained from the measured surface temperatures and the bulk mean temperatures estimated by a linear interpolation between *measured* inlet temperature, T_{in}, and *measured* outlet temperature, T_{out}, is shown in Fig. 2.4. Petukhov and Yusin (1961) have presented a method of estimating local bulk mean

temperature of liquid metal flowing in a pipe by a linear interpolation between inlet and outlet liquid temperatures with an additional correction term which takes account of axial heat conduction effect in liquid and in a pipe wall as well. For a concentric annulus, the local bulk mean temperature estimated by a method similar to that by Petukhov et al is expressed as follows:

$$T_m(x) = T_{in} + (T_{out} - T_{in})(X/L) + \Delta T_c, \quad \text{for} \quad 0 \leqq X \leqq L \qquad (2.23)$$

where $\Delta T_c = (k_w A_w + k_l A_l + k_p A_p)[(T_{out} - T_{in})/L]/(\rho_l c_{pl} A_l u)$. The Nusselt number obtained from the *measured* surface temperatures and the local bulk mean temperatures given by Eq. (2.23), Nu_{ec}, is also shown in Fig. 2.4 in comparison with Nu_{e0}, based on the local bulk mean temperatures without ΔT_c .

In addition, the Nusselt number, Nu_{c0}, obtained from the *calculated* surface temperatures and the corresponding local bulk mean temperatures based on a linear temperature distribution given by the *calculated* T_{in} and T_{out}, and the Nusselt number based on the *calculated* wall surface temperatures and the local bulk mean temperatures obtained by substituting the *calculated* T_{in} and T_{out} into Eq. (2.23), Nu_{cc}, are also shown in Fig. 2.4 in comparison with those obtained similarly from the *measured* T_{in} and T_{out} as mentioned above.

Although the values of Nu_{e0} based on the *measured* temperatures are in agreement with Nu_{c0} based on the *calculated* ones for the Péclet numbers ranging from 0.7 to 71.7, both of them decrease remarkably with decreasing the Péclet number and are about 97 percent lower than the rigorous theoretical value of 6.8 at Pe = 0.7. The values of Nu_{cc} based on the *calculated* temperatures and Nu_{ec} based on the *measured* temperatures also agree with each other in a whole range of the Péclet number. However, Nu_{ec} is still 63

percent lower than the rigorous theoretical value at Pe = 0.7. It is expected therefore that the calculated surface temperatures, inlet and outlet liquid temperatures are in agreement with those measured experimentally, but the numerical solution for local bulk mean temperatures are not properly estimated by Eq. (2.23).

The axial distributions of surface and liquid bulk mean temperatures obtained numerically for L = 52 mm for Pe = 3.1 and 20.2 are shown in Figs. 2.5(a) and 2.5(b) respectively in comparison with the experimental data. As shown in the figures, the experimental data of the heater surface temperatures at all measuring points (X=10.5, 21.5, 32.5, and 43.0 mm) and the outlet liquid temperatures measured at X=121 mm agree well with the corresponding numerical solutions for each Péclet number. The local liquid mean temperatures evaluated by substituting the numerical solutions of T_{in} and T_{out} into Eq. (2.23) for Pe = 3.1 and 20.2 are also shown respectively in Fig. 2.5(a) and in Fig. 2.5(b) for comparison. Although the value of temperature correction term, ΔT_c , in Eq. (2.23) increases with decreasing Péclet number, the temperature difference between the liquid mean temperature evaluated by Eq. (2.23) and that by Eq. (2.20) is already observable at $X = 0$ mm, and its difference becomes large as the Péclet number becomes lower, causing the decrease in fully developed Nusselt number as mentioned before. Furthermore, for smaller Péclet number as seen in Fig. 2.5(a), the distribution of liquid mean temperatures at the heated section tends to become nonlinear especially in the region near the exit of the heated section, and as a result the assumption of a linear profile of liquid mean temperature on a heated section becomes invalid at low Péclet numbers.

Fig. 2.6 shows the profiles of the local heat flux at the surface of the heated section. Here, the heat flux q was calculated as $q = \{(R_{in} - \delta_w)/R_{in}\}q_w$ by assuming no heat loss in axial direction. It is seen from the figure that the surface heat flux is almost uniform for

Pe > 20 except the regions near both ends of the heated section. However, the value of q_x/q becomes lower with decreasing Péclet number at large X. This is attributed to the end effect due to axial heat loss by conduction, which may cause the nonlinear profile of liquid bulk mean temperature near the downstream end of the heated section as mentioned before. And it was also confirmed that, for the Péclet numbers ranging from 20.4 down to 0.7, the value of q_x/q as well as its distribution are not significantly affected by the variation in heat flux but are determined chiefly by the magnitude of the Péclet number. The above results have exhibited that the liquid sodium laminar combined forced and free convection heat transfer in a concentric annulus at low Péclet numbers can be evaluated by the present numerical analysis, but cannot be accurately evaluated as far as the simple method based on a linear interpolation is used for estimating local bulk mean temperatures.

2.3.2 Effect of Heated Length

Figure 2.7 shows the distributions of the local Nusselt number obtained numerically for the heated sections of 52 mm and 156 mm in length for $\mathrm{Pe} = 10.1$. In performing numerical analysis for each heated length, the parameters other than the heated length—heat flux, liquid inlet velocity, and liquid inlet temperature—were kept unchanged. As shown in the figure, the numerical solutions of the Nusselt number for both heated lengths agree well with each other at the same position of X. The Nusselt number obtained from the calculated wall surface temperature and the local bulk mean temperature estimated by Eq. (2.23) for $L = 52$ mm and 156 mm, Nu_{cc}, is also shown in the figure for comparison. It is seen that in the fully developed region the values of Nu_{cc} for both heated lengths are 15 to 20 percent lower than the numerical solutions. It was confirmed that, even if the heated length becomes longer, Eq. (2.23) calculates the local bulk mean temperature to be lower than the numerical

solutions and always results in underestimation of the heat transfer coefficients at low Péclet numbers.

2.3.3 Effect of Heat Flux

Immediately after the reactor shutdown followed by a loss of flow accident, decay heat generated in FBR core is designed to decrease down to about 5 percent and, in about 24 hours down to less than one percent of an initial value at rated operating condition. In the previous sections of this chapter, the discussion has been restricted to the heat transfer phenomena for the heat flux listed in Table 2.1; for Pe $\geqq$ 7.6, the value of the heat flux employed in the numerical and experimental studies is approximately equal to that under the rated operating condition of FBRs. In this section, to investigate the effect of heat flux, the numerical results obtained with the heat fluxes other than those listed in Table 2.1 will be reported.

Figure 2.8 shows the effect of heat flux on the local Nusselt number for Pe = 20.2 ($q = 1.17\times10^6$ and 5.85×10^6 W/m^2, Gr*/Re^2 = 0.0629 and 0.314) and for Pe = 0.7 ($q = 1.96\times10^4$ and 1.96×10^5 W/m^2, Gr*/Re^2 = 0.821 and 8.21) for L = 52 mm. At every position on the heated section, the Nusselt number increases with heat flux for each Péclet number. And also, it tends to increase with X in fully developed region for higher heat fluxes in each case. This is supposed to be mostly due to the contribution of free convection, because the tendency is more noticeable at high heat fluxes and appears to be more emphasized at low flow velocity.

Figure 2.9 shows the axial flow velocity distributions in the gap at X = 40 mm on the heated section for $q = 1.96\times10^5$, 1.96×10^4, and 0 W/m^2 for Pe = 0.7. The velocity distribution for q = 0 W/m^2 was obtained from Eqs. (2.18) and (2.19). As shown in the

figure, the velocity distribution for $q = 1.96 \times 10^4$ W/m^2 almost coincides with that for $q = 0$ W/m^2, indicating little natural convection effect. In contrast, for $q = 1.96 \times 10^5$ W/m^2, the maximum value of the velocity becomes greater than that for smaller heat flux, and simultaneously the peak velocity location shifts towards the heated inner wall. In addition, it was confirmed by the above results that fully developed Nusselt numbers on heated surfaces with various lengths and heat fluxes for all the Péclet numbers investigated in the present analysis never fall below the value of 6.

2.3.4 Approximate Analytical Solution of Laminar Forced Convection Heat Transfer

As pointed out in the preceding section, liquid sodium laminar combined forced and free convection heat transfer in a concentric annulus can be described by the numerical analysis, while the simple method for estimating local bulk mean temperatures based on the linear interpolation between inlet and outlet temperatures always leads to underestimation of the heat transfer coefficient at low Péclet numbers. For practical use, however, it is necessary to estimate properly the local bulk mean temperatures from the measured inlet and outlet temperatures. For this purpose, an approximate analytical solution for the local bulk mean temperature was derived as follows.

The energy balance within a control volume at a heated section shown in Fig. 2.10 can be expressed by the following equation:

$$\rho_l c_{pl} A_l \Delta X \frac{\Delta T}{\Delta t} = q\pi D_{in} \Delta X + A_l \left[k_l \frac{\Delta T}{\Delta X}\bigg|_{X+\Delta X} - k_l \frac{\Delta T}{\Delta X}\bigg|_{X} \right]$$

$$+ A_w \left[k_w \frac{\Delta T}{\Delta X}\bigg|_{X+\Delta X} - k_w \frac{\Delta T}{\Delta X}\bigg|_{X} \right] + A_p \left[k_p \frac{\Delta T}{\Delta X}\bigg|_{X+\Delta X} - k_p \frac{\Delta T}{\Delta X}\bigg|_{X} \right] . \qquad (2.24)$$

Cross sectional area is represented by A and the subscripts l, w, and p denote sodium, heater-sheath, and outer pipe respectively. By putting $V_0 = \Delta X / \Delta t$, the above equation becomes as follows for a heated section:

$$\frac{d^2T}{dX^2} - \frac{\rho_l c_{pl} V_0}{k_l^*}\frac{dT}{dX} + \frac{q\pi D_{in}}{A_l k_l^*} = 0 \ , \tag{2.25}$$

where

$$k_l^* = k_l\left(1 + \frac{k_w}{k_l}\frac{A_w}{A_l} + \frac{k_p}{k_l}\frac{A_p}{A_l}\right). \tag{2.26}$$

Eq. (2.25) is integrated with respect to X to give

$$T(X) = c_1 \exp\left(\frac{\rho_l c_{pl} V_0}{k_l^*} X\right) + \alpha X + c_2 \ , \tag{2.27}$$

where $\alpha \equiv q\pi D_{in} / \left(\rho_l c_{pl} u A_l\right)$.

For a non-heated section at $X < 0$ mm where $q = 0$ W/m^2, Eq. (2.25) reduces to

$$\frac{d^2T}{dX^2} - \frac{\rho_l c_{pl} V_0}{k_l^*}\frac{dT}{dX} = 0 \ . \tag{2.28}$$

By integrating Eq. (2.28), one obtains

$$T(X) = c_3 \exp\left(\frac{\rho_l c_{pl} V_0}{k_l^*} X\right) + T_{in} \ . \tag{2.29}$$

The constants c_1, c_2, and c_3 are determined by the boundary conditions of temperature continuity at $X = 0$ mm, and $T = T_{in} + \alpha L$ at $X = L$. The analytical solutions for local bulk mean temperatures are obtained as follows:

$$T(X) = \frac{k_l^* \alpha}{\rho_l c_{pl} V_0}\left\{1 - \exp\left(-\frac{\rho_l c_{pl} V_0}{k_l^*} L\right)\right\}\exp\left(\frac{\rho_l c_{pl} V_0}{k_l^*} X\right) + T_{in} \ , \quad \text{for} \quad X < 0, \tag{2.30}$$

$$T(X)=\frac{k_l^*\alpha}{\rho_l c_{pl} V_0}\left[1-\exp\left\{\frac{\rho_l c_{pl} V_0}{k_l^*}(X-L)\right\}\right]+\alpha X+T_{in}\ , \qquad \text{for } 0 \le X \le L. \tag{2.31}$$

The local bulk mean temperatures obtained from Eqs. (2.30) and (2.31) are shown in Fig. 2.11 for Pe=3.1 in comparison with the numerical solution. The values by Eqs. (2.30) and (2.31) are found to be lower than the numerical solution at all locations of X though temperature gradients in X-direction on the heated section agree with each other.

The average inlet flow velocity, V_0, in the region of $X < 0$ mm is corrected so that the approximate analytical solutions obtained for a variety of heated lengths agree with the numerical solutions at $X = 0$ mm. The values of corrected velocity u^* are shown in Fig. 2.12 and are approximated by

$$\log_{10}\left(\frac{u^*}{V_0}\right)=-0.0467-0.0987(\log_{10}\mathrm{Pe})-0.178(\log_{10}\mathrm{Pe})^2-0.0165(\log_{10}\mathrm{Pe})^3 \tag{2.32}$$

for $0.7 \le \mathrm{Pe} \le 71.7$. By substituting the corrected velocity for $X < 0$ mm into Eq. (2.28) instead of V_0, we obtain the solution for local bulk mean temperature in a similar manner as the foregoing procedure. Finally the local bulk mean temperatures for a heated section as well as for a non-heated section are expressed by the following formulas:

$$T(X)=\frac{k_l^*\alpha}{\rho_l c_{pl} u^*}\left\{1-\exp\left(-\frac{\rho_l c_{pl} u^*}{k_l^*}L\right)\right\}\exp\left(\frac{\rho_l c_{pl} u^*}{k_l^*}X\right)+T_{in}\ , \qquad \text{for } X<0, \tag{2.33}$$

$$T(X)=\frac{k_l^*\alpha}{\rho_l c_{pl} u^*}\left[1-\exp\left\{\frac{\rho_l c_{pl} V_0}{k_l^*}(X-L)\right\}\right]+\alpha X+T_{in}\ , \qquad \text{for } 0 \le X \le L. \tag{2.34}$$

The local bulk mean temperatures calculated from Eqs. (2.33) and (2.34) for Pe=3.1 are also shown in Fig. 2.11. Strictly speaking, the local bulk mean temperatures at X=0 mm calculated by Eq. (2.33) and Eq.(2.34) do not coincide with each other, since Eq. (2.34) still

involves V_0 instead of u^* in the right side, however, the difference is negligible for the Péclet numbers investigated. The specific heat c_{pl} in Eqs. (2.33) and (2.34) is evaluated at outlet temperature, while the thermophysical properties other than c_{pl} are evaluated at inlet temperature.

The distributions of the local bulk mean temperatures calculated by Eqs. (2.33) and (2.34) for L = 52 mm and L = 156 mm for Pe = 2.2 are compared with the numerical solutions in Figs. 2.13(a) and 2.13(b) respectively. The approximate analytical solution for each heated length agrees well with the corresponding numerical solution not only at each heated section but also in the upstream region of $X < 0$ mm where the liquid temperature already increases from inlet temperature by axial heat conduction.

Figure 2.7 shows the distributions of the local Nusselt number, Nu_{ap}, derived from the calculated wall surface temperatures and the local bulk mean temperatures obtained from the approximate analytical solution for Pe = 10.1, $q = 1.2 \times 10^6$ W/m^2 for L = 52 mm and 156 mm in comparison with the numerical solutions. It can be seen from the figure that the values of Nu_{ap} for L = 52 mm agree with the numerical solution within 3 percent errors in thermally fully developed region. Good agreement is also observed for L = 156 mm at $X < L/2$, however, Nu_{ap} begins to decrease progressively at $X > L/2$ and becomes about 15 percent lower than the numerical solution near the exit of a heated section. This may arises from the assumption employed in deriving the approximate analytical solution, in which the effect of natural convection is not taken into consideration.

Figure 2.14 shows the comparison of the numerically obtained local Nusselt numbers with Nu_{ap} based on the approximate analytical solution for L = 156 mm and $q = 1.5 \times 10^5$ W/m^2—heat flux of 12.5 % of that shown in Fig. 2.7. The values of Nu_{ap} agree well with the numerical solution on the entire heated length, and as a result, the approximate analytical

solution proved to be more valid as heat flux is smaller. Namely the approximate analytical solution is expected to fairly well predict local bulk mean temperatures for the heat flux of the decay heat level in FBR core being much smaller than the case of Fig. 2.14.

Fig. 2.15 shows the Nusselt numbers, Nu_{ap}, obtained from the calculated wall surface temperatures and the local bulk mean temperatures given by Eq. (2.34) at $X = L/2$ for $L = 52$ mm, 104 mm, and $L = 156$ mm for the Péclet numbers ranging from 1.6 to 71.7 in comparison with the numerical solutions and with Nu_{cc} based on the local bulk mean temperatures evaluated from Eq. (2.23). As shown in the figure, the values of Nu_{ap} based on the approximate analytical solutions for a variety of heated lengths agree well with the numerical solutions for $Pe > 3.1$. Compared with Nu_{cc} for $L = 52$ mm, which is 53 percent lower than the rigorous value of 6.7 at $Pe = 1.6$, the value of Nu_{ap} at $Pe = 1.6$ is only 20 percent lower than the numerical solution. It was confirmed that the method for estimation of the local bulk mean temperature from inlet and outlet liquid temperatures is greatly improved by the approximate analytical solution.

2.4 Conclusions

1) Rigorous theoretical solution of combined forced and free convection heat transfer was obtained numerically for fully developed flow of liquid sodium in a vertical concentric annulus with the same geometry as that used for the experiments for the Péclet numbers ranging from 0.7 to 71.7. The numerical solutions of heater surface temperatures and outlet liquid temperatures agree well with the corresponding experimental results.

2) The theoretical analysis disregarding axial heat conduction leads to serious underestimation of the absolute value of local bulk mean temperature especially at low Péclet numbers, though the apparent local Nusselt numbers—namely temperature difference

between the heated surface and bulk liquid—in thermally fully developed region, are almost in agreement with the numerical results of the conjugate heat transfer analysis.

3) The local bulk mean temperatures estimated by a simple method based on linear interpolation between inlet and outlet liquid temperatures become lower than the numerical solutions even if the correction term—which takes account of axial heat conduction effect—is added. As a result, the Nusselt numbers based on the liquid temperatures estimated by this method decrease from the numerical solution with decreasing Péclet number from around 20. It was confirmed that liquid sodium laminar combined forced and free convection heat transfer in a concentric annulus at low Péclet numbers can be described by the numerical analysis but cannot be evaluated accurately by the simple method based on the linear interpolation between T_{in} and T_{out}.

4) As far as the parameters other than the heated length such as heat flux, liquid inlet temperature, liquid inlet velocity are kept unchanged, the theoretical Nusselt numbers for a variety of heated lengths agree well with each other at the same distance from the beginning of respective heated sections. Fully developed Nusselt numbers obtained by the numerical analysis range between 6 and 7 for the Péclet numbers and heat fluxes tested in this work.

5) Approximate analytical solution, capable of describing the numerical solution for local bulk mean temperature obtained for a variety of heated lengths, was derived.

Nomenclature

A	cross sectional area, m^2
a	thermal diffusivity, m^2/s
c_p	specific heat, J/(kg K)
D_{in}	inner cylinder diameter, m
D_{out}	inside diameter of a pipe, m
Fr	Froude number, $V_0^2/(g\,L_D)$
Gr*	Grashof number for constant heat flux, $g\beta_0\,q_w L_D^4/(k_0\,\nu_0^2)$
g	acceleration of gravity, m/s^2
h_x	heat transfer coefficient, $W/(m^2\,K)$
k	thermal conductivity, W/(m K)
L	heated length, m
L_D	reference length, D_{out} - D_{in}, m
Nu	Nusselt number on heated section at the inner wall of an annulus, Eq. (2.22)
Nu_{ap}	Nusselt number obtained from calculated surface temperature and corresponding bulk liquid temperature given by approximate analytical solution, Eq. (2.34)
Nu_{c0}	Nusselt number obtained from calculated surface temperature and corresponding bulk liquid temperature based on linear bulk liquid temperature distribution given by T_{in} and calculated outlet temperatures
Nu_{cc}	Nusselt number obtained from calculated surface temperature and corresponding bulk liquid temperature given by Eq. (2.23)
Nu_{e0}	Nusselt number obtained from measured surface temperature and corresponding bulk liquid temperature based on linear bulk liquid temperature distribution given by measured inlet and outlet temperatures
Nu_{ec}	Nusselt number obtained from measured surface temperature and corresponding bulk liquid temperature given by Eq. (2.23)
p	pressure, Pa

Pe	RePr, Péclet number
Pr	Prandtl number, $\mu_0 c_{p0}/k_0$
Q	volumetric flow rate, m^3/s
q_w	uniform heat input supplied to the inner surface of heater sheath, W/m^2
q_x	local heat flux in r direction at the outer surface of inner cylinder, W/m^2
Re	Reynolds number, $\rho_0 V_0 L_D/\mu_0$
R	radial coordinate, m
R_{in}	inner cylinder radius, $D_{in}/2$, m
R_{out}	inside radius of outer wall, $D_{out}/2$, m
r	dimensionless radial coordinate, R/L_D
T	temperature, K
T_{in}	fluid inlet temperature, K
T_m	fluid bulk mean temperature, K
T_{out}	fluid outlet temperature, K
T_w	surface temperature on the inner cylinder, K
t	time, s
u^*	modified fluid velocity, m/s
V_0	fully developed axial mean flow velocity at the upstream boundary of calculation domain, m/s
V_x	fluid velocity component in x direction, m/s
V_r	fluid velocity component in r direction, m/s
$v_{x_{in}}$	dimensionless velocity profile at the upstream boundary of calculation domain
X	axial coordinate, m
x	dimensionless axial coordinate, X/L_D

Greek Symbols

β	volumetric expansion coefficient, K^{-1}
δ	thickness, m
μ	viscosity, Pa s
ν	kinematic viscosity, m^2/s
ρ	density, kg/m^3
τ	dimensionless time, $V_0\ t/L_D$

Subscripts

l	fluid
0	values evaluated at fluid inlet temperature
p	outer wall of concentric annulus
w	heater sheath of inner cylinder

References

Andoh, T., 1979, "*Ryuutai no Rikigaku(in Japanese)*," Baifuu-kan, Tokyo.

Hatton, A. P., and Quarmby, A., 1962, "Heat Transfer in the Thermal Entry Length with Laminar Flow in an Annulus," *Int. J. Heat Mass Transfer*, Vol. 5, pp. 973-980.

Lundberg, R. E., McCuen, P. A., and Reynolds, W. C., 1963, "Heat Transfer in Annular Passages. Hydrodynamically Developed Laminar Flow with Arbitrarily Prescribed Wall Temperatures or Heat Fluxes," *Int. J. Heat Mass Transfer*, Vol. 6, pp. 495-529.

Patankar, S. V., 1980, "*Numerical Heat Transfer and Fluid Flow*," McGraw-Hill, New York.

Petukhov, B. S., and Yusin, A. Y., 1961, August, "Heat Exchange During Liquid Metal Flow in the Laminar and Transition Regions," *Soviet Physics-Doklady*, Vol. 6.

Rensen, Q., 1981, "Experimental Investigation of Turbulent Heat Transfer to Liquid Sodium in the Thermal Entrance Region of an Annulus," *Nucl. Eng. Design*, Vol. 68, pp. 397-404.

Shiotsu, M., Hata, K., Takeuchi, Y., and Sakurai, A., 1993, "Heat Transfer from Inner Surface of a Concentric Annulus to Forced Flow of Liquid Sodium in the Laminar and Transition Regions," *Proceedings of the 6th International Topical Meeting on NUCLEAR REACTOR THERMAL HYDRAULICS*, Vol. 2, pp. 1292-1301.

Table 2.1 Parameters for numerical analysis equivalent to experimental conditions.

Pe	Surface Heat Flux	Flow Rate	T_{in}	$Re \times 10^{-2}$	$Fr \times 10^{4}$	$Gr^*/Re^2 \times 10^2$
	W/m^2	l/min	℃	—	—	—
0.7	1.96×10^5	0.049	249.1	1.07	7.52	821
1.6	3.95×10^5	0.114	265.9	2.61	41.4	308
2.2	1.96×10^5	0.154	249.1	3.38	75.6	81.8
3.1	3.90×10^5	0.213	287.0	5.12	145	88.4
4.5	3.90×10^5	0.313	287.0	7.53	312	40.9
7.6	1.20×10^6	0.519	315.0	13.3	858	47.1
10.1	1.20×10^6	0.697	308.0	17.5	1550	25.9
20.2	1.17×10^6	1.390	295.8	34.1	6160	6.29
42.4	1.20×10^6	2.920	295.0	71.5	27200	1.46
71.7	1.20×10^6	4.940	292.1	120	77700	0.514

Table 2.2 Bulk liquid temperatures at *X* = 0 mm for various Péclet numbers.

Pe	0.70	1.6	2.2	3.1	4.5	7.6	10.1	20.2	42.4	71.7
T_m-T_{in} (K)	78.1	32.8	9.00	10.4	5.40	8.00	5.10	2.00	0.820	0.400

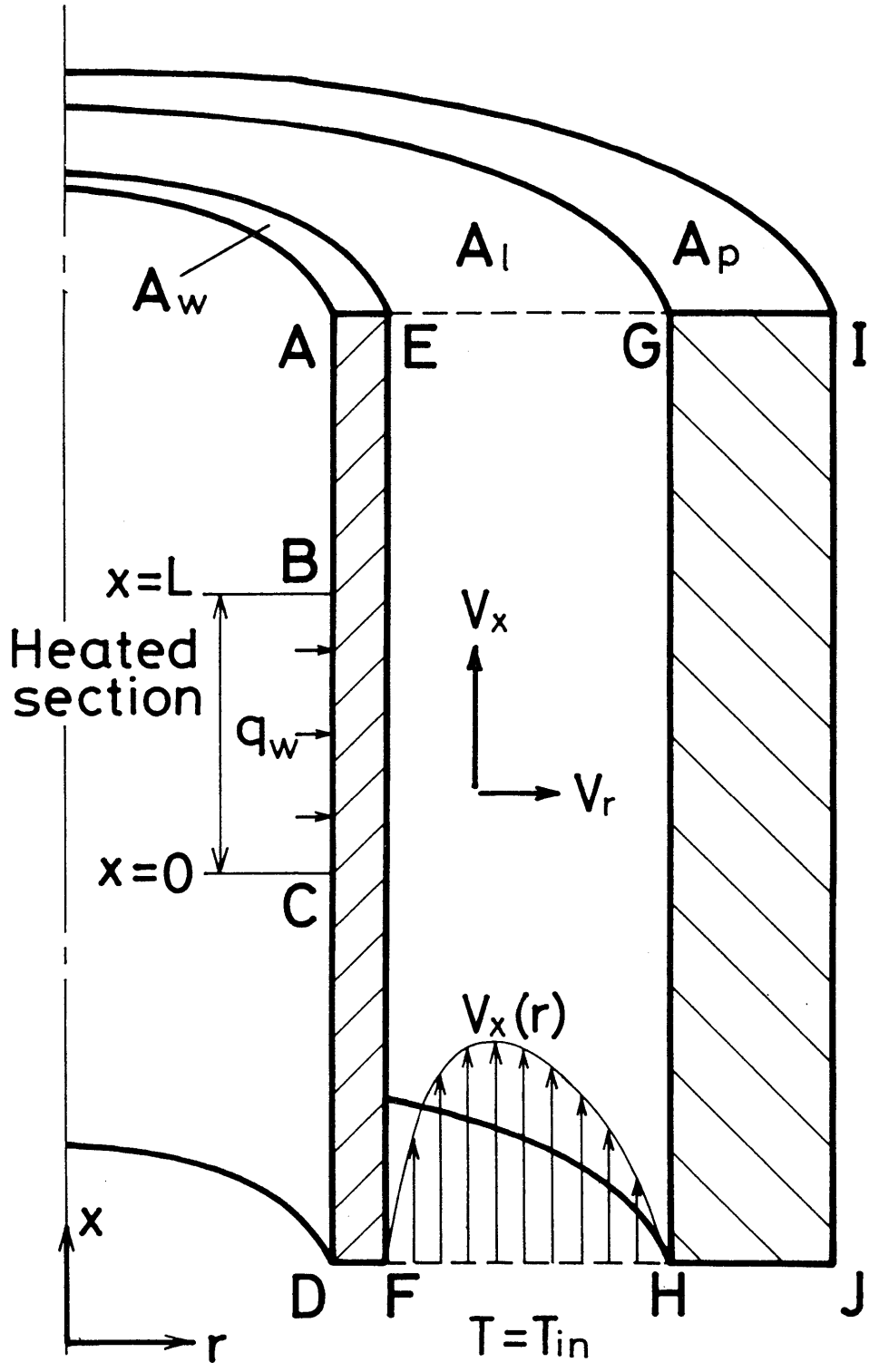

Fig. 2.1 Physical model and coordinates for numerical analysis.

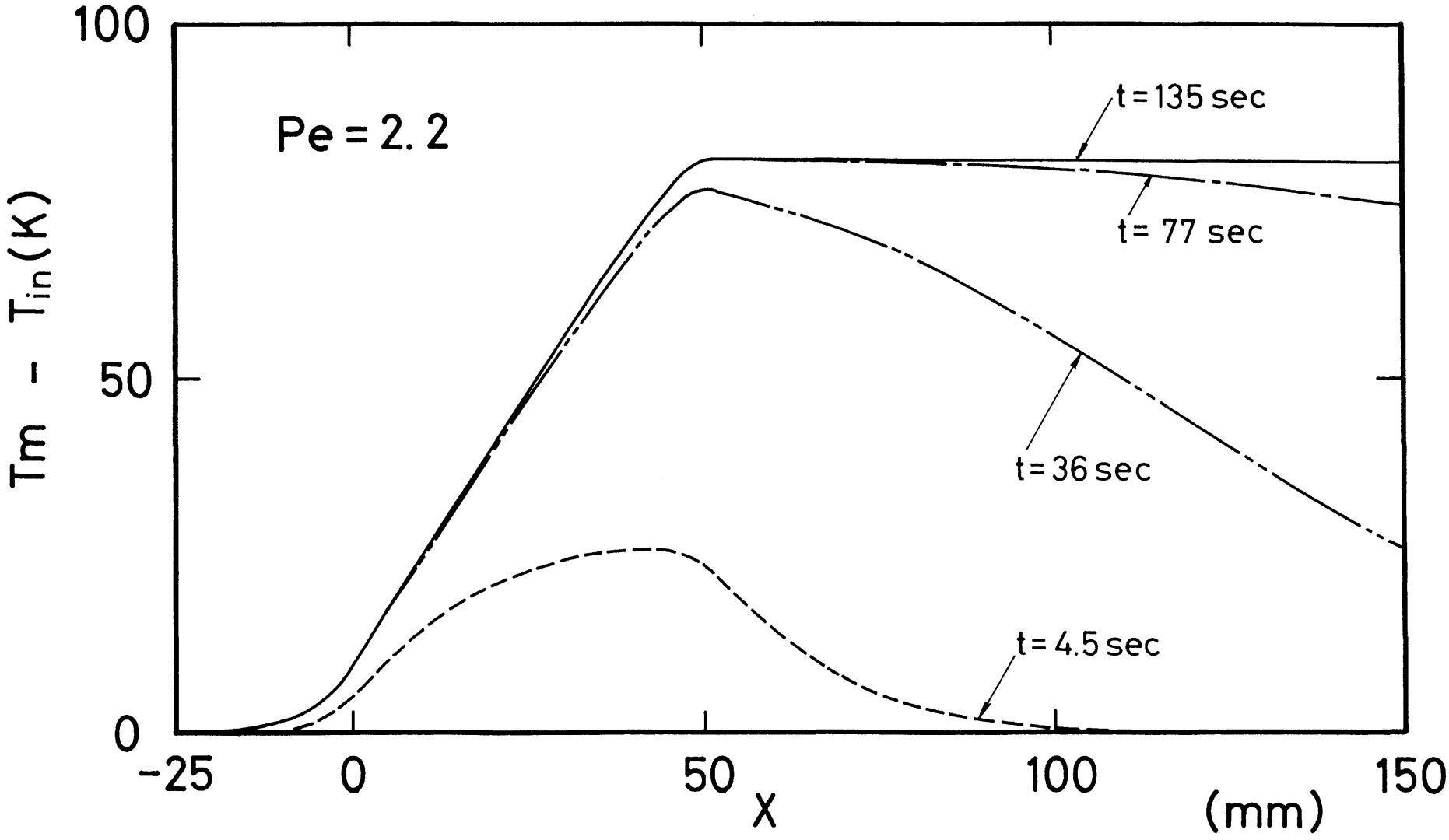

Fig. 2.2(a) Variation in liquid mean temperature distribution during transient process after step-wise heat input for Pe = 2.2.

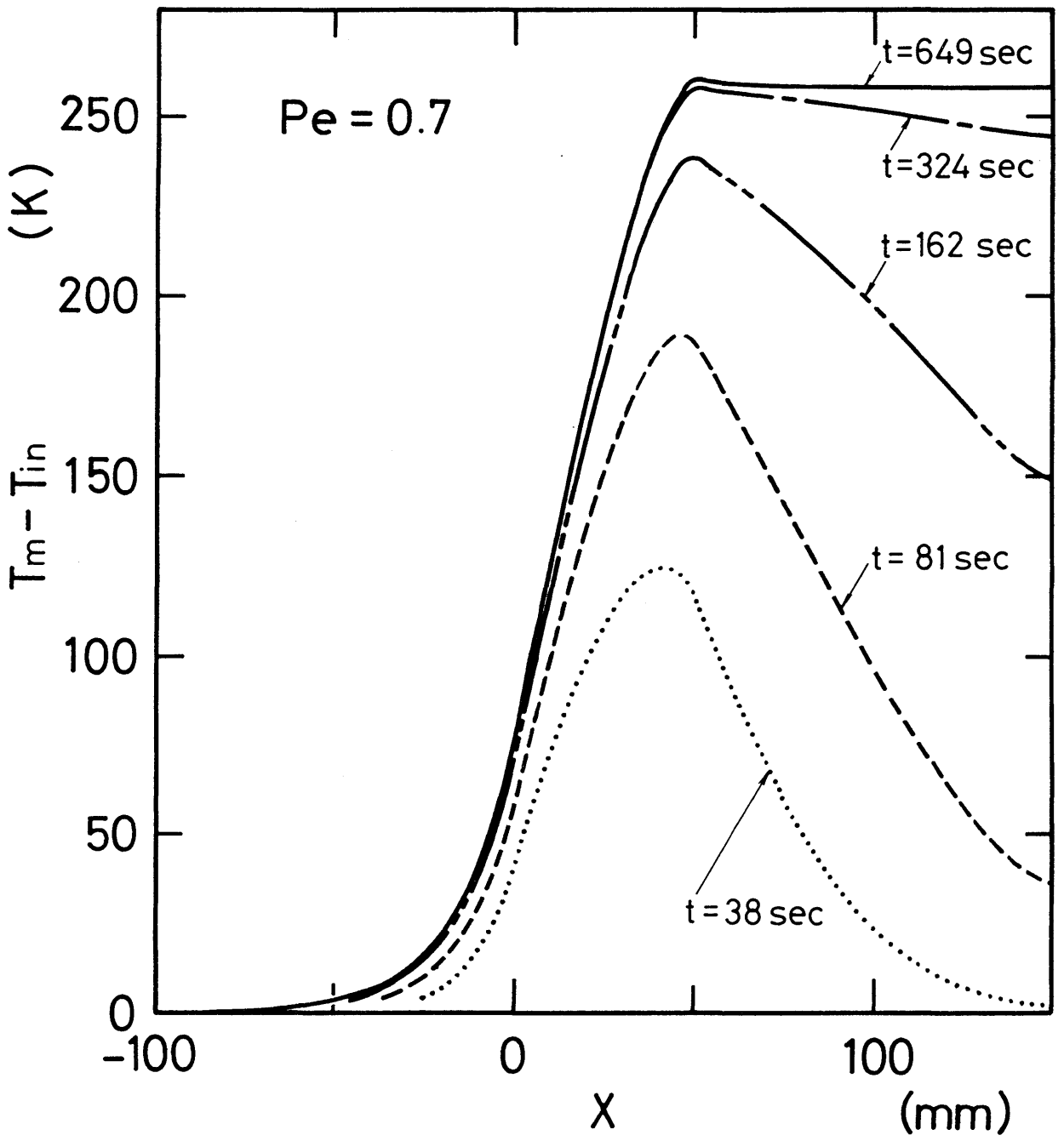

Fig. 2.2(b) Variation in liquid mean temperature distribution during transient process after step-wise heat input for Pe = 0.7.

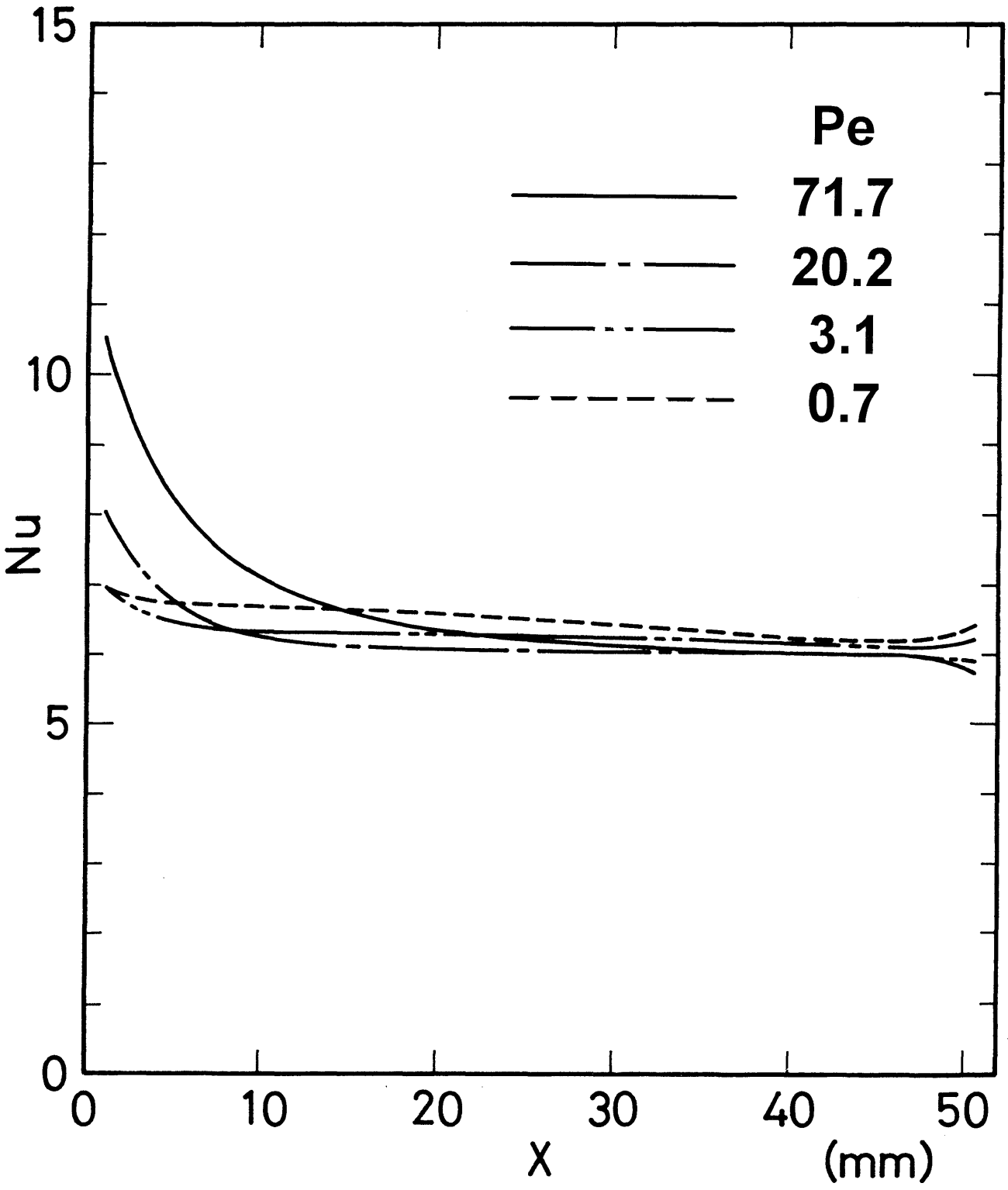

Fig. 2.3 Distributions of local Nusselt number obtained by numerical analysis for Pe= 0.7, 3.1, 20.2, and 71.7.

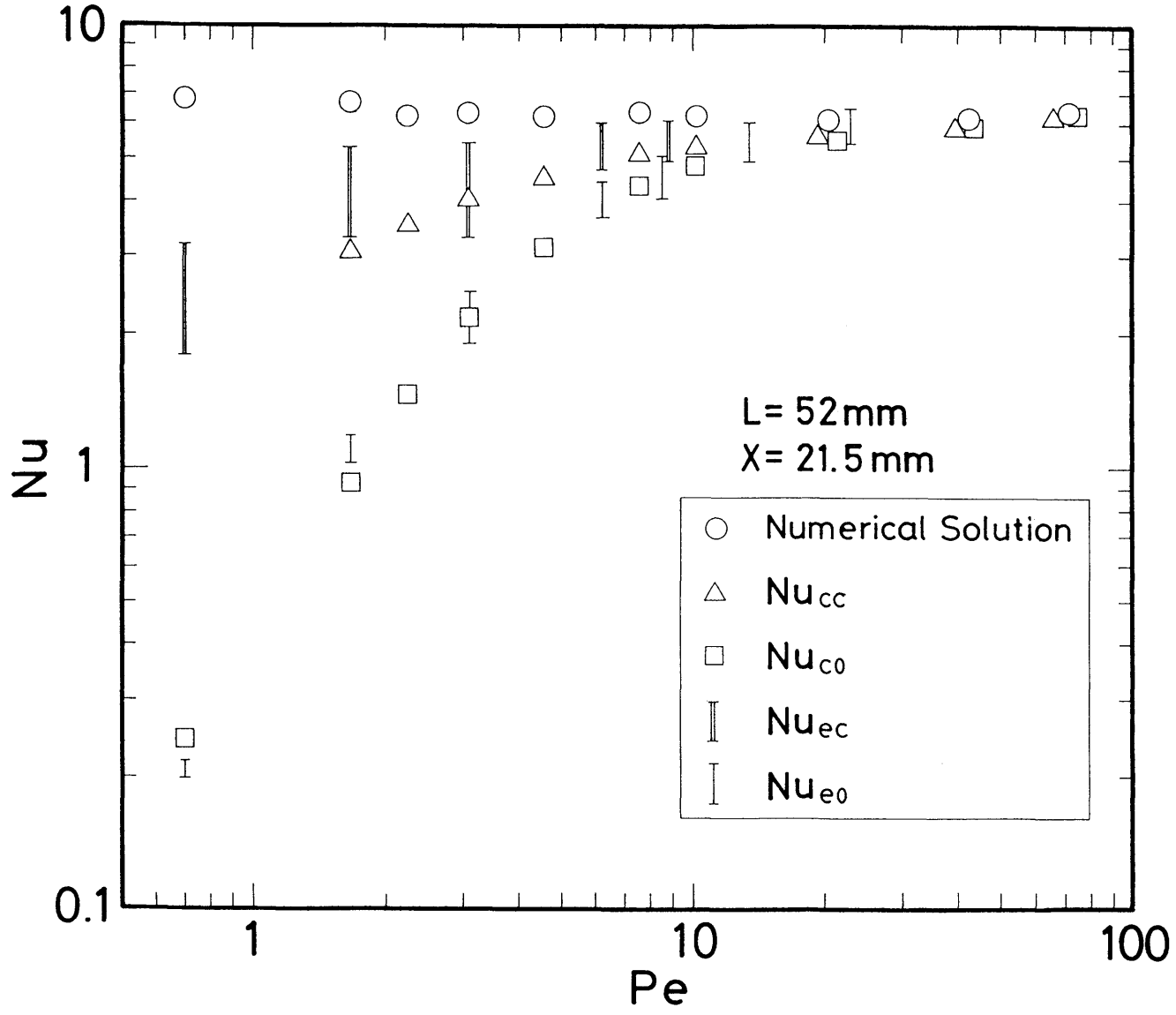

Fig. 2.4 **Local Nusselt numbers at X=21.5 mm obtained numerically based on the bulk mean temperature defined by Eq.(2.20) compared to those based on Eq.(2.23) with calculated T_{in} and T_{out} (Nu_{cc}), and with measured T_{in} and T_{out} (Nu_{ec}). The values represented by Nu_{c0} and Nu_{e0} are based on Eq.(2.23), in which numerical and experimental T_{in} and T_{out} are substituted respectively, without the temperature correction term ΔT_c.**

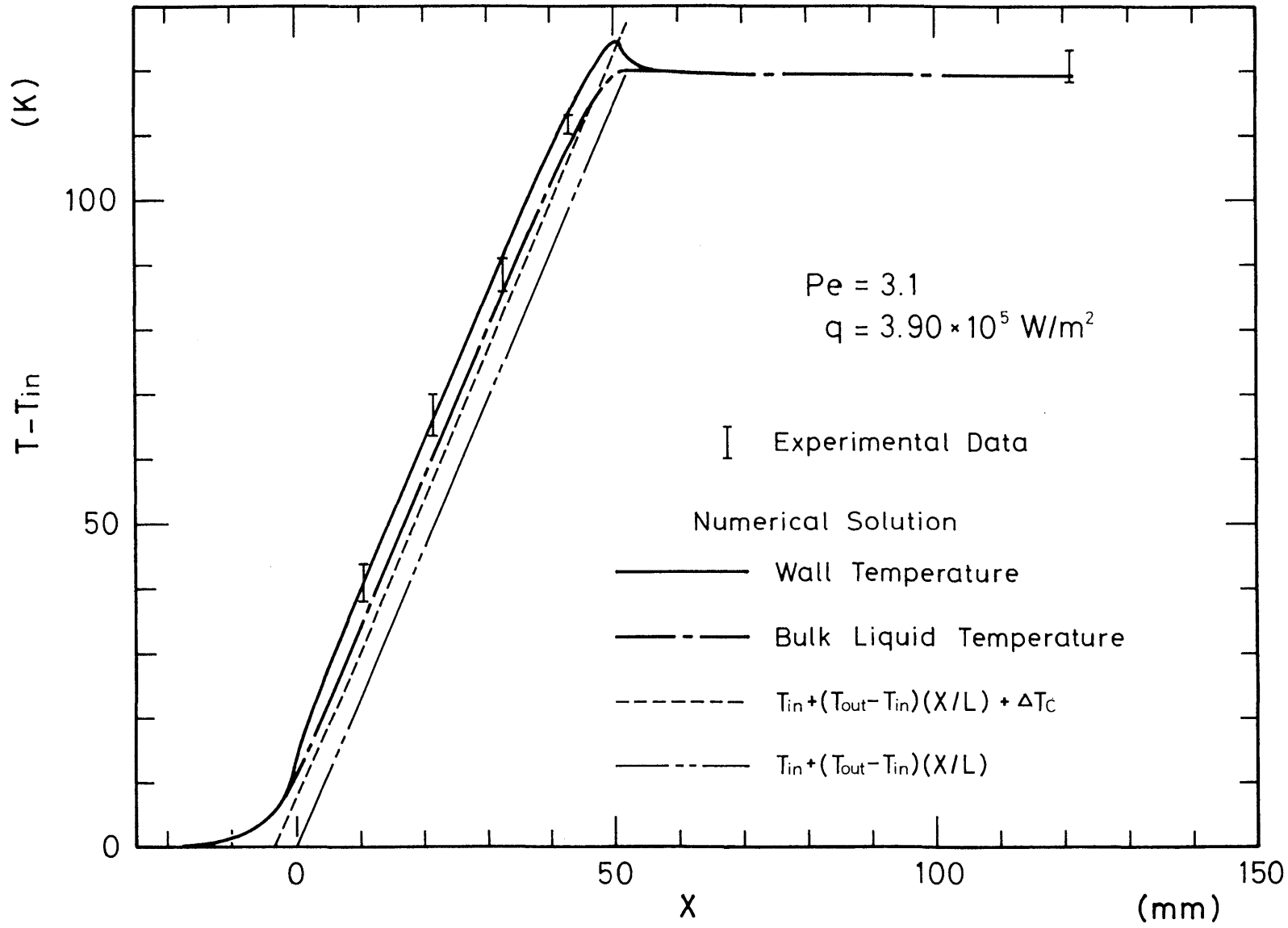

Fig. 2.5(a) Comparison of numerical solutions for wall and bulk liquid temperatures for Pe=3.1 with experimental data and with bulk liquid temperatures estimated by Eq. (2.23).

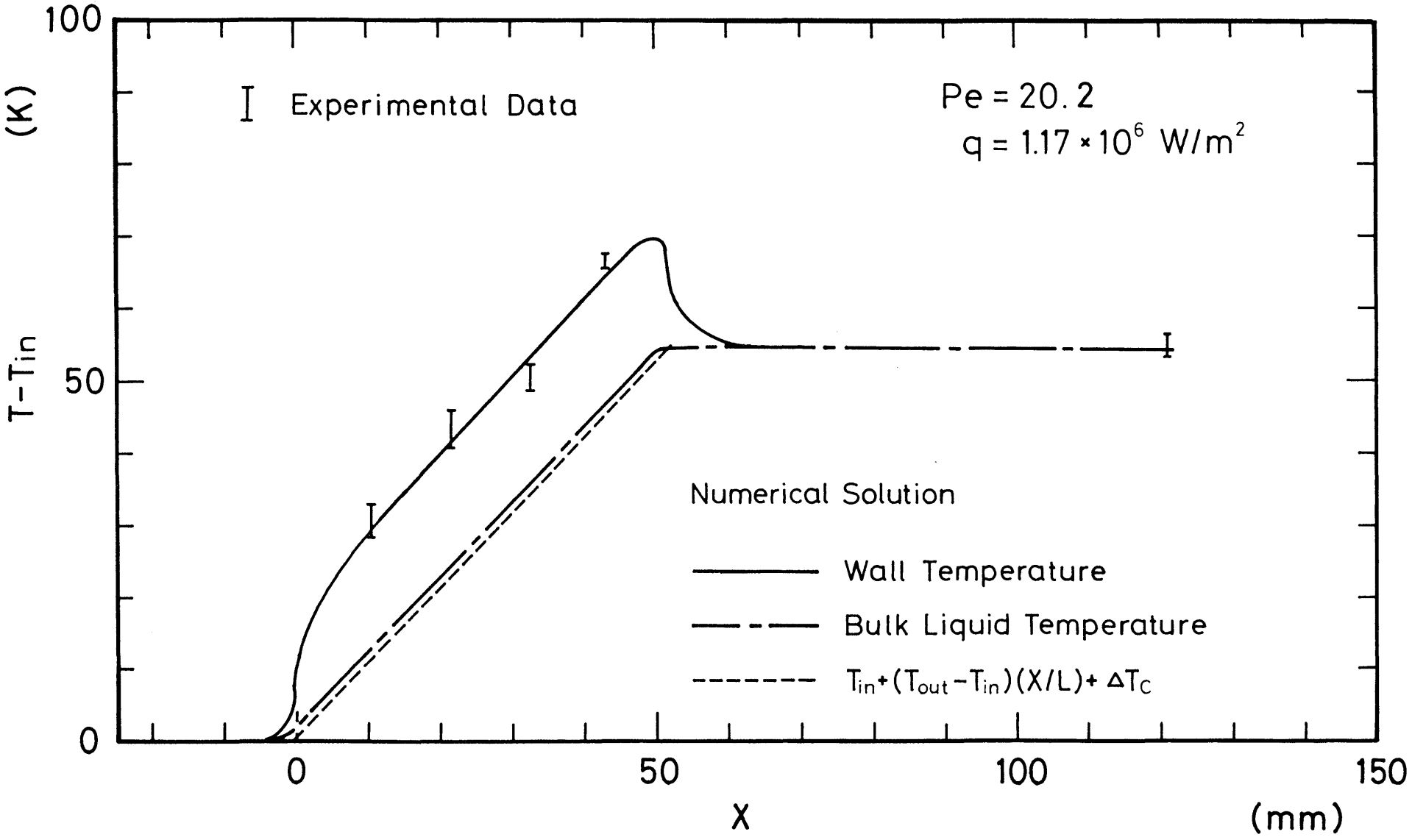

Fig. 2.5(b) Comparison of numerical solutions for wall and bulk liquid temperatures for Pe=20.2 with experimental data and with bulk liquid temperatures estimated by Eq. (2.23).

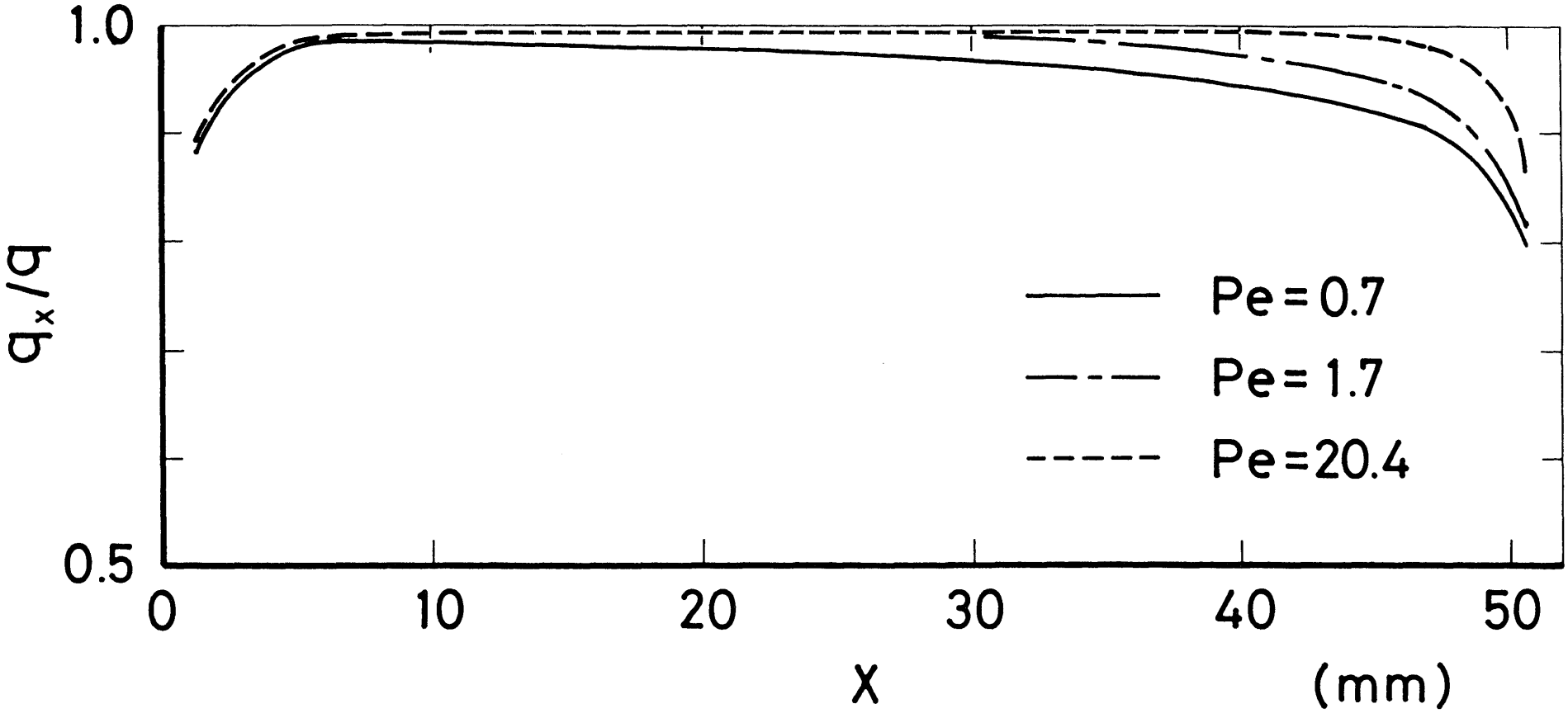

Fig. 2.6 Profiles of the heat flux at the outer surface of inner cylinder obtained numerically for Pe=0.7, 1.7, and 20.4.

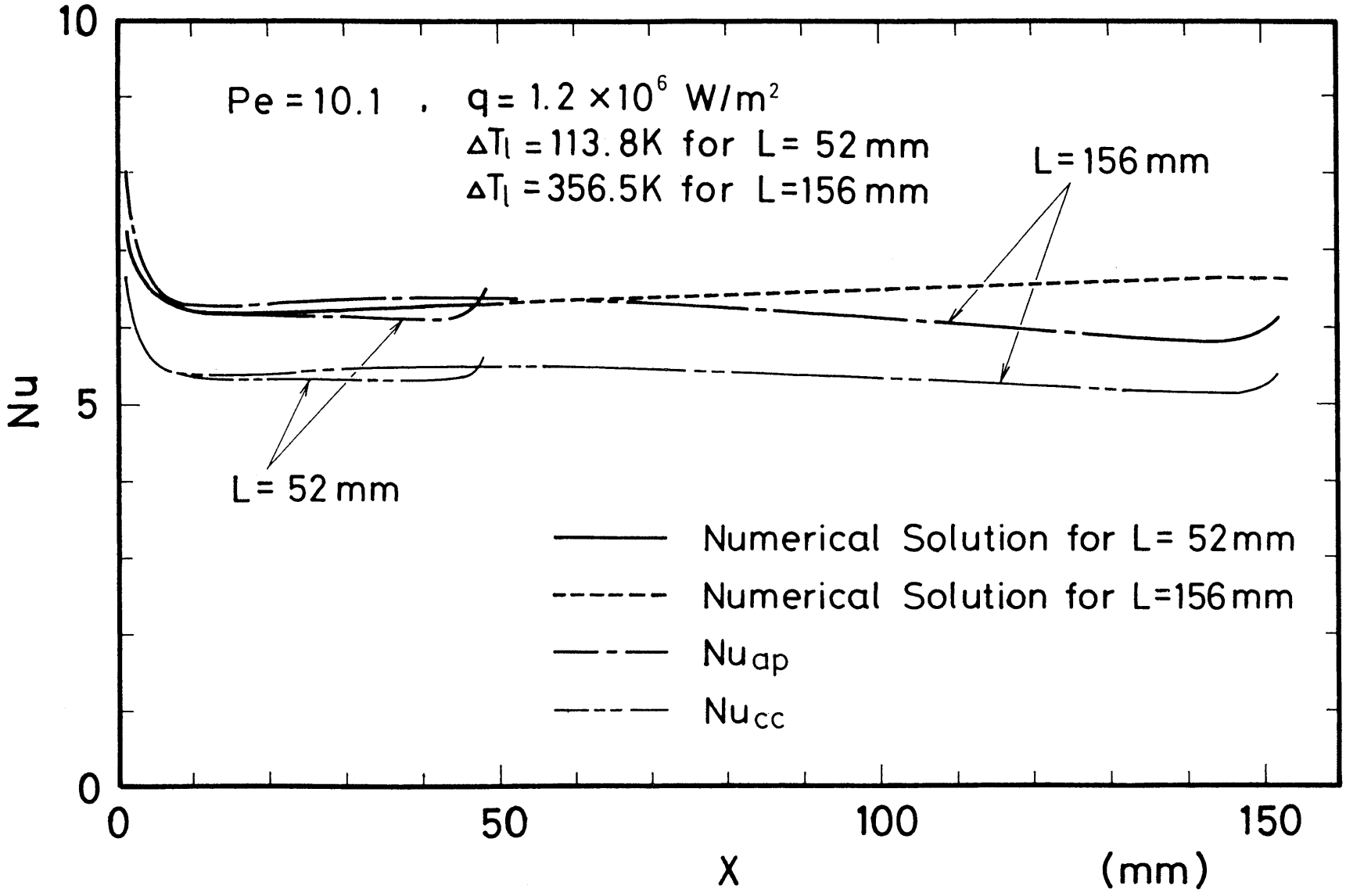

Fig. 2.7 **Comparison of the local Nusselt numbers obtained numerically for *L*=52 mm and 156 mm with those based on the liquid temperatures estimated by the method of linear interpolation between T_{in} and T_{out} (Nu_{cc}), and with those based on the liquid temperatures estimated by approximate analytical solution (Nu_{ap}).**

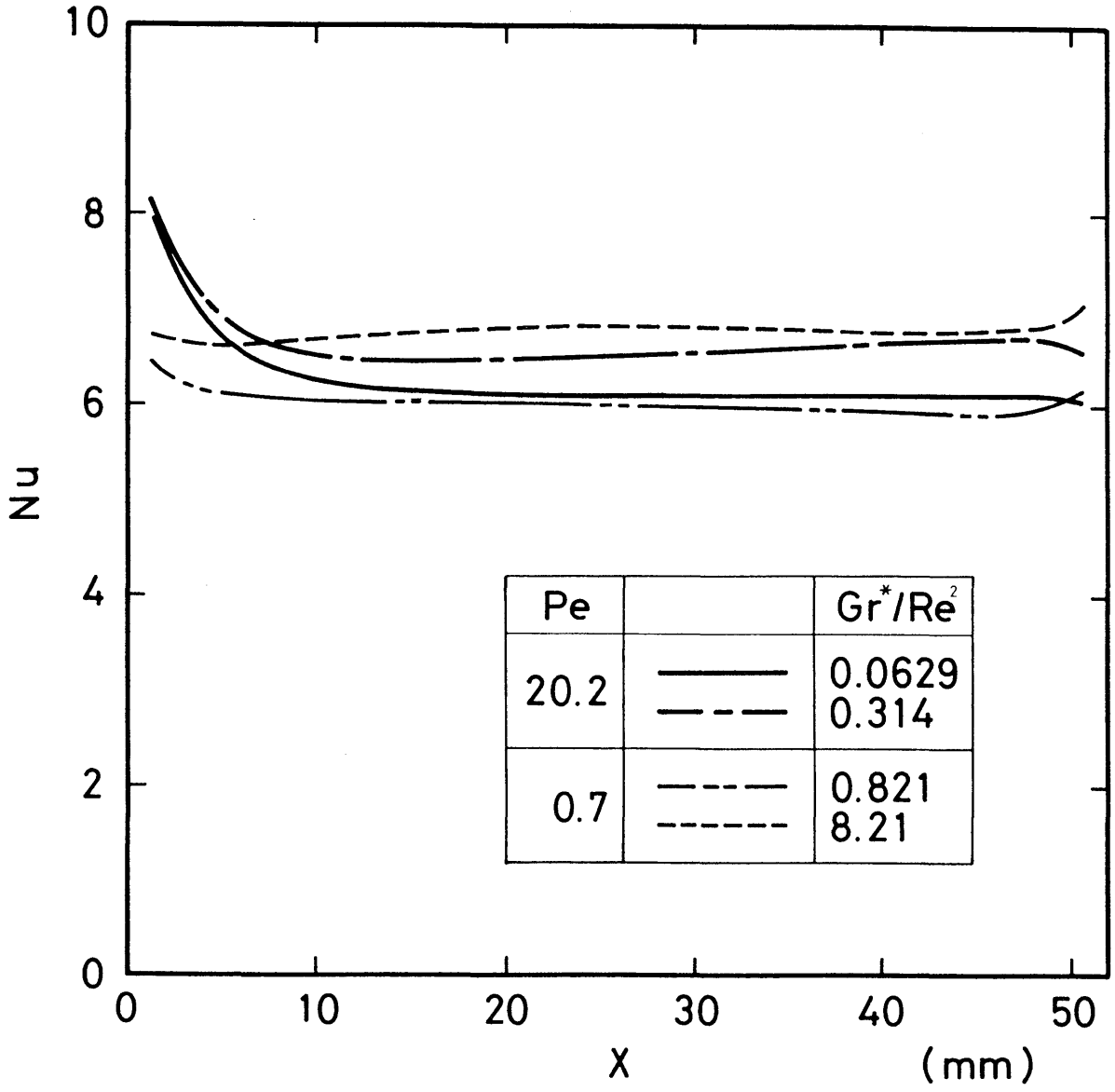

Fig. 2.8 **Distributions of local Nusselt number for various heat fluxes for Pe=0.7 and 20.2 on the heated section of 52 mm in length.**

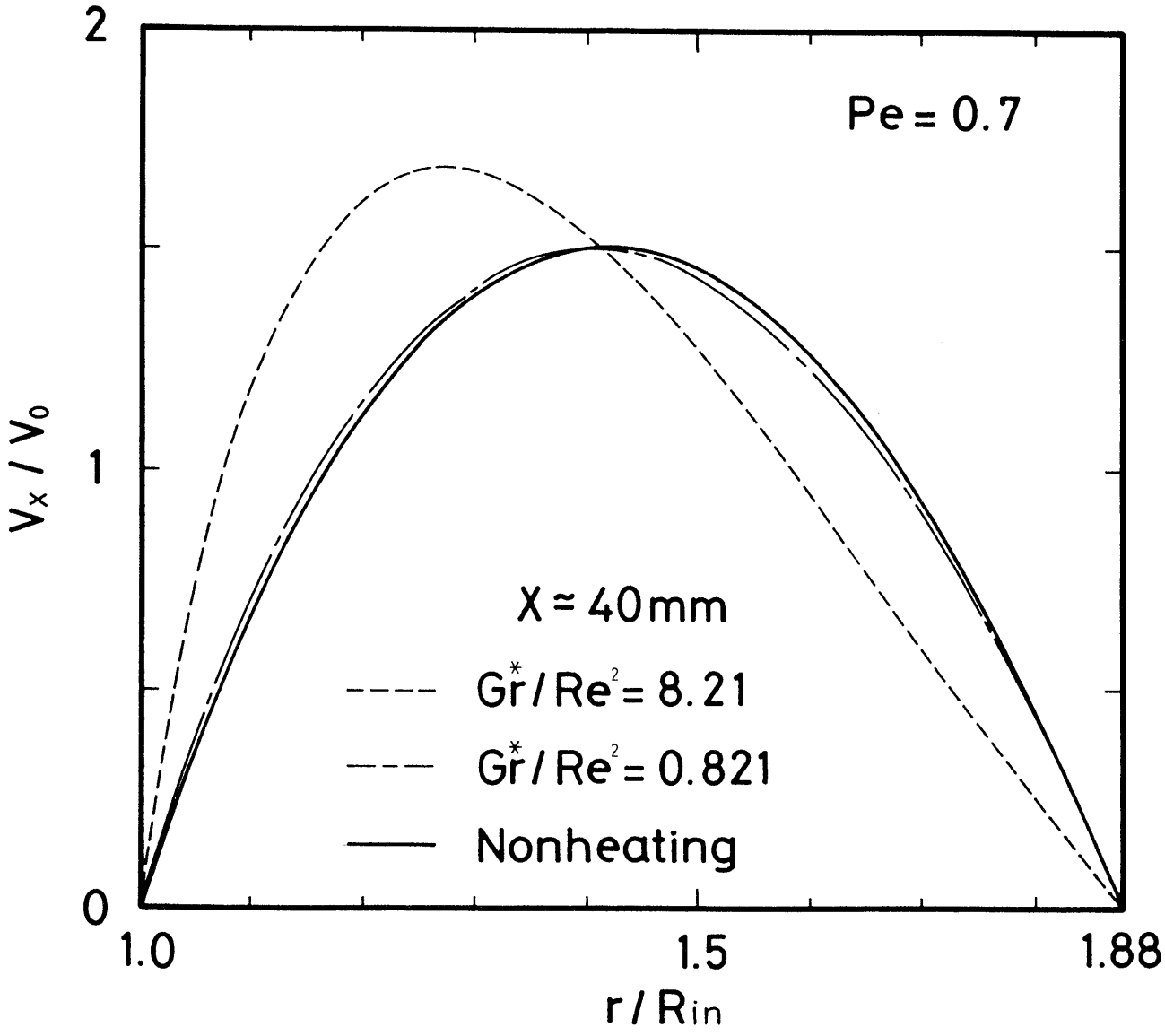

Fig. 2.9 Distributions of axial flow velocity obtained numerically for various heat fluxes.

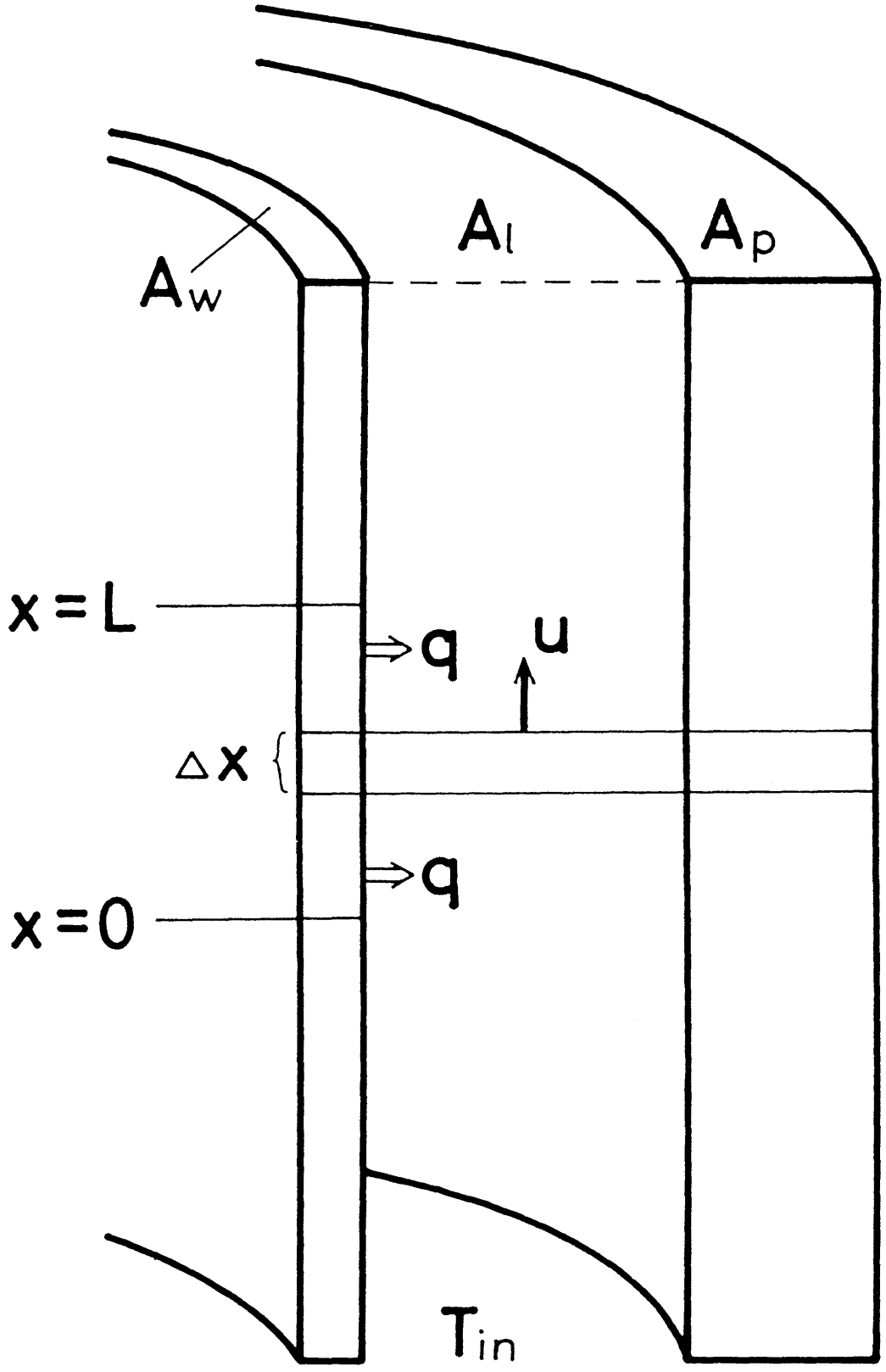

Fig. 2.10 Physical model for derivation of approximate analytical solution for bulk liquid temperature.

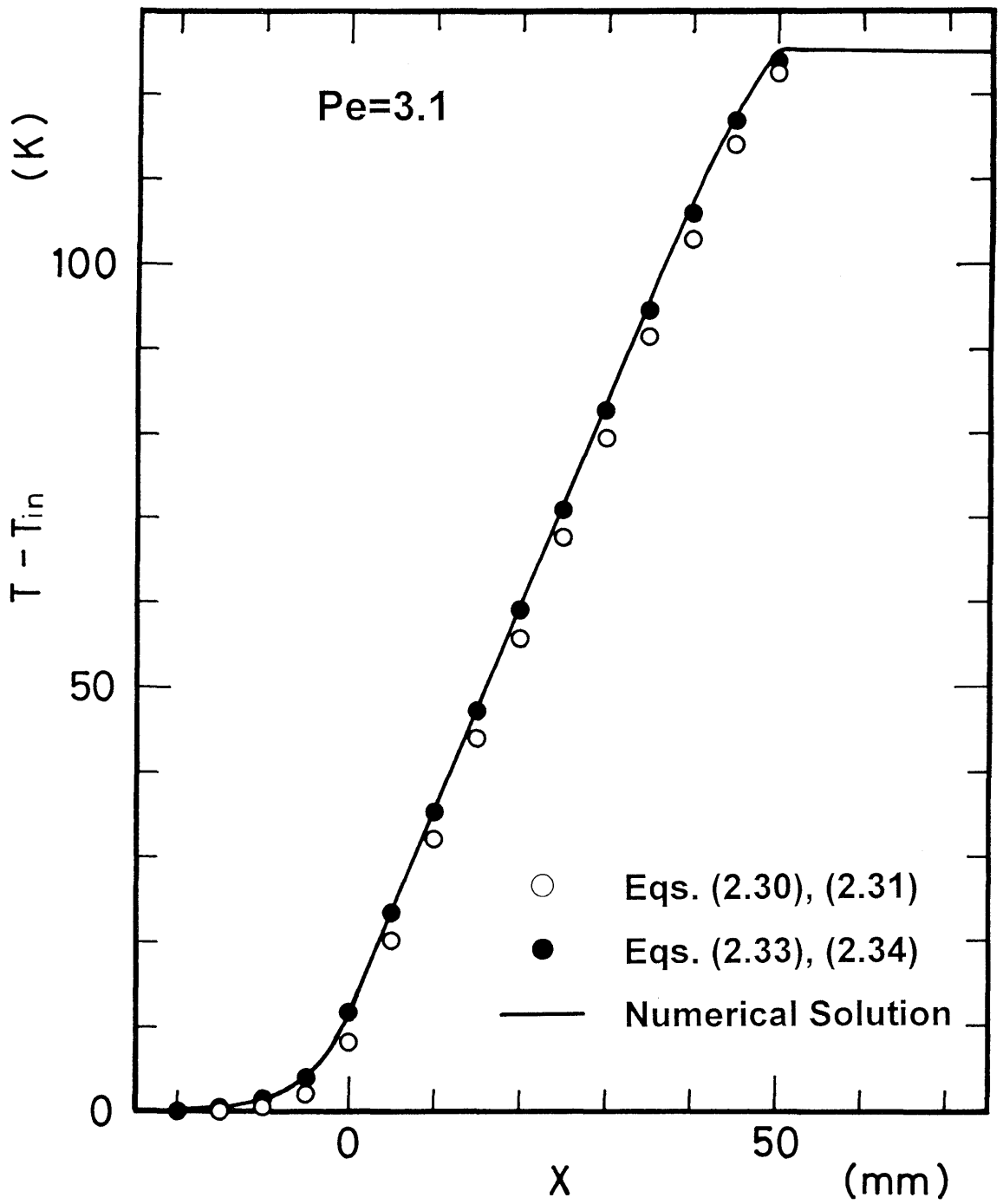

Fig. 2.11 Bulk liquid temperatures calculated from approximate analytical solution for Pe=3.1.

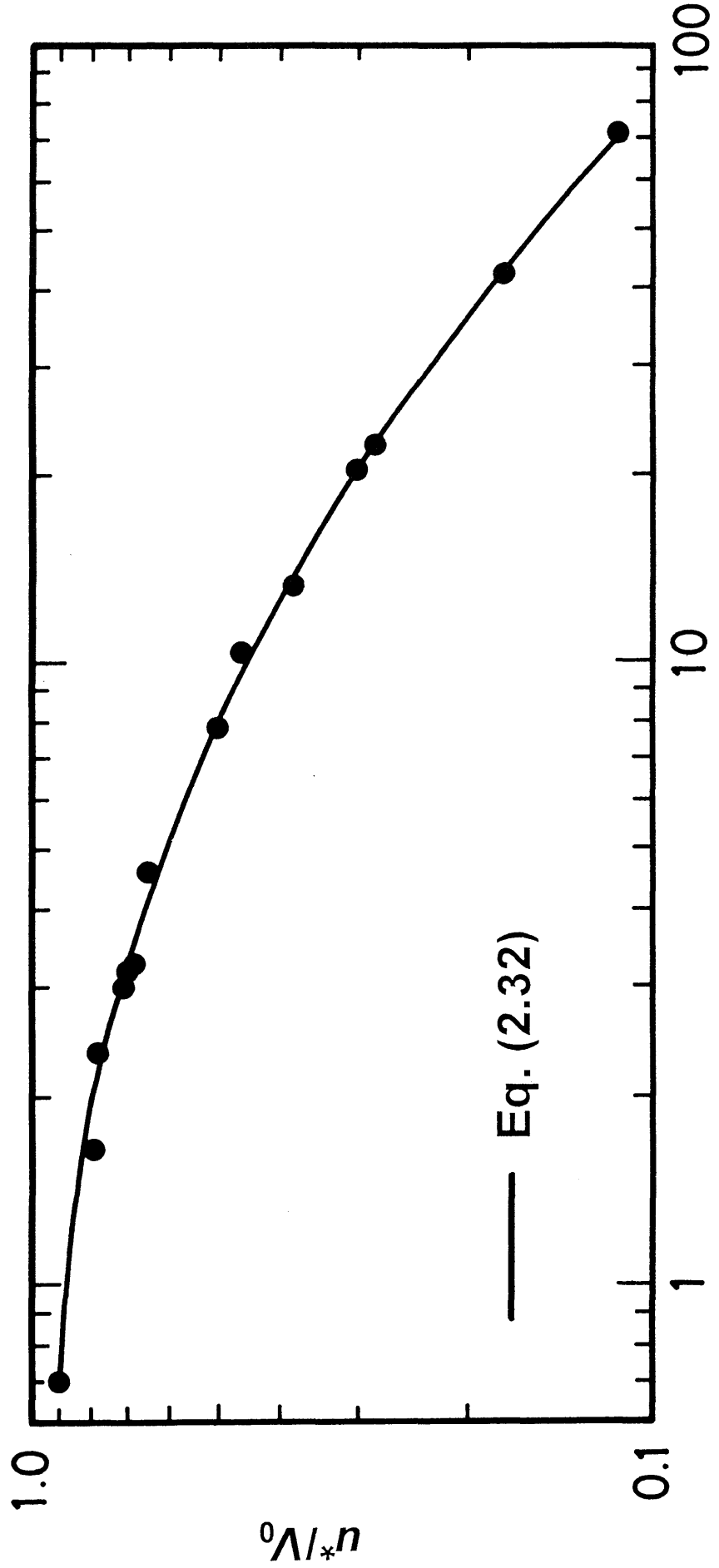

Fig. 2.12 Liquid inlet mean velocities used for approximate analytical solution.

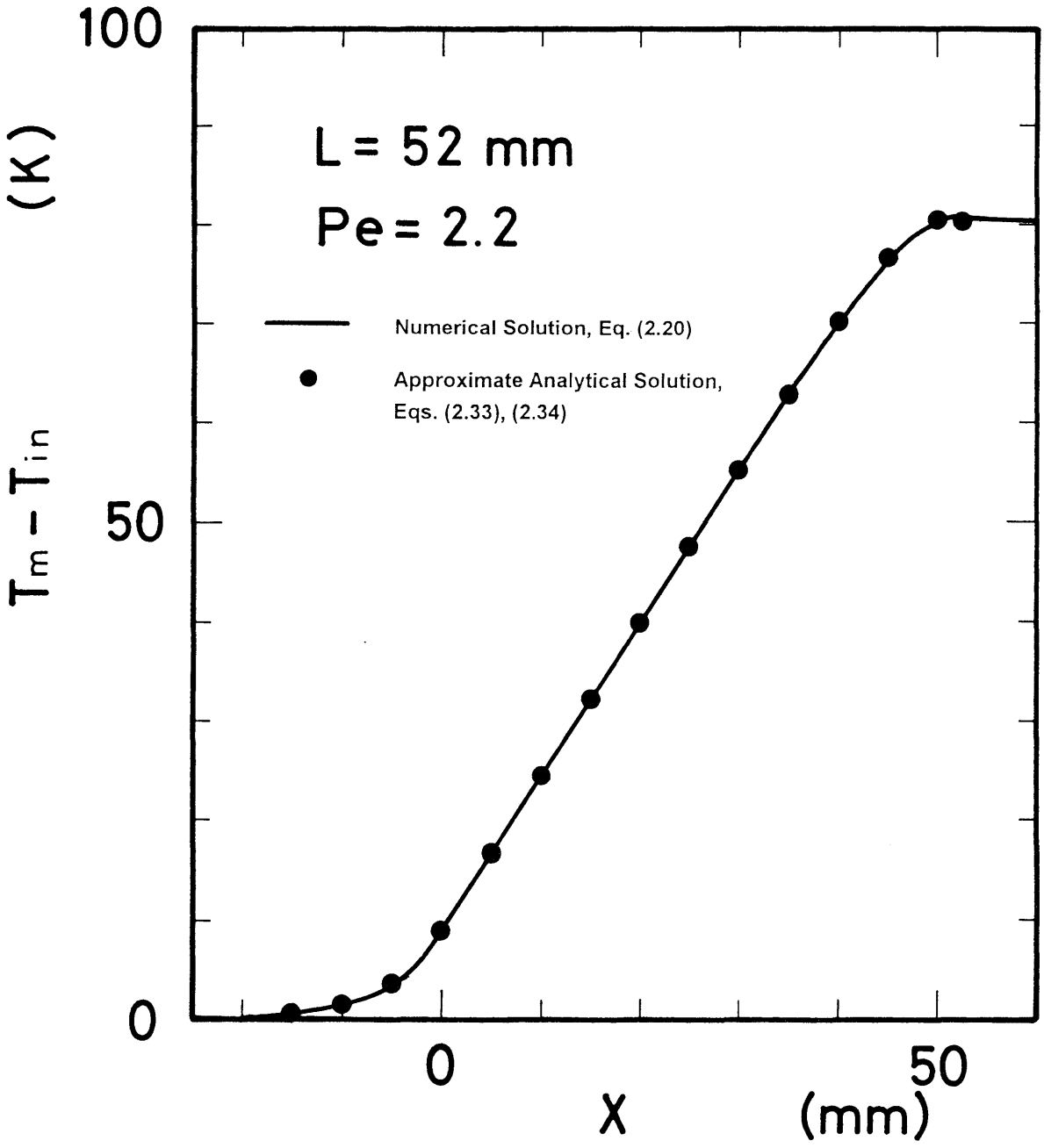

Fig. 2.13(a) Comparison of approximate analytical solution for bulk liquid temperature for Pe=2.2 and *L*=52 mm with numerical solution.

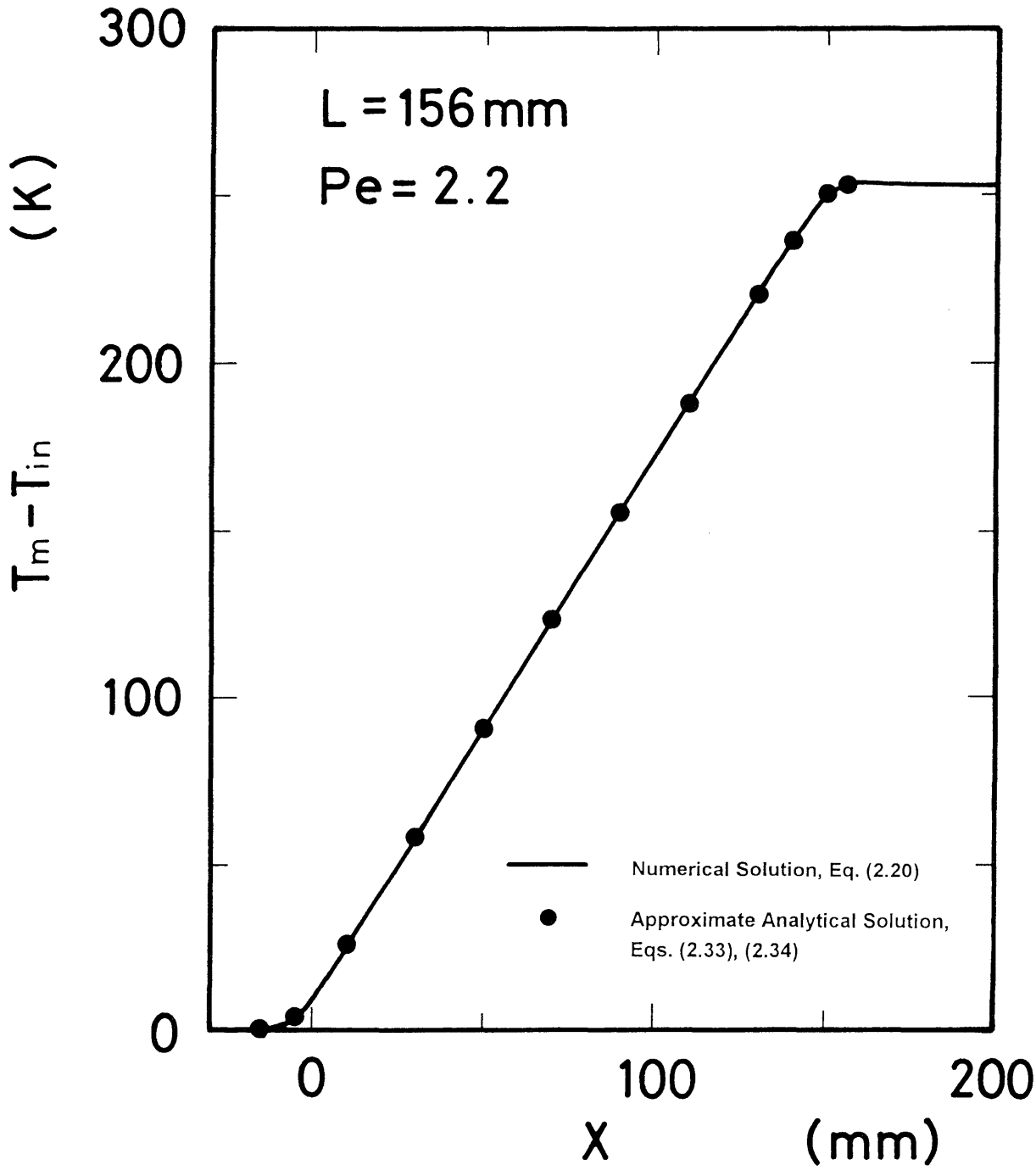

Fig. 2.13(b) Comparison of approximate analytical solution for bulk liquid temperature for Pe=2.2 and *L*=156 mm with numerical solution.

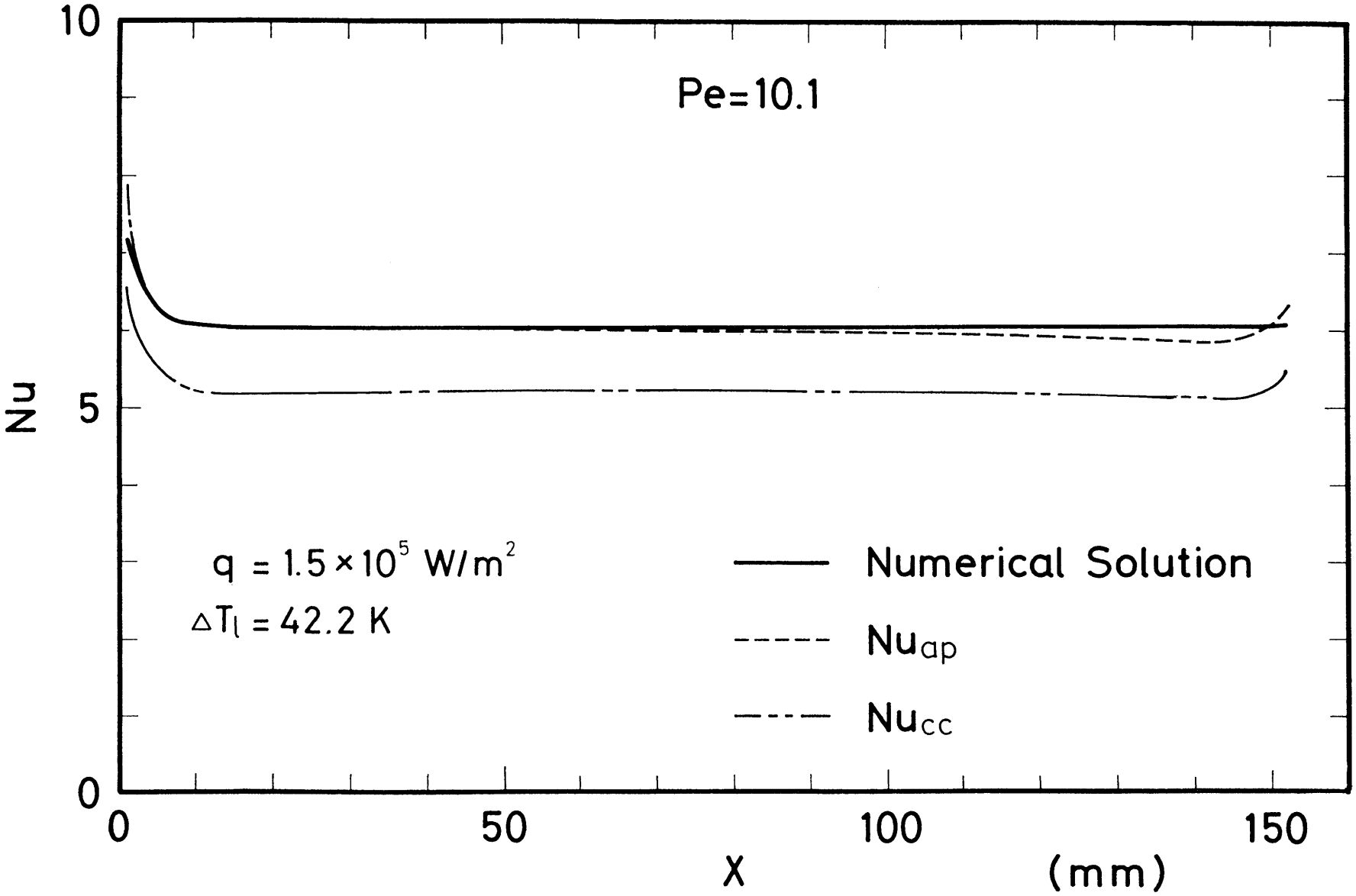

Fig. 2.14 Comparison of the local Nusselt numbers obtained numerically for $q = 1.5 \times 10^5$ W/m^2 and L=156 mm with those based on the liquid temperatures estimated by the method of linear interpolation between T_{in} and T_{out} (Nu_{cc}), and with those based on the liquid temperatures estimated by approximate analytical solution (Nu_{ap}).

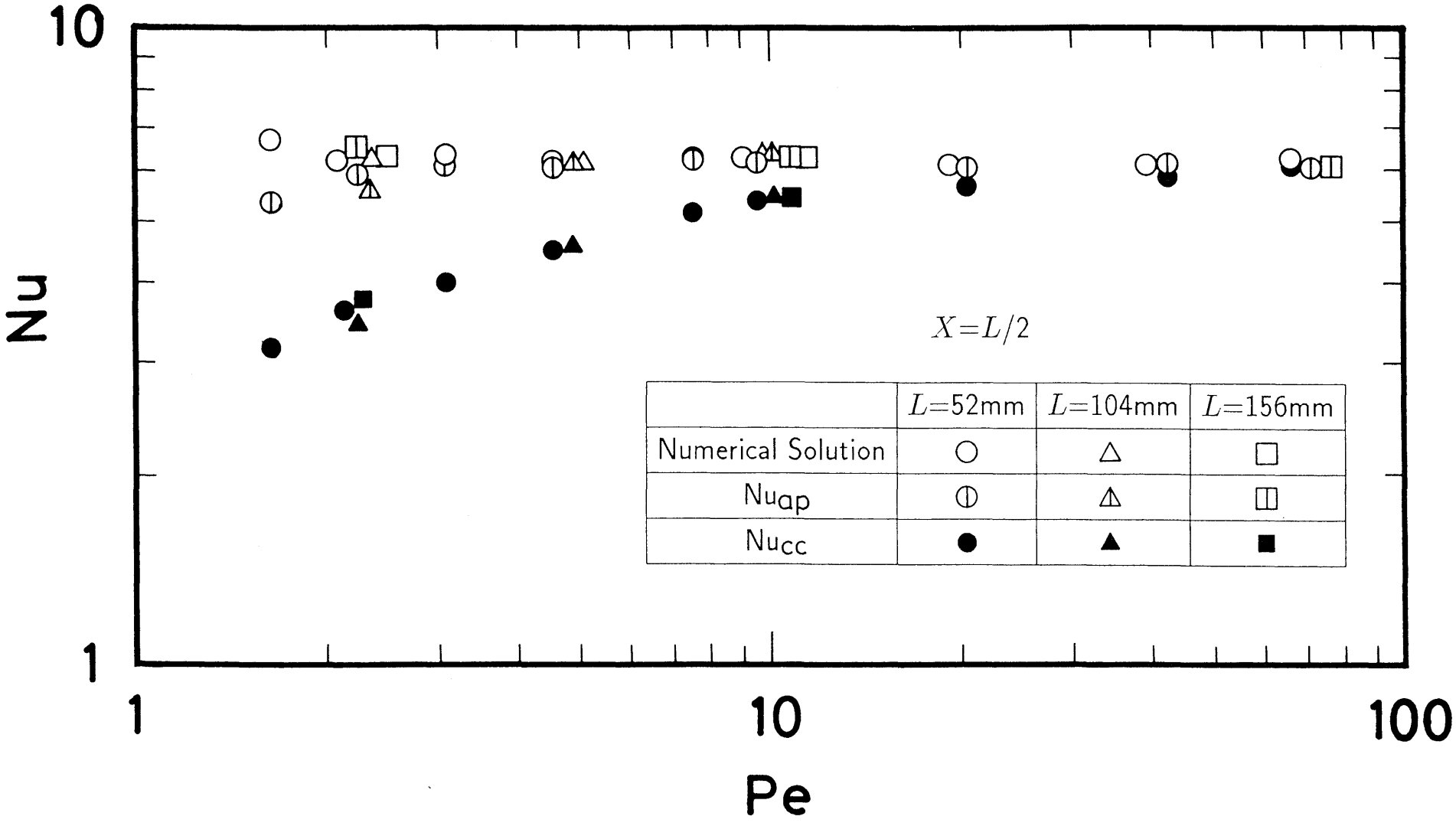

Fig. 2.15 Comparison of the local Nusselt numbers at $X = L/2$ for L=52 mm, 104 mm, and 156 mm obtained by numerical analysis with those based on liquid temperatures estimated by approximate analytical solution (Nu_{ap}), and with those based on the liquid temperatures estimated by the method of linear interpolation between T_{in} and T_{out} (Nu_{cc}).

Appendix C

Experiments of Liquid Sodium Forced Convection Heat Transfer in a Concentric Annulus

The experimental facilities are shown schematically in Fig. A-1 on page 51 and the schematic of forced convection test section is shown in Fig. C-1. Experiments of forced convection heat transfer, from a 7.6 mm-diameter inner rod heater with a heated section of 52 mm in length to liquid sodium flowing in a concentric annulus (the outer pipe of 14.3 mm in inside diameter), were performed for inlet liquid temperature of about 573 K for the flow rates ranging from 0.007 to 6.5 m/s (Péclet numbers from 0.7 to 650). In general, the temperature difference between a heated surface and local bulk liquid becomes so small at low Péclet numbers that it makes evaluation of local heat transfer coefficients very difficult. For this reason, the heated section of 52 mm in length was adopted to achieve relatively large temperature difference with heat fluxes ranging from 2×10^5 to 1×10^6 W/m^2, and also not to make liquid sodium temperature exceed its boiling point at the downstream end of the heated section where the liquid temperature becomes maximum. Surface heat flux was calculated from the measured values of the heating current and the terminal voltage of the test heater. Figure C-2 shows the schematic of thermocouple locations. The thermocouple for liquid inlet temperature measurement is located 310 mm upstream from the lower end of the heated section, and that for outlet liquid temperature measurement is 69 mm downstream from the upper end of the heated section in the vertical annular passage. The thermocouples for surface temperature measurements are embedded diagonally to a surface depth of 0.25 mm at X = 10.5, 21.5, 32.5, and 43 mm. Heater surface temperatures were calculated from the measured temperatures by solving heat conduction equation in the

heater sheath supposing uniform surface heat flux. Local bulk mean temperature distribution was estimated by means of linear interpolation between the measured inlet and outlet bulk liquid temperatures, which was corrected by the Petukhov et al's method which takes account of axial conduction effect in liquid sodium and in the walls of the concentric annulus. The experimental conditions for the Péclet numbers below 100 are listed in Table 2.1 on page 103. Detailed explanation about the experiments was reported by Shiotsu et al (1993).

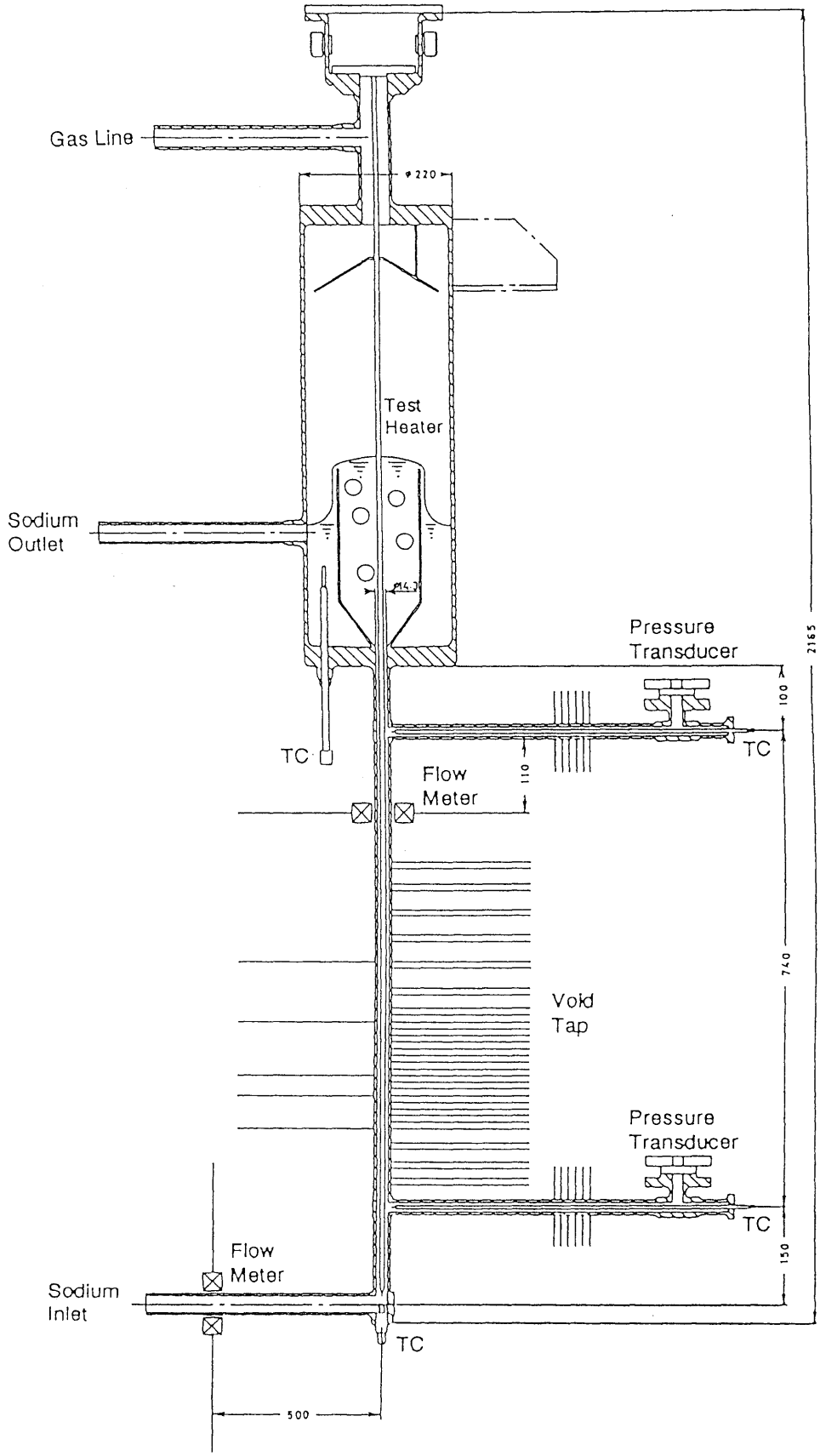

Fig. C-1 Schematic of forced convection test section.

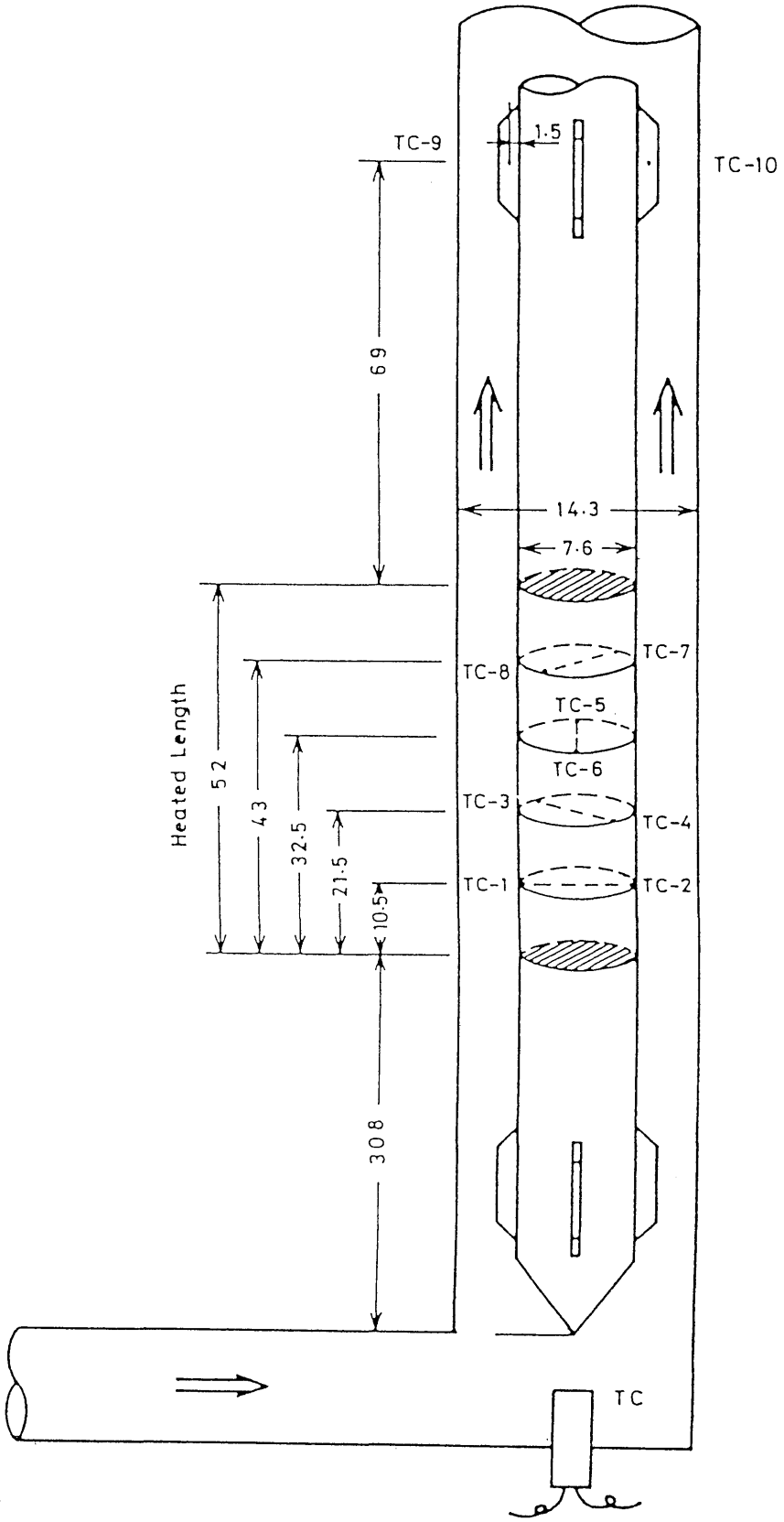

Fig. C-2 Schematic of thermocouple locations.

Appendix D

Source program with flowchart used for numerical analysis

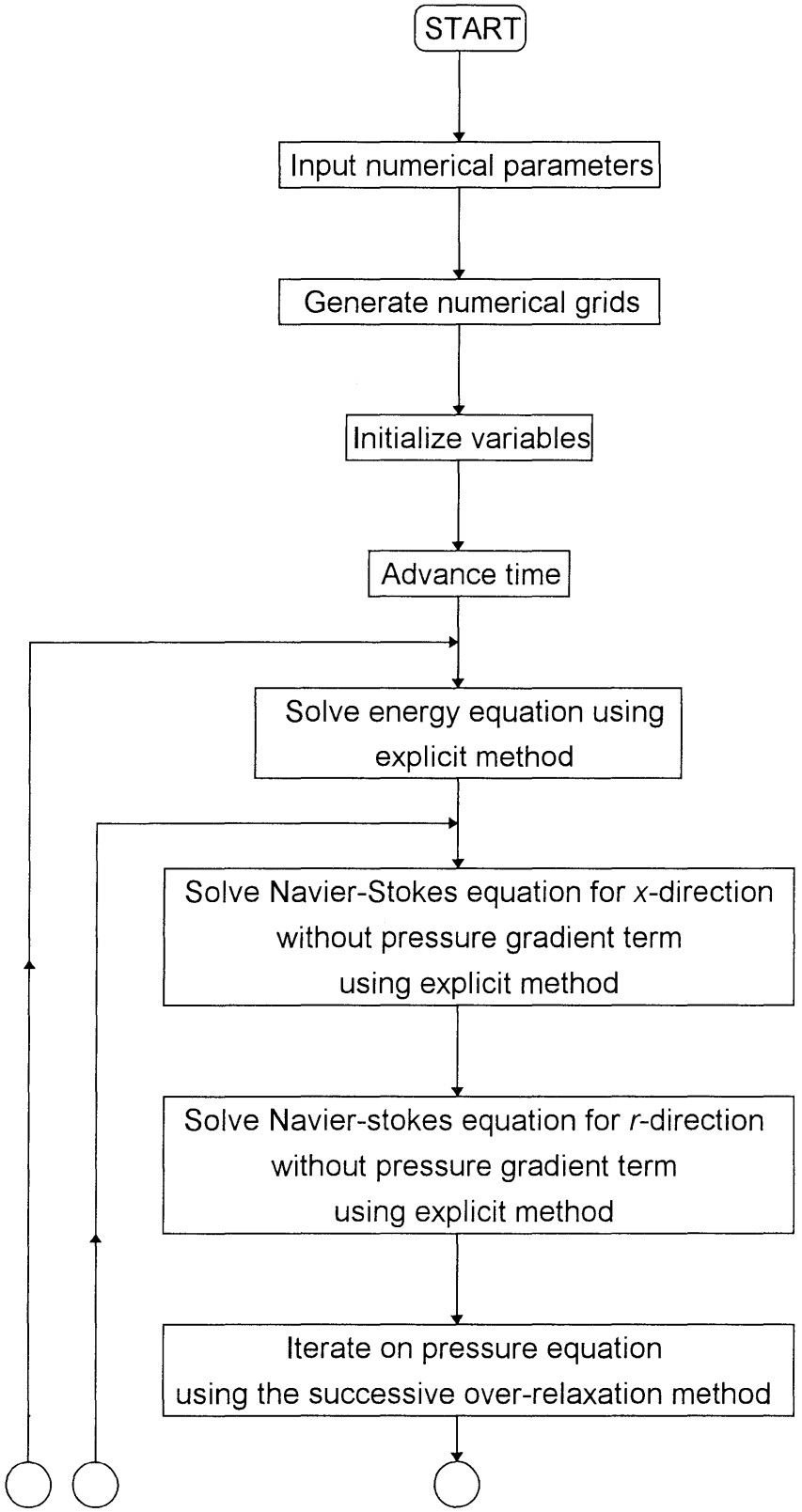

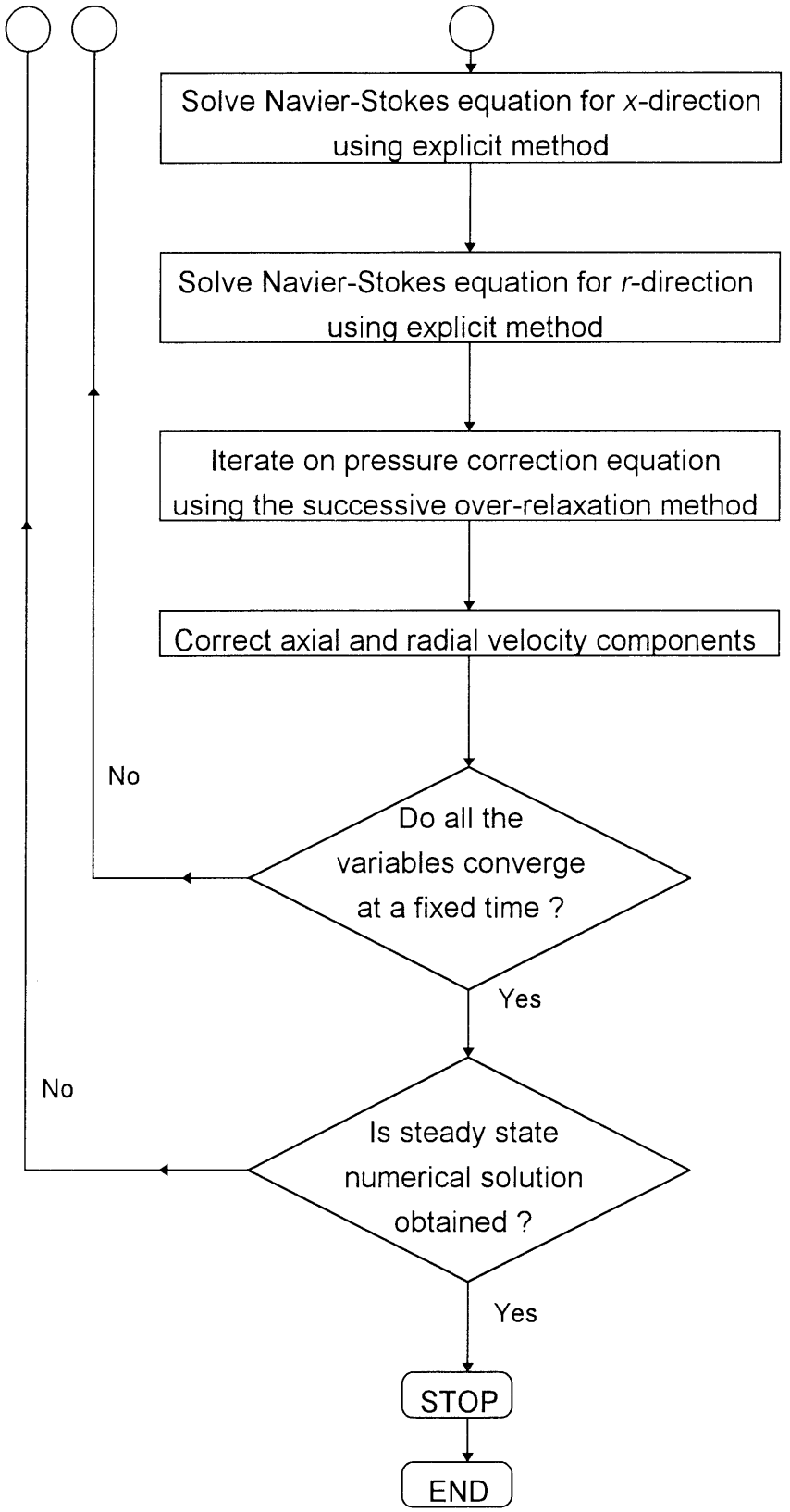

Fig. D-1 Flow chart of numerical procedure using SIMPLER algorithm.

```
      IMPLICIT REAL*8 (A-H,O-Z)
C
      COMMON /CO1/ RUR(25),RUZ(25),ZUR(200),ZUZ(200)
     &           /CO2/ DR1,DR,DRM1,DZ1,DZ,DZN1
     &           /SOLD/ VR(25,200),VZ(25,200),T(25,200),
     &                  UR(25,200),UZ(25,200),UT(25,200),
     &                  PUR(25,200),PUZ(25,200),PUT(25,200),
     &                  FUR(25,200),FUZ(25,200),FUT(25,200),
     &                  P(25,200),FP(25,200)
     &         /UM/ URM(25,200),UZM(25,200)
     &         /UA/ URA(25,200),UZA(25,200),PD(25,200),
     &              FPD(25,200)
     &         /CST0/ GV,PRES,TF,QV,QW,QRT
     &         /CST1/ DIA,RIN,ROUT,RATIO
     &         /DLP/ RE,GRQ,FR,PR,RF
     &         /XYZ/ XX,YY,ZZ
     &         /CST2/ M0,M1,M2,M3,N0,N1,N2,N3
     &         /CST22/ NWI,NWO,IN,MOUT
     &         /SOL/ HTNUM
     &         /CST5/ PAI,DTIM,TIM,RDTIM
     &         /CST8/ OMG,KVR,KVZ,KT,KPA,KPD,KE,NM,NB,IMAX,KMAX
     &         /CST9/ ERT,ERVO,ERST
     &         /CST11/ ZN1,WQ1,WQ2
     &         /CST14/ IVI,IP
     &         /CST16/ ITE
     &         /VEL/ V0
     &         /BC/ IBCT
     &         /CST20/ COEF,IU,IUST
     &         /PROP0/ RO0,VIS0,CP0,TC0,VIK0,TD0,BETA0
     &         /ERMAX/ PTMAX,PSMAX,PTER,PSER,PSM
     &         /TTIME/ TIM1,TIM2,TIM3,TIM4,TIM5,TIM6,IHT
     &         /IJOB/ JOBITE
     &         /STEP/ KESTEP
     &         /REFL/ RL
     &         /THICK/ TATHCK
     &         /IFC/ IFCHT
      COMMON /ROCONST/ TEMPRO
C
      OPEN(55,FILE='../FCPROG_3/data_cont1')
C
      OPEN(2,FILE='../FCPROG_3/FCDATA/1L_Pe_72_hcap_0',
     &       FORM='UNFORMATTED')
      OPEN(20,FILE='../FCPROG_3/FCDATA/1L_Pe_72_25_hcap_0',
     &       FORM='UNFORMATTED')
      OPEN(21,FILE='../FCPROG_3/FCDATA/1L_Pe_72_200_hcap_0',
     &       FORM='UNFORMATTED')
      OPEN(22,FILE='../FCPROG_3/FCDATA/1L_Pe_72_25200_hcap_0',
     &       FORM='UNFORMATTED')
C
      OPEN(3,FILE='../FCPROG_3/FCDATA/1L_Pe_72_hcap_1',
     &       FORM='UNFORMATTED')
      OPEN(30,FILE='../FCPROG_3/FCDATA/1L_Pe_72_25_hcap_1',
     &       FORM='UNFORMATTED')
      OPEN(31,FILE='../FCPROG_3/FCDATA/1L_Pe_72_200_hcap_1',
     &       FORM='UNFORMATTED')
      OPEN(32,FILE='../FCPROG_3/FCDATA/1L_Pe_72_25200_hcap_1',
     &       FORM='UNFORMATTED')
c
      OPEN(8,FILE='../FCPROG_3/1L_Pe_72_hcap_1')
C
        CALL PRDATA
C
      RF=1.D0/FR
      RL=2.D0*(ROUT-RIN)
C
      READ(55,50) KESTEP,DTIM,TIM1,TIM2,TIM3,TIM4,TIM5,TIM6,IHT,NB
   50 FORMAT(10X,I10/6X,E10.3,6(/35X,F12.7),/35X,I4/35X,I3)
      READ(55,51) IMAX
   51 FORMAT(6X,I5)
      WRITE(6,*) OMG
      READ(55,52) DOMG
   52 FORMAT(6X,F7.4)
      OMG=OMG+DOMG
      WRITE(6,*) OMG
      READ(55,505) IU
      READ(55,506) IUST
      READ(55,507) COEF
  505 FORMAT(24X,I5)
  506 FORMAT(25X,I5)
  507 FORMAT(6X,F10.4)
C
      KMAX=9999999
C
      M0=M1+1
      N0=N1+1
      WRITE(8,601) M0,N0,DTIM
  601 FORMAT(1H ,30X,'M0=',I3,'     N0=',I3,'     DTIM=',E10.3,
     &       '(SEC)')
      WRITE(8,602) NWI,NWO
  602 FORMAT(1H ,30X,'NWI=',I3,'     NWO=',I3)
C
      DZDR=DZ/DR
      WRITE(8,6499) DR,DZ,DZDR
 6499 FORMAT(1H ,10X,'DR=',E11.4,' DZ=',E11.4,' DZ/DR =',E11.4)
      WRITE(8,6500) RIN,ROUT,RATIO
 6500 FORMAT(1H ,10X,'RIN=',E11.4,'(M) :   ROUT=',E11.4,
     &       '(M)*****   ; ROUT/RIN =',F10.3)
      WRITE(8,6510) WQ1,WQ2
```

```
 6510 FORMAT(1H ,10X,'WQ1=',E11.4,' :   WQ2=',E11.4)
      WRITE(8,6501) TF,QV,QW,V0
 6501 FORMAT(1H ,10X,'Liquid Temp. (C) :        TF =',F6.1/
     &        1H ,10X,'Flow Rate (m3/s):         QV =',E10.3/
     &        1H ,10X,'Heat Flux (W/m2) :        QW =',E11.4/
     &        1H ,10X,'Fluid Velocity (m/s) : V0 =',E10.3)
      WRITE(8,678) RE,GRQ,FR,PR
  678 FORMAT(1H ,'@@@@@@@@@@@@@@   Re=',E11.4,'   Grq=',E11.4,
     &        '   Fr=',E11.4,'   Pr=',E11.4)
C
      SS=PAI*(ROUT*ROUT-RIN*RIN)
      SL=2.D0*PAI*(RIN+ROUT)
      REM=4.D0*V0*SS/VIK0/SL
      PEC=REM*PR
      QVL=QV*60.D0*1000.D0
      WRITE(8,630) REM,PEC,QVL
  630 FORMAT(/1H ,'++++<Rem>=',E11.4,'     <Pe>=',E11.4,'   QVL=',
     &        F7.4,'(l/min)')
C
      WRITE(8,650) XX,YY,ZZ
  650 FORMAT(1H ,' XX=',E11.4,' YY=',E11.4,' ZZ=',E11.4)
C
      WRITE(8,603) OMG,DOMG
  603 FORMAT(1H ,20X,'RELAXATION FACTOR ;   OMG=',F7.4,'   DOMG=',F7.4)
C
      WRITE(8,6004) TIM1,TIM2,TIM3,TIM4,TIM5,TIM6
 6004 FORMAT(1H ,'   TIM1=',E11.4,'   TIM2=',E11.4,'   TIM3=',E11.4,'   TIM4
     &=',E11.4,'   TIM5=',E11.4,'   TIM6=',E11.4)
      WRITE(8,660) COEF,NB,IU
  660 FORMAT(1H ,20X,'COEF=',F10.4,'   SHUUSOKUHANTEI(NB)',I3,
     &   ' KAI-OKI   UCHIDASHI-KANKAKU(IU) WA KE GA ',I5,' KAI-OKI DESU')
      WRITE(8,661) IMAX
  661 FORMAT(1H ,20X,'IMAX=',I6)
C
C
 9999 CONTINUE
C
C------ calculation of Tm for density of Na --------
      IFCHT=0
      IF(KE.GE.2) CALL FCHT
C
      KE=KE+1
C
      ITE=0
 8888 CONTINUE
C
C
C-------- CALCULATION OF TEMPERATURE DISTRIBUTION ----------
CCCCCC       non-heating     CCCC
      IF(QW.eq.0.D0) go to 2
CCCCCC       non-heating     CCCC
C
      CALL TEMP
      ISTOP=0
      IF(ISTOP.NE.1) go to 2
      CALL PRINT
      STOP
    2 continue
C
C-------- CALCULATION OF URM ----------
      IP=0
      CALL VRVR
C
C-------- CALCULATION OF UZM ----------
      CALL VZVZ
C
C-------- PRESSURE EQUATION ----------
      CALL PRESS
      IF(KPA.GE.IMAX) GO TO 1234
C-------- CALCULATION OF URA ----------
      IP=1
      CALL VRVR
C
C-------- CALCULATION OF UZA ----------
      CALL VZVZ
C
C-------- CALCULATION OF MASS SOURCE AND PRESSURE CORRECTION
EQUATION
      CALL PMOD
      IF(KPD.GE.IMAX) GO TO 1234
C
      CALL NCCON

      GO TO 9999
C
 1234 CALL PRINT
      CALL BUFFER
           CLOSE(2)
           CLOSE(20)
           CLOSE(21)
           CLOSE(22)
           CLOSE(3)
           CLOSE(30)
           CLOSE(31)
           CLOSE(32)
           CLOSE(55)
           CLOSE(8)
      STOP
```

```
      END
C-------- NEW.FORT77(COGKE) ---------------------------
C
      SUBROUTINE NCCON
C
      IMPLICIT REAL*8 (A-H,O-Z)
C
      COMMON /CO1/ RUR(25),RUZ(25),ZUR(200),ZUZ(200)
     &           /CO2/ DR1,DR,DRM1,DZ1,DZ,DZN1
     &           /CST8/ OMG,KVR,KVZ,KT,KPA,KPD,KE,NM,NB,IMAX,KMAX
     &           /SOLD/ VR(25,200),VZ(25,200),T(25,200),
     &                  UR(25,200),UZ(25,200),UT(25,200),
     &                  PUR(25,200),PUZ(25,200),PUT(25,200),
     &                  FUR(25,200),FUZ(25,200),FUT(25,200),
     &                  P(25,200),FP(25,200)
     &           /PFT/   PT(25,200),FT(25,200)
     &           /PFVR/   PVR(25,200),FVR(25,200)
     &           /PFVZ/   PVZ(25,200),FVZ(25,200)
     &           /YYY/ YUT(25,200),YUR(25,200),YUZ(25,200)
     &           /YYYY/ YT(25,200)
     &           /SOL/ HTNUM
     &           /CST0/ GV,PRES,TF,QV,QW,QRT
     &           /CST1/ DIA,RIN,ROUT,RATIO
     &           /CST2/ M0,M1,M2,M3,N0,N1,N2,N3
     &           /CST4/ DY2,C1,CD3,DD0,D1
     &           /CST5/ PAI,DTIM,TIM,RDTIM
     &           /CST9/ ERT,ERVO,ERST
     &           /CST14/ IVI,IP
     &           /CST20/ COEF,IU,IUST
     &           /CST22/ NWI,NWO,IN,MOUT
     &           /ERMAX/ PTMAX,PSMAX,PTER,PSER,PSM
     &           /TTIME/ TIM1,TIM2,TIM3,TIM4,TIM5,TIM6,IHT
     &           /NTIME/ MT1,MT2,MT3,MT4,MT5,MT6,ICONV
     &           /IJOB/ JOBITE
     &           /STEP/ KESTEP
     &           /VEL/ V0
     &           /REFL/ RL
     &           /IFC/ IFCHT
C
      TIM=FLOAT(KE)*DTIM*RL/V0
C
      IF(IVI.NE.0) GO TO 570
      IUR=0
      IUZ=0
      IT=0
      ICONV=0
C
      IF(IU.LT.IUST.AND.KE.LT.IUST) GO TO 7
      IF((KE/IU*IU-KE).NE.0) GO TO 7
      WRITE(8,61) KE,TIM,PTER,PSER
   61 FORMAT(/1H ,120('-')
     &       /1H ,40X,'@@ KE=',I8,'   TIM=',F15.6,'(SEC)',
     &       '   PTER=',E11.4,'   PSER=',E11.4)
      CALL PRINT
    7 CONTINUE
C
      IF(KE/NB*NB-KE) 564,8,564
    8 IF(KE.EQ.NB) GO TO 564
C
      PSM=PSMAX
      PTMAX=1.D0
      PSMAX=0.D0
      DO 563 J=1,N1
      DO 563 I=IN,MOUT
      IF(ABS(UZ(I,J)).GT.PSMAX) PSMAX=ABS(UZ(I,J))
  563 CONTINUE
      DPSM=PSMAX-PSM
      IF(PSMAX.NE.0.D0) DPCON=ABS(DPSM/PSMAX)
      PTER=ERT*PTMAX*COEF
      PSER=ERST*PSMAX*COEF
C
      IF(KE.EQ.1) GO TO 564
      DO 562 J=1,N1
      DO 562 I=2,M1
      DDTY=T(I,J)-YT(I,J)
      DTY=ABS(T(I,J)-YT(I,J))
      ITY=I
      JTY=J
      IF(DTY.LE.PTER) GO TO 562
      GO TO 564
  562 CONTINUE
      print*,'++++ T CONVERGED !! ++++'
      IT=1
C
      DO 466 J=2,N2
      DO 466 I=IN,MOUT
      DDSY=UZ(I,J)-YUZ(I,J)
      DSY=ABS(UZ(I,J)-YUZ(I,J))
      IF(DSY.LE.PSER) GO TO 466
      print*,'(',I,',',J,')       UZ=',UZ(I,J)
      print*,'(',I,',',J,')     YUZ=',YUZ(I,J),'DZY=',DDSY
      GO TO 564
  466 CONTINUE
      print*,'**** UZ CONVERGED !! ****'
      IUZ=1
C
      DO 566 J=2,N1
```

```
      DO 566 I=IN,MOUT-1
      DDSY=UR(I,J)-YUR(I,J)
      DSY=ABS(UR(I,J)-YUR(I,J))
      IF(DSY.LE.PSER) GO TO 566
      print*,'(',I,',',J,')     UR=',UR(I,J)
      print*,'(',I,',',J,')    YUR=',YUR(I,J),'DSY=',DDSY
      GO TO 564
  566 CONTINUE
      print*,'>>>> UR CONVERGED !! <<<<'
      IUR=1
C
      IF((IT.NE.1).OR.(IUR.NE.1).OR.(IUZ.NE.1)) GO TO 564
                              ICONV=1
      WRITE(8,1000) PTER,PSER,DPSM,KE,TIM
 1000 FORMAT(/1H ,'$$$$$$$$$$   CONVERGED   !!!!!!!!!   PTER=',E11.4,
     &        '   PSER=',E11.4,'   DPSM=',E11.4,'   KE=',I8,'   TIM=',E11.4,
     &        '(SEC)')
C
      WRITE(8,666)
  666 FORMAT(/1H ,'   ¥¥¥ CONVERGED !!!')
      GO TO 570
C
  564 CONTINUE
C
 8888 DO 565 J=1,N0
      DO 565 I=1,M0
      PUR(I,J)=UR(I,J)
      PUZ(I,J)=UZ(I,J)
      PUT(I,J)=UT(I,J)
      PVR(I,J)=VR(I,J)
      PVZ(I,J)=VZ(I,J)
      PT(I,J)=T(I,J)
      IF(KE/NB*NB-KE) 565,567,565
  567 YUR(I,J)=UR(I,J)
      YUZ(I,J)=UZ(I,J)
      YT(I,J)=T(I,J)
  565 CONTINUE
C
      IF(KE.Lt.KESTEP) GO TO 234
      WRITE(8,667) KESTEP,KE,TIM
  667 FORMAT(/1H ,'******** KESTEP =',I8,'       KE=',I8,'   TIM=',
     &        F15.6,'(SEC)')
      IFCHT=1
      CALL FCHT
      CALL PRINT
      CALL BUFFER
      STOP
  234 CONTINUE
C
      IF((KE/IHT*IHT-KE).EQ.0) WRITE(8,213) TIM,KE,KPA,KPD
      IFCHT=1
      IF((KE/IHT*IHT-KE).EQ.0) CALL FCHT
C
                  IF((KE.LE.KESTEP).AND.(KE.NE.MT1).AND.(KE.NE.MT2).AND.
     &               (KE.NE.MT3).AND.(KE.NE.MT4).AND.(KE.NE.MT5).AND.
     &               (KE.NE.MT6).AND.((KE/IHT*IHT-KE).NE.0)) RETURN
  213 FORMAT(1H ,'<<<<< TIM=',F15.6,'(SEC) >>>>>      KE=',I8,
     &        '   KPA=',I4,'   KPDmod=',I4)
      KV=1
C
      GO TO 5700
C
  570 CONTINUE
C-----  CALCULATION OF HEATTRANSFER COEFFICIENT
      IFCHT=1
      CALL FCHT
 5700 CONTINUE
C
      IF(IVI.NE.0) GO TO 2000
      IF((ICONV.NE.1).AND.(KE.LE.KESTEP)) RETURN
      CALL PRINT
      CALL BUFFER
      IF(ICONV.EQ.1) STOP
C
 2000 IF(IVI.EQ.1) RETURN
      END
```

```
C
      SUBROUTINE PRDATA
C
      IMPLICIT REAL*8 (A-H,O-Z)
C
      COMMON /CO1/ RUR(25),RUZ(25),ZUR(200),ZUZ(200)
     &            /CO2/ DR1,DR,DRM1,DZ1,DZ,DZN1
     &            /SOLD/ VR(25,200),VZ(25,200),T(25,200),
     &                   UR(25,200),UZ(25,200),UT(25,200),
     &                   PUR(25,200),PUZ(25,200),PUT(25,200),
     &                   FUR(25,200),FUZ(25,200),FUT(25,200),
     &                   P(25,200),FP(25,200)
     &            /PFT/ PT(25,200),FT(25,200)
     &            /PFVR/ PVR(25,200),FVR(25,200)
     &            /PFVZ/ PVZ(25,200),FVZ(25,200)
     &            /UM/ URM(25,200),UZM(25,200)
     &            /UA/ URA(25,200),UZA(25,200),PD(25,200),
     &                 FPD(25,200)
     &            /CST0/ GV,PRES,TF,QV,QW,QRT
     &            /CST1/ DIA,RIN,ROUT,RATIO
```

```
     &            /CST2/ M0,M1,M2,M3,N0,N1,N2,N3
     &            /CST22/ NWI,NWO,IN,MOUT
     &            /SOL/ HTNUM
     &            /CST5/ PAI,DTIM,TIM,RDTIM
     &            /CST8/ OMG,KVR,KVZ,KT,KPA,KPD,KE,NM,NB,IMAX,KMAX
     &            /CST9/ ERT,ERVO,ERST
     &            /CST10/ ICON
     &            /CST11/ ZN1,WQ1,WQ2
     &            /CST14/ IVI,IP
      COMMON /PROP0/ RO0,VIS0,CP0,TC0,VIK0,TD0,BETA0
     &            /DLP/   RE,GRQ,FR,PR,RF
     &            /XYZ/   XX,YY,ZZ
     &            /VEL/ V0
     &            /BC/ IBCT
     &            /CST20/ COEF,IU,IUST
     &            /ERMAX/ PTMAX,PSMAX,PTER,PSER,PSM
     &            /TTIME/ TIM1,TIM2,TIM3,TIM4,TIM5,TIM6,IHT
     &            /BB/ B(25,200),BD(25,200)
     &            /THICK/ TATHCK
C
        PRINT*,'>>> prd.f <<<'
      READ(20) RUR
      READ(20) RUZ
      READ(21) ZUR
      READ(21) ZUZ
      READ(22) UR
      READ(22) PUR
      READ(22) UZ
      READ(22) PUZ
      READ(22) UT
      READ(22) PUT
      READ(22) VR
      READ(22) PVR
      READ(22) VZ
      READ(22) PVZ
      READ(22) T
      READ(22) PT
      READ(22) URM
      READ(22) UZM
      READ(22) URA
      READ(22) UZA
      READ(22) P
      READ(22) FP
      READ(22) PD
      READ(22) FPD
      READ(22) BD
      READ(2) GV
      READ(2) PRES
      READ(2) TF
      READ(2) QV
      READ(2) QW
      READ(2) V0
      READ(2) QRT
      READ(2) DR
      READ(2) DZ
      READ(2) M0
      READ(2) M1
      READ(2) M2
      READ(2) M3
      READ(2) N0
      READ(2) N1
      READ(2) N2
      READ(2) N3
      READ(2) NWI
      READ(2) NWO
      READ(2) IN
      READ(2) MOUT
      READ(2) IBCT
      READ(2) PAI
      READ(2) DTIM
      READ(2) TIM
      READ(2) RDTIM
      READ(2) DIA
      READ(2) RIN
      READ(2) ROUT
      READ(2) RATIO
      READ(2) ZN1
      READ(2) WQ1
      READ(2) WQ2
      READ(2) OMG
      READ(2) KVR
      READ(2) KVZ
      READ(2) KT
      READ(2) KE
      READ(2) KPA
      READ(2) KPD
      READ(2) NM
      READ(2) NB
      READ(2) IMAX
      READ(2) KMAX
      READ(2) IVI
      READ(2) ERT
      READ(2) ERVO
      READ(2) ERST
      READ(2) ICON
      READ(2) COEF
      READ(2) IU
      READ(2) IUST
```

```
      READ(2) PTMAX
      READ(2) PSMAX
      READ(2) PTER
      READ(2) PSER
      READ(2) PSM
      READ(2) RO0
      READ(2) VIS0
      READ(2) CP0
      READ(2) TC0
      READ(2) VIK0
      READ(2) TD0
      READ(2) BETA0
      READ(2) RE
      READ(2) GRQ
      READ(2) FR
      READ(2) PR
      READ(2) XX
      READ(2) YY
      READ(2) ZZ
      READ(2) TIM1
      READ(2) TIM2
      READ(2) TIM3
      READ(2) TIM4
      READ(2) TIM5
      READ(2) TIM6
      READ(2) IHT
      READ(2,END=999) TATHCK
  999 print*,'(TATHCK) O.K.'
C
      RETURN
      END

------------------------------------------------------------------------

      SUBROUTINE BUFFER
C
      IMPLICIT REAL*8 (A-H,O-Z)
C
      COMMON /CO1/ RUR(25),RUZ(25),ZUR(200),ZUZ(200)
     &           /CO2/ DR1,DR,DRM1,DZ1,DZ,DZN1
     &           /SOLD/ VR(25,200),VZ(25,200),T(25,200),
     &                  UR(25,200),UZ(25,200),UT(25,200),
     &                  PUR(25,200),PUZ(25,200),PUT(25,200),
     &                  FUR(25,200),FUZ(25,200),FUT(25,200),
     &                  P(25,200),FP(25,200)
     &           /PFT/ PT(25,200),FT(25,200)
     &           /PFVR/ PVR(25,200),FVR(25,200)
     &           /PFVZ/ PVZ(25,200),FVZ(25,200)
     &           /UM/ URM(25,200),UZM(25,200)
     &           /UA/ URA(25,200),UZA(25,200),PD(25,200),
     &                FPD(25,200)
     &           /CST0/ GV,PRES,TF,QV,QW,QRT
     &           /CST1/ DIA,RIN,ROUT,RATIO
     &           /CST2/ M0,M1,M2,M3,N0,N1,N2,N3
     &           /CST22/ NWI,NWO,IN,MOUT
     &           /SOL/ HTNUM
     &           /CST5/ PAI,DTIM,TIM,RDTIM
     &           /CST8/ OMG,KVR,KVZ,KT,KPA,KPD,KE,NM,NB,IMAX,KMAX
     &           /CST9/ ERT,ERVO,ERST
     &           /CST10/ ICON
     &           /CST11/ ZN1,WQ1,WQ2
     &           /CST14/ IVI,IP
      COMMON /PROP0/ RO0,VIS0,CP0,TC0,VIK0,TD0,BETA0
     &           /DLP/ RE,GRQ,FR,PR,RF
     &           /XYZ/ XX,YY,ZZ
     &           /VEL/ V0
     &           /BC/ IBCT
     &           /CST20/ COEF,IU,IUST
     &           /ERMAX/ PTMAX,PSMAX,PTER,PSER,PSM
     &           /TTIME/ TIM1,TIM2,TIM3,TIM4,TIM5,TIM6,IHT
     &           /THICK/ TATHCK
     &           /BB/ B(25,200),BD(25,200)
C
      JUKE=1
      IF(JUKE.NE.1) RETURN
                    REWIND 3
                    REWIND 30
                    REWIND 31
                    REWIND 32
      PRINT*,'!! PRINT.F !!'
C
      WRITE(30) RUR
      WRITE(30) RUZ
      WRITE(31) ZUR
      WRITE(31) ZUZ
      WRITE(32) UR
      WRITE(32) PUR
      WRITE(32) UZ
      WRITE(32) PUZ
      WRITE(32) UT
      WRITE(32) PUT
      WRITE(32) VR
      WRITE(32) PVR
      WRITE(32) VZ
      WRITE(32) PVZ
      WRITE(32) T
      WRITE(32) PT
      WRITE(32) URM
      WRITE(32) UZM
```

```
      WRITE(32) URA
      WRITE(32) UZA
      WRITE(32) P
      WRITE(32) FP
      WRITE(32) PD
      WRITE(32) FPD
      WRITE(32) BD
      WRITE(3) GV
      WRITE(3) PRES
      WRITE(3) TF
      WRITE(3) QV
      WRITE(3) QW
      WRITE(3) V0
      WRITE(3) QRT
      WRITE(3) DR
      WRITE(3) DZ
      WRITE(3) M0
      WRITE(3) M1
      WRITE(3) M2
      WRITE(3) M3
      WRITE(3) N0
      WRITE(3) N1
      WRITE(3) N2
      WRITE(3) N3
      WRITE(3) NWI
      WRITE(3) NWO
      WRITE(3) IN
      WRITE(3) MOUT
      WRITE(3) IBCT
      WRITE(3) PAI
      WRITE(3) DTIM
      WRITE(3) TIM
      WRITE(3) RDTIM
      WRITE(3) DIA
      WRITE(3) RIN
      WRITE(3) ROUT
      WRITE(3) RATIO
      WRITE(3) ZN1
      WRITE(3) WQ1
      WRITE(3) WQ2
      WRITE(3) OMG
      WRITE(3) KVR
      WRITE(3) KVZ
      WRITE(3) KT
      WRITE(3) KE
      WRITE(3) KPA
      WRITE(3) KPD
      WRITE(3) NM
      WRITE(3) NB
      WRITE(3) IMAX
      WRITE(3) KMAX
      WRITE(3) IVI
      WRITE(3) ERT
      WRITE(3) ERVO
      WRITE(3) ERST
      WRITE(3) ICON
      WRITE(3) COEF
      WRITE(3) IU
      WRITE(3) IUST
      WRITE(3) PTMAX
      WRITE(3) PSMAX
      WRITE(3) PTER
      WRITE(3) PSER
      WRITE(3) PSM
      WRITE(3) RO0
      WRITE(3) VIS0
      WRITE(3) CP0
      WRITE(3) TC0
      WRITE(3) VIK0
      WRITE(3) TD0
      WRITE(3) BETA0
      WRITE(3) RE
      WRITE(3) GRQ
      WRITE(3) FR
      WRITE(3) PR
      WRITE(3) XX
      WRITE(3) YY
      WRITE(3) ZZ
      WRITE(3) TIM1
      WRITE(3) TIM2
      WRITE(3) TIM3
      WRITE(3) TIM4
      WRITE(3) TIM5
      WRITE(3) TIM6
      WRITE(3) IHT
      WRITE(3) TATHCK
c
      RETURN
      END

------------------------------------------------------------------------

      SUBROUTINE TEMP
C
      IMPLICIT REAL*8 (A-H,O-Z)
C
      COMMON /CO1/ RUR(25),RUZ(25),ZUR(200),ZUZ(200)
     &           /CO2/ DR1,DR,DRM1,DZ1,DZ,DZN1
     &           /SOLD/ VR(25,200),VZ(25,200),T(25,200),
```

```
     &                    UR(25,200),UZ(25,200),UT(25,200),
     &                    PUR(25,200),PUZ(25,200),PUT(25,200),
     &                    FUR(25,200),FUZ(25,200),FUT(25,200),
     &                    P(25,200),FP(25,200)
     &          /PFT/ PT(25,200),FT(25,200)
     &          /PFVR/ PVR(25,200),FVR(25,200)
     &          /PFVZ/ PVZ(25,200),FVZ(25,200)
     &          /CST0/ GV,PRES,TF,QV,QW,QRT
     &          /CST1/ DIA,RIN,ROUT,RATIO
     &          /CST2/ M0,M1,M2,M3,N0,N1,N2,N3
     &          /CST22/ NWI,NWO,IN,MOUT
     &          /CST5/ PAI,DTIM,TIM,RDTIM
     &          /CST8/ OMG,KVR,KVZ,KT,KPA,KPD,KE,NM,NB,IMAX,KMAX
     &          /CST9/ ERT,ERVO,ERST
     &          /CST10/ ICON
     &          /CST11/ ZN1,WQ1,WQ2
     &          /CST14/ IVI,IP
     &          /BC/ IBCT
     &          /PROP0/ RO0,VIS0,CP0,TC0,VIK0,TD0,BETA0
     &          /XYZ/ XX,YY,ZZ
     &          /REFL/ RL
C
      KT=1
C
    1 CONTINUE
C
      DO 100 J=2,N1
      DO 200 I=2,M1
C
      TIJ=PT(I,J)
      TIP1=PT(I+1,J)
      TIM1=PT(I-1,J)
      TJP1=PT(I,J+1)
      TJM1=PT(I,J-1)
C
      CTIJ=TIJ*QRT+TF
      CTIP1=TIP1*QRT+TF
      CTIM1=TIM1*QRT+TF
      CTJP1=TJP1*QRT+TF
      CTJM1=TJM1*QRT+TF
C
      RLOG1=LOG(RUZ(I+1)/RUZ(I))
      RLOG2=LOG(RUR(I)/RUZ(I))
      RLOG3=LOG(RUZ(I+1)/RUR(I))
      RLOG4=LOG(RUZ(I)/RUZ(I-1))
      RLOG5=LOG(RUR(I-1)/RUZ(I-1))
      RLOG6=LOG(RUZ(I)/RUR(I-1))
C
      IF((I.GE.IN).AND.(I.LE.MOUT)) GO TO 20
      IF(I.GT.MOUT) GO TO 21
C
      RCPIJ=ROT(CTIJ)*CPT(CTIJ)/RO0/CP0
C
      FN=RUR(I)*RLOG1/(RLOG2*TC0/TCT(CTIJ)
     &   +RLOG3*TC0/TCT(CTIP1))
      IF(I.EQ.IN-1) FN=RUR(I)*RLOG1/(RLOG2*TC0/TCT(CTIJ)
     &                  +RLOG3*TC0/TC(CTIP1))
      FS=RUR(I-1)*RLOG4/(RLOG5*TC0/TCT(CTIM1)
     &   +RLOG6*TC0/TCT(CTIJ))
      HE=2.D0*TCT(CTJP1)*TCT(CTIJ)
     &    /(TCT(CTIJ)+TCT(CTJP1))/TC0
      HW=2.D0*TCT(CTIJ)*TCT(CTJM1)
     &    /(TCT(CTIJ)+TCT(CTJM1))/TC0
      D1=(FN*(TIP1-TIJ)-FS*(TIJ-TIM1))/DR/DR
      D4=(HE*(TJP1-TIJ)-HW*(TIJ-TJM1))/DZ/DZ
C
      TMP=T(I,J)*QRT+TF
      RCP=ROT(TMP)*CPT(TMP)/RO0/CP0
      AT=ZZ*(-D1/RUZ(I)-D4)
      T(I,J)=(RCPIJ*TIJ-DTIM*AT)/RCP
      GO TO 200
   21 RCPIJ=ROH(CTIJ)*CPH(CTIJ)/RO0/CP0
      FN=RUR(I)*RLOG1/(RLOG2*TC0/TCH(CTIJ)
     &   +RLOG3*TC0/TCH(CTIP1))
      FS=RUR(I-1)*RLOG4/(RLOG5*TC0/TCH(CTIM1)
     &   +RLOG6*TC0/TCH(CTIJ))
      IF(I.EQ.MOUT+1) FS=RUR(I-1)*RLOG4/(RLOG5*TC0/TC(CTIM1)
     &                  +RLOG6*TC0/TCH(CTIJ))
      HE=2.D0*TCH(CTJP1)*TCH(CTIJ)
     &   /(TCH(CTIJ)+TCH(CTJP1))/TC0
      HW=2.D0*TCH(CTIJ)*TCH(CTJM1)
     &    /(TCH(CTIJ)+TCH(CTJM1))/TC0
      D1=(FN*(TIP1-TIJ)-FS*(TIJ-TIM1))/DR/DR
      D4=(HE*(TJP1-TIJ)-HW*(TIJ-TJM1))/DZ/DZ
C
      TMP=T(I,J)*QRT+TF
      RCP=ROH(TMP)*CPH(TMP)/RO0/CP0
      AT=ZZ*(-D1/RUZ(I)-D4)
      T(I,J)=(RCPIJ*TIJ-DTIM*AT)/RCP
      GO TO 200
C
   20 CONTINUE

      RCPIJ=RO(CTIJ)*CP(CTIJ)/RO0/CP0
C
      CPNA=CP(CTIJ)/CP0
C
      IF(I.EQ.IN) CTIM1=CTIJ
```

```
      IF(I.EQ.MOUT) CTIP1=CTIJ
C
      RIJ=RO(CTIJ)/RO0
      RIP1=RO(CTIP1)/RO0
      RIM1=RO(CTIM1)/RO0
      RJM1=RO(CTJM1)/RO0
      RJP1=RO(CTJP1)/RO0
C
  223 IF(I.NE.IN) GO TO 80
      VRIM2=-PVR(IN,J)
      GO TO 81
   80 VRIM2=PVR(I-2,J)
   81 IF(I.NE.MOUT) GO TO 82
      VRIP1=-PVR(MOUT-1,J)
      GO TO 83
   82 VRIP1=PVR(I+1,J)
C
   83 VRIJ=0.5D0*(PVR(I-1,J)+PVR(I,J))
      VRIF=0.5D0*(PVR(I,J)+VRIP1)
      VRIP=0.5D0*(VRIM2+PVR(I-1,J))
      FRC=RIJ*RUZ(I)*VRIJ*TIJ
      IF(VRIJ.LT.0.D0) GO TO 70
      FRP=RIM1*RUZ(I-1)*VRIP*TIM1
      C1=CPNA*(FRC-FRP)/DR
      GO TO 71
   70 FRF=RIP1*RUZ(I+1)*VRIF*TIP1
      C1=CPNA*(FRF-FRC)/DR
C
   71 IF(J.NE.2) GO TO 84
      VZJM2=PVZ(I,1)
      GO TO 85
   84 VZJM2=PVZ(I,J-2)
   85 IF(J.NE.N1) GO TO 86
      VZJP1=PVZ(I,N1)
      GO TO 87
   86 VZJP1=PVZ(I,J+1)
C
   87 VZIJ=0.5D0*(PVZ(I,J-1)+PVZ(I,J))
      VZJF=0.5D0*(PVZ(I,J)+VZJP1)
      VZJP=0.5D0*(PVZ(I,J-1)+VZJM2)
      FZC=RIJ*VZIJ*TIJ
      IF(VZIJ.LT.0.D0) GO TO 72
      FZP=RJM1*VZJP*TJM1
      C2=CPNA*(FZC-FZP)/DZ
      GO TO 73
   72 FZF=RJP1*VZJF*TJP1
      C2=CPNA*(FZF-FZC)/DZ
C
   73 TEMPC=TIJ*QRT+TF
      TEMPF=TIP1*QRT+TF
      TEMPP=TIM1*QRT+TF
      FN=ZZ*RUR(I)*RLOG1/(RLOG2*TC0/TC(TEMPC)
     &   +RLOG3*TC0/TC(TEMPF))
      FS=ZZ*RUR(I-1)*RLOG4/(RLOG5*TC0/TC(TEMPP)
     &   +RLOG6*TC0/TC(TEMPC))
      IF(I.EQ.IN) FS=ZZ*RUR(I-1)*RLOG4/(RLOG5*TC0/TCT(TEMPP)
     &              +RLOG6*TC0/TC(TEMPC))
      IF(I.EQ.MOUT) FN=ZZ*RUR(I)*RLOG1/(RLOG2*TC0/TC(TEMPC)
     &                 +RLOG3*TC0/TCH(TEMPF))
      TEMPF=TJP1*QRT+TF
      TEMPP=TJM1*QRT+TF
      HE=ZZ*2.D0*TC(TEMPF)*TC(TEMPC)
     &    /(TC(TEMPC)+TC(TEMPF))/TC0
      HW=ZZ*2.D0*TC(TEMPC)*TC(TEMPP)
     &    /(TC(TEMPC)+TC(TEMPP))/TC0
      D1=(FN*(TIP1-TIJ)-FS*(TIJ-TIM1))/DR/DR
      D4=(HE*(TJP1-TIJ)-HW*(TIJ-TJM1))/DZ/DZ
C
      TMP=T(I,J)*QRT+TF
      RCP=RO(TMP)*CP(TMP)/RO0/CP0
      AT=(C1-D1)/RUZ(I)+(C2-D4)
      T(I,J)=(RCPIJ*TIJ-DTIM*AT)/RCP
C
  200 CONTINUE
  100 CONTINUE
C
  356 DO 110 J=1,N0
      UT(M0,J)=UT(M1,J)
      T(M0,J)=T(M1,J)
      ZX=ZUR(J)
      IF(ZX.GT.WQ1)   GO TO 40
      UT(1,J)=UT(2,J)
      T(1,J)=T(2,J)
      GO TO 110
   40 IF(ZX.GT.WQ2) GO TO 41
C
      KTW=0
   43 KTW=KTW+1
      TW=0.5D0*(T(1,J)+T(2,J))*QRT+TF
      T(1,J)=T(2,J)+DR/TCT(TW)*TC0
      T1=T(1,J)*QRT+TF
      IF(KTW.EQ.1) GO TO 45
      if(KTW/10*10-KTW.eq.0)PRINT*,'              KTW =',KTW
      if(KTW/10*10-KTW.eq.0)PRINT*,' T1=',T1,' TT1=',TT1
      IF(T1.GE.0.D0) GO TO 777
      print*,'** T(1,',J,')=',T(1,J),' < TF DE STOP'
      CALL PRINT
      STOP
```

```
  777 TTS=ABS(T1-TT1)
      IF(TTS.LE.(T1*1.E-10)) GO TO 44
   45 TT1=T1
      GO TO 43
   44 UT(1,J)=T(1,J)*ROT(T1)*CPT(T1)/RO0/CP0
      GO TO 110
   41 T(1,J)=T(2,J)
  110 CONTINUE
C
      DO 1011 I=1,M0
      T(I,1)=0.D0
      IF((I.LT.IN).OR.(I.GT.MOUT)) T(I,1)=T(I,2)
      T(I,N0)=T(I,N1)
 1011 CONTINUE
C
      return
      END
```

```
C
      SUBROUTINE VRVR
C
      IMPLICIT REAL*8 (A-H,O-Z)
C
      COMMON /CO1/ RUR(25),RUZ(25),ZUR(200),ZUZ(200)
     &           /CO2/ DR1,DR,DRM1,DZ1,DZ,DZN1
     &           /SOLD/ VR(25,200),VZ(25,200),T(25,200),
     &                  UR(25,200),UZ(25,200),UT(25,200),
     &                  PUR(25,200),PUZ(25,200),PUT(25,200),
     &                  FUR(25,200),FUZ(25,200),FUT(25,200),
     &                  P(25,200),FP(25,200)
     &           /PFT/ PT(25,200),FT(25,200)
     &           /PFVR/ PVR(25,200),FVR(25,200)
     &           /PFVZ/ PVZ(25,200),FVZ(25,200)
     &           /UM/ URM(25,200),UZM(25,200)
     &           /UA/ URA(25,200),UZA(25,200),PD(25,200),
     &                FPD(25,200)
     &           /CST0/ GV,PRES,TF,QV,QW,QRT
     &           /CST1/ DIA,RIN,ROUT,RATIO
     &           /CST2/ M0,M1,M2,M3,N0,N1,N2,N3
     &           /CST22/ NWI,NWO,IN,MOUT
     &           /CST5/ PAI,DTIM,TIM,RDTIM
     &           /CST8/ OMG,KVR,KVZ,KT,KPA,KPD,KE,NM,NB,IMAX,KMAX
     &           /CST9/ ERT,ERVO,ERST
     &           /CST10/ ICON
     &           /CST14/ IVI,IP
     &           /BC/ IBCT
     &           /PROP0/ RO0,VIS0,CP0,TC0,VIK0,TD0,BETA0
     &           /DLP/   RE,GRQ,FR,PR,RF
     &           /XYZ/   XX,YY,ZZ
C
      KVR=1
C
    1 CONTINUE
C
      DO 100 J=2,N1
      DO 200 I=IN,MOUT-1
C
      TIJ=PT(I,J)
      TIP1=PT(I+1,J)
    3 TIP2=PT(I+2,J)
    4 TIM1=PT(I-1,J)
      TJP1=PT(I,J+1)
      TJM1=PT(I,J-1)
C
      CTIJ=TIJ*QRT+TF
      CTIP1=TIP1*QRT+TF
      CTIP2=TIP2*QRT+TF
      CTIM1=TIM1*QRT+TF
      CTJP1=TJP1*QRT+TF
      CTJM1=TJM1*QRT+TF
C
      IF(I.EQ.IN) CTIM1=CTIJ
      IF(I.EQ.MOUT-1) CTIP2=CTIP1
C
      VRIJ=PVR(I,J)
      VRIF=PVR(I+1,J)
      VRIP=PVR(I-1,J)
      VRJF=PVR(I,J+1)
      VRJP=PVR(I,J-1)
      ROIJ=RO(CTIJ)/RO0
      ROIP1=RO(CTIP1)/RO0
      ROIP2=RO(CTIP2)/RO0
      ROIM1=RO(CTIM1)/RO0
      FRC=0.5D0*(ROIJ+ROIP1)*RUR(I)*VRIJ*VRIJ
      IF(VRIJ.LT.0.D0) GO TO 70
      FRP=0.5D0*(ROIM1+ROIJ)*RUR(I-1)*VRIP*VRIP
      C1=(FRC-FRP)/DR
      GO TO 71
   70 FRF=0.5D0*(ROIP1+ROIP2)*RUR(I+1)*VRIF*VRIF
      C1=(FRF-FRC)/DR
C
   71 IF(J.NE.2) GO TO 80
      VZJM2=PVZ(I+1,1)
      VZJM22=PVZ(I,1)
      GO TO 81
   80 VZJM2=PVZ(I+1,J-2)
      VZJM22=PVZ(I,J-2)
```

```
   81 IF(J.NE.N1) GO TO 82
      VZJP1=PVZ(I,N1)
      VZJP11=PVZ(I+1,N1)
      GO TO 83
   82 VZJP1=PVZ(I,J+1)
      VZJP11=PVZ(I+1,J+1)
C
   83 VZIJ=0.25D0*(PVZ(I,J)+PVZ(I+1,J)+PVZ(I+1,J-1)+PVZ(I,J-1))
      VZJF=0.25D0*(PVZ(I,J)+PVZ(I+1,J)+VZJP11+VZJP1)
      VZJP=0.25D0*(PVZ(I,J-1)+PVZ(I+1,J-1)+VZJM2+VZJM22)
      ROJP1=RO(CTJP1)/RO0
      ROJM1=RO(CTJM1)/RO0
      CTIPJP=PT(I+1,J+1)*QRT+TF
      CTIPJM=PT(I+1,J-1)*QRT+TF
      FZC=0.5D0*(ROIJ+ROIP1)*VRIJ*VZIJ
      IF(VZIJ.LT.0.D0) GO TO 72
      FZP=0.5D0*(ROJM1+RO(CTIPJM)/RO0)*VRJP*VZJP
      C2=(FZC-FZP)/DZ
      GO TO 73
   72 FZF=0.5D0*(ROJP1+RO(CTIPJP)/RO0)*VRJF*VZJF
      C2=(FZF-FZC)/DZ
C
   73 TEMPC=TIJ*QRT+TF
      TEMPF=TIP1*QRT+TF
      FN=4.D0/3.D0/RE*RUZ(I+1)*VIS(TEMPF)/VIS0
      FS=4.D0/3.D0/RE*RUZ(I)*VIS(TEMPC)/VIS0
      D1=(FN*(VRIF-VRIJ)-FS*(VRIJ-VRIP))/DR/DR
      AN=0.5D0*(VRIF+VRIJ)*VIS(TEMPF)/VIS0
      AS=0.5D0*(VRIP+VRIJ)*VIS(TEMPC)/VIS0
      D2=XX*(AN-AS)/DR
      FN=XX*RUZ(I+1)*VIS(TEMPF)/VIS0
      FS=XX*RUZ(I)*VIS(TEMPC)/VIS0
      D3=(FN*(PVZ(I+1,J)-PVZ(I+1,J-1))
     &            -FS*(PVZ(I,J)-PVZ(I,J-1)))/DR/DZ
      T4E=0.25D0*(TIP1+PT(I+1,J+1)+TJP1+TIJ)
      T4W=0.25D0*(PT(I+1,J-1)+TIP1+TIJ+TJM1)
      TEMPE=T4E*QRT+TF
      TEMPW=T4W*QRT+TF
      FE=YY*VIS(TEMPE)/VIS0
      FW=YY*VIS(TEMPW)/VIS0
      D4=(FE*(VRJF-VRIJ)-FW*(VRIJ-VRJP))/DZ/DZ
      D5=(FE*(PVZ(I+1,J)-PVZ(I,J))
     &            -FW*(PVZ(I+1,J-1)-PVZ(I,J-1)))/DR/DZ
      IF(VRIJ.LT.0.D0) GO TO 230
      HVR=(VRIF-VRIJ)/DR
      GO TO 232
  230 HVR=(VRIJ-VRIP)/DR
  232 IF(VZIJ.LT.0.D0) GO TO 234
      HVZ=(VZJF-VZIJ)/DZ
      GO TO 235
  234 HVZ=(VZIJ-VZJP)/DZ
  235 TEMPH=0.5D0*(TIJ+TIP1)*QRT+TF
      H=FLOAT(IP)*(P(I+1,J)-P(I,J))/DR
     & -XX/RUR(I)*VIS(TEMPH)/VIS0*(HVR+HVZ-2.D0*VRIJ/RUR(I))
C
      TT=T(I,J)*QRT+TF
      TTI=T(I+1,J)*QRT+TF
      ROIJ=0.5D0*(RO(TT)+RO(TTI))/RO0
      PROIJ=0.5D0*(RO(CTIJ)+RO(CTIP1))/RO0
      AR=(C1-D1+D2+D3)/RUR(I)+(C2-D4-D5)+H
      VR(I,J)=(PROIJ*PVR(I,J)-DTIM*AR)/ROIJ
C
      UR(I,J)=ROIJ*VR(I,J)
  200 CONTINUE
  100 CONTINUE
C
C---------- normal velocity component ----------
      DO 110 J=1,N0
      UR(IN-1,J)=0.D0
      UR(MOUT,J)=0.D0
      VR(IN-1,J)=0.D0
      VR(MOUT,J)=0.D0
  110 CONTINUE
C
C---------- boundary ----------
      igo=0
      if(igo.eq.1) go to 555
C---------- boundary ----------
      DO 1011 I=IN,MOUT-1
      UR(I,1)=0.D0
      UR(I,N0)=UR(I,N1)
      VR(I,1)=0.D0
      VR(I,N0)=VR(I,N1)
 1011 CONTINUE
C
  555 continue
c
      DO 800 J=1,N0
      DO 800 I=IN-1,MOUT
      IF(IP.EQ.0) URM(I,J)=VR(I,J)
      IF(IP.EQ.1) URA(I,J)=VR(I,J)
  800 CONTINUE
C
      return
      END

C
```

```
      SUBROUTINE VZVZ
C
      IMPLICIT REAL*8 (A-H,O-Z)
C
      COMMON /CO1/ RUR(25),RUZ(25),ZUR(200),ZUZ(200)
     &           /CO2/ DR1,DR,DRM1,DZ1,DZ,DZN1
     &           /SOLD/ VR(25,200),VZ(25,200),T(25,200),
     &                  UR(25,200),UZ(25,200),UT(25,200),
     &                  PUR(25,200),PUZ(25,200),PUT(25,200),
     &                  FUR(25,200),FUZ(25,200),FUT(25,200),
     &                  P(25,200),FP(25,200)
     &           /PFT/ PT(25,200),FT(25,200)
     &           /PFVR/ PVR(25,200),FVR(25,200)
     &           /PFVZ/ PVZ(25,200),FVZ(25,200)
     &           /UM/ URM(25,200),UZM(25,200)
     &           /UA/ URA(25,200),UZA(25,200),PD(25,200),
     &                FPD(25,200)
     &           /CST0/ GV,PRES,TF,QV,QW,QRT
     &           /CST1/ DIA,RIN,ROUT,RATIO
     &           /CST2/ M0,M1,M2,M3,N0,N1,N2,N3
     &           /CST22/ NWI,NWO,IN,MOUT
     &           /CST5/ PAI,DTIM,TIM,RDTIM
     &           /CST8/ OMG,KVR,KVZ,KT,KPA,KPD,KE,NM,NB,IMAX,KMAX
     &           /CST9/ ERT,ERVO,ERST
     &           /CST10/ ICON
     &           /CST14/ IVI,IP
     &           /BC/ IBCT
     &           /PROP0/ RO0,VIS0,CP0,TC0,VIK0,TD0,BETA0
     &           /DLP/ RE,GRQ,FR,PR,RF
     &           /XYZ/ XX,YY,ZZ
C
      KVZ=1
C
    1 CONTINUE
C
      DO 100 J=2,N2
      DO 200 I=IN,MOUT
C
      TIJ=PT(I,J)
      TIP1=PT(I+1,J)
      TIM1=PT(I-1,J)
      TJP1=PT(I,J+1)
      IF(J.NE.N2) GO TO 3
      TJP2=PT(I,N1)
      GO TO 4
    3 TJP2=PT(I,J+2)
    4 TJM1=PT(I,J-1)
C
      CTIJ=TIJ*QRT+TF
      CTIP1=TIP1*QRT+TF
      CTIM1=TIM1*QRT+TF
      CTJP1=TJP1*QRT+TF
      CTJP2=TJP2*QRT+TF
      CTJM1=TJM1*QRT+TF
C
      IF(I.EQ.IN) CTIM1=CTIJ
      IF(I.EQ.MOUT) CTIP1=CTIJ
C
      ROIJ=RO(CTIJ)/RO0
      ROIP1=RO(CTIP1)/RO0
      ROIM1=RO(CTIM1)/RO0
      ROJP1=RO(CTJP1)/RO0
      ROJP2=RO(CTJP2)/RO0
      ROJM1=RO(CTJM1)/RO0
      CTIMJP=PT(I-1,J+1)*QRT+TF
      CTIPJP=PT(I+1,J+1)*QRT+TF
C
      IF(I.EQ.IN) CTIMJP=CTJP1
      IF(I.EQ.MOUT) CTIPJP=CTJP1
C
      VZIJ=PVZ(I,J)
      VZIF=PVZ(I+1,J)
      VZIP=PVZ(I-1,J)
      VZJF=PVZ(I,J+1)
      VZJP=PVZ(I,J-1)
C
  223 IF(I.NE.IN) GO TO 80
      VRIM2=-PVR(IN,J)
      VRIM22=-PVR(IN,J+1)
      GO TO 81
   80 VRIM2=PVR(I-2,J)
      VRIM22=PVR(I-2,J+1)
   81 IF(I.NE.MOUT) GO TO 82
      VRIP1=-PVR(MOUT-1,J)
      VRIP11=-PVR(MOUT-1,J+1)
      GO TO 83
   82 VRIP1=PVR(I+1,J)
      VRIP11=PVR(I+1,J+1)
C
   83 VRIJ=0.25D0*(PVR(I,J)+PVR(I,J+1)+PVR(I-1,J+1)+PVR(I-1,J))
      VRIF=0.25D0*(PVR(I,J)+VRIP1+VRIP11+PVR(I,J+1))
      VRIP=0.25D0*(PVR(I-1,J+1)+PVR(I-1,J)+VRIM2+VRIM22)
      FZC=0.5D0*(ROIJ+ROJP1)*RUZ(I)*VRIJ*VZIJ
      IF(VRIJ.LT.0.D0) GO TO 70
      FZP=0.5D0*(ROIM1+RO(CTIMJP)/RO0)*RUZ(I-1)*VRIP*VZIP
      C1=(FZC-FZP)/DR
      GO TO 71
   70 FZF=0.5D0*(ROIP1+RO(CTIPJP)/RO0)*RUZ(I+1)*VRIF*VZIF
```

```
      C1=(FZF-FZC)/DR
   71 FZC=0.5D0*(ROIJ+ROJP1)*VZIJ*VZIJ
      IF(VZIJ.LT.0.D0) GO TO 72
      FZP=0.5D0*(ROJM1+ROIJ)*VZJP*VZJP
      C2=(FZC-FZP)/DZ
      GO TO 73
   72 FZF=0.5D0*(ROJP1+ROJP2)*VZJF*VZJF
      C2=(FZF-FZC)/DZ
C
   73 TEMPN=0.25D0*(TIP1+PT(I+1,J+1)+TJP1+TIJ)*QRT+TF
      TEMPS=0.25D0*(TIJ+TJP1+PT(I-1,J+1)+TIM1)*QRT+TF
C
      FN=YY*RUR(I)*VIS(TEMPN)/VIS0
      FS=YY*RUR(I-1)*VIS(TEMPS)/VIS0
      D1=(FN*(PVR(I,J+1)-PVR(I,J))-FS*(PVR(I-1,J+1)-PVR(I-1,J)))/DR/DZ
      TEMPE=TJP1*QRT+TF
      TEMPW=TIJ*QRT+TF
      BE=0.5D0*(PVR(I,J+1)+PVR(I-1,J+1))/RUZ(I)*VIS(TEMPE)/VIS0
      BW=0.5D0*(PVR(I-1,J)+PVR(I,J))/RUZ(I)*VIS(TEMPW)/VIS0
      D5=XX*(BE-BW)/DZ
      D2=(FN*(VZIF-VZIJ)
     &            -FS*(VZIJ-VZIP))/DR/DR
      EE=XX*VIS(TEMPE)/VIS0
      EW=XX*VIS(TEMPW)/VIS0
      D4=(EE*(PVR(I,J+1)-PVR(I-1,J+1))-EW*(PVR(I,J)-PVR(I-1,J)))/DR/DZ
      HE=2.D0*XX*VIS(TEMPE)/VIS0
      HW=2.D0*XX*VIS(TEMPW)/VIS0
      D6=(HE*(VZJF-VZIJ)
     &            -HW*(VZIJ-VZJP))/DZ/DZ
      H=FLOAT(IP)*(P(I,J+1)-P(I,J))/DZ
     & +(RF-GRQ*0.5D0*(TIJ+TJP1)/RE/RE)
C
      TT=T(I,J)*QRT+TF
      TTI=T(I,J+1)*QRT+TF
      ROIJ=0.5D0*(RO(TT)+RO(TTI))/RO0
      PROIJ=0.5D0*(RO(CTIJ)+RO(CTJP1))/RO0
      AZ=(C1-D1-D2)/RUZ(I)+(C2+D4+D5-D6)+H
      VZ(I,J)=(PROIJ*PVZ(I,J)-DTIM*AZ)/ROIJ
C
      IF((I.GE.IN).AND.(I.LE.MOUT))
     &            UZ(I,J)=ROIJ*UZ(I,J)
  200 CONTINUE
  100 CONTINUE
C
      DO 110 J=1,N1
      UZ(IN-1,J)=-UZ(IN,J)
      UZ(MOUT+1,J)=-UZ(MOUT,J)
      VZ(IN-1,J)=-VZ(IN,J)
      VZ(MOUT+1,J)=-VZ(MOUT,J)
  110 CONTINUE
C
C------------- boundary --------------
      igo=0
      if(igo.eq.1) go to 555
C------------- normal velocity component ---------------
      DO 1011 I=IN-1,MOUT+1
      UZ(I,N1)=UZ(I,N2)
      VZ(I,N1)=VZ(I,N2)
 1011 CONTINUE
C
555       continue
C
      DO 800 J=1,N1
      DO 800 I=IN-1,MOUT+1
      IF(IP.EQ.0) UZM(I,J)=VZ(I,J)
      IF(IP.EQ.1) UZA(I,J)=VZ(I,J)
  800 CONTINUE
C
      return
      END
```

```
C
      SUBROUTINE PRESS
C
      IMPLICIT REAL*8 (A-H,O-Z)
C
      COMMON /CO1/ RUR(25),RUZ(25),ZUR(200),ZUZ(200)
     &      /CO2/ DR1,DR,DRM1,DZ1,DZ,DZN1
     &      /SOLD/ VR(25,200),VZ(25,200),T(25,200),
     &            UR(25,200),UZ(25,200),UT(25,200),
     &            PUR(25,200),PUZ(25,200),PUT(25,200),
     &            FUR(25,200),FUZ(25,200),FUT(25,200),
     &            P(25,200),FP(25,200)
     &      /PFT/ PT(25,200),FT(25,200)
     &      /CST0/ GV,PRES,TF,QV,QW,QRT
     &      /CST1/ DIA,RIN,ROUT,RATIO
     &      /CST2/ M0,M1,M2,M3,N0,N1,N2,N3
     &      /CST22/ NWI,NWO,IN,MOUT
     &      /CST5/ PAI,DTIM,TIM,RDTIM
     &      /CST8/ OMG,KVR,KVZ,KT,KPA,KPD,KE,NM,NB,IMAX,KMAX
     &      /CST9/ ERT,ERVO,ERST
     &      /CST10/ ICON
     &      /CST14/ IVI,IP
     &      /BC/ IBCT
     &      /PROP0/ RO0,VIS0,CP0,TC0,VIK0,TD0,BETA0
     &      /DLP/ RE,GRQ,FR,PR,RF
```

```
     &            /XYZ/ XX,YY,ZZ
     &            /LWSTEP/   LW
     &            /UM/ URM(25,200),UZM(25,200)
     &            /UA/ URA(25,200),UZA(25,200),PD(25,200),
     &                 FPD(25,200)
     &            /BB/ B(25,200),BD(25,200)
     &            /PFVZ/ PVZ(25,200),FVZ(25,200)
C
      KPA=0
C
      IF(KE.GT.1) GO TO 2
      DO 11 J=1,N0
      DO 11 I=1,M0
      P(I,J)=0.D0
   11 CONTINUE
C
C------- Pressure Equation --------------
C
    2 DO 10 J=2,N1
      DO 20 I=IN,MOUT
      TMP=T(I,J)*QRT+TF
      TIP1=T(I+1,J)*QRT+TF
      TIM1=T(I-1,J)*QRT+TF
      TJP1=T(I,J+1)*QRT+TF
      TJM1=T(I,J-1)*QRT+TF
      PTEM=PT(I,J)*QRT+TF
C
      IF(I.EQ.IN) TIM1=TMP
      IF(I.EQ.MOUT) TIP1=TMP
C
      ROIJ=RO(TMP)/RO0
      ROIP1=RO(TIP1)/RO0
      ROIM1=RO(TIM1)/RO0
      ROJP1=RO(TJP1)/RO0
      ROJM1=RO(TJM1)/RO0
      PROIJ=RO(PTEM)/RO0
      URMIJ=URM(I,J)
      URMIJP=URM(I-1,J)
      UZMIJ=UZM(I,J)
      UZMIJP=UZM(I,J-1)
      IF(I.EQ.IN) URMIJP=0.D0
      IF(I.EQ.MOUT) URMIJ=0.D0
      IF(J.EQ.2) UZMIJP=PVZ(I,1)
      IF(J.EQ.N1) UZMIJ=PVZ(I,N1)
      B(I,J)=(PROIJ-ROIJ)/DTIM-(0.5D0*(ROIJ+ROIP1)*
     &       RUR(I)*URMIJ-0.5D0*(ROIM1+ROIJ)*RUR(I-1)*URMIJP)
     &   /RUZ(I)/DR-0.5D0*((ROIJ+ROJP1)*UZMIJ-(ROJM1+ROIJ)*UZMIJP)/DZ
   20 CONTINUE
   10 CONTINUE
C
      DZZ=DTIM/DZ/DZ
      DRR=DTIM/DR/DR
C
    1 CONTINUE
C
      DO 100 J=2,N1
      AE=DZZ
      AW=DZZ
      IF(J.EQ.2) AW=0.D0
      IF(J.EQ.N1) AE=0.D0
C
      DO 200 I=IN,MOUT
      AN=RUR(I)/RUZ(I)*DRR
      AS=RUR(I-1)/RUZ(I)*DRR
c
      IF(I.EQ.IN) AS=0.D0
      IF(I.EQ.MOUT) AN=0.D0
c
      AP=AE+AW+AN+AS
C
      PE=P(I,J+1)
      PW=P(I,J-1)
      PN=P(I+1,J)
      PS=P(I-1,J)
C
      P(I,J)=(1.D0-OMG)*P(I,J)+OMG*(AE*PE+AW*PW+AN*PN+AS*PS
     &                              +B(I,J))/AP
      IF(ABS(P(I,J)).LT.1.E8) GO TO 200
      WRITE(8,838) KE,KPA,I,J,P(I,J)
  838 FORMAT(/1H ,'** KE=',I8,' KPA=',E11.4,' P(',I3,',',
     &       I3,')=',E11.4,'   DE STOP')
      STOP
  200 CONTINUE
  100 CONTINUE
C
      IF(KPA.EQ.0) GO TO 330
      if(KPA/2000*2000-KPA.eq.0)print*,'KPA=',KPA
      IF(KPA.GT.(IMAX/5)) GO TO 331
C
      SMAX=0.D0
      DO 320 J=2,N1
      DO 320 I=IN,MOUT
      ERS=ABS(P(I,J))*ERT
      SAMS=ABS(P(I,J)-FP(I,J))
      IF(SAMS.GT.ERS) GO TO 321
  320 CONTINUE
      RETURN
C
```

```
  331 SMAX=0.D0
      DO 319 J=2,N1
      DO 319 I=IN,MOUT
C
      IF(ABS(P(I,J)).LE.SMAX) GO TO 319
      SMAX=ABS(P(I,J))
C
  319 CONTINUE
      ERS=ERT*SMAX
      DO 332 J=2,N1
      DO 332 I=IN,MOUT
      SAMS=ABS(P(I,J)-FP(I,J))
      IF(SAMS.GT.ERS) GO TO 321
  332 CONTINUE
      RETURN
  321 IF(KPA.LT.IMAX) GO TO 330
      WRITE(8,61) KE,TIM,IMAX
   61 FORMAT(1H ,'### KE=',I9,'   TIM=',E11.4,'(SEC)    IMAX=',I5)
C
      WRITE(8,30) KE,I,J,P(I,J),FP(I,J),SAMS,ERS
   30 FORMAT(1H ,'KE=',I5,'   P(',I3,',',I2,')=',E11.4,' FP=',E11.4,
     &       '   SAMS=',E11.4,' >',E11.4,'(ERS) DE STOP')
      IVI=1
      RETURN
C
  330 CONTINUE
      DO 335 J=1,N0
      DO 335 I=IN,MOUT
      FP(I,J)=P(I,J)
  335 CONTINUE
C
      KPA=KPA+1
      GO TO 1
      END
```

```
C
      SUBROUTINE PMOD
C
      IMPLICIT REAL*8 (A-H,O-Z)
C
      COMMON /CO1/ RUR(25),RUZ(25),ZUR(200),ZUZ(200)
     &           /CO2/ DR1,DR,DRM1,DZ1,DZ,DZN1
     &           /SOLD/ VR(25,200),VZ(25,200),T(25,200),
     &                  UR(25,200),UZ(25,200),UT(25,200),
     &                  PUR(25,200),PUZ(25,200),PUT(25,200),
     &                  FUR(25,200),FUZ(25,200),FUT(25,200),
     &                  P(25,200),FP(25,200)
     &           /PFT/ PT(25,200),FT(25,200)
     &           /CST0/ GV,PRES,TF,QV,QW,QRT
     &           /CST1/ DIA,RIN,ROUT,RATIO
     &           /CST2/ M0,M1,M2,M3,N0,N1,N2,N3
     &           /CST22/ NWI,NWO,IN,MOUT
     &           /CST5/ PAI,DTIM,TIM,RDTIM
     &           /CST8/ OMG,KVR,KVZ,KT,KPA,KPD,KE,NM,NB,IMAX,KMAX
     &           /CST9/ ERT,ERVO,ERST
     &           /CST10/ ICON
     &           /CST14/ IVI,IP
     &           /BC/ IBCT
     &           /PROP0/ RO0,VIS0,CP0,TC0,VIK0,TD0,BETA0
     &           /DLP/ RE,GRQ,FR,PR,RF
     &           /UM/ URM(25,200),UZM(25,200)
     &           /UA/ URA(25,200),UZA(25,200),PD(25,200),
     &                FPD(25,200)
     &           /BB/ B(25,200),BD(25,200)
     &           /PFVZ/ PVZ(25,200),FVZ(25,200)
     &           /JC/ jcon
C
      KPD=0
C
      IF(KE.GT.1) GO TO 2
      DO 11 J=1,N0
      DO 11 I=1,M0
      PD(I,J)=0.D0
   11 CONTINUE
C
C------- Pressure Correction Equation ----------
C
    2 DO 10 J=2,N1
      DO 20 I=IN,MOUT
      TMP=T(I,J)*QRT+TF
      TIP1=T(I+1,J)*QRT+TF
      TIM1=T(I-1,J)*QRT+TF
      TJP1=T(I,J+1)*QRT+TF
      TJM1=T(I,J-1)*QRT+TF
      PTEM=PT(I,J)*QRT+TF
C
      IF(I.EQ.IN) TIM1=TMP
      IF(I.EQ.MOUT) TIP1=TMP
C
      ROIJ=RO(TMP)/RO0
      ROIP1=RO(TIP1)/RO0
      ROIM1=RO(TIM1)/RO0
      ROJP1=RO(TJP1)/RO0
      ROJM1=RO(TJM1)/RO0
      PROIJ=RO(PTEM)/RO0
C---- Mass Source ---------
      URAIJ=URA(I,J)
```

```
      URAIJP=URA(I-1,J)
      UZAIJ=UZA(I,J)
      UZAIJP=UZA(I,J-1)
      IF(I.EQ.IN) URAIJP=0.D0
      IF(I.EQ.MOUT) URAIJ=0.D0
      IF(J.EQ.2) UZAIJP=PVZ(I,1)
      IF(J.EQ.N1) UZAIJ=PVZ(I,N1)
      BD(I,J)=(PROIJ-ROIJ)/DTIM-(0.5D0*(ROIJ+ROIP1)*
     &     RUR(I)*URAIJ-0.5D0*(ROIM1+ROIJ)*RUR(I-1)*URAIJP)
     &   /RUZ(I)/DR-0.5D0*((ROIJ+ROJP1)*UZAIJ-(ROJM1+ROIJ)*UZAIJP)/DZ
   20 CONTINUE
   10 CONTINUE
C
    1 CONTINUE
C
      DZZ=DTIM/DZ/DZ
      DRR=DTIM/DR/DR
C
      DO 100 J=2,N1
      AE=DZZ
      AW=DZZ
      IF(J.EQ.2) AW=0.D0
      IF(J.EQ.N1) AE=0.D0
      DO 200 I=IN,MOUT
      AN=RUR(I)/RUZ(I)*DRR
      AS=RUR(I-1)/RUZ(I)*DRR
      IF(I.EQ.IN) AS=0.D0
      IF(I.EQ.MOUT) AN=0.D0
      AP=AE+AW+AN+AS
C
      PE=PD(I,J+1)
      PW=PD(I,J-1)
      PN=PD(I+1,J)
      PS=PD(I-1,J)
C
      PD(I,J)=(1.D0-OMG)*PD(I,J)+OMG*(AE*PE+AW*PW+AN*PN+AS*PS
     &                                +BD(I,J))/AP
  200 CONTINUE
  100 CONTINUE
C
      IF(KPD.EQ.0) GO TO 330
      if(KPD/2000*2000-KPD.eq.0) print*,'              KPD =',KPD
      IF(KPD.GT.(IMAX/5)) GO TO 331
      SMAX=0.D0
      DO 320 J=1,N1
      DO 320 I=IN,MOUT
      ERS=ABS(PD(I,J))*ERT
      SAMS=ABS(PD(I,J)-FPD(I,J))
      IF(SAMS.GT.ERS) GO TO 321
  320 CONTINUE
      GO TO 500
  331 SMAX=0.D0
      DO 319 J=1,N1
      DO 319 I=IN,MOUT
      IF(ABS(PD(I,J)).LE.SMAX) GO TO 319
      SMAX=ABS(PD(I,J))
  319 CONTINUE
      ERS=ERT*SMAX
      DO 332 J=1,N1
      DO 332 I=IN,MOUT
      SAMS=ABS(PD(I,J)-FPD(I,J))
      IF(SAMS.GT.ERS) GO TO 321
  332 CONTINUE
      GO TO 500
  321 IF(KPD.LT.IMAX) GO TO 330
      WRITE(8,61) KE,TIM,IMAX
   61 FORMAT(1H ,'### KE=',I5,'   TIM=',E11.4,'(SEC)     IMAX=',I5)
C
      WRITE(8,30) KE,I,J,PD(I,J),FPD(I,J),SAMS,ERS
   30 FORMAT(1H ,'KE=',I5,'   PD(',I3,',',I3,')=',E11.4,' FPD=',E11.4,
     &       '   SAMS=',E11.4,' >',E11.4,'(ERS) DE STOP')
      IVI=1
      RETURN
C
  330 CONTINUE
C
      DO 335 J=1,N0
      DO 335 I=IN,MOUT
      FPD(I,J)=PD(I,J)
  335 CONTINUE
C
      KPD=KPD+1
      GO TO 1
C
C------- Correction of Mass Flux -----------------
  500 DO 300 J=2,N1
      DO 400 I=IN,MOUT-1
      TIJ=T(I,J)*QRT+TF
      TIP1=T(I+1,J)*QRT+TF
      ROIJR=0.5D0*(RO(TIJ)+RO(TIP1))/RO0
      VR(I,J)=URA(I,J)-DTIM/DR*(PD(I+1,J)-PD(I,J))/ROIJR
      UR(I,J)=ROIJR*VR(I,J)
  400 CONTINUE
  300 CONTINUE
C
      DO 310 I=1,M1
      UR(I,1)=0.D0
      VR(I,1)=0.D0
```

```
      UR(I,N0)=UR(I,N1)
      VR(I,N0)=VR(I,N1)
  310 CONTINUE
C
      DO 301 J=2,N2
      DO 401 I=IN,MOUT
      TIJ=T(I,J)*QRT+TF
      TJP1=T(I,J+1)*QRT+TF
      ROIJZ=0.5D0*(RO(TIJ)+RO(TJP1))/RO0
      VZ(I,J)=UZA(I,J)-DTIM/DZ*(PD(I,J+1)-PD(I,J))/ROIJZ
      UZ(I,J)=ROIJZ*VZ(I,J)
      IF(VZ(I,J).GE.0.D0) GO TO 401
  401 CONTINUE
  301 CONTINUE
C
      DO 110 J=1,N1
      UZ(IN-1,J)=-UZ(IN,J)
      UZ(MOUT+1,J)=-UZ(MOUT,J)
      VZ(IN-1,J)=-VZ(IN,J)
      VZ(MOUT+1,J)=-VZ(MOUT,J)
  110 CONTINUE
C
      DO 311 I=1,M0
      UZ(I,N1)=UZ(I,N2)
      VZ(I,N1)=VZ(I,N2)
  311 CONTINUE
C
      RETURN
      END
```

```
C        CALCULATION OF HEATTRANSFER COEFFICIENT
      SUBROUTINE FCHT
C
      IMPLICIT REAL*8 (A-H,O-Z)
C
      COMMON /CO1/ RUR(25),RUZ(25),ZUR(200),ZUZ(200)
     &           /CO2/ DR1,DR,DRM1,DZ1,DZ,DZN1
     &           /SOLD/ VR(25,200),VZ(25,200),T(25,200),
     &                  UR(25,200),UZ(25,200),UT(25,200),
     &                  PUR(25,200),PUZ(25,200),PUT(25,200),
     &                  FUR(25,200),FUZ(25,200),FUT(25,200),
     &                  P(25,200),FP(25,200)
     &           /SOL/ HTNUM
     &           /CST0/ GV,PRES,TF,QV,QW,QRT
     &           /CST1/ DIA,RIN,ROUT,RATIO
     &           /CST2/ M0,M1,M2,M3,N0,N1,N2,N3
     &           /CST22/ NWI,NWO,IN,MOUT
     &           /CST5/ PAI,DTIM,TIM,RDTIM
     &           /CST8/ OMG,KVR,KVZ,KT,KPA,KPD,KE,NM,NB,IMAX,KMAX
     &           /CST14/ IVI,IP
     &           /BC/ IBCT
     &           /CST11/ ZN1,WQ1,WQ2
     &           /REFL/ RL
     &           /TR1/ HNEX(200)
     &           /TR0/ HTN(200)
     &           /TTIME/ TIM1,TIM2,TIM3,TIM4,TIM5,TIM6,IHT
     &           /NTIME/ MT1,MT2,MT3,MT4,MT5,MT6,ICONV
     &           /STEP/ KESTEP
     &           /VEL/ V0
     &           /ROCONST/ TEMPRO
     &           /THICK/ TATHCK
     &           /IFC/ IFCHT
      dimension QWCAL(200)
C
      ATA=PAI*(RIN**2-(RIN-TATHCK)**2)
      ATNA=PAI*(ROUT**2-RIN**2)
      ATHX=PAI*((ROUT+3.7D-3)**2-ROUT**2)
      XOUT=WQ2*RL+0.069D0
      TOUT=0.D0
      IREF=(IN+MOUT)/2
      DO 13 J=5,N0
      ZX=ZUR(J)
      IF(ABS(ZX-XOUT/RL).GT.(DZ/2.D0)) GO TO 13
      TOUT=T(IREF,J)*QRT+TF
      JT=J
      GO TO 14
   13 CONTINUE
   14 CONTINUE
      IF(TOUT.NE.0.D0) GO TO 15
      WRITE(8,666) ZX,DZ
  666 FORMAT(1H ,'>>>>> TOUT = 0 (C) DE STOP AT ZX=',E10.3,
     &       ' DZ=',E10.3)
      CALL PRINT
      STOP
   15 TMM=0.5D0*(TF+TOUT)
C
      ITW=0
      TWW1=0.D0
      DO 16 J=2,N1
      IF((ZUR(J).LT.WQ1).OR.(ZUR(J).GT.WQ2)) GO TO 16
      ITW=ITW+1
      TWW2=0.5D0*(T(IN-1,J)+T(IN,J))*QRT+TF
      TWW1=TWW1+TWW2
   16 CONTINUE
      TWAV=TWW1/FLOAT(ITW)
C
      DO 20 J=1,N0
```

```
      ZX=ZUR(J)
      IF(ZX.LT.WQ1) GO TO 20
      QQ1=ZX-0.5D0*DZ
      GO TO 21
   20 CONTINUE
C
   21 T1=TF
      T2=TF
      DO 572 J=2,N1
      IW1=0
      IW2=0
      ZX=ZUR(J)
C
      ZXM=(ZX-QQ1)*RL*1000.D0
C
      HTN(J)=0.D0
C
      TW=0.5D0*(T(IN-1,J)+T(IN,J))
      TWALL=TW*QRT+TF
      TWALLP=TW*QRT
C
      CALL SUBTRP (J,TM)
C
      TMIX=TM*QRT+TF
      TMIXP=TM*QRT
c
      zw1=ABS(ZX-WQ1)
      zw2=ABS(ZX-WQ2)
      IF(ABS(ZX-WQ1).LT.(DZ/2.D0)) IW1=1
      IF(ABS(ZX-WQ2).LT.(DZ/2.D0)) IW2=2
      IF(ABS(ZX-WQ1).LT.(DZ/2.D0)) T1=TMIX
      IF(ABS(ZX-WQ2).LT.(DZ/2.D0)) T2=TMIX
      if(IW1.ne.1) go to 44
   44 if(IW2.ne.2) go to 45
   45 continue
C
      DTC=(TCT(TWAV)*ATA+TC(TMM)*ATNA+TCH(TMM)*ATHX)
     &    *(TOUT-TF)/(WQ2-WQ1)/RL/RO(TMM)/CP(TMM)/V0/ATNA
      TMEX0=TF+(TOUT-TF)*(ZX-QQ1)/(WQ2-WQ1)
      TMEX=TF+(TOUT-TF)*(ZX-QQ1)/(WQ2-WQ1)+DTC
      TMEXP=(TOUT-TF)*(ZX-QQ1)/(WQ2-WQ1)+DTC
C
      ALFA=0.D0
      IF(ABS(TWALL-TMIX).LE.1.D-10) GO TO 11
C
  412 format(/1h ,'J=',I2,' TF=',F8.3,' TOUT=',F8.3,
     &      ' JT=',I3,' TMM=',F8.3,' DTC=',E10.3,' TW=',F8.3,
     &      ' TMEX=',F8.3/1h ,'ALFA=',e11.4,' BETA=',e11.4,
     &   ' REFTC=',e11.4,' REFEX=',e11.4)
C
      CTE=T(IN,J)*QRT+TF
      CTP=T(IN-1,J)*QRT+TF
      QWCAL(J)=(LOG(RUZ(IN)/RUZ(IN-1))
     &          /(LOG(RUR(IN-1)/RUZ(IN-1))/TCT(CTP)
     &          +LOG(RUZ(IN)/RUR(IN-1))/TC(CTE)))
     &          *(CTP-CTE)/(RUZ(IN)-RUZ(IN-1))/RL
C
      ALFA=QWCAL(J)/(TWALL-TMIX)
      QWEX=QW/RIN/1000.D0*(RIN*1000.D0-TATHCK*1000.D0)
      BET0=QWEX/(TWALL-TMEX0)
      BETA=QWEX/(TWALL-TMEX)
   11 TREF=0.5D0*(TWALL+TMIX)
      TREFEX=0.5D0*(TWALL+TMEX)
      TREFEX0=0.5D0*(TWALL+TMEX0)
      REFRO=RO(TREF)
      REFVIS=VIS(TREF)
      REFCP=CP(TREF)
      REFTC=TC(TREF)
      REFEX=TC(TREFEX)
      REFEX0=TC(TREFEX0)
      REFVIK=REFVIS/REFRO
      REFTD=REFTC/REFRO/REFCP
      REFPR=REFVIK/REFTD
      REFRE=V0*RL/REFVIK
      REFPEC=REFRE*REFPR
      HTN(J)=ALFA*RL/REFTC
      HNEX(J)=BETA*RL/REFEX
      HNEX0=BET0*RL/REFEX0
C
      if(IFCHT.ne.1) go to 572
      IF((KE/IHT*IHT-KE).EQ.0)
     & WRITE(8,6000) HTN(J),HNEX(J),HNEX0,QWCAL(J),ZXM,
     &               TWALLP,TMIXP,TMEXP
      IF(((KE/IHT*IHT-KE).EQ.0).AND.(ICONV.NE.1)) GO TO 572
C
      if(IFCHT.ne.1) go to 572
c
      IF((KE.EQ.MT1).OR.(KE.EQ.MT2).OR.(KE.EQ.MT3).OR.(KE.EQ.MT4).OR.
     &(KE.EQ.MT5).OR.(KE.EQ.MT6).OR.(ICONV.EQ.1).OR.(KE.GE.KESTEP).OR.
     &    (IVI.EQ.1))
     & WRITE(8,6000) HTN(J),HNEX(J),HNEX0,QWCAL(J),ZXM,
     &               TWALLP,TMIXP,TMEXP
 6000 FORMAT(1H ,'NU =',E11.4,'   Nuex=',E11.4,' Nu0=',E11.4,
     &         '  QW=',E11.4,
     &         '  ZQ =',E11.4,'(mm)   Tw=',F8.3,
     &         '  Tm=',F8.3,' Tex=',F8.3)
C
  572 CONTINUE
```

```
c
      TEMPRO=0.5D0*(T1+T2)
      IF((KE/IHT*IHT-KE).NE.0) RETURN
C
      WRITE(8,888) WQ1
  888 FORMAT(1H ,'***** AT htr_new_rc_mod.f ; WQ1=',E11.4)
      IGO=1
      IF(IGO.EQ.1) RETURN
      IF((KE/IHT*IHT-KE).NE.0) RETURN
      WRITE(8,6003) HTNUM
 6003 FORMAT(1H ,10X,'NUM=',E11.4)
      RETURN
      END

C------- DENSITY OF SODIUM (kg/m3)
      FUNCTION RO(TT)
C
      IMPLICIT REAL*8 (A-H,O-Z)
      COMMON /ROCONST/ TEMPRO
     &             /CST8/ OMG,KVR,KVZ,KT,KPA,KPD,KE,NM,NB,IMAX,KMAX
C
      DL1=0.95017D0-2.2978D-4*TT-1.4606D-8*TT**2+5.6384D-12*TT**3
      IF(KE.GE.2)
     &DL1=0.95017D0-2.2978D-4*TEMPRO-1.4606D-8*TEMPRO**2
     &    +5.6384D-12*TEMPRO**3
      RO=DL1*1000.D0
      RETURN
      END
C------- SPECIFIC HEAT CAPACITY OF SODIUM
      FUNCTION CP(TT)
C
      IMPLICIT REAL*8 (A-H,O-Z)
C
      CPZ7=0.343221D0-1.3869D-4*TT+1.1054D-7*TT**2
      CP=CPZ7*4.184D3
      RETURN
      END
C------- THERMAL CONDUCTIVITY OF LIQUID SODIUM
      FUNCTION TC(TT)
C
      IMPLICIT REAL*8 (A-H,O-Z)
C
      WK7=0.22203D0-1.3875D-4*TT+2.8013D-8*TT**2
      BKZ7=360.D0*WK7
      TC=BKZ7*1.162D0
      RETURN
      END
C------- VISCOSITY OF LIQUID SODIUM
      FUNCTION VIS(TT)
C
      IMPLICIT REAL*8 (A-H,O-Z)
C
      X7=0.5108D0+220.65D0/(TT+273.D0)
      Y7=0.4925*(LOG(TT+273.D0)/LOG(10.D0))
      A7=X7-Y7
      VIS=1.D-3*EXP(LOG(10.D0)*A7)
      RETURN
      END

C------- DENSITY OF Tantalum
      FUNCTION ROT(TT)
C
      IMPLICIT REAL*8 (A-H,O-Z)
C
C      ROT=16.6D0*1000.D0
      ROT=0.16621408D5-0.35776258D0*TT-0.72586262D-4*TT**2
     &    +0.14931845D-6*TT**3-0.86284131D-10*TT**4
      RETURN
      END
C------- SPECIFIC HEAT CAPACITY OF Tantalum
      FUNCTION CPT(TT)
C
      IMPLICIT REAL*8 (A-H,O-Z)
C
      CPT=0.1358344D3+0.69916403D-01*TT-0.129859D-3*TT**2
     &    +0.13049321D-6*TT**3-0.48799534d-10*TT**4
      RETURN
      END
C------- THERMAL CONDUCTIVITY OF Tantalum
      FUNCTION TCT(TT)
C
      IMPLICIT REAL*8 (A-H,O-Z)
C
      TCT=0.71714351D2-0.1962555D-01*TT+0.1922828D-4*TT**2
     &    -0.16051834D-7*TT**3+0.67099359D-11*TT**4
      RETURN
      END

C------- DENSITY OF Hastelloy X
      FUNCTION ROH(TT)
C
      IMPLICIT REAL*8 (A-H,O-Z)
C
      ROH=0.82398665D4-0.37451248D0*TT-0.77658294D-4*TT**2
     &    +0.12860041D-6*TT**3-0.63734668D-10*TT**4
```

```
      RETURN
      END
C------- SPECIFIC HEAT OF Hastelloy X
      FUNCTION CPH(TT)
C
      IMPLICIT REAL*8 (A-H,O-Z)
C
      CPH=0.12D0*4187.D0
      RETURN
      END
C------- THERMAL CONDUCTIVITY OF Hastelloy X
      FUNCTION TCH(TT)
C
      IMPLICIT REAL*8 (A-H,O-Z)
C
      TCH=0.98334611D1+0.14090929D-01*TT+0.15820335D-4*TT**2
     &    -0.26096088D-7*TT**3+0.16066076D-10*TT**4
      RETURN
      END
```

```
C
      SUBROUTINE PRINT
C
      IMPLICIT REAL*8 (A-H,O-Z)
C
      COMMON /CO1/ RUR(25),RUZ(25),ZUR(200),ZUZ(200)
     &           /CO2/ DR1,DR,DRM1,DZ1,DZ,DZN1
     &           /SOLD/ VR(25,200),VZ(25,200),T(25,200),
     &                  UR(25,200),UZ(25,200),UT(25,200),
     &                  PUR(25,200),PUZ(25,200),PUT(25,200),
     &                  FUR(25,200),FUZ(25,200),FUT(25,200),
     &                  P(25,200),FP(25,200)
     &           /UA/ URA(25,200),UZA(25,200),PD(25,200),
     &                FPD(25,200)
     &           /BB/ B(25,200),BD(25,200)
     &           /NTIME/ MT1,MT2,MT3,MT4,MT5,MT6,ICONV
     &           /SOL/ HTNUM
     &           /CST0/ GV,PRES,TF,QV,QW,QRT
     &           /CST1/ DIA,RIN,ROUT,RATIO
     &           /CST2/ M0,M1,M2,M3,N0,N1,N2,N3
     &           /CST5/ PAI,DTIM,TIM,RDTIM
     &           /CST8/ OMG,KVR,KVZ,KT,KPA,KPD,KE,NM,NB,IMAX,KMAX
     &           /CST10/ ICON
     &           /CST14/ IVI,IP
     &           /CST22/ NWI,NWO,IN,MOUT
     &           /STEP/ KESTEP
     &           /ZMET/ ZM(200)
     &           /REFL/ RL
     &           /PRO3/ UZSUM(200)
     &           /PTEM/ TTT(25,200)
     &           /AAA/ RRR(25),RZZ(25)
C
      DO 55 J=1,N1
      UZSUM(J)=0.D0
      DO 56 I=IN,MOUT
      UZSUM(J)=UZ(I,J)+UZSUM(J)
   56 CONTINUE
   55 CONTINUE
C
      DO 100 J=1,N0
      DO 100 I=1,M0
      TTT(I,J)=T(I,J)*QRT
  100 CONTINUE
C
      DO 110 I=1,M0
      RRR(I)=RUR(I)*RL
      RZZ(I)=RUZ(I)*RL
  110 CONTINUE
C
      MM=12
      WRITE(8,610) KVR,KE
      MP=1
      KW=1
      MS=1
      IF(MOUT+1.LT.12) MM=MOUT
      ME=MM
C
    1 IF(KW.EQ.1) GO TO 2
      MS=MS+MM
      ME=ME+MM
      IF(ME.GE.MOUT+1) ME=MOUT
    2 WRITE(8,614) (I,I=MS,ME,MP)
      WRITE(8,615) (RRR(I),I=MS,ME,MP)
      NMP=1
      DO 650 J=1,N0,NMP
      ZM(J)=ZUR(J)*RL
      WRITE(8,620) ZM(J),(VR(I,J),I=MS,ME,MP)
  650 CONTINUE
C
C
      KW=KW+1
      IF(ME.LT.MOUT) GO TO 1
C
  610 FORMAT(/1H ,10X,'KVR=',I4,' ;; KE=',I8)
  611 FORMAT(/1H ,10X,'KVZ=',I4,' ;; KE=',I8)
 6110 FORMAT(/1H ,10X,'DISTRIBUTION OF Uz',I4,' ;; KE=',I8)
 6119 FORMAT(/1H ,10X,' UZSUMJ')
```

```
  612 FORMAT(/1H ,10X,'KT=',I4,' ;; KE=',I8,
     &          10X,' >> JOUSHOU ONDO(K) <<')
  614 FORMAT(/1H ,'     I =        ',1X,12(4X,I6))
  615 FORMAT(1H ,'     RUR',6X,12(F10.7))
  616 FORMAT(1H ,'     RUZ',6X,12(F10.7))
  620 FORMAT(1H ,F7.3,5X,12E10.3)
C
  400 WRITE(8,611) KVZ,KE
      MM=12
      MP=1
      KW=1
      MS=1
      ME=MM
C
   11 IF(KW.EQ.1) GO TO 22
      MS=MS+MM
      ME=ME+MM
   22 IF(ME.GE.MOUT+1) ME=MOUT+1
      WRITE(8,614) (I,I=MS,ME,MP)
      WRITE(8,616) (RZZ(I),I=MS,ME,MP)
      NMP=1
      DO 651 J=1,N1,NMP
      ZM(J)=ZUZ(J)*RL
      WRITE(8,620) ZM(J),(VZ(I,J),I=MS,ME,MP)
  651 CONTINUE
C
      KW=KW+1
      IF(ME.LT.MOUT+1) GO TO 11
      IA=1
      IF(IA.EQ.1) GO TO 321
C
      WRITE(8,6110) KVZ,KE
      MM=12
      MP=1
      KW=1
      MS=1
      ME=MM
C
  101 IF(KW.EQ.1) GO TO 202
      MS=MS+MM
      ME=ME+MM
  202 IF(ME.GE.MOUT+1) ME=MOUT+1
      WRITE(8,614) (I,I=MS,ME,MP)
      WRITE(8,616) (RZZ(I),I=MS,ME,MP)
      NMP=1
      DO 5 J=1,N1,NMP
      ZM(J)=ZUZ(J)*RL
      WRITE(8,620) ZM(J),(VZ(I,J),I=MS,ME,MP)
    5 CONTINUE
C
      KW=KW+1
      IF(ME.LT.MOUT+1) GO TO 101
  321 DO 7 J=1,N1
    7 write(8,865) J,ZM(J),UZSUM(J)
  865 FORMAT(1h ,'J=',I3,'   ZM=',F11.3,'   Uz sum=',E11.4)
C
      WRITE(8,612) KT,KE
      MP=1
      KW=1
      MS=1
      ME=MM
C
  111 IF(KW.EQ.1) GO TO 222
      MS=MS+MM
      ME=ME+MM
  222 IF(ME.GE.M0) ME=M0
      WRITE(8,614) (I,I=MS,ME,MP)
      WRITE(8,616) (RZZ(I),I=MS,ME,MP)
      NMP=1
      DO 652 J=1,N0,NMP
      ZM(J)=ZUR(J)*RL
      WRITE(8,620) ZM(J),(TTT(I,J),I=MS,ME,MP)
  652 CONTINUE
C
      KW=KW+1
      IF(ME.LT.M0) GO TO 111
      IF(KE.EQ.1) RETURN
C
  500 WRITE(8,642) KE,KPA
      MP=1
      KW=1
      MS=1
      ME=MM
C
 1111 IF(KW.EQ.1) GO TO 2222
      MS=MS+MM
      ME=ME+MM
 2222 IF(ME.GE.MOUT+1) ME=MOUT+1
      WRITE(8,614) (I,I=MS,ME,MP)
      WRITE(8,616) (RZZ(I),I=MS,ME,MP)
      NMP=1
      DO 653 J=1,N0,NMP
      ZM(J)=ZUR(J)*RL
      WRITE(8,640) ZM(J),(P(I,J),I=MS,ME,MP)
      IF(KPA.GE.IMAX) WRITE(8,641) (FP(I,J),I=MS,ME,MP)
  642 FORMAT(/1H ,10X,'KE=',I8,' ;; KPA=',I5,'   pres.f')
  640 FORMAT(1H ,F7.3,5X,12E10.3)
  641 FORMAT(1H ,12X,12E10.3)
```

```
  653 CONTINUE
C
      KW=KW+1
      IF(ME.LT.MOUT+1) GO TO 1111
C
      WRITE(8,645) KE,KPD
      MP=1
      KW=1
      MS=1
      ME=MM
C
 1112 IF(KW.EQ.1) GO TO 2223
      MS=MS+MM
      ME=ME+MM
 2223 IF(ME.GE.MOUT+1) ME=MOUT+1
      WRITE(8,614) (I,I=MS,ME,MP)
      WRITE(8,616) (RZZ(I),I=MS,ME,MP)
      NMP=1
      DO 658 J=1,N0,NMP
      ZM(J)=ZUR(J)*RL
      WRITE(8,640) ZM(J),(PD(I,J),I=MS,ME,MP)
      IF(KPD.GE.IMAX) WRITE(8,641) (FPD(I,J),I=MS,ME,MP)
  645 FORMAT(/1H ,10X,'KE=',I8,' ;; KPD=',I5,'   pmod.f')
  658 CONTINUE
C
      KW=KW+1
      IF(ME.LT.MOUT+1) GO TO 1112
C
      WRITE(8,646) KE
      MP=1
      KW=1
      MS=1
      ME=MM
C
 1113 IF(KW.EQ.1) GO TO 2224
      MS=MS+MM
      ME=ME+MM
 2224 IF(ME.GE.MOUT+1) ME=MOUT+1
      WRITE(8,614) (I,I=MS,ME,MP)
      WRITE(8,616) (RZZ(I),I=MS,ME,MP)
      NMP=1
      DO 659 J=1,N0,NMP
      ZM(J)=ZUR(J)*RL
      WRITE(8,640) ZM(J),(BD(I,J),I=MS,ME,MP)
  646 FORMAT(/1H ,10X,'KE=',I8,' MASS SOURCE (BD)')
  659 CONTINUE
C
      KW=KW+1
      IF(ME.LT.MOUT+1) GO TO 1113
      RETURN
C
      END
```

```
      SUBROUTINE SUBTRP (J,TM)
      IMPLICIT REAL*8(A-H,O-Z)
C
      COMMON /CO1/ RUR(25),RUZ(25),ZUR(200),ZUZ(200)
     &       /CO2/ DR1,DR,DRM1,DZ1,DZ,DZN1
     &       /SOLD/ VR(25,200),VZ(25,200),T(25,200),
     &              UR(25,200),UZ(25,200),UT(25,200),
     &              PUR(25,200),PUZ(25,200),PUT(25,200),
     &              FUR(25,200),FUZ(25,200),FUT(25,200),
     &              P(25,200),FP(25,200)
     &       /CST2/ M0,M1,M2,M3,N0,N1,N2,N3
     &       /CST22/ NWI,NWO,IN,MOUT
     &       /CST0/ GV,PRES,TF,QV,QW,QRT
     &       /PROP0/ RO0,VIS0,CP0,TC0,VIK0,TD0,BETA0
C
      SOLF=0.D0
      SOLG=0.D0
      DO 10 I=IN-1,MOUT-1
      UZS=0.25D0*(VZ(I,J)+VZ(I,J-1)+VZ(I+1,J)+VZ(I+1,J-1))
      UZS2=0.25D0*(VZ(I+1,J)+VZ(I+1,J-1)+VZ(I+2,J)+VZ(I+2,J-1))
      TIJ=0.5D0*(T(I,J)+T(I+1,J))
      TIJ2=0.5D0*(T(I+1,J)+T(I+2,J))
C
      CT1=TIJ*QRT+TF
      CT2=TIJ2*QRT+TF
      CP1=CP(CT1)/CP0
      CP2=CP(CT2)/CP0
      F1=CP1*RUR(I)*UZS*DR
      F2=CP2*RUR(I+1)*UZS2*DR
C
      SOLF=0.5D0*(F1+F2)+SOLF
C
      G1=CP1*RUR(I)*UZS*TIJ*DR
      G2=CP2*RUR(I+1)*UZS2*TIJ2*DR
C
   10 SOLG=0.5D0*(G1+G2)+SOLG
      HSOLF=0.5D0*SOLF
      HSOLG=0.5D0*SOLG
      TM=HSOLG/HSOLF
C
      RETURN
      END
```

Fig. D-2 Source program list used for numerical analysis.

Chapter 3

Unsteady Combined Forced and Free Convection Heat Transfer Due to Rapid Decrease in Liquid Sodium Flow Rate in a Concentric Annulus

3.1 Introduction

With respect to decay heat removal in reactor core by natural circulation of coolant, study of unsteady combined forced and free convection heat transfer under rapid decrease in liquid sodium flow rate accompanied by pump coast down is important to understand cooling characteristics of reactor core under loss of flow accident.

In chapter 2, the steady combined forced and free convection heat transfer from the inner cylinder (7.6 mm in diameter, heater sheath of 1.1 mm in thickness, and heated section of 52 mm in length) to liquid sodium flowing inside a vertical concentric annulus (diameter ratio of 1.88, and outer pipe thickness of 3.7 mm) was investigated experimentally for the Péclet numbers ranging from 650 down to 0.7 (Shiotsu et al, 1993). At the same time the author have developed a numerical model which incorporates the effects of heat conduction in liquid sodium and in annulus walls, the temperature dependence of thermophysical

properties, and the natural convection due to buoyancy force on heat transfer. Based on the experimental and theoretical results, the mechanism of steady state heat transfer phenomena at low Péclet numbers has been clarified (Takeuchi et al, 1993). Irrespective of important necessity for fast reactor safety design, however, no basic study on the transient heat transfer caused by decrease in sodium flow rate in a concentric annulus has been reported.

The purpose of this study is threefold. First is to develop a numerical model for analyzing *unsteady forced convection heat transfer* (*UFCHT*) by extending a previously developed model for *steady forced convection heat transfer* (*SFCHT*) for constant flow rates, and simultaneously to obtain experimentally the time variation in heated surface temperature during liquid sodium flow reduction. Second is to obtain the numerical solution using the *UFCHT* model with the parameters identical to the experimental conditions. By comparing the numerical results with the experimental data, the validity of the model will be examined. Third is, based on the *UFCHT* and *SFCHT* models, to investigate the effect of flow reduction period on time variation in heated surface temperature and on transient heat transfer coefficient.

3.2 Numerical Model for unsteady combined forced and free convection heat transfer

The geometry to be considered and the fundamental equations—continuity, momentum, and energy for liquid sodium as well as heat conduction equation for heater sheath and outer pipe—are identical to those employed for the steady combined forced and free convection heat transfer (*SFCHT*) model described in the previous chapter.

By employing the numerical solutions of both velocity components and temperatures obtained with the *SFCHT* model for an initial condition, the numerical analysis was

performed until a steady state was established. In numerical analysis, with constant heat flux across the inner surface of the heater sheath, the flow rate of liquid sodium at the upstream boundary of a calculation domain was reduced from an initial value to a lower constant value within a certain period of time. Independent of variation in flow rate, the dimensionless velocity distribution of a developed flow at the entrance of calculation domain was kept unchanged. In contrast, the dimensionless numbers—Re, Fr, and Pe—as well as the time step, $\Delta t = L_D \Delta\tau / V_0$, involving the average inlet velocity, V_0, were simultaneously varied with variation in V_0. Other boundary conditions, configuration and dimensions of calculation domain, and mesh sizes are identical to those employed in the *SFCHT* model described in chapter 2.

Figure 3.1 shows the numerical results for time variation in inner rod surface temperature-rise from inlet liquid temperature for the flow reduction of the Péclet number decreasing almost linearly from 72 to 6.4 within 24 sec with constant heat flux, $q = 1 \times 10^6$ W/m^2, and constant liquid sodium inlet temperature, T_{in} = 573 K. The position of X = 0 mm corresponds to the upstream end of a heated section. At the initial equilibrium state, Pe = 72 (t = 0 sec), the surface temperature begins to rise from inlet temperature at about $X = -5$ mm, and increases with X on the heated section to a maximum value of 27 K near the downstream end of the heated section. In the region downstream of the heated section, the wall temperature decreases rapidly to the value almost equivalent to outlet liquid sodium temperature. Once the flow rate begins to decrease, the wall temperatures keep increasing from the initial values. Just after the flow rate reaches a lower constant value, Pe = 6.4 (t = 25 sec), the temperature profile is seen to be nonlinear on the heated section and the maximum wall superheat becomes 120 K at X = 50 mm. Moreover, it decreases continuously to 45 K at the downstream of the heated section, which may result in

significant heat loss in a flow direction. Finally, the wall temperature reaches a steady state at $t = 66\,\mathrm{sec}$, indicating almost linearly increasing profile on the heated section and a flat profile at the downstream. At this time, the thermal boundary layer begins to develop at $X = -10\,\mathrm{mm}$. Obviously the starting point of a thermal boundary layer tends to move upstream with the decrease in the Péclet number due to the contribution of axial heat conduction in liquid sodium and in the inner and outer walls of a concentric annulus.

3.3 Results and Discussion

In this section, for examination of the applicability of the *UFCHT* model for transient heat transfer, the numerical results will be first compared with experimental results. After that, the numerical analysis with the steady state model (*SFCHT*) is performed for several sodium flow rates corresponding to those encountered in the flow transient case analyzed with the *UFCHT* model. Based on the theoretical results, the possibility of predicting the unsteady combined forced and free convection heat transfer by the *SFCHT* model will be discussed.

3.3.1 Comparison of Numerical Results with Experimental Data

Experiments of unsteady forced convection heat transfer from a heated surface of 52 mm in length on an inner cylinder of 7.6 mm in diameter to liquid sodium flowing in a vertically orientated concentric annulus with an inside diameter of 14.3 mm were performed systematically. The facilities, test section, and test heater are the same as those used in the steady convection heat transfer experiments described in the previous chapter (also see Appendix E).

With constant heat flux of $q = 1.0 \times 10^6\,\mathrm{W/m^2}$, liquid sodium flow rate was reduced

ramp-wise from an initial equilibrium state (T_{in} = 573 K, U = 5 l/min, Pe=72) to the value of 0.46 l/min (Pe = 6.4) within 24 seconds and was then maintained constant. And another experimental condition of the flow rate range was from Pe = 141 (U=10 l/min) to 11.5 (U = 0.8 l/min) at $q=1.0\times10^6$ W/m^2 and T_{in} = 573 K. In the latter case, the flow rate was reduced ramp-wise within 27 seconds. For simplicity's sake, hereafter, let us refer to the former flow reduction range as *Case A*, and the latter as *Case B*.

Figures 3.2(a) and 3.2(b) show the time variation in surface temperature-rise from sodium inlet temperature, (T_w-T_{in}), at the measuring points on the heated section (X = 10.5, 21.5, 32.5, and 43.0 mm) for the *Case A* and *Case B* respectively. In the figures, the numerical results obtained with the *UFCHT* model with the parameters identical to the respective experimental conditions are also shown for comparison. The transient flow rate used in the analysis was approximated by the fourth-order of polynomials as a function of time, which estimates the experimental values within ±4 percent errors.

As shown in Fig. 3.2(a), it is observed from the experimental results that, in the first 10 seconds after the flow rate begins to decrease and amounts to about 70 percent of its initial value, the surface temperatures at all measuring points remain almost unchanged, however, they turn to increase remarkably at about t = 20 seconds. After the flow rate ceases to decrease at t = 24 sec, the surface temperatures at each location still keep rising and finally converge into each constant value. The amount of temperature rise increases as X is larger: in this case the surface temperature difference between the initial and steady states is about 40K at X = 10.5 mm and 120K at X = 43 mm. As shown in Fig. 3.2(b), the experimental results exhibit that the transient phenomena for the *Case B* are essentially similar to those for the *Case A*. At steady state, the surface temperatures at each location are lower than those for the *Case A* since the final flow rate is greater than that for the *Case A*.

And also, even though the flow reduction periods for both cases are almost the same, the time required for surface temperatures to reach a steady state is found to be more dependent on the magnitude of a final flow rate than on the variation range of a flow rate. Although the time delay of one or two seconds is observed during rapid increase in surface temperatures at the time between 20 and 30 seconds, the numerical solution of heater surface temperatures at the four locations corresponding to the measuring points agree well with the experimental results obtained for the two different flow transient conditions covering the Péclet number range from 141 down to 6.4. It is concluded therefore that the *UFCHT* model appropriately describes the unsteady combined forced and free convection heat transfer caused by a decrease in sodium flow rate in a vertical concentric annular passage.

3.3.2 Effect of Flow Reduction Period on Time Variation in Heated Surface Temperature

As basic knowledge for reactor safety design providing against loss of flow accident, effect of flow reduction period on forced convection heat transfer is technically of great interest in designing pump capacity as well as in choosing pump type. In this section, numerical results obtained with the *UFCHT* model for various flow reduction periods will be reported. And also, an attempt will be made to test the validity of the *SFCHT* model for predicting time variation in heater surface temperatures due to flow reduction.

For this purpose, the numerical analysis with the *SFCHT* model was first performed for the flow rates of 10, 5.5, 5.0, 2.75, 1.38, 1.0, 0.5, and 0.386 l/min for T_{in} = 573 K and $q = 1 \times 10^6$ W/m^2 to clarify the relationship between sodium flow rate and heated surface temperature at steady state. The Péclet numbers corresponding to these flow rates are 143, 79, 72, 40, 20, 14, 7.2, and 5.6 respectively. Figure 3.3 shows the steady state numerical

solutions of heated surface temperatures at X = 10.5, 21.5, 32.5, and 43.0 mm calculated by the *SFCHT* model at the various flow rates described above. To estimate local surface temperatures at an arbitrary sodium flow rate from the *SFCHT* model, the following equations were derived by approximating the numerical solutions using the method of least squares;

$$\left.\begin{aligned} T_w - T_{in} &= 30.0 - 39.5y + 52.5y^2 - 51.7y^3 + 20.9y^4, && \text{for } X = 10.5 \text{ mm} \\ T_w - T_{in} &= 44.1 - 71.2y + 94.3y^2 - 82.4y^3 + 30.6y^4, && \text{for } X = 21.5 \text{ mm} \\ T_w - T_{in} &= 58.0 - 104.0y + 135.4y^2 - 112.7y^3 + 41.0y^4 && \text{for } X = 32.5 \text{ mm} \\ T_w - T_{in} &= 71.3 - 135.2y + 173.0y^2 - 139.6y^3 + 50.1y^4 && \text{for } X = 43.0 \text{ mm} \end{aligned}\right\} \quad (3.1)$$

where $y = log_{10} U$. The curves obtained from the above equations are shown in Fig. 3.3. The experimental results for a variety of constant flow rates of 10, 5.0, 2.9, 1.5, 0.9, and 0.4 l/min are also shown in the figure for comparison. The experimental values at each measuring point agree with the respective approximate curves. From Eq. (3.1) the heated surface temperatures at each location were evaluated at an arbitrary flow rate corresponding to that for the flow reduction used in the *UFCHT* model.

On the other hand, the numerical analysis with the *UFCHT* model was performed for the flow reduction periods, τ, of 24, 10, 5, and 2 seconds for the *Case A*, and for τ = 27, 10, 5, and 2 seconds for the *Case B* respectively. In each case, the flow rate was reduced linearly from an initial value to a lower constant value. The time variations in heated surface temperatures based on the *SFCHT* model are compared with the numerical solutions obtained with the *UFCHT* model for the *Case A* with τ = 24 and 2 sec in Figs. 3.4(a) and 3.4(b), and for the *Case B* with τ = 27 and 2 sec in Figs. 3.5(a) and 3.5(b) respectively.

For the *Case A* at τ = 24 sec as shown in Fig. 3.4(a), in the first 10 seconds after the onset of flow reduction, the surface temperatures obtained with the *SFCHT* and *UFCHT*

models agree with each other on each location of X, without indicating remarkable temperature rise. On starting rapid temperature rise at about t = 20 seconds, however, the values predicted by the *SFCHT* model tend to increase faster than the numerical solution obtained with the *UFCHT* model. When the flow rate stopped decreasing at t = 24 sec, the surface temperatures estimated by the *SFCHT* model simultaneously reach each steady state constant value depending on X.

In contrast, even after the sodium flow rate reaches its lower constant value at t = 24 sec, the surface temperatures by the *UFCHT* model are lower than those by the *SFCHT* model and still keep increasing with time delay before reaching the steady state: at X = 43 mm for example, the period of about 20 seconds is still required for the surface temperature to be almost equal to the steady state value. For this reason as mentioned before (Fig. 3.1), the temperatures of liquid sodium, heater sheath, and outer pipe at the downstream from a heated section are still lower than those at the exit of the heated section, which results in heat loss by heat conduction in the flow direction. Thereafter the surface temperatures obtained with the *UFCHT* model asymptotically approach the values predicted by the *SFCHT* model with the increase in temperature at the non-heated section.

For τ = 2 sec as shown in Fig. 3.4(b), although the flow rate decreases as if it falls almost stepwise from an initial value to a lower constant value, the time delay of the numerical solutions by the *UFCHT* model from the values by the *SFCHT* model at a fixed wall temperature is almost equal to that for τ = 24 sec in Fig. 3.4(a). Namely, the effect of flow reduction period on time delay is unexpectedly little for τ ranging from 24 down to 2 sec. As shown in Fig. 3.5(a) and 3.5(b), the relationship between the surface temperatures obtained with the *UFCHT* model and those with the *SFCHT* model for the *Case B* is observed to be qualitatively similar to that for the *Case A*.

Figure 3.6 shows the time delay in heated surface temperatures, calculated by the *UFCHT* model for all the flow reduction periods for the *Case A*, from those predicted by the *SFCHT* model at fixed temperatures. At each location of X, the amounts of time delay become slightly large as τ is smaller, however, they agree with each other within about 2 seconds. Essentially the time delay is to become zero as τ approaches infinity. So the above results imply that the flow reduction period of $\tau = 24$ sec is short enough to be regarded as almost saturated. Namely, even if the flow reduction period becomes shorter than 24 seconds, the time delay from the value predicted by the *SFCHT* model will not become considerably larger. The similar results have been obtained for the *Case B*. From the above discussions, the amount of time delay is expected to be probably dependent on the heat capacity of a region corresponding to a heated length, however, further investigation is required to confirm the physical background of the phenomena. In summary, the *SFCHT* model is likely to overestimate transient temperature rise particularly when a final flow rate is small, and the surface temperatures calculated by the *UFCHT* model prove to be always equal to or lower than those by the *SFCHT* model for all the investigated ranges of the Péclet number and flow reduction period. Accordingly, it is concluded that the *SFCHT* model is effective as a simple method for safety evaluation of transient heated wall temperature rise caused by a rapid decrease in liquid sodium flow rate for the flow reduction periods ranging from 2 seconds to infinity.

3.3.3 Effect of Flow Reduction Period on Local Heat Transfer Coefficient

Figures 3.7(a) and 3.7(b) show the distributions of the transient local Nusselt numbers at Pe = 40, 20, and 6.4 for the *Case A* with $\tau = 24$ and 2 sec, and at Pe = 73, 40, and 11.5 for the *Case B* with $\tau = 27$ and 2 sec respectively. In each figure, the steady state

local Nusselt numbers at the corresponding Péclet numbers are also shown for comparison. For both cases, the fully developed Nusselt numbers obtained with the *SFCHT* model are observed to be about 6. For Pe = 6.4 in Fig. 3.7(a), however, the fully developed Nusselt numbers illustrated by a broken line tend to increase with X and become 8 percent greater than those for other cases. For this reason, the effect of local free convection developed near the heated surface is probably emphasized with the decrease in flow rate. As shown in the figures, the distributions of the transient local Nusselt numbers are almost the same as those for the steady state values for τ =24 and 27 sec especially in thermal entrance regions. For τ =2 sec, however, as illustrated by the symbol (▼), they become about 15 percent lower than the steady state values (— — —) in fully developed regions immediately after the end of flow reduction. At this time, the heat flux across the heated surface proved to be about eight percent lower than the predicted value of 1×10^6 W/m^2 in spite of the heat flux supplied to the inner surface of the heater sheath being kept constant. This is attributed to the heat loss in the flow direction as mentioned before. Besides, compared to the steady state values, the local temperature difference between the heated surface and bulk liquid becomes about 3 percent greater, and the thermal conductivity is also evaluated several percent greater. All these factors cause the decrease in the local Nusselt numbers in fully developed regions. As the time proceeds, the temperatures at the non-heated section rise with the decrease in the axial heat loss in the heated section, which induces the free convection effect. Finally the developed Nusselt numbers gradually approach the steady state distribution illustrated by the broken line in each figure.

3.4 Summary and Concluding Remarks

1) Liquid sodium unsteady laminar forced convection heat transfer in a concentric annulus

was experimentally investigated for the two flow reduction cases: one is for the Péclet number decreasing from 72 down to 6.4 and the other from 141 to 11.5. In each case, the flow rate was reduced ramp-wise within about 25 seconds from an initial equilibrium value to a lower constant value with constant heat flux and constant liquid inlet temperature. The experimental results have revealed that, after the onset of flow reduction, the surface temperature at first remains almost unchanged from its initial value, however, it turns to increase remarkably in about 20 seconds. After the end of flow reduction, the surface temperature still continues to rise before converging into constant value at steady state.

2) The numerical model for analyzing unsteady combined forced and free convection heat transfer due to a decrease in liquid sodium flow rate in a concentric annulus, the *UFCHT* model, was developed by extending the *SFCHT* model for constant sodium flow rates. With the *UFCHT* model, numerical analysis was performed with the same parameters—heat flux, inlet temperature of liquid sodium, and transient flow rate—as the experimental conditions. Time variations in heater surface temperatures obtained numerically agree with the experimental results for the two different flow transient conditions covering the Péclet number range from 141 down to 6.4. Thus the *UFCHT* model appropriately describes the unsteady combined forced and free convection heat transfer caused by a rapid decrease in sodium flow rate in a vertical annular passage.

3) The *SFCHT* model is valid as a simple method for safety evaluation of transient heated wall temperature rise caused by a rapid decrease in liquid sodium flow rate, because the wall temperatures calculated by the *UFCHT* model are always equal to or lower than those by the *SFCHT* model for all the investigated ranges of the Péclet number and flow reduction period.

Nomenclature

c_p	specific heat, J/(kg K)
D_{in}	inner cylinder diameter, m
D_{out}	inside diameter of a pipe, m
Fr	Froude number, $V_0^2/(g\, L_D)$
g	acceleration of gravity, m/s^2
k	thermal conductivity, W/(m K)
L	heated length, m
L_D	reference length , D_{out} - $D_{in,}$ m
Nu_X	local Nusselt number defined as Eq. (2.22)
Pe	RePr, Péclet number
Pr	Prandtl number, $\mu_0\, c_{p0}/k_0$
q	heat flux in r direction at the outer surface of inner cylinder evaluated by $q = q_w(R_{in}- \delta)/R_{in}$, W/m^2
q_w	uniform heat input supplied to the inner surface of heater sheath, W/m^2
R	radial distance from the center of inner cylinder, m
Re	Reynolds number, $\rho_0\, V_0\, L_D/\mu_0$
R_{in}	inner cylinder radius, $D_{in}/2$, m
r	dimensionless radial coordinate, R/L_D
T	temperature, K
T_{in}	fluid inlet temperature, K
T_w	surface temperature on the inner cylinder, K
t	time, s
U	flow rate, l/min

V_0 axial fully developed flow mean velocity at the entrance of calculation domain, m/s

X axial coordinate, m

x dimensionless axial coordinate, X/L_D

Greek Symbols

β volumetric expansion coefficient, K^{-1}

δ thickness of heater sheath, m

μ viscosity, Pa s

ν kinematic viscosity, m^2/s

ρ density, kg/m^3

τ period of flow rate reduction, sec

Subscript

0 values evaluated at fluid inlet temperature

References

M. Shiotsu, K. Hata, Y. Takeuchi, and A. Sakurai, 1993, "Heat Transfer from Inner Surface of a Concentric Annulus to Forced Flow of Liquid Sodium in the Laminar and Transition Regions," *Proc. 6th International Topical Meeting on NUCLEAR REACTOR THERMAL HYDRAULICS*, Vol. 2, pp. 1292-1301.

Y. Takeuchi, M. Shiotsu, K. Hata, and A. Sakurai, 1993, "Numerical Analysis for Heat Transfer from Inner Surface of a Concentric Annulus to Laminar Forced Flow of Liquid Sodium at Low Péclet Numbers," *General Papers on Convection*, ASME Publication HTD-Vol. 256, pp. 21-28.

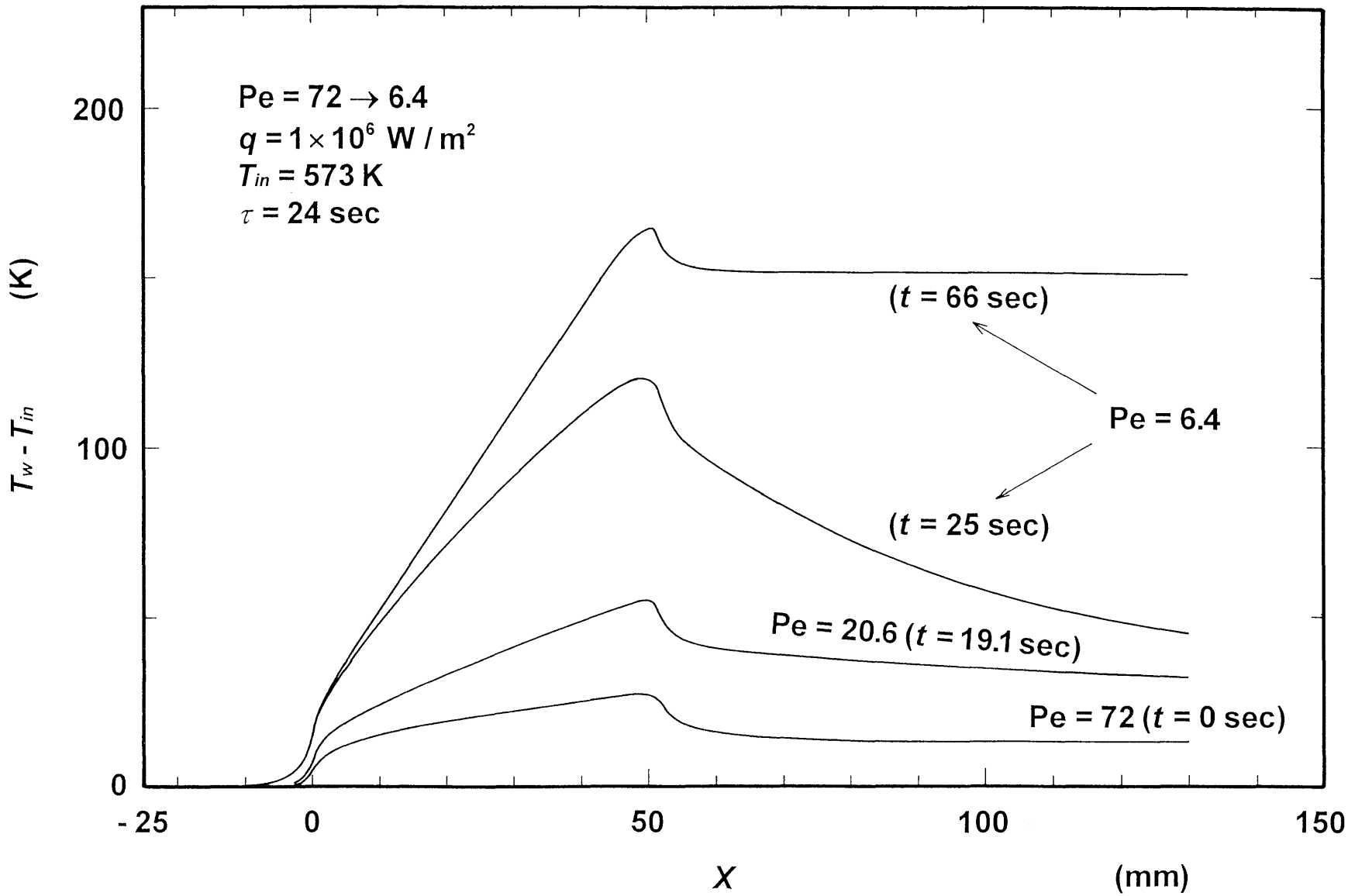

Fig. 3.1 **Time variation in the axial temperature distribution on inner rod surface for the Péclet number decreasing from 72 down to 6.4 within 24 sec.**

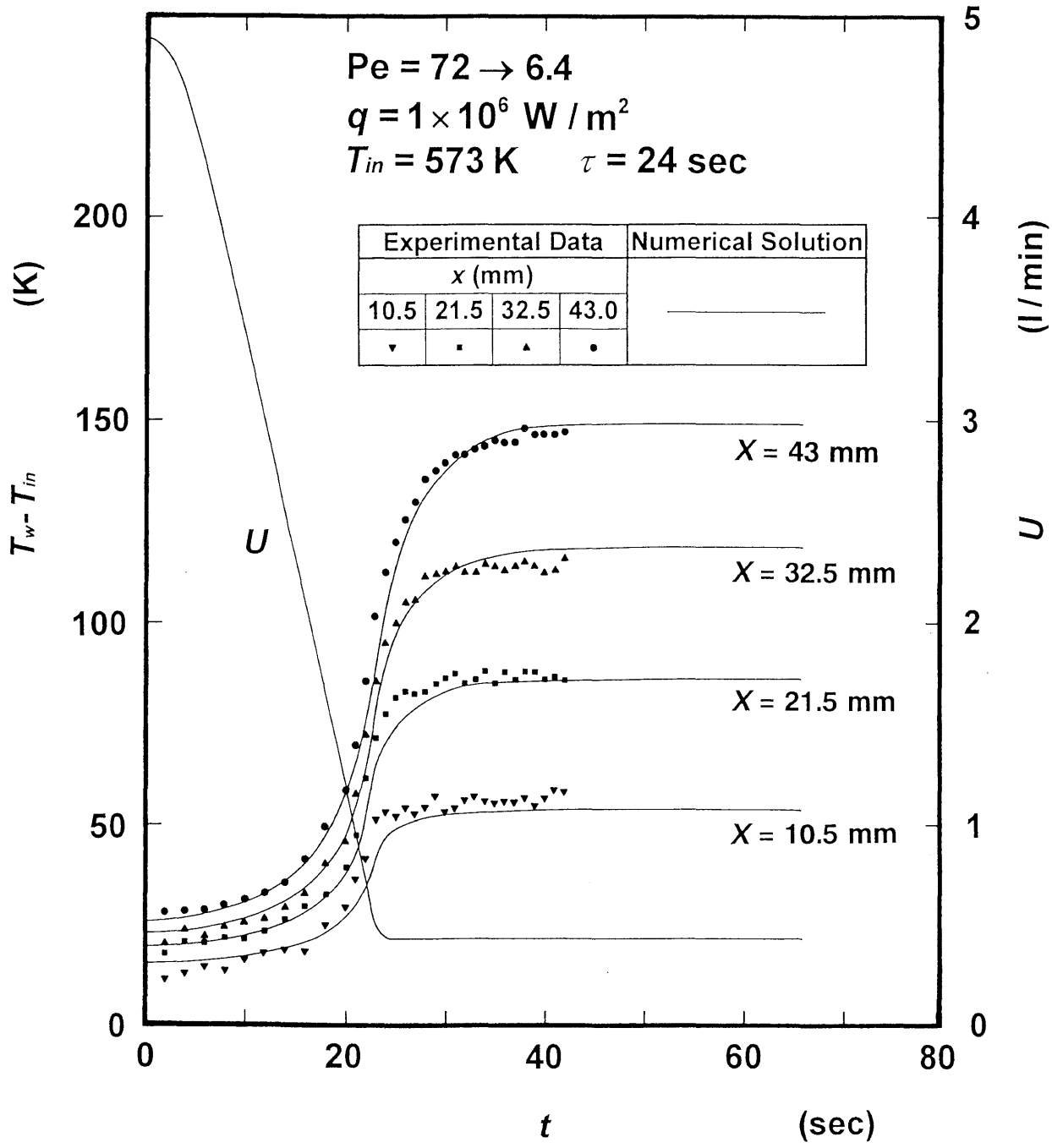

Fig. 3.2(a) Time variations in heated surface temperatures measured at X=10.5, 21.5, 32.5, and 43.0 mm for the Péclet number decreasing from 72 down to 6.4 compared with numerical solutions calculated by the *UFCHT* model.

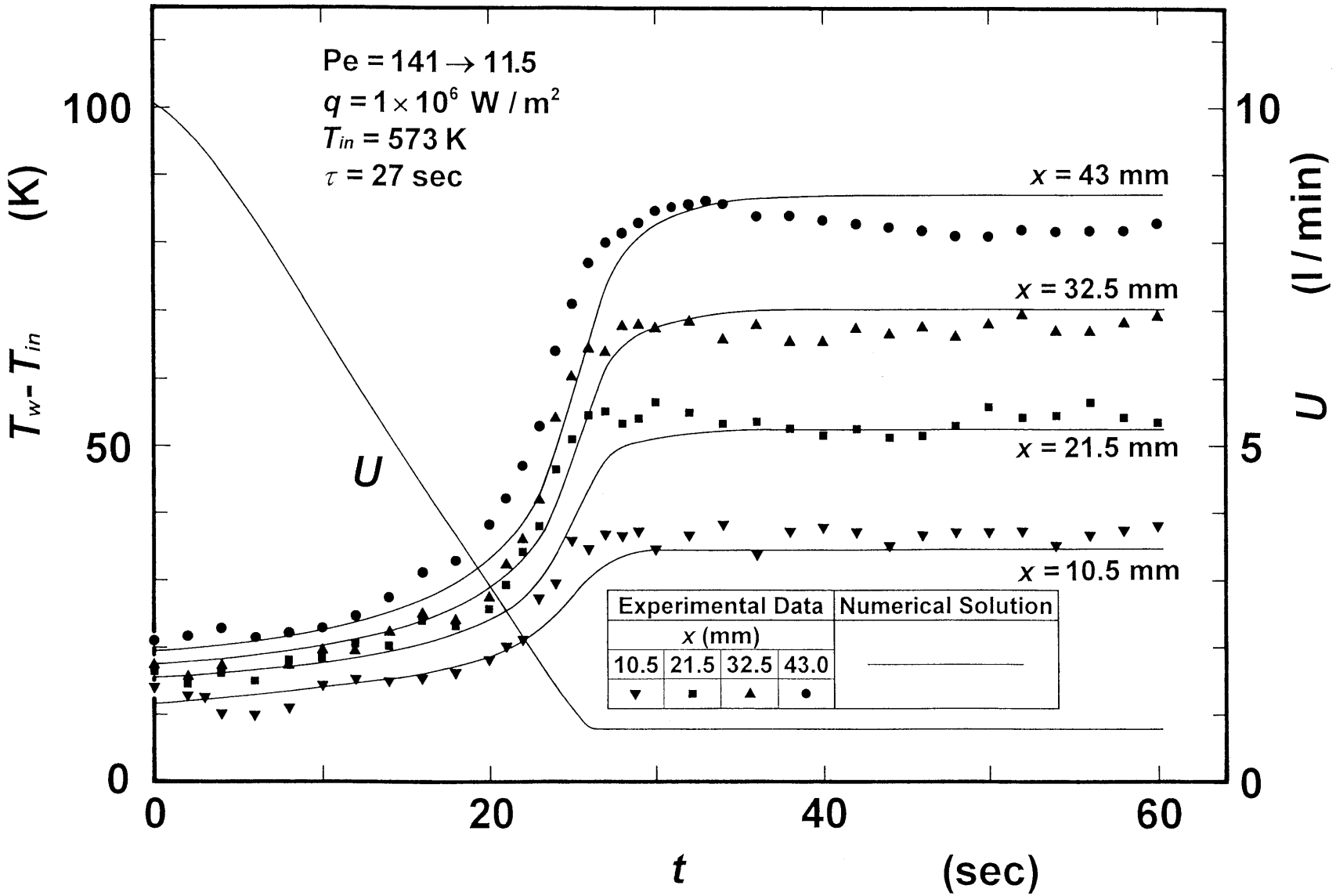

Fig. 3.2(b) Time variations in heated surface temperatures measured at *X*=10.5, 21.5, 32.5, and 43.0 mm for the Péclet number decreasing from 141 down to 11.5 compared with numerical solutions calculated by the *UFCHT* model.

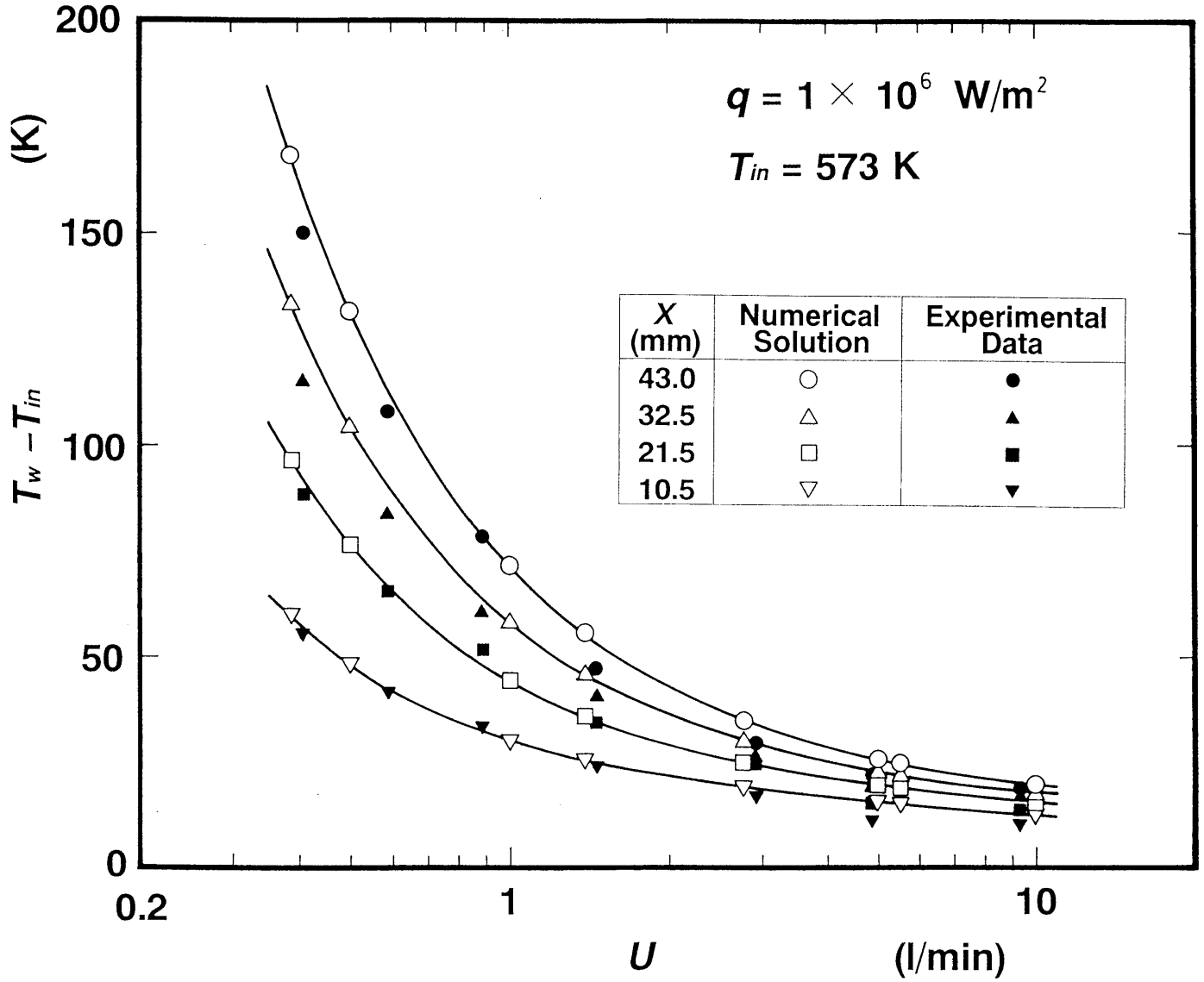

Fig. 3.3 Relationship between steady state liquid sodium flow rate and heated surface temperatures at *X*=10.5, 21.5, 32.5, and 43.0 mm obtained with the *SFCHT* model and experiments. The curves indicated are calculated by Eq. (3.1).

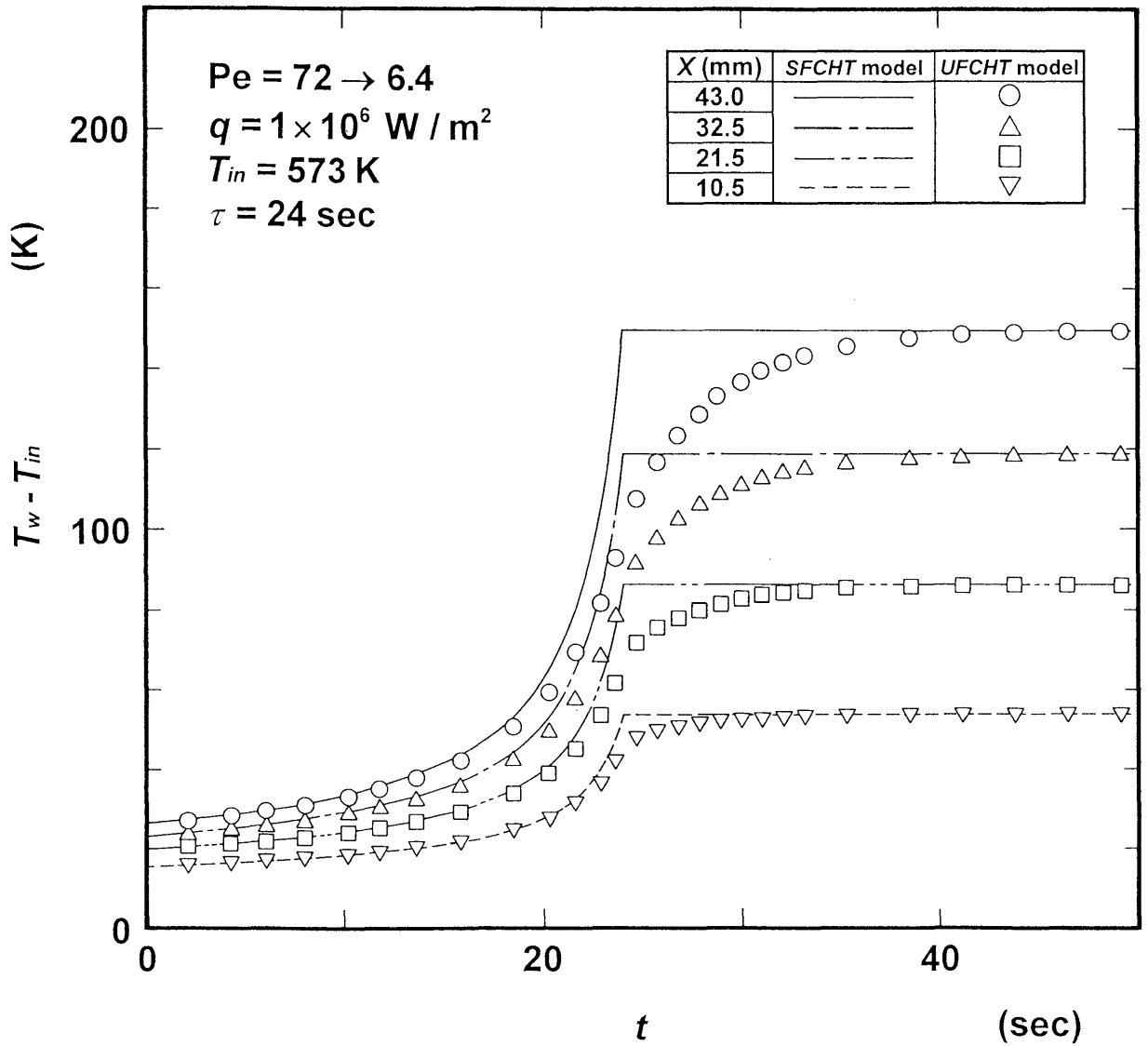

Fig. 3.4(a) Time variations in heated surface temperatures at *X*=10.5, 21.5, 32.5, and 43.0 mm calculated by the *UFCHT* model for the Péclet number decreasing from 72 down to 6.4 within 24 sec compared with those predicted by the *SFCHT* model.

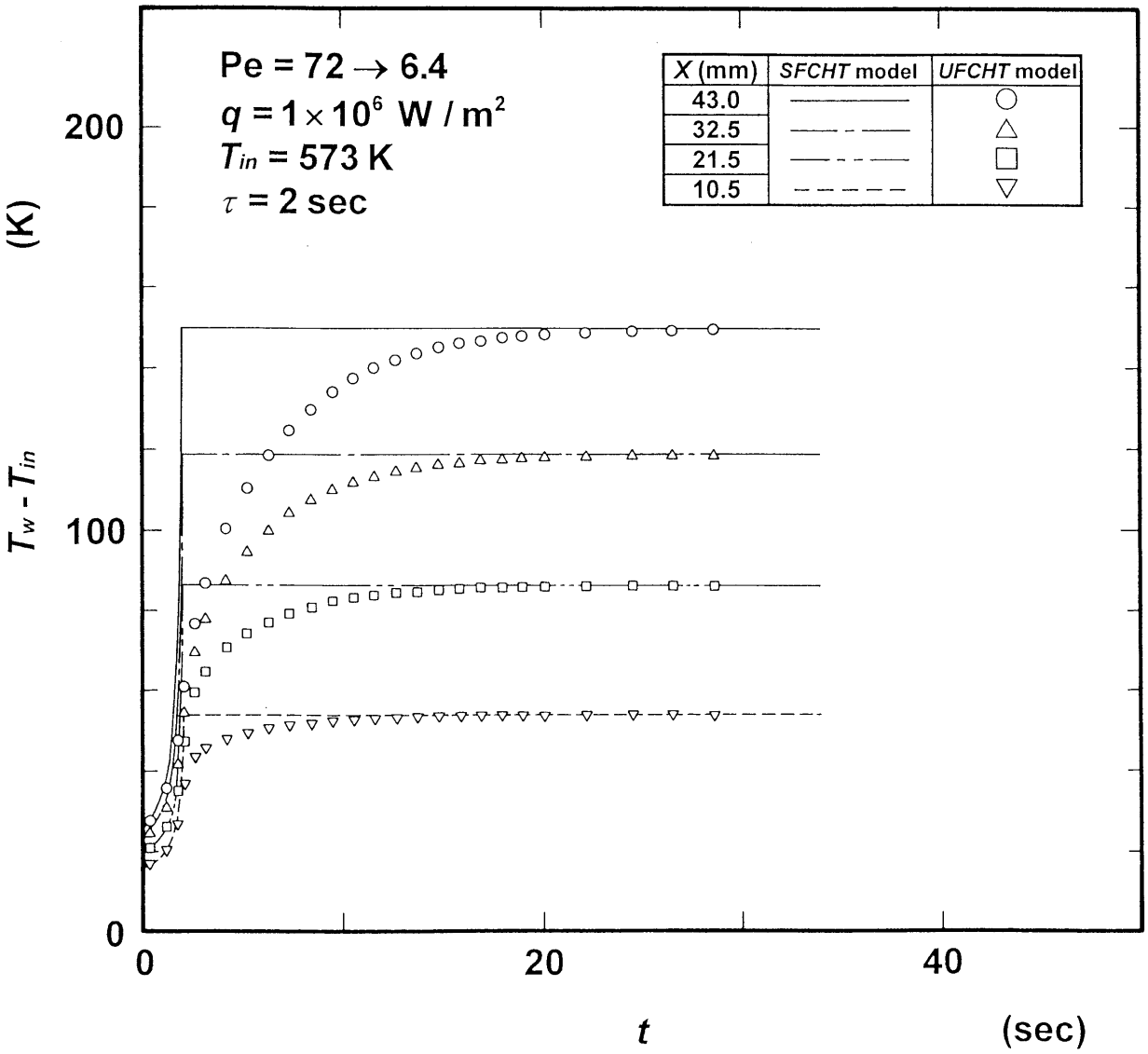

Fig. 3.4(b) Time variations in heated surface temperatures at *X*=10.5, 21.5, 32.5, and 43.0 mm calculated by the *UFCHT* model for the Péclet number decreasing from 72 down to 6.4 within 2 sec compared with those predicted by the *SFCHT* model.

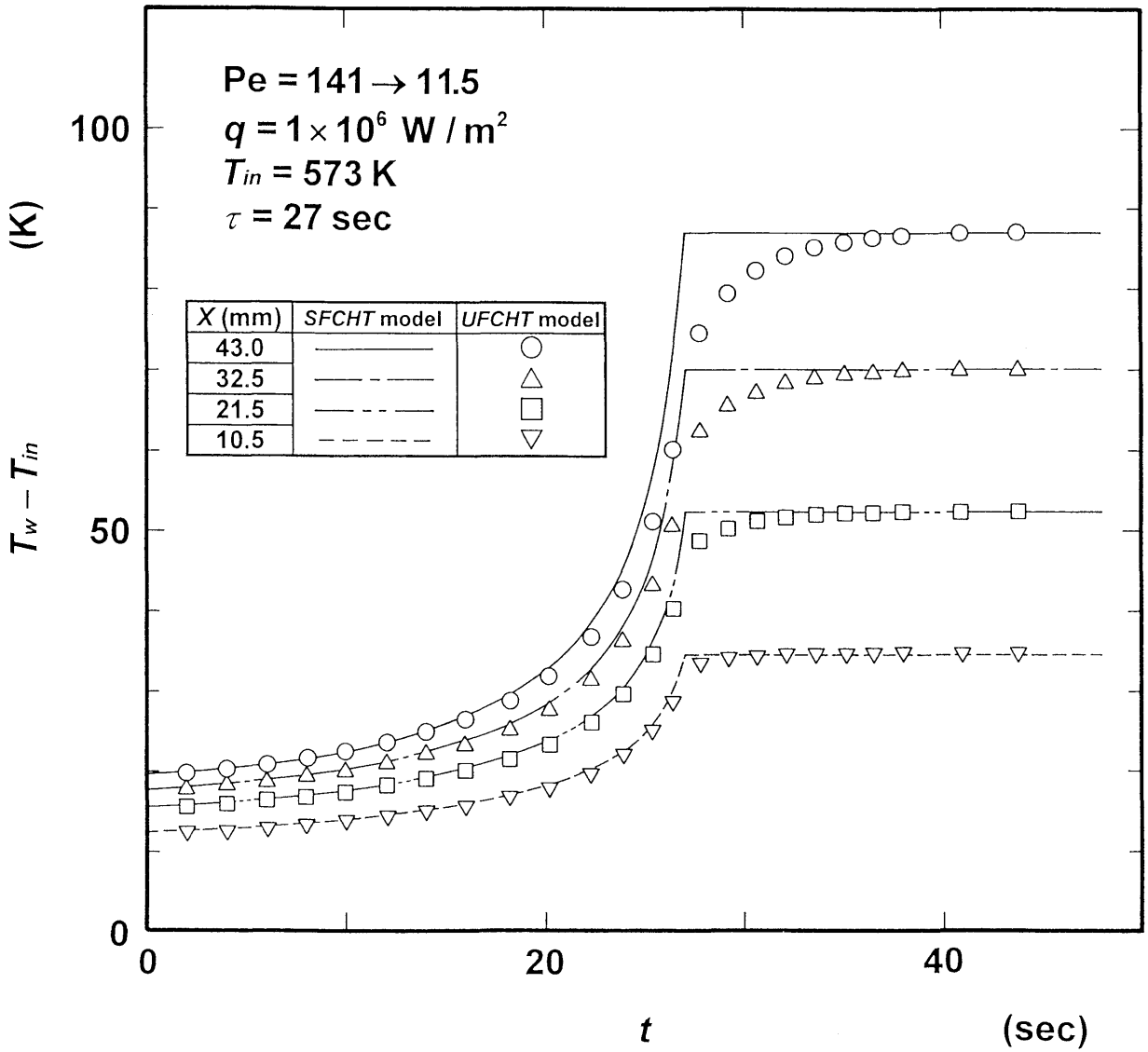

Fig. 3.5(a) Time variations in heated surface temperatures at X=10.5, 21.5, 32.5, and 43.0 mm calculated by the *UFCHT* model for the Péclet number decreasing from 141 down to 11.5 within 27 sec compared with those predicted by the *SFCHT* model.

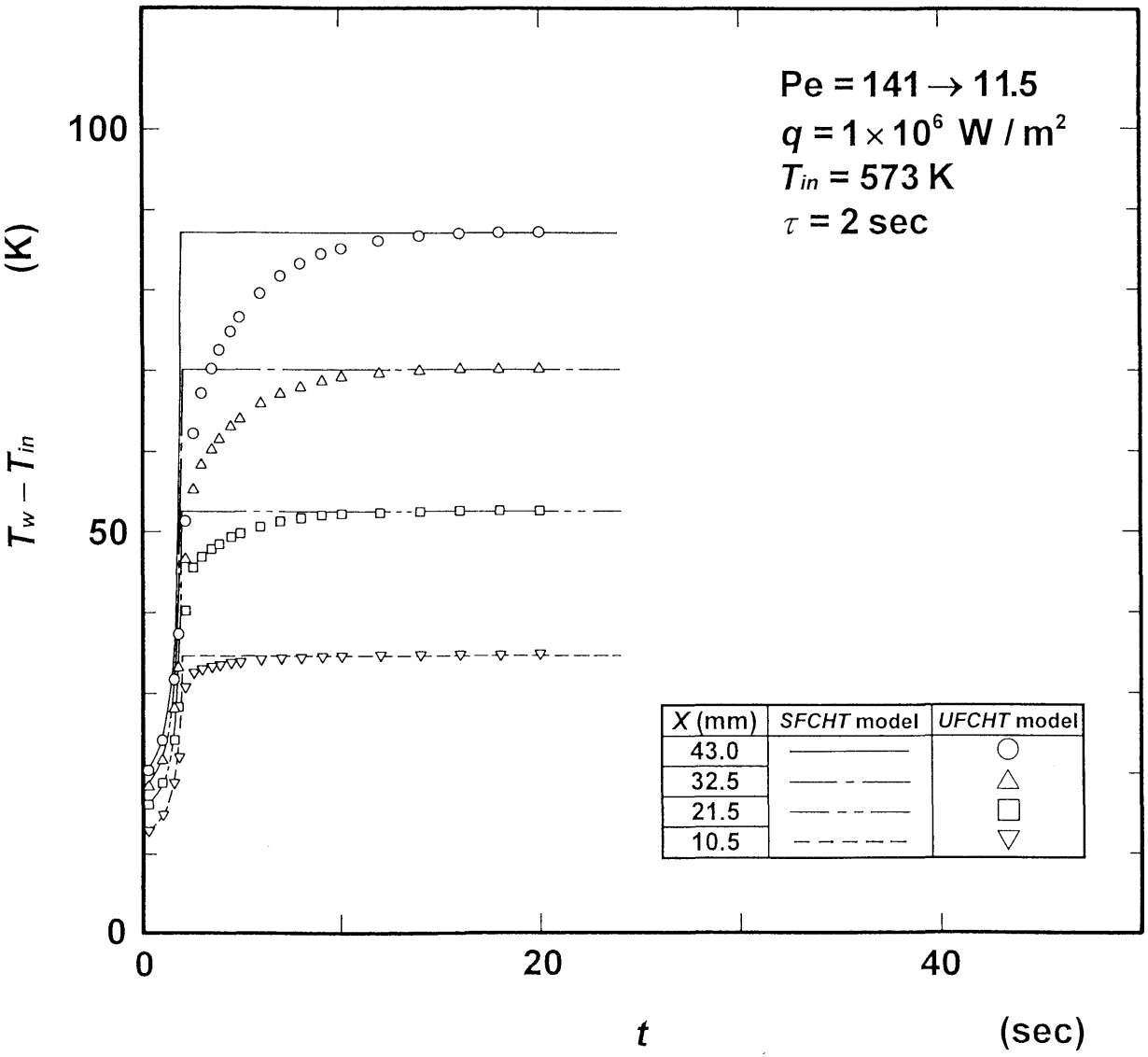

Fig. 3.5(b) Time variations in heated surface temperatures at X=10.5, 21.5, 32.5, and 43.0 mm calculated by the *UFCHT* model for the Péclet number decreasing from 141 down to 11.5 within 2 sec compared with those predicted by the *SFCHT* model.

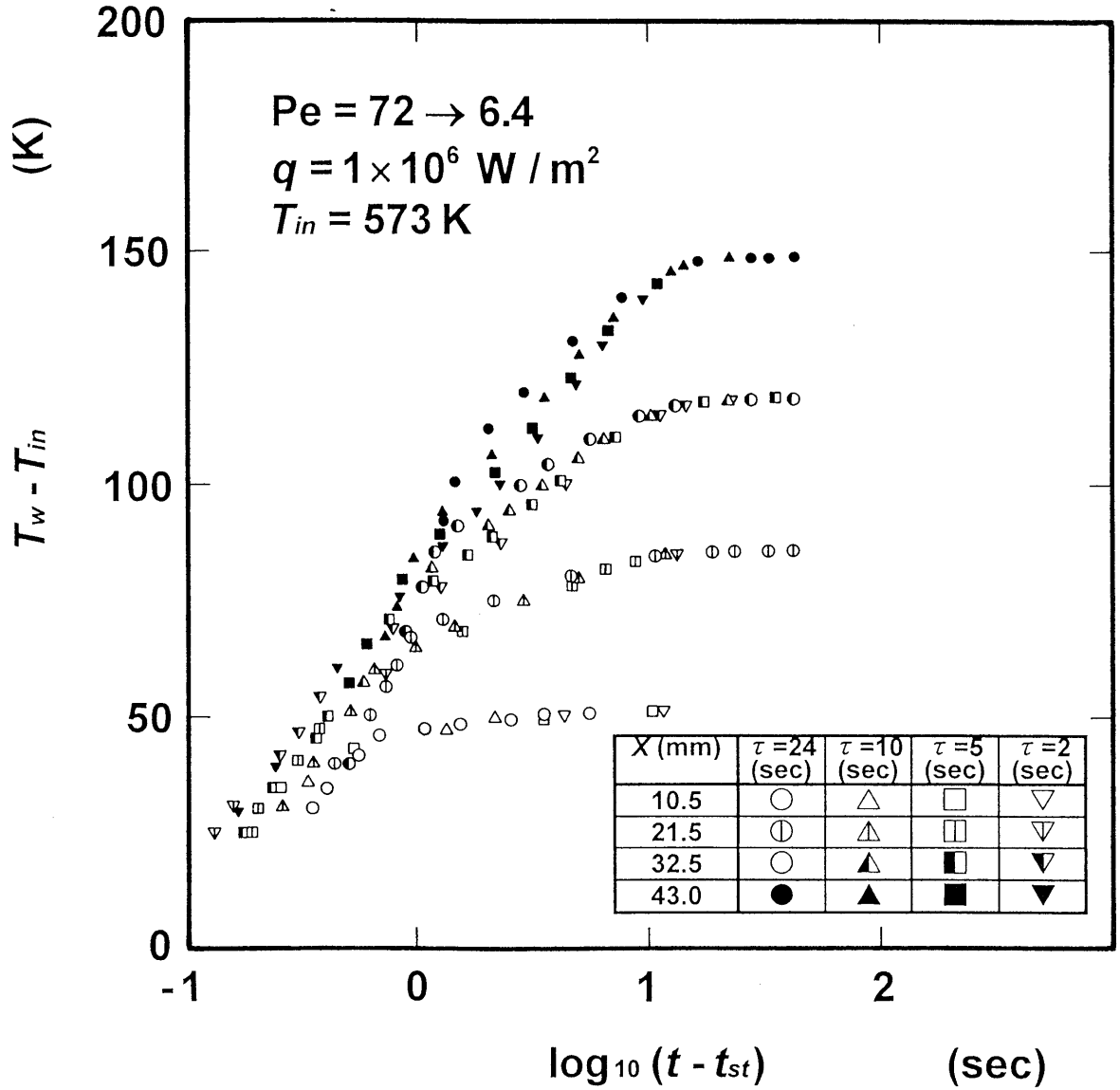

Fig. 3.6 Time delays in surface temperature rise obtained with the *UFCHT* model from that with the *SFCHT* model at *X*=10.5, 21.5, 32.5, and 43.0 mm for the flow reduction periods of 24, 10, 5, and 2 seconds for the Case *A*.

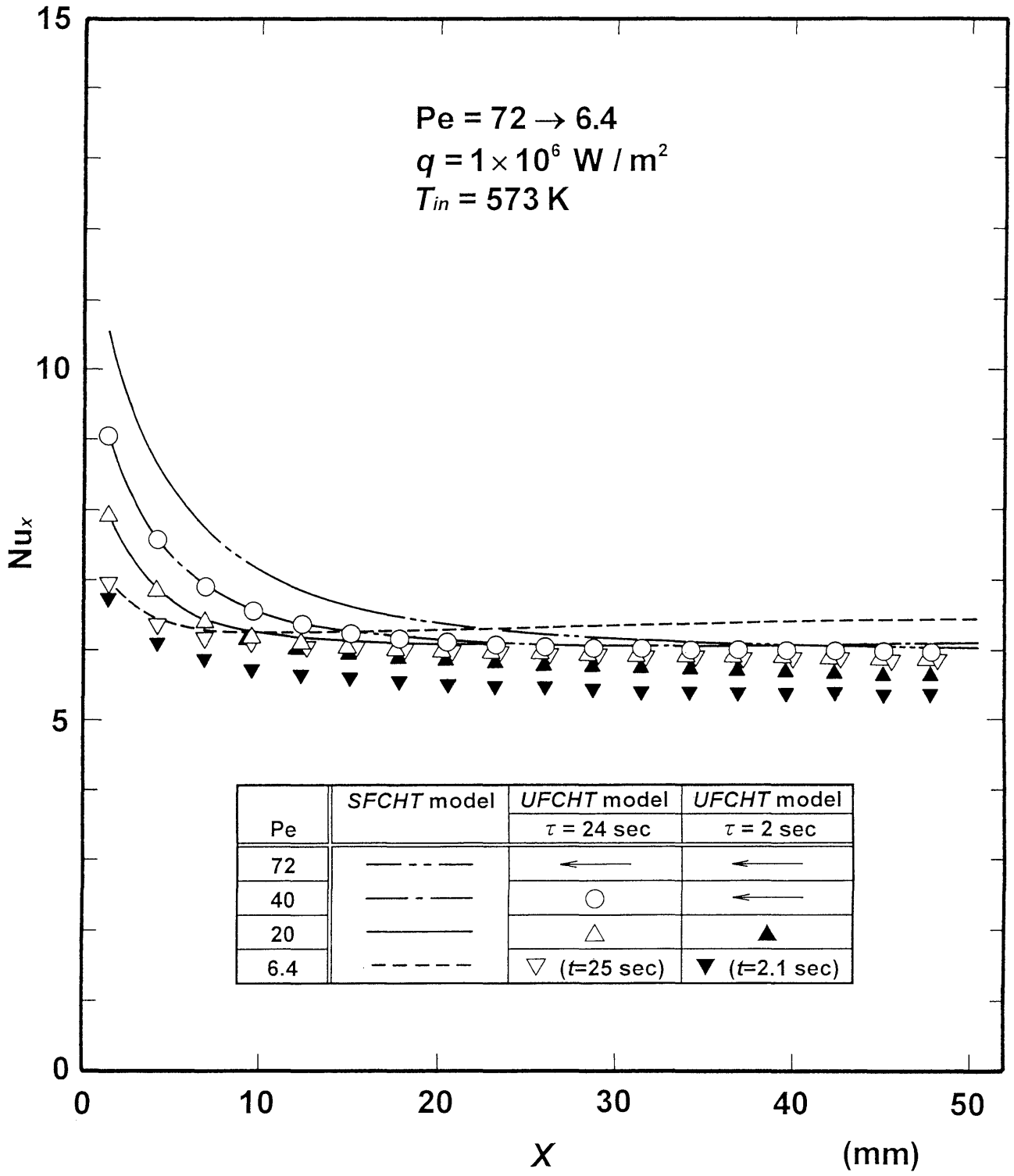

Fig. 3.7(a) **Distributions of transient local Nusselt number calculated by the *UFCHT* model for the Péclet number decreasing from 72 to 6.4 at flow reduction periods of 24 and 2 sec compared with those by the *SFCHT* model at corresponding flow rates.**

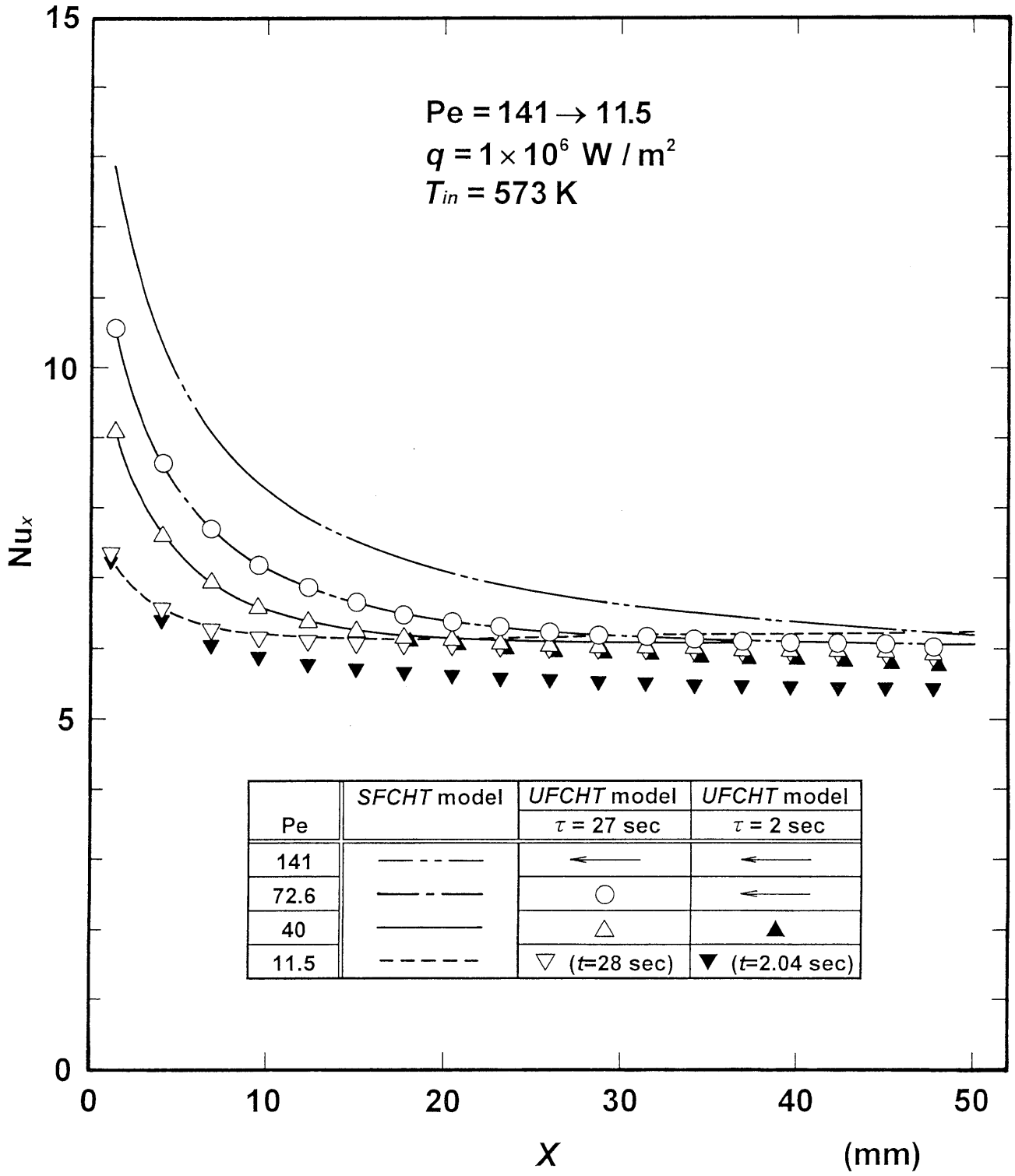

Fig. 3.7(b) Distributions of transient local Nusselt number calculated by the *UFCHT* model for the Péclet number decreasing from 141 to 11.5 at flow reduction periods of 27 and 2 sec compared with those by the *SFCHT* model at corresponding flow rates.

Appendix E

Experimental Apparatus and Method

The experimental facilities including test section and test heater are the same as those used in the experiments of steady forced convection heat transfer described in chapter 2. All the experiments of unsteady forced convection heat transfer were performed for an inlet liquid temperature of about 573 K at atmospheric pressure. Liquid sodium flow rate was adjusted to a desired value by manually regulating the input voltage of electromagnetic pumps, and was measured by electromagnetic flow meters. Measurements of heat flux, heated surface temperature, and liquid inlet/outlet temperatures have been performed as is the case for the experiments of steady forced convection heat transfer.

Chapter 4

Conclusions

A series of basic studies described in this thesis have been performed with a consistent purpose of providing the new knowledge of laminar convective heat transfer associated with reactor passive safety based on both theoretical and experimental findings.

Chapter 1 is intended to present a general correlation for natural convection heat transfer from single horizontal cylinders in liquids and gases with all existent Prandtl numbers.

1. Natural convection heat transfer coefficients on single horizontal cylinders with uniform surface heat fluxes were derived numerically from the basic equations by finite difference method without the boundary layer approximation for a wide range of Rayleigh numbers for Pr = 0.005, 0.7, 10, 100, 1000 and 3000. On the basis of the numerical results, a correlation for laminar natural convection heat transfer from single

horizontal cylinders was derived. The general correlation describes the numerical solutions of the average Nusselt numbers for the dimensionless number R_m ranging from 1.09×10^{-7} to 2.15×10^{9} within $\pm$ 5 percent errors.

2. The author's experimental results, for various liquids such as water, ethanol, glycerin, sodium, nitrogen, and helium obtained for a wide range of bulk liquid temperatures and system pressures with a variety of cylinder diameters, agree with the general correlation on the graph of $\log_{10}$ Nu vs. $\log_{10}$ R_m within $\pm$ 10 percent errors for the Prandtl numbers ranging from 0.005 to 18000, provided the liquid properties are evaluated at the reference temperature given by $T_f = T_w - 0.7(T_w - T_\infty)$. Other researchers' experimental data obtained for air, He, Ar, H_2, O_2, N_2, CO_2 gases, silicone oils and some liquid metals such as sodium, mercury and tin agree with the general correlation within $\pm$ 20 percent errors.

3. Some conventional correlation equations for natural convection heat transfer from a horizontal cylinder were compared with the general correlation: McAdams's correlation appears to be inappropriate for prediction of the average Nusselt numbers for fluids of extremely high or low Prandtl numbers even in a region where the boundary layer approximation is appropriate; the correlation presented by Churchill and Chu is not in agreement with the general correlation or with the experimental results for the Prandtl numbers tested in this work; Raithby and Hollands's correlation, based on other workers' experimental data, will probably predict the natural convection heat transfer from single horizontal cylinders with the same accuracy as other workers' experimental errors.

Chapter 2 is devoted to clarify the mechanism of laminar combined forced and free convection heat transfer in liquid sodium flowing in a vertical concentric annulus.

4. Rigorous theoretical solution of heat transfer for fully developed flow of liquid sodium in a vertical concentric annulus was obtained numerically with the same geometry as that used for the author's experiments. The numerical solutions of heater surface temperatures and outlet liquid temperatures obtained for the Péclet numbers ranging from 0.7 to 71.7 agree well with the corresponding experimental results.
5. Every theoretical analysis disregarding axial heat conduction leads to serious underestimation of the absolute values of bulk liquid temperature especially at low Péclet numbers, though the apparent local Nusselt number—namely the temperature difference between the heated surface and bulk liquid—in a thermally fully developed region, is almost in agreement with the present numerical results of the conjugate heat transfer analysis.
6. The local bulk liquid temperatures estimated by a simple method based on the linear interpolation between inlet and outlet liquid temperatures become lower than the numerical solutions even if the correction term, which takes account of axial heat conduction effect, is added. As a result, the Nusselt numbers based on the liquid temperatures estimated by this method decrease from the present numerical results with decreasing the Péclet number from around 20. It was confirmed that liquid sodium laminar forced convection heat transfer in a concentric annulus at low Péclet numbers can be described by the present numerical analysis but cannot be evaluated accurately by the simple method based on the linear interpolation between inlet and outlet liquid temperatures.
7. The fully developed Nusselt numbers obtained by the present numerical analysis range

between 6 and 7 for the Péclet numbers and heat fluxes investigated. The theoretical Nusselt numbers for a variety of heated lengths coincide with each other at the same distance measured from the beginning of respective heated section, as far as the parameters other than heated length—heat flux, liquid inlet temperature, liquid inlet velocity—are kept unchanged.

8. Approximate analytical solution capable of describing the numerical solution for bulk liquid temperature obtained for a variety of heated lengths was derived.

Chapter 3 is concerned with unsteady combined forced and free convection heat transfer due to rapid decrease in liquid sodium flow rate in a vertical concentric annulus.

9. Liquid sodium unsteady laminar combined forced and free convection heat transfer in a concentric annulus was experimentally investigated for the two flow reduction cases: one is for the Péclet number decreasing from 72 down to 6.4 and the other from 141 to 11.5. In each case, the flow rate was reduced ramp-wise within about 25 seconds from an initial equilibrium value to a lower constant value with constant heat flux and liquid inlet temperature. The experimental results have revealed that, after the onset of flow reduction, the surface temperature remains almost unchanged from its initial value, however, it turns to increase remarkably in about 20 seconds. After the end of flow reduction, the surface temperature still continues to rise before converging into constant value.

10. A numerical model for analyzing combined forced and free convection heat transfer under rapid decrease in liquid sodium flow rate in a concentric annulus, the *UFCHT*

model, was developed by extending the steady combined forced and free convection heat transfer (*SFCHT*) model for constant sodium flow rate. With the *UFCHT* model, numerical analysis was performed with the same parameters—heat flux, inlet temperature of liquid sodium, and transient flow rate—as the experimental conditions. The numerical solutions of heater surface temperatures agree with the experimental results obtained for the two different flow transient conditions covering the Péclet number range from 141 down to 6.4. Thus the *UFCHT* model proves to be valid for describing the unsteady combined forced and free convection heat transfer caused by rapid decrease in liquid sodium flow rate in the annular passage.

11. The *SFCHT* model is valid as a simple method for safety evaluation of transient heated wall temperature rise caused by rapid decrease in liquid sodium flow rate, because the surface temperatures calculated by the *UFCHT* model are always equal to or lower than those by the *SFCHT* model for all the investigated ranges of the Péclet number and flow reduction period.